THE IMPACT OF AGING, EXERCISE AND MUSCLE DISUSE ON SKELETAL MUSCLE AUTOPHAGY, MITOPHAGY AND LYSOSOME BIOGENESIS

MATTHEW TRIOLO

A DISSERTATION SUBMITTED TO THE FACULTY OF GRADUATE STUDIES

IN PARTIAL FULFILLMENT OF THE REQUIREMENTS FOR THE DEGREE OF

DOCTOR OF PHILOSOPHY

GRADUATE PROGRAM IN KINESIOLOGY AND HEALTH SCIENCE

YORK UNIVERSITY

TORONTO, ONTARIO

December 2021

ABSTRACT

Inactivity and age-related sarcopenia similarly lead to a loss of muscle mass and function. This has largely been attributed to deficits in the synthesis of proteins and organelles, yet the processes that govern the clearance of such constituents remain unexplored. The maintenance of the latter is integral, as damaged proteins/organelles perpetuate functional impairments within the tissue. The autophagy-lysosome system (ALS), which entails the selective tagging of damaged proteins and organelles, followed by their digestion in the lysosomes, is one such method. When confined to the mitochondria, the energy producing organelles, this process is termed mitophagy. Our work is focused on the regulation of intracellular degradation through the ALS, in both disuse and aging models, with implications for mitochondrial and tissue health.

To examine the dynamic effects of muscle disuse, we unilaterally denervated the hindlimb muscle of rats for 1, 3 or 7 days. Our results indicate that autophagy and mitophagy flux are biphasic, being upregulated in the early time points (i.e., 1 and 3 days) and downregulated at the latter time point. Increases in lysosomal protein levels were promoted by the upregulation and nuclear activation of the transcriptional regulator of lysosomal protein synthesis (Tfeb). Utilizing electron microscopy, we measured an increase in vacuolar inclusions, indicative of lysosomal dysfunction with prolonged denervation.

In aged muscle we similarly report elevations in ALS components and higher nuclear TFEB versus young mice. Uniquely, female mice had a greater abundance of ALS-related proteins and indices of autophagosomal turnover. This indicates that biological sex influences the capacity for autophagy. Paradoxically, catabolic events are also transiently upregulated in response to exercise, serving to “prune” the tissue’s faulty parts, including the mitochondria. Thus, we subjected young and aged mice to exhaustive exercise. Young male mice were able to activate

autophagy and lysosome biogenesis to a greater extent than female counterparts. This effect was blunted in aged mouse muscle, independent of sex.

We have uncovered how autophagy and mitophagy are differentially regulated in denervated and aged muscle. Further, we were able to show that biological sex influences the regulation of the autophagy-lysosome system in young, aged, and exercised muscle.

ACKNOWLEDGMENTS

No words can describe the gratitude I have for the many important people who have made this dream a reality.

First and foremost, I must thank Dr. David Hood for everything he has done for me. Five years ago, I joined the lab with some pretty high expectations, and they were greatly exceeded. You have provided me with endless guidance and support both inside and outside of the lab.. You have shown me the importance of being rigorous in scientific thinking and the value of balance. Your constant willingness to provide opportunities for professional and personal development have made me into the person I am today I am extremely thankful for the past five years, and I am proud to call you my mentor and friend. I will most definitely miss Friday beers. I hope to one day provide mentorship and support to others the way you have for me.

To my lab mates – what an incredible journey it has been. I have been fortunate to work alongside many great people and I could write pages about every one of you. Working with all of you throughout the years was an absolute pleasure. At times the research environment can be tough, but having you there made it much easier. I leave the Hood Lab with more than just a PhD in hand. I am grateful to walk away with life-long friends. I cannot wait to see where each of our path's lead.

To my parents, you have been a constant source of love and support. From a young age you taught me to dream big and work hard, and it is because of you that this is possible. I appreciate all the sacrifices you made to allow me to explore my passions. To my brothers, you two are, and always will be, my best friends. Thank you for consistently lightening the mood and keeping me sane – it made the tough days that much easier.

Finally, and most importantly, to Kelsey. None of this would have been possible without you. We met as I began this journey, and ever since day one you have been supportive of my aspirations. Although I have often been preoccupied by my work, you have always been understanding and motivating. You have helped me remain positive after long days at the lab. Your love and support mean the world to me, and for that I am eternally grateful.

TABLE OF CONTENTS

LIST OF TABLES

Chapter 4:

Chapter 5:

LIST OF FIGURES

Chapter 2:

Chapter 4:

LIST OF ABBREVIATIONS

Ach	Acetylcholine
ADP	Adenosine diphosphate
AIF	Apoptosis-Inducing Factor
Akt	Protein kinase B
ALS	Autophagy-lysosome system
AMBRA1	Activating molecule in beclin-1-regulated autophagy
AMP	Adenosine monophosphate
AMPK	AMP-activated protein kinase
ANOVA	Analysis of variance
Atg	Autophagy-related genes
ATP	Adenosine triphosphate
ATP5A	ATP synthase subunit 5a
BCL-2	B-cell lymphoma 2
BNIP3	BCL2/adenovirus E1B 19-kDa-interacting protein 3
BNIP3L/NIX	BCL2/adenovirus E1B 19-kDa protein-interacting protein 3-like
Ca^{2+}	Calcium
CaMK	Ca2+/calmodulin-dependent protein kinase
cAMP	Cyclic AMP
CARM1	Coactivator associated arginine methyltransferase 1
CHOP	C/EBP homologous protein
CLEAR	Coordinated lysosomal expression and regulation
ClpP	Caseinolytic mitochondrial matrix peptidase proteolytic subunit
CMA	Chaperone-mediated autophagy
COLCH	Colchicine
COX	Cytochrome oxidase
COX I	Cytochrome oxidase subunit I
COX IV	Cytochrome oxidase subunit IV
CnA	Calcineurin
CoQ	Coenzyme Q

CRE	cAMP response element
CREB	cAMP response element binding protein
CS	Citrate synthase
Cyto c	Cytochrome c
DCF	2',7'-Dichlorofluorescin
DEN	Denervation
DHPR	Dihydropyridine receptors
DNA	Deoxyribonucleic acid
Drp1	Dynamin-realted protein 1
E-box	Enhancer box
ECC	Excitation contraction coupling
EDL	Extensor digitorum longus
ENDO G	Endonuclease G
ER	Endoplasmic reticulum
ERR (α, β, γ)	Estrogen-related receptors (alpha, beta, gamma)
ETC	Electron transport chain
FAD+	Flavin adenine dinucleotide - oxidized
$FADH_2$	Flavin adenine dinucleotide - reduced
FIP200	FAK family-interacting protein of 200 kDa
Fis1	Mitochondrial fission 1 protein
FoxO3	Forkhead box O3
Fundc1	FUN14 Domain Containing 1
GABARAP	Gamma-aminobutyric acid receptor-associated protein
GAPDH	Glyceraldehyde-3-Phosphate Dehydrogenase
GATE 16	Golgi-associated ATPase enhancer of 16 kDa
gDNA	Genomic DNA
GF	Growth factor
GFP	Green fluorescent protein
H^+	Hydrogen ion
H_2O_2	Hydrogen peroxide

H_2O	Water
HDAC	Histone deacetylase
HRP	Horseradish peroxidase
HSC70	Heat shock cognate 70 kDa protein
i.p.	Intraperitoneal
IGF-1	Insulin-like growth factor 1
IL	Interleukin
IMF	Intermyofibrillar
IMM	Inner mitochondrial membrane
IMS	Intermembrane space
KD	Knockdown
KO	Knockout
Lamp	Lysosomal-associated membrane protein
LC3-I	Microtubule-associated proteins 1A/1B light chain 3-I
LC3-II	Microtubule-associated proteins 1A/1B light chain 3-II
LIR	LC3-interacting region
LonP	Lon peptidase
Lmp	Lysosome membrane proteins
MAFbx	Muscle atrophy F-box / Atrogin-1
MCOLN1	Mucolipin 1
MEF2	Myocyte-enhancer factor 2
Mff	Mitochondrial fission factor
Mfn1/2	Mitofusin-1/2
MHC	Myosin heavy chain
MiD49/51	Mitochondrial dynamics proteins of 49 and 51 kDa
MnSOD	Manganese Superoxide Dismutase
Mpp	Mitochondrial processing peptidase
mRNAs	Messenger RNA
mtDNA	Mitochondrial DNA
MuRF1	Muscle ring finger 1

MTCO1	Mitochondrially encoded cytochrome c oxidase 1
mTORC	Mechanistic target of rapamycin complex
mtPTP	Mitochondrial permeability transition pore
mtUPR	Mitochondrial unfolded protein response
MuSC	Muscle stem cell
Na^+	Sodium
NAD+	Nicotinamide adenine dinucleotide - oxidized
NADH	Nicotinamide adenine dinucleotide – reduced
NADPH	Nicotinamide adenine dinucleotide phosphate
NBR1	Neighbour of BRCA-1
Ndp52	Nuclear dot protein 52
NDUFB8	NADH:ubiquinone oxidoreductase subunit B8
NF-κβ	Nuclear Factor-kappa beta
Nrf2	Nuclear factor, erythroid 2 like 2
NMJ	Neuromuscular junction
NRF-1/2	Nuclear respiratory factor-1 / 2
NuGEMPs	Nuclear genes encoding mitochondrial proteins
O_2	Oxygen
$O_2^{\bullet-}$	Superoxide
$OH^{\bullet}$	Hydroxyl
OMM	Outer mitochondrial membrane
Opa1	Optic atrophy 1
OPTN	Optineurin
OXPHOS	Oxidative phosphorylation
P_i	Inorganic phosphate
p38-MAPK	p38 mitogen activated kinase
p53	Tumor Suppressor protein 53
p62/SQSTM1	sequestosome 1
pAMPK	phospho-AMPK
PARL	Presenilins-associated rhomboid-like protein

PCR	Polymerase chain reaction
PCr/CK	Phosphocreatine/creatine kinase system
PE	phosphatidylethanolamine
PGC-1α	peroxisome proliferator activated receptor gamma coactivator 1 alpha
PI3K	Phosphatidylinositol-4,5-bisphosphate 3-kinase
PI3KC3-C1	Class III phosphatidylinositol 3-kinase complex I
PI(3)P	Phosphatidylinositol 3-phosphate
PIM	Protein import machinery
Pink1	PTEN-induced putative kinase 1
p-p38	Phospho-p38
POLRMT	RNA Polymerase Mitochondrial
PPAR (α,β,γ)	Peroxisome proliferator-activated receptor (alpha, beta, gamma)
PTM	Post-translational modification
qPCR	Quantitative polymerase chain reaction
RAB7	Ras-related protein 7
RFP	Red fluorescent protein
RLU	Relative light units
RNA	Ribonucleic Acid
ROS	Reactive oxygen species
RyR	Ryanodine receptor
SAL	Saline
SDHB	Succinate dehydrogenase subunit B
SDS-PAGE	Sodium dodecyl sulfate polyacrylamide gel electrophoresis
SERCA	Sarco/endoplasmic reticulum Ca2+-ATPase
Sirt1	Sirtuin 1
SR	Sarcoplasmic reticulum
SS	Subsarcolemmal
STAT3	signal transducers and activators of transcription 3
TA	Tibialis anterior
TCA	Tricarboxylic acid cycle

TFB2M	Transcription factor B2, mitochondrial
Tfam	Mitochondrial transcription factor A
Tfeb	Transcription factor EB
Tfe3	Transcription factor E3
TGF-β	Transforming growth factor beta
Tim	Translocase of the inner membrane
TNF-α	Tumor necrosis factor alpha
Tollip	Toll interacting protein
Tom	Translocase of the outer membrane
TGN	Trans-golgi network
Trpml1	Transient receptor potential mucolipin 1
TSC1/2	Tuberous sclerosis proteins 1 and 2
TT	Transverse tubules
Ub	Ubiquitin
UBD	Ubiquitin binding domain
ULK1	Unc-51 like kinase 1
UPS	Ubiquitin proteasome system
USF-1	Upstream stimulatory factor 1
UQCRC2	Ubiquinol-cytochrome c reductase core protein 2
v-ATPase	Vacuolar-type H + -ATPase
VDAC	Voltage dependent anion channel
VEH	Vehicle
Vsp	Vacuolar sorting proteins
ΔΨ	Mitochondrial membrane potential

Chapter One: Introduction

Skeletal muscle is the largest organ system in the human body, and plays a significant role in locomotion, motor task execution and in the control of whole-body metabolism. As such, preserving healthy muscle throughout our lifespan is integral to the maintenance of quality of life. Importantly, muscle displays a high degree of plasticity, adapting to the demands placed upon it. These demands include contractile activity, or lack thereof, and metabolic cues. This plasticity contributes to the beneficial effects of exercise, but also the decrements in muscle quality observed with sedentarism and aging. Thus, understanding the consequences of these adaptations has implications for the increasing aging population, and for those who are restricted in physical activity due to sedentary behavior or injury.

Chronic muscle disuse is commonly associated with loss of muscle mass (i.e., atrophy), function and metabolic efficiency. The natural aging process produces similar characteristics in a condition known as sarcopenia, which can be exacerbated by prolonged periods of inactivity. Fortunately, exercise can restore muscle health following periods of disuse, and can serve to slow age-related muscle wasting. Thus, further understanding of the molecular differences between young and old muscle, and the differential effects of physical activity and inactivity on these populations will guide the development of strategies to enhance skeletal muscle health with increasing age.

Skeletal muscle mitochondria are primarily responsible for energy production. When these organelles become dysfunctional there are detrimental effects on the muscle through both a lack of energy production and the damaging effects of reactive oxygen species. The volume of these organelles within muscle is regulated by the balance of opposing processes of their synthesis (biogenesis) and degradation, the latter via a specific form of autophagy, termed mitophagy.

Mitophagy contributes to the loss of mitochondrial volume and the preservation of their function through the removal of organelles that become defective.

Autophagy is a cellular quality control mechanism that digests and recycles impaired organelles and protein aggregates at the lysosomes. This process is required in a balanced manner, as overactivation has catabolic effects, whereas loss of autophagy prevents the removal of damaging constituents. Recently, lysosomes, acidic digestive organelles, have been established as a regulator of muscle quality through their ability to terminally degrade cellular components, such as mitochondria.

With the rapid increase in the aging population, and with inactivity rates on the rise, it is essential to uncover the mechanisms responsible for the preservation of skeletal muscle health. Overall, investigating the disuse and age-induced responses in autophagy, mitophagy and the regulation of the lysosomes are avenues worthy of exploration. Furthermore, understanding the molecular control of the beneficial effects of exercise will guide future interventions aimed at mitigating the negative effects of age and disuse on the skeletal muscle health. Thus, the goal of this dissertation is to examine how disuse, in the form of neuromuscular denervation, and advancing age impact the autophagy-lysosome system in skeletal muscle, with the further aim of exploring how exercise may positively influence these processes.

CHAPTER 2: REVIEW OF LITERATURE

2.1. Overview of Skeletal Muscle Form and Function:

2.1.1. SKELETAL MUSCLE ANATOMY

Skeletal muscle comprises approximately 40% of total body mass and is integral for locomotion and whole-body metabolic control (1, 2). Muscle is a "long" tissue that is attached to the bone on both ends via tendons. As such when contraction occurs, the muscle shortens, effectively pulling the attached bones together. Typically thought of as a layered tissue (3), bundled within a muscle are multiple fascicles, which contain myofibers (muscle cells). Each myofiber membrane is termed the sarcolemma, and within it the boundaries of this membrane are subunits called myofibrils, which contain the contractile apparatus. A series of sarcomeres (thousands to millions) make up myofibrils, of which boundaries are defined by z-lines (Figure 1). With actin and titin anchored to these z-lines, and myosin closely associated, each sarcomere has the machinery to contract when signaled to. As a cell, muscle fibers contain capillaries for nutrients exchange, and nervous innervation through neuromuscular junctions.

Inside and around the muscle fiber is an intricate network of membrane-bound structures termed transverse-tubules (TT) and sarcoplasmic reticulum (SR). The TT are invaginations of the sarcolemma, that allow for action potentials to penetrate the myofiber, and ultimately promote contraction (see below). These TT are flanked by SR, which act as a Ca^{2+} storage depot. This sophisticated anatomy allows for control of muscular contraction.

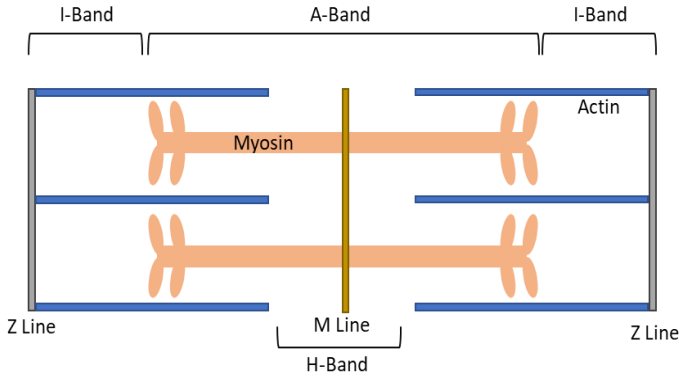

Figure 1. Schematic Depiction of a Skeletal Muscle Sarcomere. A sarcomere boundary is within two Z-Lines. Actin, the "thin filament", made up of globular actin subunits, is tethered to the Z-Line. Myosin, the "thick filament" is contained within the mid-portion of the sarcomere. Each myosin contains two-heavy and four-light chains, making it a hexamer. Anatomically, the I-Band is a region where only actin can be seen microscopically, the A-Band is the region where both Actin and Myosin can be observed, the M-Line is the middle of the Sarcomere, and the H-Band is a region where only Myosin is observed.

2.1.2. CONTROL OF MUSCULAR CONTRACTION

Muscular contraction is an intricate process that begins at the α-motorneuron. Depolarization at the pre-synaptic membrane will lead to the release of the neurotransmitter, acetylcholine (Ach), at the neuromuscular junction (NMJ). Ach diffuses across the synaptic cleft and binds to post-synaptic nicotinic Ach-receptors housed within the sarcolemma. This acts to open Na^+ channels, and an influx of Na^+ leads to an action potential at the sarcolemma. This action potential propagates down the TT, activating dihydropyridine receptors (DHRP). Through physical interaction with Ryanodine Receptors (RYR) of the SR, Ca^{2+} will be released into the sarcoplasm, where it can promote muscular contraction (4, 5). In a process called excitation-contraction coupling (ECC), Ca^{2+} will bind to troponin c, and effectively release its inhibition on myosin binding sites within the actin molecules, allowing for the complexes to interact and promote contraction through crossbridge cycling (4, 5). This process requires an abundance of energy in the form of adenosine triphosphate (ATP). Following the cessation of an action potential, the Ca^{2+} that has flooded into

the muscle will be reuptaken into the SR via the sarco/endoplasmic reticulum Ca^{-2+}-ATPase (SERCA) pump (6).

An important concept in control of muscle contraction is that of a motor unit, which is essentially an α-motorneuron and all the muscle fibers it innervates. Thus, a single α-motorneuron will branch to create a variety of NMJs on several muscle fibers within a muscle. Since a muscle contains 100's to 1000's of muscle fibers, and it will have numerous motor neurons innervating a variety of these fibers. It has long been known that each muscle fiber in a motor unit has the same contractile and metabolic properties (7, 8), and that recruitment occurs based on the size recruitment principal (9, 10).

2.1.3. MUSCLE METABOLISM

Myofibers, like all cell types, rely on multiple metabolic pathways to create the ATP required for contraction and other maintenance events. These are categorized as the phosphocreatine/ creatine kinase (PCr/CK) system, glycolysis, and oxidative phosphorylation (OXPHOS) (Figure 2). The PCr/CK system is primarily responsible for ATP production when there is a high metabolic demand in which ATP breakdown exceeds the ability to be regenerated by the other systems (11). These situations arise at the onset of activity or during high-intensity exercise. Essentially, this metabolic pathway utilized CK to create ATP from free ADP and creatine-bound P_i (PCr) (11). When muscle activity lasts longer than a few seconds, the energy required to regenerate ATP is derived from blood glucose and intramuscular glucose through its breakdown in glycolysis (12, 13). This pathway produces ATP directly, but also produce NADH and pyruvate, which can be utilized in OXPHOS. Typically, OXPHOS is the predominant energy source when muscle activity is prolonged (i.e., running a marathon) at a lower intensity (12, 13). OXPHOS relies on mitochondria, the "powerhouse of the cell", to produce mass quantities of ATP while utilizing

oxygen in the process (Reviewed in Chapter 2.3.1). Importantly, the relative contribution of these metabolic pathways differs based on the level (i.e., high intensity vs low intensity exercise) and duration (short-term vs prolonged) muscular activity, but also based on muscle fiber-type.

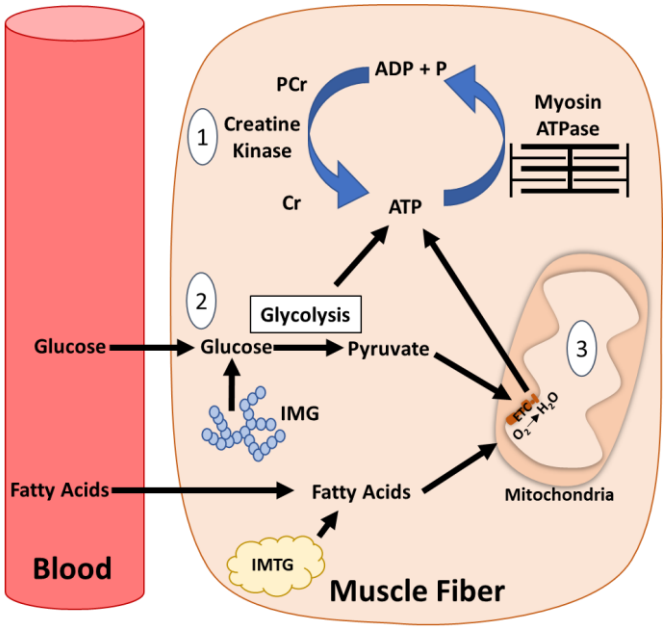

Figure 2. Overview of Metabolism in Skeletal Muscle. During exercise, ATP is hydrolyzed into ADP + P_i by Myosin ATPase during contraction. Three systems will work to regenerate ATP. The first is mediate by the enzyme Creatine Kinase (CK), which will utilize the P_i from Phosphocreatine (PCr) to create ATP, leaving Creatine (Cr) to then be utilized to restore PCr. The second is via glycolysis, in which glucose from the blood or intramuscular glycogen (IMG) it utilized to generate ATP and pyruvate for the final system, which is OXPHOS in the mitochondria. In addition to pyruvate, fatty acids from the blood and intramuscular triglycerides (IMTGs) will be utilized by the mitochondrial electron transport chain (ETC) to create ATP in the presence of oxygen.

2.1.4. MUSCLE FIBER TYPES

Typically, muscle fiber type is categorized based on the innervation they receive, the isoform of the contractile properties they contain (i.e., myosin ATPase isoform), metabolic properties and/or color. Type I (slow and oxidative) fibers have high capillarization to foster nutrient exchange, an abundance of mitochondria to support OXPHOS, slow shortening velocity and easy excitability/recruit ability. Muscles belonging to this group are typically smaller, tonic,

and the most fatigue resistant. Conversely, Type II fibers can be categorized as IIa (fast, oxidative) and IIx (fast-glycolytic). IIa fibers are intermediary of I and IIx. Type IIx fibers have the greatest capacity for force generation due to their size, but they are also the most fatigable due to a low abundance of OXPHOS machinery. Muscle fibers that are IIx require the larges stimulus for motor neuron depolarization, and thus, are only recruited when high levels of force production is required. Interestingly, it has been noted that rodents (i.e., mice and rats), which are typically used in research settings, contain subtle differences in their fiber-type categorizations, containing Type IIb fibers (14).

2.2. The Autophagy-Lysosome System:

2.2.1. OVERVIEW OF THE AUTOPHAGY PATHWAY

The literal definition of autophagy is self (auto) eat (phagy) in Greek, coined by Dr. Christian de Duve in the 1960s. Although discovered in the 1950s most of the seminal work in the autophagy field began when Dr. Dr. Yoshinori Oshumi studied the regulation of this process in yeast in the 1990s (15, 16), for which he won the 2016 Nobel Prize in Physiology or Medicine. Specifically, Dr. Oshumi's group were the first to identify autophagy-related genes (Atg), and the field rapidly evolved shortly thereafter (17).

Typically, autophagy is categorized as either 1) the non-selective process in which small cytoplasmic proteins are internalized into the lysosome via membrane invaginations, termed microautophagy (18); 2) chaperone mediated autophagy (CMA) the selective process that requires heat shock conjugate 70 protein (Hsc70) to bind to soluble proteins, and transport them to the lysosome-associated membrane protein (Lamp) type 2A receptor on lysosomes (19); or 3)

macroautophagy, the bulk degradation of macromolecules, protein aggregates and organelles. Although distinct, all are complete with the delivery of cargo to the lysosome.

Autophagy is a major catabolic system within the cell, principally responsible for the selective degradation of long-lived proteins, protein aggregates, macromolecules and organelles via lysosomes (20). Although paradoxical in nature, this highly conserved process is protective in cells, aiding in the removal of damaged cellular components (i.e., macromolecules and organelles), and liberating their constituents for cellular processes (i.e., energy metabolism and biosynthesis). In steady state conditions, autophagy is continually ongoing. Importantly, autophagic breakdown is essential for the maintenance of cell health through the removal of damaged or dysfunctional cellular components, such as mitochondria via mitophagy. In skeletal muscle, inhibition of autophagy elicits atrophy, perturbations in sarcomere structure, neuromuscular junction decay, and weakness (21–25). Furthermore, a hallmark of various myopathies aberrant autophagy (26–32). Cumulatively, these findings highlight the importance of understanding the processes that govern this proteolytic system in skeletal muscle tissue.

2.2.2. TRANSCRIPTIONAL CONTROL OF AUTOPHAGY

Gene expression of the autophagy-lysosome system is primarily mediated by two groups of transcription factors. The first is the forkhead box O (FoxO) family of transcription factors. Of the numerous FoxO isoforms (i.e., 1, 3, 4 and 6), FoxO3 is the most understood and studied in the context of skeletal muscle. Early studies demonstrated that 1) FoxO3 overexpression *in vitro*, 2) activation via mutagenesis and 3) activation in response to nutrient depravation *in vivo* induces atrogin-1, an E3-ubiquitin ligase, expression thereby promoting muscle atrophy through upregulation of the ubiquitin-proteasome pathway (33). The complexity of FoxO3 in inducing muscle atrophy was uncovered shortly thereafter, whereby two subsequent studies demonstrated

that FoxO3 promotes the expression of both proteasome- and autophagy-related genes, leading to muscle atrophy (34, 35). Furthermore, FoxO3 promotes mitophagy through Bcl3 and adenovirus E1b 19-kDa-interacting protein 3 (Bnip3) and Bnip3-like (Nix) gene expression (35). In fact, blunted FoxO3 activity prevents stimulus-induced atrophy of muscle fibers through perturbations in both proteasomal and autophagic pathways (33, 36–43). Although FoxO3 is the most well-characterized, other FoxO family members have been shown to act in a similar manner within muscle (44), but the vitality of these in the regulation of autophagy is not fully elucidated.

The second class of transcription factors that is integral in the activation of the autophagic genetic program are members of the MiTE/TFE family, specifically Tfeb and Tfe3. A series of intricate studies performed by the groups of Andrea Ballabio and Rosa Puertollano helped to identify these transcription factors and their mechanism of action (45–49). Functionally, Tfeb and Tfe3 homodimerize and/or heterodimerize to interact with E-box and M-box elements in promoters (45, 50, 51) and regulate the expression of both lysosome and autophagy-related genes via their ability to activate the coordinated lysosome enhancement and regulation (CLEAR) network of genes (45–49). Although the work in skeletal muscle is limited, studies are beginning to explore these transcription factors in muscle physiology and pathophysiology. Uniquely, Tfeb can promote mitochondrial biogenesis in muscles, and the absence of Tfeb limits muscular endurance, which may be autophagy-independent (52). However, more work is required to understand this phenomenon and to determine if Tfe3 acts in a similar manner within muscle.

2.2.3. AUTOPHAGY: FROM ACTIVATION TO EXECUTION

The process of macroautophagy, herein referred to autophagy, can be broken down into a series of steps, including initiation/activation, nucleation, elongation/maturation, transport, fusion with lysosomes, and degradation (Figure 3). Although not fully characterized in muscle, the

information provided below serves as a framework, which has been utilized to study autophagy in this organ system.

Autophagy begins with the induction of a pre-autophagosomal structure, mediated by the Ulk1 complex containing the yeast *Atg1* homolog unc-51-like kinase (Ulk1), family-interacting protein 200kDa (FIP200), Atg13 and Atg101, which are integral in complex stabilization and function (53–58). For example, Atg101 prevents Atg13 and Ulk1 proteasomal breakdown through phosphorylation. Ulk1 functions as a serine/threonine kinase, the activity of which is negatively regulated by the mammalian target of rapamycin complex 1 (mTORC1), and positively regulated by AMP-activated protein kinase (AMPK) in both direct and indirect mechanisms (59–61). As such, the induction of autophagy is tightly controlled based on cellular demands, as discussed further below. The utility of Ulk1, and its isoform, Ulk2, in muscle have recently been demonstrated, whereby their deletion perturbs autophagy flux and promotes muscular weakness (62, 63).

Activated Ulk1 stimulates the class III PI3K Complex I (PI3KC3-C1), which consists of vacuolar sorting proteins (Vps) 15 and 34, Atg14, Beclin1 and Ambra1 (64–66) to promote nucleation of the autophagosomal membrane. Specifically, the Ulk1 complex will enhance the lipid kinase activity of Vps34 through phosphorylation (67) leading to the production of the phospholipid phosphatidylinositol-3-phosphate [PI(3)P], which is utilized in the nucleation of autophagosomal membranes. This occurs whilst Ulk1-mediated phosphorylation of Beclin1 (67, 68) and Ambra1 (64) help release the complex from the cytoskeleton for successful activity. At the present time, the source of this phagophore membrane is unknown, however there is evidence suggesting that it may originate from a variety of organelles and could differ in response to the cell the type and physiological conditions that active autophagy (69). More work is required to

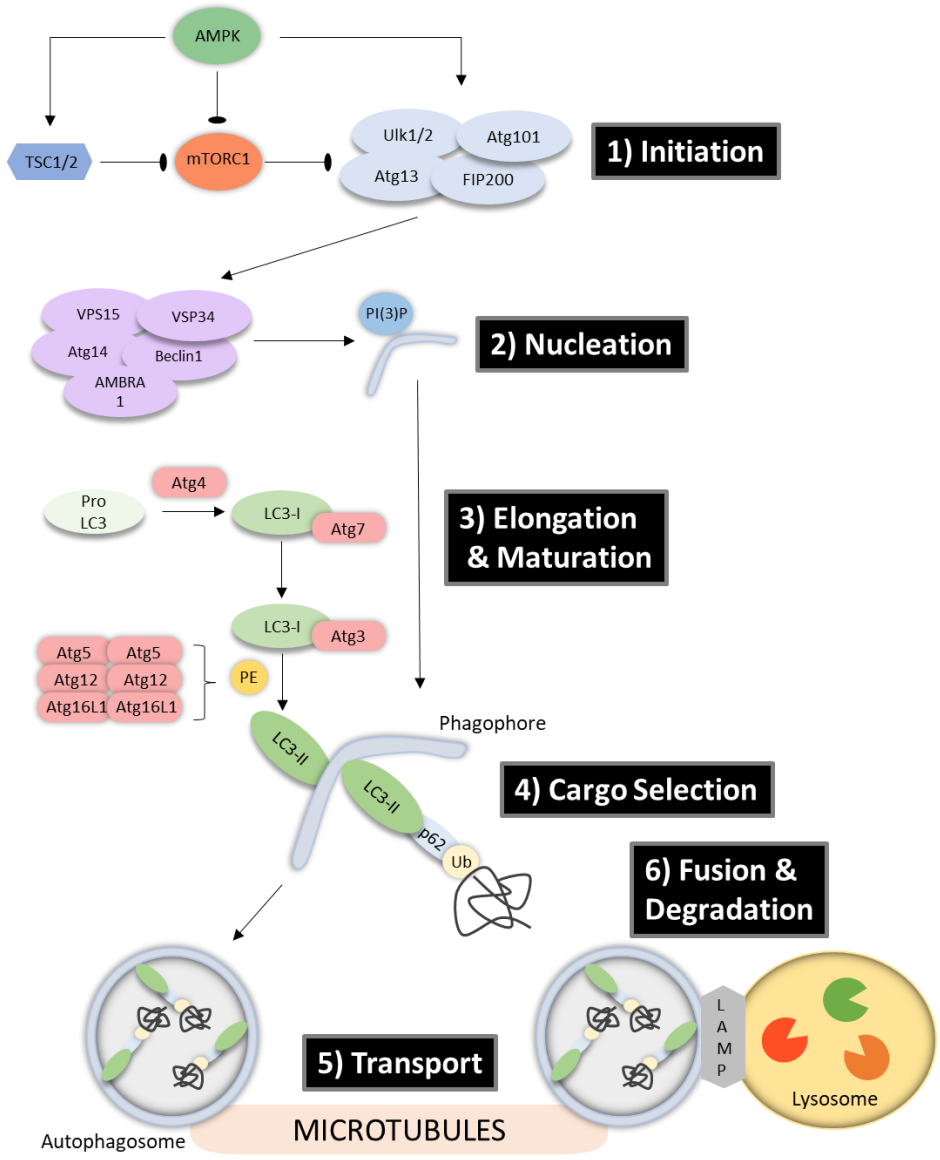

Figure 3. Overview of the autophagy pathway. 1) Initiation of autophagy occurs during times of cellular stress. As such, AMPK is activated and can inhibit mTORC1 to suppress its inhibitory role on Ulk1 activity and autophagy. Furthermore, AMPK can directly phosphorylate Ulk1, thereby activating it. Functional Ulk1 can then phosphorylate and mobilize the **2)** Nucleation complex, to create PI(3)P and begin the process of forming the phagophore, which will act as a scaffold for the mature autophagosome. **3)** Maturation and elongation of the phagophore occurs through a series of conjugation reactions. Firstly, Atg4 creates LC3-I from pro-LC3. LC3-I is the processed by Atg7 and Atg3. The Atg5-12-16L1 complex is created through its own conjugation reactions and acts to assist in the addition of PE to LC3-I to create mature, autophagosomal LC3-II. **4)** As the membrane expands, cargo will be selected via the interaction of adaptor proteins with autophagosomal LC3-II. **5)** Once autophagosomes are formed, they will transport to the lysosomes, where the **6)** membranes will fuse and degradation will take place.

determine the membrane origin of autophagosomes in muscle. In addition, Atg9 rich membranes, originating from intracellular vesicles, are thought to donate lipids to promote further nucleation and expansion of the phagophore (69, 70). Expansion of the phagophore subsequently occurs through two ubiquitin-like conjugation systems. The first is mediated through the Atg12-Atg5-Atg16L1complex. This complex is formed by E1-activating enzyme Atg7 and E2-conjugating enzyme Atg10, which work to link Atg12 to Atg5, which, when dimerized will recruit Atg16L1 (71). This complex will then dimerize with an identical complex, which is essential for activating late-steps in the second conjugation system. The second conjugation system involves the conversion of yeast *Atg 8* homolog, pro-microtubule-associated proteins 1A/1B light chain 3 (LC3) into its lipidated form LC3-I and subsequently its active, autophagosome embedded form, LC3-II. This begins with Atg4-mediated cleavage of pro-LC3 into LC3-I. Subsequently, Atg7, as an E1-like enzyme, will activate and transfer LC3-I to the E2-like enzyme Atg3, where it will be conjugated to phosphatidylethanolamine (PE) by the initial Atg-12-5-16L1 complex (71, 72). LC3-II will then embed itself in the autophagosomal membrane, where it contributes to expansion of the structure, acts as a receptor for cargo selection, and a marker for autophagosome membrane (73, 74). Both gamma-aminobutyric acid receptor-associated protein (GABARAP), and Golgi-associated ATPase enhancer of 16kDa (GATE16) follow a similar mechanism of conjugation and play a role in autophagosome maturation like LC3 (73, 74). There is controversary in the muscle literature whereby some believe that slow muscle has a great abundance of autophagosomes and autophagic breakdown (75), whereas others believe the opposite (76, 77) in a basal state. However, these studies unanimously show that in response to exercise and starvation, fast muscle has a greater induction of autophagic breakdown (75–77).

As the autophagosome begins to mature, cargo selection will begin to take place. This process is highly selective and can be ubiquitin (Ub) -dependent or -independent, ultimately working to tether digestible components to the autophagosome (78–80). As the name suggests, Ub-dependent autophagy relies on the presence of a Ub chains on proteins, followed by the tethering of these proteins to autophagosomal embedded LC3-like proteins via a receptor. In ubiquitin-independent autophagy, autophagy receptors recognize cellular constituents such as proteins, lipids, and sugars directly. Such receptors include p62 (Sqstm1) (81), neighbor of BRCA1 gene 1 (NBR1) (82), Optineurin (OPTN) (83, 84), and Toll-interacting protein (Tollip) (85). Uniquely, these receptors possess both Ub-binding domains (UBD) and LC3- interacting regions (LIR) allowing for the selective degradation of various intracellular components (86, 87).

Once closure of the autophagosome occurs and its constituents are engulfed, the structure is destined for transport to the lysosomes. Movement of autophagosomes is via microtubule tracts and microtubule associated motor proteins (88, 89). This process is not well studied, especially in the context of skeletal muscle. However, it has been demonstrated that treatment with colchicine, a microtubule destabilizer, prevents autophagic vesicles from reaching the lysosome, and thus debris accumulates within the cell (90, 91), highlighting the importance of autophagosomal transport in the autophagy-lysosome system. Once delivered to the lysosome, the membranes of the two compartments will fuse, forming an autolysosome. This has vaguely been characterized in mammalian cells, but Ras-related protein 7 (Rab7) is responsible for tethering autophagosomes to microtubule motor proteins, whereas SNARE proteins are thought to be responsible for fusion events at the lysosome membrane in conjunction with Lamp proteins (88).

Degradation will take place then take place at the lysosomes, highly acid organelles that contain an abundance of proteins to aid in the breakdown of autophagic substrates. Maintenance

of the proper pH (4.5-5.0) is integral for the functioning of these organelles, and vacuolar-type H+-ATPase (v-ATPase) is primarily responsible for this (92). It should be noted that there is an evolving understanding of acidification mechanisms that suggest other players involved (92). Integral lysosomal membrane proteins (Lmp), lysosome associated membrane proteins (Lamp) and lysosomal hydrolases make up the lysosome (i.e. proteases, glycosidases, lipases, and nucleases) (93, 94). This heterogeneity allows for the digestion of and array of intracellular compounds into their basic constituents. Typically thought of as the digestive organelle, an abundance of literature has implicated the lysosomes as a significant component in the monitoring and subsequent response to changes in the cellular milieu. For example, lysosomes are sensitive to changes in nutrient and amino acid availability, discussed briefly below (94, 95). Furthermore, lysosomes are important in organellar communication, for example, between them and the mitochondria (96–98), but more work is required to understand this phenomenon in skeletal muscle.

Lysosomal membranes are generated via the endocytotic pathway, whereby internalized vesicles are delivered to early endosomes and subsequently late endosomes. These late endosomes will then receive enzymes and membrane proteins from the Golgi, to help establish the lysosome milieu (93, 94). This occurs concurrently with the production of lysosomal proteins, through the activation by Tfeb/Tfe3, as discussed earlier. Importantly, to ensure enzyme stability of these proteins, they are processed by the *trans*-golgi network (TGN) prior to their incorporation in the lysosome. Alternatively, some proteins make their way to lysosomes through secretion and re-uptake via endocytosis (93, 99).

2.2.4. ACTIVATION OF THE AUTOPHAGY-LYSOSOME SYSTEM

Sensing of the cellular milieu is required to enhance the expression autophagic and lysosome related genetic programs and active the process. As such, FoxO3, Tfeb, Tfe3, and Ulk1 undergo a serious of post-translational modifications (PTMs) which serve to coordinate this process (Summarized in Figure 4). As transcription factors, PTMs on FoxO3 and Tfeb/3 regulate their nuclear localization and activity, whereas PTMs on Ulk1 dictate relative activity in upstream autophagy induction. It is important to keep in mind that Ulk1 is furthest upstream in the pathway and thus more work is required to determine how other modifications within the autophagy pathway dictate the systems functional capacity.

Under homeostatic conditions, FoxO3, Tfeb and Tfe3 remain primarily localized within the cytosol due to an intricate network of repressing PTMs. Specifically, AKT, which is active in fed states, promotes FoxO3 cytosolic localization via phosphorylation on a variety of residues (Thr32, Ser352, Ser315) (100). It was also recently shown that AKT represses Tfeb via phosphorylation (101), a mechanism which may also serve to inhibit Tfe3 as well. Furthermore, mTORC1, positioned downstream, is localized to the lysosome, where it acts to phosphorylate Tfeb on Ser211 (102) and Tfe3 on Ser321 (47), promoting the interaction of these proteins with 14-3-3 in the cytosolic compartment, rendering them inactive (47, 102–104). mTORC1 also acts as an inhibitor of Ulk1 though direct interactions and phosphorylation (105).

AMPK has been identified as a potent activator of FoxO3 (100, 106, 107), Tfeb and Tfe3 (108) through localization independent mechanisms. Additionally, AMPK acts to promote Ulk1 activity (107, 109). Thus, in a homeostatic milieu, whereby AMPK activity is low, its ability to active FoxO3, Tfeb and Ulk1-complex via phosphorylation is minimal. In contrast, under energy-stress, AMPK is active and enhances FoxO3 (100, 106, 107) and Tfeb (108) function, promoting the

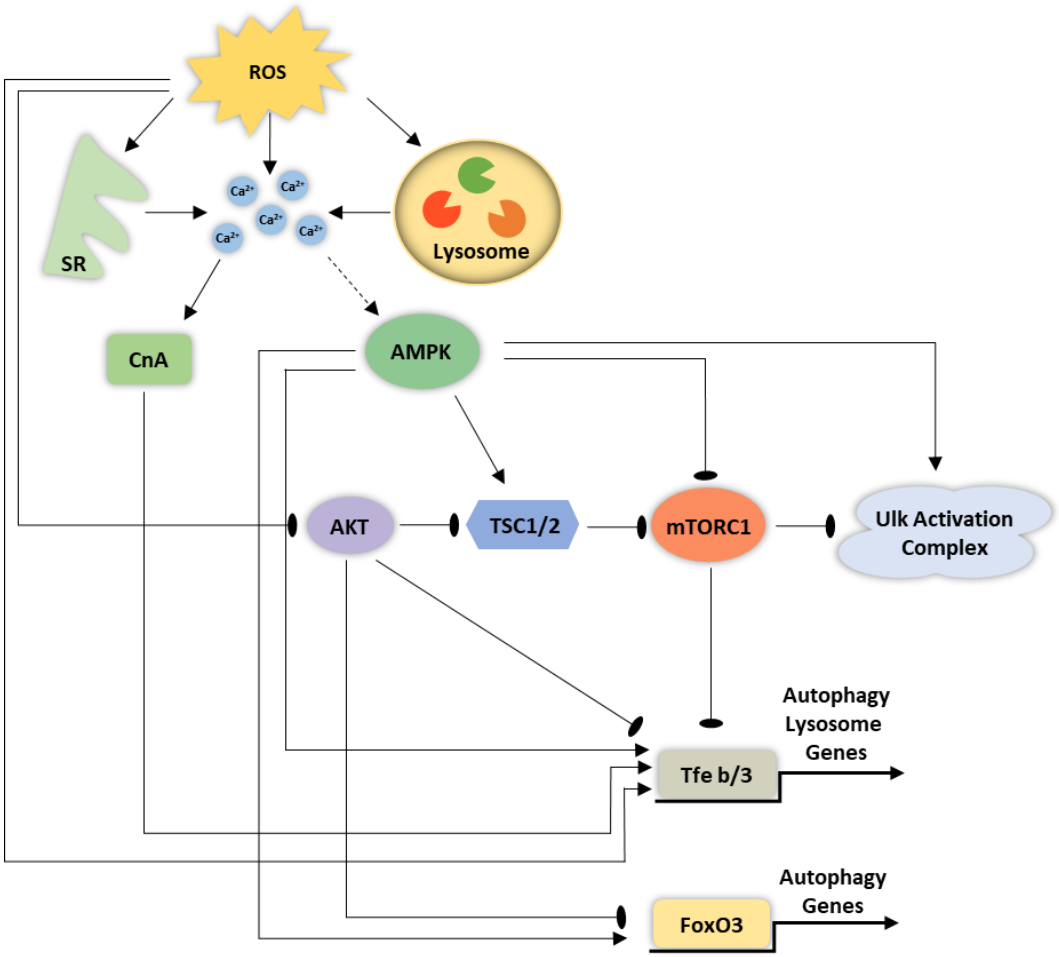

Figure 4. Coordination of the Autophagy-Lysosome System. Proposed coordination of pathways that regulate the autophagy-lysosome System (ALS). ROS and cytosolic calcium ($[Ca2+]_{IC}$) act as upstream signaling mechanisms that converge on the gene expression and protein activation of the ALS. AMPK is activated directly via compromised energy status (increase AMP:ADP), and indirectly through $[Ca2+]_{IC}$ via CaMKII (not shown). Elevated $[Ca2+]_{IC}$ may occur due to the damaging effects of elevated ROS on the sarcoplasmic reticulum and lysosomes. AMPK synchronously activates FoxO3, Tfeb and Tfe3 (Tfeb/3) through (1) direct phosphorylation of FoxO3, (2) activation of TSC1/2 and (3) inhibition of mTORC1. Simultaneously, AMPK activates autophagy induction through the Ulk1 complex and by alleviating mTORC1 inhibition on this complex. In a similar cellular milieu, FoxO3 repression is alleviated via AKT inhibition. Increases in $[Ca2+]_{IC}$ activate the phosphatase CnA, which activates Tfeb/3. ROS also activate Tfeb/3 through oxidation, an added layer of coordination in this autophagy-lysosome system.

expression of autophagy-related genes. Similarly, AMPK elevates Ulk1-complex activation, and therefore autophagy initiation (107, 109). AMPK also represses mTORC1 activity both directly though phosphorylation, and indirectly through the activation of the mTORC1 inhibitor Tsc1/2 (110).

In the context of skeletal muscle, the interplay of AMPK and mTORC1 has been investigated. First, Tsc1 deletion blocks autophagy induction, and promotes muscle atrophy which can be prevented via mTORC1 inhibition with rapamycin (111). This finding highlights the importance of mTORC1 in repressing autophagic induction in muscle. Furthermore, genetic deletion of AMPK leads to an attenuation of atrophy in disuse models (112, 113) which is, at least in part, due to a failure to induce autophagy, amongst other things.

The activity of the autophagy lysosome system is also coordinatively regulated by a variety of intracellular cues. For example, reactive oxygen species (ROS) and Calcium (Ca^{2+}) are both though to activate autophagic pathways. Specifically, in muscle it has been reported that ROS activate AMPK (114) and may thereby enhance FoxO3, Tfeb, Tfe3 and Ulk1 activity. ROS have also been shown to inhibit AKT signaling pathways (115, 116) and thus ultimately mTORC1. This in theory would alleviate its suppression on Ulk1 and FoxO3, further promoting autophagic induction. The role of ROS in the regulation of lysosome biosynthesis has also recently been uncovered, whereby ROS can oxidize Tfeb on Cys212 and Tfe3 on Cys322, triggering their nuclear localization in muscle cells (117). Furthermore, ROS are capable of oxidizing lysosomal transient receptor potential mucolipin 1 (Trpml1) on lysosomes (118) and ryanodine receptors (RyR) on the SR (119), which evokes Ca^{2+} release and elevations in intracellular calcium ($[Ca^{2+}]_{IC}$) facilitating crosstalk between Ca^{2+} signaling networks. $[Ca^{2+}]_{IC,}$ a potent activator of CAMKKβ, which can activate AMPK and may in-turn act on Ulk1, FoxO3 and Tfeb/3. Importantly, $[Ca^{2+}]_{IC}$

activates the phosphatase calcineurin (CnA), which dephosphorylated Tfeb (120) and Tfe3 (121), thereby allowing for its nuclear localization and function.

2.2.5. MEASUREMENTS OF AUTOPHAGY

Autophagy is a dynamic process, with substrates being tagged and degraded consistently. Thus, measuring changes in the breakdown of autophagosomal substrates is a challenge, especially in-vivo. This challenge holds true in skeletal muscle as well. Since LC3-II and p62, amongst other adaptor proteins, are found embedded in the autophagosome, their protein levels are commonly reported to assess autophagy. If considered in conjunction with mRNA levels of these genes, an inference of autophagic breakdown can be made. Furthermore, using microscopic analysis, an increase in autophagy-puncta (i.e., LC3) or the colocalization of autophagosomal components and lysosomes have also been used to assess autophagy. Unfortunately, these snapshot measures fail to fully encapsulate the dynamic autophagic process, and only capture markers of autophagosomal number. For example, an increased number of autophagosomes could suggest increased autophagy flux or an accumulation of undigested ones. Similarly, a decrease in autophagosomes could suggest enhanced flux, as they could be degraded at a high rate.

Over the past decade methods have been developed to assess autophagy flux more accurately, both *in-vitro* and *in-vivo*. Based on the premise that Atg-8 related family members (LC3-II, Gabarap etc…) and adaptor proteins are embedded in autophagosomal membranes and degraded when membranes fuse, measurement of these proteins in a "blocked" condition, in comparison to a "normal" condition, can produce an interpretation of "flux" (Figure 5, A). Thus, two widely used method consist of either 1) pharmacologically blocking autophagosome-lysosome fusion, such as with the microtubule destabilizer colchicine or the agent bafilomycin A, or 2) inhibiting lysosome activity, such as with leupeptin or pepstatin A (90, 122, 123). Such

methodologies come with limitations, such as off-target effects of these compounds on tissue physiology. Thus, assays utilizing autophagy reporters have become increasingly common (124). One such way to do is through dual/tandem fluorophore, such as with the mCherry-GFP-LC3 (125) or mRFP-GFP-LC3 (126–128) constructs. These allow for the simultaneous assessment of autophagosomes and autolysosomes (Figure 5, B). In these models, the RFP is resistant to lysosomal digestion, and thus pure-red puncta represent autolysosomes, whereas yellow/orange puncta represent autophagosomes. Most recently, pH sensitive probes have been developed to assess autophagy flux. One such example is Keima, a coral-derived fluorophore which fluoresces differentially when exposed to the neutral pH of the cytosol (green) vs that of the acidic lysosome (red), when excited at their associated wavelengths (129) (Figure 5, C). This has been adapted and developed into a mitochondrial specific probe, termed mt-Keima, through fusion to the COX VIII subunit (130, 131). Further utilization of such models will be essential to further elucidate the mechanisms of autophagy in skeletal muscle.

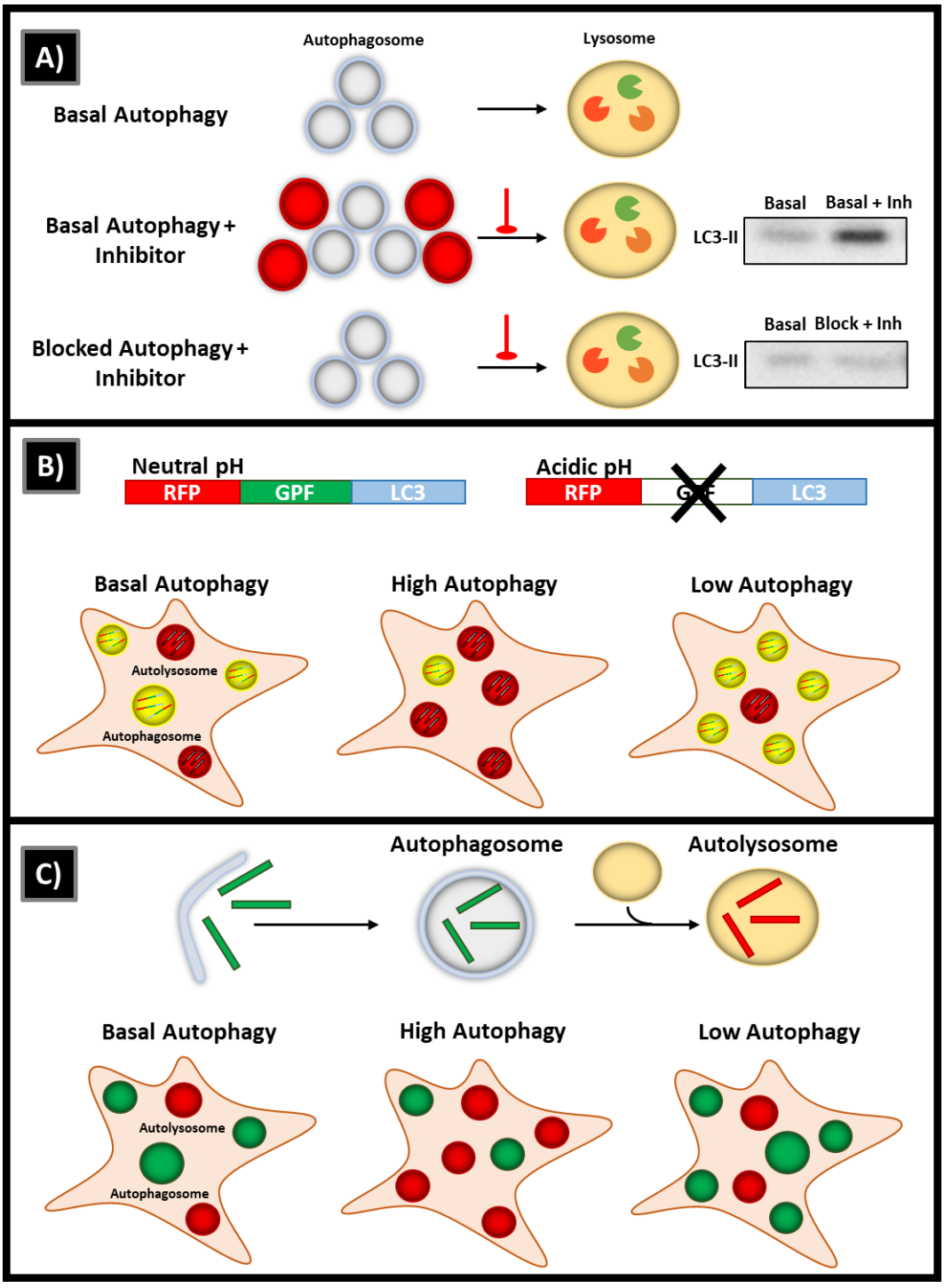

Figure 5: Methodologies in Assessing Autophagy Flux. Measuring autophagy via A) pathway inhibition; B) RFP-GFP tandem tagged LC3; and C) pH sensitive fluorophores. See text for details.

2.3. Mitochondria in Skeletal Muscle:

2.3.1 MITOCHONDRIAL STRUCTURE AND FUNCTION

Mitochondria are organelles that are primarily responsible for energy provision through the electron transport chain (ETC). These organelles also play an essential role within muscle through the production of reactive oxygen species (ROS), in Ca^{2+} handling (132), and in apoptotic signaling. Typically, mitochondrial content within a cell is determined based on the metabolic needs of the tissue. For example, within cardiac muscle, a highly oxidative organ that is consistently requiring ATP, 30% of cell volume is consumed by mitochondria (133). Comparatively, mitochondrial content in skeletal muscle is low, making up approximately 2 to 7% of muscle cell volume, depending on the fiber-type of the muscle (134–136). Just as muscle is said to exhibit plasticity, so do the mitochondria within it, whereby they adapt to the changing energy demands within the tissue, such as with exercise or inactivity (discussed below in more detail).

Mitochondria are composed of two separate compartments, bordered by two lipid membranes (Figure 6). The outer mitochondrial matrix (OMM) creates a boundary between the cytoplasm and the internal portion of the organelle and contains protein import machinery termed translocate of the outer membrane (TOM). These allow for the entry of nuclear genomic products (discussed below). Within the confinement of the OMM is the intermembrane space (IMS), which encloses on the mitochondrial matrix via the inner mitochondrial membrane (IMM). The matrix contains an abundance of enzymes for the TCA/Krebs' cycle, which provide cofactors for the ETC to create energy (discussed below).

Within skeletal muscle, mitochondria exist in two discrete locations. These geographic populations of mitochondria were discovered in the 1980s, however, with modern microscopy

techniques, these organelle populations are being further characterized. The mitochondria that reside underneath the sarcolemma, termed subsarcolemmal (SS) mitochondria, provide energy for membrane and nuclear events (137–140), and lie in close proximity to capillaries for nutrient exchange (141). Conversely, intermyofibrillar mitochondria (IMF), which provide energy to fuel contraction, reside intertwined in a reticular network surrounding the myofibrils (139, 140, 142, 143). Importantly, these subpopulations of mitochondria have distinct structural and biochemical properties whereby, SS have higher membrane potential (144) and ROS emission (145) and IMF have greater respiration (145, 146), protein import rates (147), protein synthesis (145), and OXPHOS-related proteins (148). The following subsections will highlight the various roles of mitochondria within cells, skeletal muscle included.

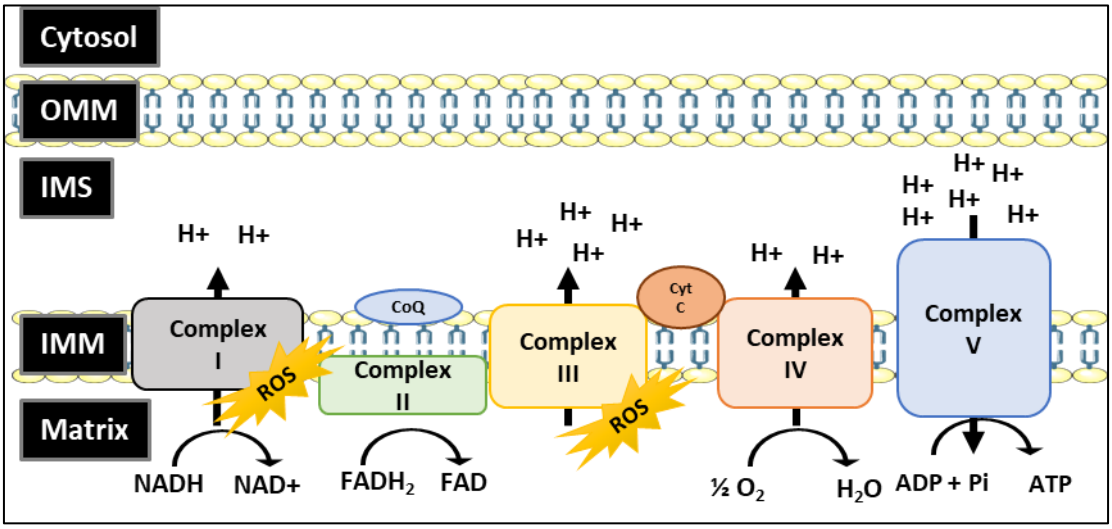

Figure 6. Schematic of the Electron Transport Chain (ETC). The process of OXPHOS begins with the oxidation of the cofactor NADH at Complex I and $FADH_2$ at Complex II. These oxidation reactions lead to electron transfer from Complex I and II to a carrier molecule, coenzyme Q (CoQ), which will subsequently shuttle the electrons to Complex III, Cytochrome C (CytoC) and ultimately Complex IV. The electrons accepted by Complex IV reduce oxygen into water (H_2O). The shuttling of electrons is coupled to the transfer of protons (H+) from the Matrix to the IMS. This creates a membrane potential, which will be dissipated through Complex V in the presence of ADP and Phosphate (P_i), and ultimately fuel the production of ATP. Complex I and III are considered the primary sites of reactive oxygen species production (ROS), as electrons "leak" and react with O_2 to produce superoxide (O_2^-).

2.3.1.1. Mitochondrial Respiration

Energy production within mitochondria begins within the matrix, which houses the Krebs/TCA cycle enzymes. The process initiates, when acetyl coenzyme A is produced, in the mitochondria, as a byproduct of macromolecule breakdown. This two-carbon molecule will fuel a series of intricate TCA cycle reactions to not only create a small amount of ATP, but to also produce cofactors required for the ETC (Figure 6). These cofactors, nicotinamide adenine dinucleotide (NAD) and flavin adenine dinucleotide (FAD), are reduced into NADH and $FADH_2$, respectively. Complex I of the ETC (NADH Dehydrogenase) oxidizes NADH into NAD^+, gaining an electron, whilst simultaneously pumping a proton (H^+) across to the IMS. This electron will ultimately be shuttled to Complex III (Cytochrome bc_1 complex) via Coenzyme Q. $FADH_2$ is oxidized at Complex II (Succinate Dehydrogenase), whereby the liberated electrons are also transferred to Complex III. The subsequent transfer of these electrons to Complex IV (Cytochrome C Oxidase) via Cytochrome C will also drive H^+ into the IMS. At Complex IV, the terminal electron acceptor, oxygen is reduced to water, which will also promote the shuttling of H^+ into the IMS. Thus, since O_2 consumption is proportional to ETC activity it is utilized a measure of ETC/mitochondrial function (149–151). This shunting of H^+ into the IMS generates a membrane potential between the IMS and the matrix. To dissipate this gradient H+ flow towards the matrix through Complex V (ATP Synthase), and the energy of transport fuels the production of ATP from its precursors, ADP and P_i.

2.3.1.2. Mitochondrial Reactive Oxygen Species

Unfortunately, this process of ATP production at the ETC is not flawless. In fact, a natural biproduct of this system is the production of ROS. This occurs via electrons that “slip” from the ETC followed by their subsequent transfer to oxygen (152). This is thought to occur mainly at

Complex I and Complex III of the ETC (153). Ultimately, this reduced O_2 creates a highly reactive species $O2^{\bullet-}$, which is damaging to lipid membranes and proteins. ROS production is determined by the activity of these organelles. In isolated mitochondria, basal respiration (State IV), the absence of ADP creates less need for electron transport through OXPHOS. This creates a backflow of electrons that can react to form $O2^{\bullet-}$, and per O_2 being consumed, ROS production is high. Supply of ADP to isolated mitochondria (active respiration, State III) increases absolute ROS production, simply as byproduct of more flux through the system. However, mitochondria in these states are far more efficient, and thus per O_2 consumed, these is less ROS production.

Luckily, mitochondria contain innate antioxidant enzymes, such as manganese superoxide dismutase (MnSOD), which catalyzes the conversion of $O2^{\bullet-}$ to O_2 and hydrogen peroxide (H_2O_2) (154), and due to its ability to permeate membranes, can function as a signaling molecule (155, 156). Although historically thought of as damaging to cells via their membrane, protein and DNA damaging effects, in moderation, ROS can act as a signaling molecule (157, 158). As is the case in muscle with physical exercise, whereby there is evidence that antioxidant supplementation may impair the adaptive potential of the tissue (159). Thus, it is evident that ROS, within reasonable limits, can be beneficial, yet sustained ROS production, from the mitochondria or elsewhere can be damaging and promote aging (160).

2.3.1.3. Cell Death via Apoptosis

While mitochondria provide energy, they are also regulators of apoptosis, which is a form of programmed cell death. Although the intricacies of this process are outside of the scope of this thesis, the concept is an important one, especially in the context of aging and denervation in skeletal muscle, as discussed in the appropriate sections. Mitochondria house proteins such as cytochrome c, apoptosis-inducing factor (AIF) and endonuclease G (Endo G). Briefly, when

mitochondria become dysfunctional, the mitochondrial permeability transition pore (mtPTP) in the OMM will reconfigure to become "open". This will allow for the entry of water, causing organelle swelling and the subsequent release of these proteins from the mitochondria to the cytosol. In the cytosol, these proteins trigger a series of caspase-dependent or caspase-independent events, which ultimately lead to the fragmentation of DNA and cell death (161). However, since myocytes are multi-nucleated, the result of these apoptotic events are quite unique, whereby they lead to the loss of a population of nuclei, that may lead to less gene-expression capability in the local region. This is hypothesized to ultimately promote atrophy in the local environment (162, 163), however there is some controversy in this (164).

2.3.2. MITOCHONDRIAL LIFE CYCLE

Mitochondrial content and function within muscle are depends on organellar turnover. This process is dictated by the balance between the synthesis of new, health mitochondrial organelles via biogenesis, and the recycling of damaged or dysfunction mitochondria through a specific form of autophagy, termed mitophagy. These ongoing processes ensure that the mitochondrial reticulum within muscle is producing ATP and generating ROS at sufficient levels to maintain tissue homeostasis. Under steady-state conditions, this removal process is balanced by an equal rate of synthesis, or biogenesis, such that mitochondrial content within the cell remains unchanged. However, an imbalance in these processes can have wide-spread ramifications on the metabolic and functional health of the muscle, as seen with aging and prolonged periods of inactivity (165–167). The goal of this section is to summarize the basic principles that govern mitochondrial content and network formation, which has implications in skeletal muscle aging and disuse, topics covered later in this thesis.

2.3.2.1. Mitochondrial Dynamics: Fusion and Fission

Skeletal muscle mitochondria exist in a reticular network, which optimize the metabolic capacity of the tissue (168, 169). Furthermore, mitochondria are dynamic organelles that undergo constant remodeling. Network formation and expansion is mediated by fusion of existing mitochondrial membranes, which is under the control of the proteins mitofusin 1/2 (Mfn1/2) and optic atrophy protein 1 (Opa1) (170). However, segments of the network often become dysfunction, and the removal of these segments is through mitochondrial fission (171). This is controlled through a series of events, mediated by dynamin-related protein 1 (Drp1), mitochondrial fission protein 1 (Fis1), mitochondrial fission factor (Mff), and mitochondrial dynamics proteins of 49 and 51 kDa (MiD49/51) (170). This fission of poorly functioning mitochondrial segments primes the sequestered organelle for degradation in mitophagy(172, 173).

Maintaining this balance between fusion and fission is necessary in skeletal muscle. To uncover the essential nature of mitochondrial dynamics in skeletal muscle biology, a series of studies were conducted to examine the impact of 1) the merit of creating a greater reticular network in muscle to enhance metabolic capabilities and 2) the vitality of generating a more fragmented mitochondrial pool to accelerate mitophagy with aims of enhancing of mitochondrial quality in muscle. Of the major findings, knockout of Fis1 in adult mice, created a more reticular network. But contrary to the expected, this deletion impaired mitochondrial function and perturbed mitophagy (174). Very recently, both the groups of Dr. Gouspillou and Dr. Sandri showed that knockdown of the other pro-fission protein, Drp1, impaired mitochondrial health, autophagy and ultimately led to significant muscle fiber denervation and thus atrophy (175, 176). Thus, creating a more reticular mitochondrial network is not feasible to enhance the tissues functionality. In contrast creating a more fragmented mitochondrial pool, through the overexpression of both Fis1

and Drp1 promoted atrophy (177). Similar results were seen when creating a more fragmented mitochondrial pool through Mfn2 (178, 179) and Opa1 deletion (180). In combination, these results suggest that a balance of fusion and fission is required to maintain a healthy mitochondrial pool, which has implications for muscle health.

2.3.2.2. Mitochondrial Biogenesis: Signaling Mechanisms

Each mitochondrion possesses numerous copies of its own circular DNA (mtDNA), which is approximately 16.5 kb in size (181). However, of the approximately 1200 proteins found within the mitochondria, only 37 genes, 13 of which are proteins are encoded by the mitochondrial genome (182). The remaining proteins within the organelle are transcribed from nuclear genes encoding mitochondrial proteins (NuGEMPs). Thus, mitochondria are created through an intricate process that requires the coordination of both the nuclear and mitochondrial genomes. This process, in addition to import of NuGEMPs into mitochondria and fusion of mitochondrial membranes, is a prerequisite to enlargement of the organellar network. In muscle, this would favor oxidative metabolism and enhance endurance capacity.

At the level of the nuclear genome, many transcription factors are required to contribute to NUGEMP expression. These include nuclear respiratory factors 1 and 2 (NRF-1/2), peroxisome proliferator-activated receptor (PPAR) family members (α, β, γ) and estrogen-related receptor (ERR) family members (α, β, γ) (183–186). Proteins that are generated via the action of these transcription factors are then imported into mitochondria. Perhaps the largest discovery was that of the cold-inducible protein, peroxisome proliferator-activated receptor gamma coactivator 1 alpha (PGC-1α) (187). As a transcriptional co-activator, PGC-1a activates the previously mentioned transcription factors. Both over-expression (188, 189) and knockdown (190–194)

studies have shown that PGC1-α is a critical upstream regulator of the muscle oxidative phenotype. Importantly, activation of PGC-1α, and ultimately mitochondrial biogenesis, occurs in response to a variety of stimuli, many of which are induced with endurance style exercise (195, 196), as discussed in more detail below.

A group of critical NuGEMPs help coordinate the two genomes include are transcription factor A of the mitochondria (Tfam) (197), mitochondrial RNA polymerase (POLRMT) and mitochondrial transcription factors B1 and B2 (TFB1/2M) (198, 199). These function in mtDNA transcription and replication (198, 199). Tfam has been studied extensively in muscle biology. Briefly, Tfam contains a high-mobility group domain, which can induce a U-turn confirmation of mtDNA fostering the recruitment of TFB2M and POLRMT to the H and L promoters of mtDNA, thereby promoting transcription of mtDNA-regulated genes (200, 201). As expected, Tfam transcript, protein, and mitochondrial import are enhanced when mitochondrial biosynthesis pathways are stimulated in muscle (202–206). The tumor suppressor p53 is another coordinator of the two genomes, acting as a transcription factor in both the nuclear and mitochondrial genomes. It also functions, in conjunction with Tfam, to stabilize mtDNA (207–209).

Mitochondrial biogenesis can be stimulated via the convergence of multiple signaling pathways. The pathways essential in the field of muscle biology will be discussed briefly here, as they have implications for muscular aging and adaptation to both exercise and disuse. The most potent inducer of synthesis of mitochondria is through perturbations in cellular energy status. Hallmarks of this state are AMP-mediated AMPK activation and NAD+ mediated Silent mating type information regulation 2 homolog 1 (Sirt1) activation. Studies have shown that pharmacological activation of AMPK (210, 211) or Sirt1 enhances mitochondrial content (212–214). AMPK's mechanism of action is through the activating phosphorylation of PGC-1α (215,

216), as well as through the activation of USF-1, a transcription factor that binds to the PGC-1α promoter (114, 216). Conversely, Sirt1 deacetylates PGC-1α, promoting its nuclear localization (217–219). In fact, loss of AMPK leads to a failure to induce mitochondrial biogenesis in response to starvation (220, 221) or contractile activity (222), and limits endurance capacity due to reduced mitochondrial volume (220). Further, Sirt1 deletion reduces mitochondrial content and endurance capacity of muscle (223), cumulatively highlighting the importance of these proteins in exercise-induced adaptations.

Ca^{2+} is constantly in flux within skeletal muscle as it undergoes cycles of contraction and relaxation. Thus, researchers hypothesized that it would be a great target for inducing oxidative phenotypes. This was found to be the case, whereby pharmacological enhancement of Ca^{2+} in muscle cells increased mitochondria-related transcription and protein content in muscle cells (224–226). It was also uncovered that this was due to 1) Ca^{2+}/calmodulin dependent protein kinase II (CaMKII) and 2) calcineurin A (CnA) activation, which in turn upregulates PGC-1a transcription via activation of the transcription factors cAMP response element-binding protein (CREB), and MEF2, respectively (227–232). Furthermore, CaMKII also promotes p38- mitogen activated protein kinase (p38-MAPK) activation to potentially induce mitochondrial biogenesis (233). Importantly, electrical stimulation-induced mitochondrial biogenesis is prevented when muscle cells are co-treated with Ca^{2+} chelators (222, 226), highlighting that Ca^{2+} signaling contributes to mitochondrial biogenesis with exercise.

ROS are also implicated in promoting the synthesis of mitochondria through induction of PGC1-α expression (114, 234, 235). This occurs through 1) ROS-induced activation of AMPK (114), 2) activation of p38-MAPK, which stabilized PGC1-α (236–238) and activates the transcriptional regulators of PGC-1a, MEF2 (239) and ATF2 (240), via phosphorylation and 3)

USF-1 activity (114). Exercise stimulates p38-MAPK (222, 241–243), and its inhibition reduced the exercise-induced PGC-1α promoter activity (244). Importantly, antioxidant treatment in stimulated cells had a similar effect (222), suggesting that ROS is activating p38-MAPK to induce mitochondrial biogenesis with exercise.

2.3.2.3. Mitochondrial Degradation: Mitophagy

Mitochondrial health within muscle depends on the maintenance of a functional organellar pool within the tissue. Thus, not only do new, healthy, mitochondria need to be created, but those that are damaged must be removed to prevent the perpetuation of these damaging effects (i.e., sustained ROS). This section highlights important pathways that regulate mitophagy (Figure 7) and their importance of skeletal muscle.

The canonical mitophagy pathway is controlled by the serin/threonine kinase, PTEN-induced putative kinase 1 (Pink1) and the E3-ubiquitin ligase Parkin. This system has been primarily classified by Dr. Richard Youle's group in a series of studies beginning in the mid-2000's. Briefly, in a healthy mitochondrion, where protein import is functioning well, Pink1 is predominantly imported into the mitochondria and degraded in the matrix via mitochondrial protein peptidase (Mpp) and Lon protease (LonP) (245) or the intramembrane protease presenilin-associated rhomboid-like protease (PARL) (246, 247). Following mitochondrial stress, particularly an accumulation of damaged matrix proteins (248) or a loss of membrane potential (246, 249–251), protein import is reduced and Pink1 accumulates on the OMM where it undergoes activating autophosphorylation (252). Active Pink1 phosphorylates both Parkin (249–251, 253) and Ubiquitin (254–257) leading to polyubiquitination of OMM proteins (VDAC, Mfn1/2, TOMs, Ubiquitin), which will act in a feedforward way to recruit more Parkin and Ubiquitin to membrane (249–251, 258, 259). In addition, ubiquitination of Mfn1/2 primes it for degradation, likely to

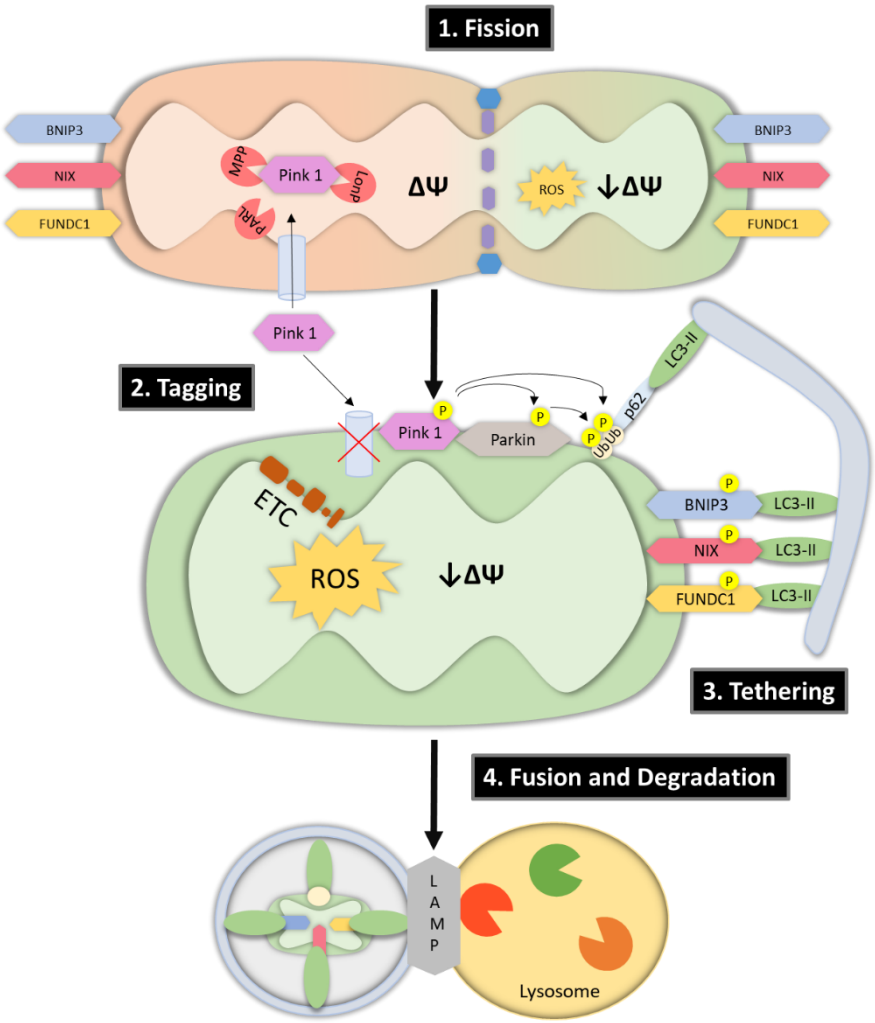

Figure 7. The Mitophagy Pathway. When a portion of the mitochondrial network becomes dysfunctional, with a low membrane potential (Ψ) and/or excessive ROS production (green mitochondria), it will undergo 1) fission, mediated by Fis1 and Drp1. The fragmented mitochondrion will then undergo 2) tagging. Briefly, Pink1, which is normally imported into healthy mitochondria and degraded by proteases (PARL, MPP, LonP), will no longer be imported and will therefore accumulate on the outer mitochondrial membrane (OMM) and undergo autophosphorylation. This "active" Pink1 will then phosphorylate and activate both Parkin and Ubiquitin (Ub). Parkin, which acts as an E3-ubiquitin ligase, will poly-ubiquitinate OMM proteins. This will lead to 3) tethering of the mitochondrion to the autophagosome via adaptor proteins that interact with them and phagophore-embedded LC3-II. Alternatively, the mitophagy receptors Bnip3, Nix and Fundc1 are OMM embedded and will undergo phosphorylation and tether to the phagophore via LC3-II. Finally, the autophagosome-bound mitochondrion will be shuttled to the lysosomes where 4) fusion of the membranes and degradation of the dysfunctional organelle will occur.

to prevent re-fusion of the damaged mitochondrion (260). Ultimately, these ubiquitin chains act as a scaffold or adaptor proteins such as p62, optineurin and Ndp52, to tether mitochondria to the autophagosome for degradation (261–263).

The vitality of this mitophagy pathway in skeletal muscle has been demonstrated in a series of studies. Firstly, Parkin knockout in drosophila promotes muscle degeneration and cell death (264). Furthermore, silencing of Parkin in cultured myotubes reduces mitochondrial respiration (265), induces insulin insensitivity (265) and increases susceptibility to mitochondrial stressors (266). In Parkin-null mice, mitochondria appear fragmented (267), corresponding to impaired respiratory capacity (267–269) and reduced mitophagy flux (268, 269). Importantly, these mice fail to moderate mitophagy in response to acute and chronic endurance exercise (268, 269). Interestingly, unlike mitochondrial dynamics-related proteins, overexpression of Parkin prevents aging-induced loss of muscle mass (270). Cumulatively, these reports highlight the importance of this mitophagy system in skeletal muscle.

Receptor mediated mitophagy is a far simpler process, that does not rely on ubiquitin for tethering to the autophagosome. Instead, mitophagy receptors, which are normally localized to the mitochondrial membrane (271–274), are phosphorylated, allowing for their interaction with autophagosomal proteins of the Atg8 family (LC3-II, Gabarap etc…) (271, 275, 276). These receptors include Bnip3 (277–279), Bnip3-like protein (Nix) (276, 280, 281), and Fun 14 domain containing protein (Fundc1) (271, 282). It is un unclear if these mechanisms occur simultaneously or independently with one another and Parkin-mediated mitophagy, however, there is evidence to suggest that Bnip/Nix promote mitochondrial Drp1 localization, which would enhance fission and aid in Parkin recruitment (283–285). It is important to note that Fundc1 can be activated by Ulk1 (282), linking upstream autophagy to mitophagy induction.

The complexities of these mitophagy receptors have only briefly been explored in skeletal muscle. Yet, in 2010, the Sandri group first observed that both Bnip3 and Nix overexpression in muscle promoted atrophy (177), suggesting that mitophagy is fine-tuned in skeletal muscle homeostasis. Since then, others have found that Bnip3 knockout in muscle cells perturbs myogenesis likely a result of the accumulation of dysfunction mitochondria (286). Interestingly, both Nix and Fundc1 knockout in cardiac progenitor cells promoted cell death (287), which may similarly impact skeletal muscle. Furthermore, Fundc1 muscle specific knockout impairs mitochondrial function and exercise capacity (288), whereas its inhibition in stimulated C2C12 myotubes prevented mitophagy induction (289). Cumulatively, these results indicate that mitochondrial degradation is fine-tuned to the maintenance of muscle mass.

2.3.3. BENEFITS OF EXERCISE ON MITOCHONDRIAL HOMEOSTASIS

Acute exercise stimulates several mechanisms that enhance mitochondrial content and quality, as summarized in Figure 8. First, acute exercise is a potent inducer of mitochondrial biogenesis. For example, work from our lab has recently shown that in-situ contractile activity enhances PGC-1α promoter activity (241), explaining the abundance of findings that measure exercise-induced elevations in PGC-1α transcript (205, 231, 241, 290). Furthermore, endurance exercise rapidly activates PGC-1α nuclear localization and function (291). This enhancement promotes the synthesis of NuGEMPs. These changes are due to activation of the pathways highlighted above (Chapter 3.2.2.). Briefly, with endurance exercise, ATP is utilized, which leads to accumulation of the metabolite AMP, thereby activating AMPK. This AMPK activation with exercise has been shown in a variety of studies (222, 241, 242, 290, 292–294), which are intensity, duration, and modality dependent (292, 295). With these metabolic changes occurring in the working muscle, NADH is oxidized to NAD+, and thereby activates PGC-1α (296–298).

Furthermore, Ca^{2+} is constantly in flux within contracting and relaxing muscle, and in culture it has been shown the treatment with calcium chelators prevents contractile activity-induced mitochondrial biogenesis (226, 231), which is though Ca^{2+} ability to activate transcription factors such as MEF2 and CREB. Finally, ROS levels are primarily enhanced with prolonged and high-intensity exercise, which may not be from mitochondrial origin (299). These ROS will activate p38, of whose activity is elevated following acute exercise (294), and ultimately enhance the transcription factors USF and ATF2 function in promoting PGC-1a transcription and protein activation. Importantly, endurance-style training has been shown to increase the expression of PIM components and enhance the kinetics of protein import into the mitochondria (203, 300, 301).

This upregulation of biogenesis explains the elevated mitochondrial content observed in trained / chronically contracted skeletal muscle (302, 303). However, they do not account for the commonly observed reduced predisposition for ROS production within trained skeletal muscle (304–307). Thus, to understand such changes, we must turn our attention to mitochondrial quality control mechanisms, specifically fission and mitophagy. Acute exercise leads to an elevation in mitochondrial Drp-1 protein likely to remove poorly functional portions of the organellar network (294). Importantly, endurance exercise serves as a stimulus to enhance mitophagic protein levels in whole muscle and isolated mitochondrial samples (269, 294, 308–311) and activate mitophagy flux (269, 294, 312). Nonetheless, these acute changes manifest as an overall reduction in basal mitophagy flux in trained skeletal muscle (305, 307, 313, 314). In fact, in response to acute exercise following training, there is a blunted mitophagy activation (268, 315), suggesting that there is a higher quality of the organelle pool, thus diminishing the necessity for mitophagy. Over time, as with a training regime, these subtle changes will manifest in an expansion of the reticular mitochondrial network, reducing diffusion distance for substrates, proving a larger capacity of

OXPHOS. These adaptations ultimately contribute to the enhancement of endurance and metabolic capacity of the tissue.

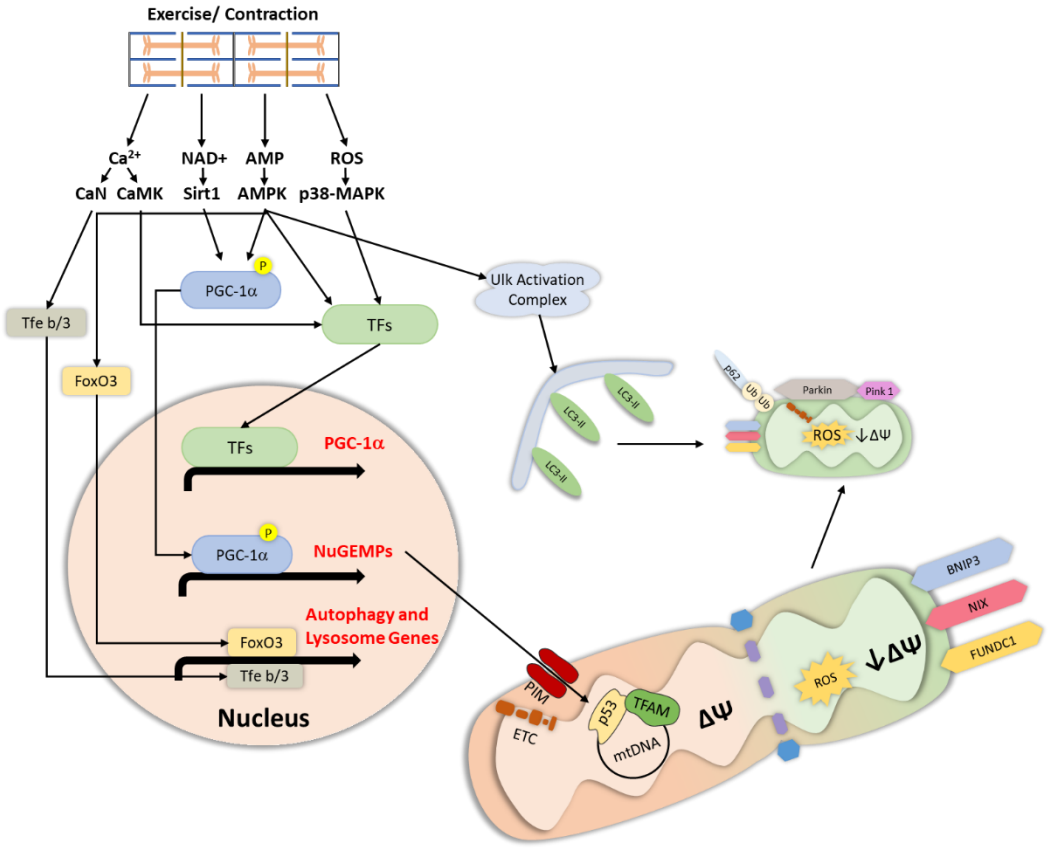

Figure 8. Exercise-Induced Mitochondrial Quality Control. In response to contractile activity a cascade of events simultaneously promotes mitochondrial biogenesis and mitophagy to enhance the organellar pool within the muscle. Signaling is mediated by: 1) Ca^{2+} release from the SR and subsequent activation of CaN and CaMK which enhance the activity of transcription factors (TFs) for mitochondrial biogenesis, and autophagy-lysosome system via Tfeb/3 and FoxO3; 2) NAD+ is produced and activates Sirt1, which deacetylates and enhances PGC-1α activity and NuGEMP expression; 3) ATP is hydrolyzed to ADP and AMP, which activate AMPK to facilitate PGC-1a activity, TF function, and autophagy induction via Ulk1, FoxO3 and Tfeb; and 4) ROS are produced, leading to the activation of p38-MAPK, which upregulates the activity of biogenesis stimulating TFs. NuGEMPs such as TFAM and ETC proteins are imported via the PIM and promote the expression of mtDNA-regulated genes, and are assembled into the organelle, respectively. Simultaneously, dysfunctional portions of the mitochondrial network undergo fission and subsequent mitophagic degradation with the autophagic machinery promoted by exercise.

2.4. Skeletal Muscle Aging:

Based on the 2016 Canadian Census, the proportion of seniors aged 65 and older has been rapidly increasing over the past 40 years (316). Seniors currently represent greater than 15% of Canadians and are projected to account for more than 25% of the Canadian population by 2036, (316). In addition, life expectancy is at an all-time high (316). Unfortunately, advanced age is associated with declines in quality of life, which are related to a higher incidence of falls, hospitalization, and co-morbidities (317). Accordingly, this increased proportion of aged individuals will impose a strain on the health care system moving forward. With aging there are multifactorial changes that occur and understanding the intricacies of such changes is integral. Although much is understood about mechanisms involved, these is a lack of clear evidence about cause and effect in aging muscle. Thus, characterization of the molecular differences between young and old muscle will guide the development of strategies to enhance skeletal muscle health with increasing age.

2.4.1. PHENOTYPIC CHANGES IN AGED SKELETAL MUSCLE

With aging there is a progressive decline in muscle mass and quality (1, 318), which is commonly referred to as “sarcopenia” (319, 320). It is thought that somewhere in an adults mid-30’s, they begin to lose as much as 3-5% of muscle mass each decade, and that this process accelerates after approximately 60-years old, where muscle mass may decline by upwards of 15% per decade (321, 322). Interestingly, the impact of sarcopenia prevalence of sarcopenia is greater in men than women (323–327) and functional deficits are more prominent in the hindlimb versus the forelimb muscles (320, 326). These changes in muscle architecture have a significant impact on locomotion and thus quality of life. Although the etiology of such changes remains unclear, one thing is for certain – age-related changes in skeletal muscle size and function are multifactorial,

with both intrinsic and extrinsic regulation (323). Importantly, sarcopenia is exacerbated by prolonged periods of inactivity (318, 319, 328). Fortunately, however, exercise can restore muscle health following periods of disuse and slowing age-related muscle wasting (167, 328–330).

2.4.1.1. Slowing of Muscle with Age

With aging there is a "slowing" of muscle (320, 331). Motor unit reorganization, favoring a fast-to-slow transformation is reported in age-related sarcopenia. Specifically, in early muscular aging, there is a transition from IIB to IIX, and with advanced age, there is a further transformation leading to an increased number of IIA and I fibers (331). Further, Type II fiber cross sectional area is decreased dramatically versus the relatively unchanged Type I fiber area (326, 332, 333). This corresponds to greater loss of force in Type II fibers versus Type I (334). These changes have been attributed to age-related remodeling of motor units, resulting in preferential denervation of Type II fiber, and re-innervation of Type I fibers, leading to an increased number of muscle fibers per motor unit (331, 335, 336). However, it is important to note that controversy around this point exists due to the recent discovery of co-expressing fibers of slow origin that may express fast MHC (337). Thus, slow myofiber atrophy could be occurring in aging muscle, and modern methodologies may help understand this phenomenon.

The slowing of muscle is also due to the loss of ECC efficiency, as a product of changes at multiple steps along the way. First, the neuromuscular junction (NMJ) becomes fragmented, disorganized, and "loose" compared to that of a young, healthy muscle (320, 338, 339). Second, in aged muscle there is perturbed RyR and SERCA function, which slows Ca^{2+} release and reuptake, leading to less Ca^{2+} transients with contraction (340–345). Finally, contractile protein function is altered with age (346), which may be due to oxidative modifications that disrupt cross-bridge cycling and a loss of elastic properties (347).

2.4.1.2. Factors Contributing to the Aged Muscle Phenotype

As summarized below, and depicted in Figure 9, there are several factors contributing to the aged muscle phenotype. First and foremost, there is an infiltration of fat in aged muscle (348–350), which can promote inflammation and insulin sensitivity in aged muscle (351). There are also accumulations of connective tissue in senescent muscle, reducing the quality of the tissue (352–354). Although the etiology of these changes is unclear, it is thought that inflammation and metabolic insufficiencies are responsible. Furthermore, mitochondrial abnormalities are also linked to fiber atrophy with age, as discussed in more detail in Chapter 4.3.

Changes in circulating factors have also been proposed in regulating age-induced muscle wasting. First, inflammation can produce muscle atrophy (355–359) and there is evidence that in aging there are elevated circulating pro-inflammatory markers (IL-1, IL-6, TNF-α), upregulated intramuscular inflammatory signaling (349, 360, 361), and reduced anti-inflammatory cytokines (IL-10, IL-15) (361). In addition, anabolic hormones such as growth hormone (GH) and insulin-like growth factor 1 (IGF-1) are essential in muscle mass maintenance. As GH is responsible for the production of IGF-1 in the liver, and thus it is not surprising that with age, both hormones are concomitantly reduced (362, 363). Furthermore, reductions in testosterone and estrogen, and elevations in myostatin are also proposed to impact muscle mass and function with age (364–366). In the context of aging, these changes foster muscle degeneration through perturbed protein synthesis, enhanced degradation, and elevated apoptotic pathways.

Muscle atrophy is a hallmark characteristic of sarcopenia, the result of a progressive loss of muscle protein over time. Such changes could be achieved by an imbalance between muscle protein synthesis and the pathways that mediate protein degradation. Muscle stem cells (MuSCs) respond to anabolic stimuli, such as resistance exercise, to promote enhanced myonuclear number,

and thus hypertrophy. In aged muscle however, literature suggests that there is MuSC exhaustion (338, 367), and this loss is greater in Type II fibers, but relatively unchanged in Type I (368). This may contribute to the more pronounced Type II atrophy with age. There is also evidence of anabolic resistance in the muscle from elderly individuals. In healthy muscle insulin stimulates glucose uptake/utilization and protein synthesis. In aged muscle, the action of insulin is blunted, suggestive of anabolic resistance (349, 369). This is further supported by blunted post-meal-induced increases in muscle protein synthesis (370), and reduced hypertrophy with resistance training (371). This perturbed stimulus-induced anabolism may explain the atrophy phenotype of aged muscle.

Muscle protein is maintained through the balance of synthesis and degradation. As detailed above, aged muscle exhibits anabolic resistance. On the other side of the story, protein degradation in myofibers is regulated by the ubiquitin proteasome system (UPS), calcium-activated proteases (i.e., calpain and caspase) and the autophagy lysosome system. The autophagy-lysosome system in aged muscle is discussed extensively in Chapter 4.2.2. of this literature review, and an overview of these other proteolytic systems is covered in Chapter 4.5. As Ca^{2+} levels are sustained in aged muscle (see below for details), it is not surprising that the activity of the calpain system is enhanced with age (372). Furthermore, UPS activity is also increased in sarcopenic muscle (373). Central to this thesis is the autophagic process, and literature searches reveal that much remains to be elucidated regarding the signaling toward, and the activity of, autophagy-lysosome regulatory proteins, which is covered extensively below.

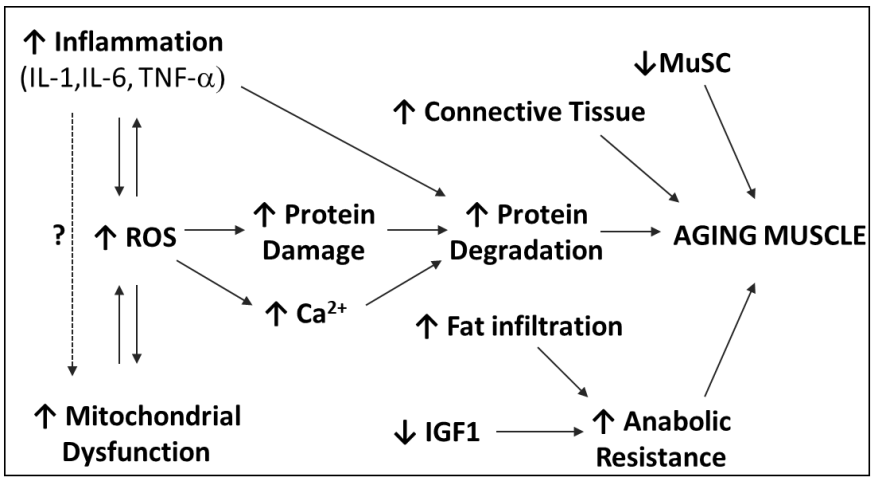

Figure 9. Factors Implicated in Muscle Aging. Muscle structure and function are altered with age. This is due to an array of changes that occur in the local environment and within the muscle, which ultimately promote a loss of muscle mass and function. See text for details.

2.4.2. THE AUTOPHAGY-LYSOSOME SYSTEM IN AGED MUSCLE

2.4.2.1 Upstream Autophagy

There is ample evidence that show that both FoxO3 (313, 374) and Tfeb (313) protein is elevated in aged muscle. If functional, these proteins would support the expression of ubiquitin-proteosome and autophagy genes in old muscle. Unfortunately, regarding FoxO3, there are no clear indications of whether AKT-mediated, inhibitory, FoxO3 phosphorylation is altered in age (375, 376). Furthermore, there are inconsistencies in findings in relation to its nuclear localization (376, 377). These inconsistencies in FoxO3 localization with age may be explained by the lack of consensus on whether AKT activity is elevated, reduced or unchanged in aged muscle (376–381). FoxO3 deacetylation by histone deacetylase 1 (HDAC1) (100, 382, 383) and co-activation by CARM1 (36, 37) enhance FoxO3 function, mechanism that have not been explored in aged muscle. Like AKT, there are reports that have observed lower basal (384, 385), unchanged AMPK (386–388) signaling in aged muscle in a basal state. The consequence of this on FoxO3 are not understood, yet in a very recent report, aged human and rat muscle were shown to contain lower

basal AMPK-activating-Ulk1 phosphorylation (62). Importantly, mTORC1 activity is sustained in aged muscle (381, 389, 390), corresponding to increased inhibitory Ulk1 phosphorylation in aged skeletal muscle (378, 381, 390). Importantly, even less is understood in regard to Tfeb and Tfe3, and the ramifications of the differences measured upstream of these proteins. There are, however, a number of studies that have reported increases in both (reactive oxygen species) ROS (165, 391, 392) and $[Ca^{2+}]_{IC}$ (119, 391, 393, 394), yet the impact of these changes on the autophagy-lysosome system in aged muscle remain unclear. Cumulatively, the lack of data signify that more work is necessary to understand the influence of age on the autophagy-lysosome system at the genetic and activation levels.

2.4.2.2. Autophagy Flux

There are inconsistencies in the understanding of autophagic resolution in aging muscle, which may be due to the use of "snapshot" measures of autophagy, looking at autophagosomal transcript and protein levels. For example, one report by Dr. Leeuwenburgh's lab shown evidence of normally functioning autophagosome formation, with impairments in the processing and degradation of autophagosomes. These interpretations stem from observed accumulations in Beclin-1, LC3-I and LC3-II, without changes in upstream autophagy markers Atg7, Atg9 of *Lc3* transcripts (395). Furthermore, various studies in rodents have shown elevations in the mature autophagosomal marker LC3-II, the LC3-II/I ratio, the LC3 processing protein Atg-7, and the adaptor protein p62 (178, 396–399). In humans, Fry et al., measured elevations in upstream autophagy proteins such as Beclin1 and Atg7, but no changes in LC3-II/I (400), whereas Balan at al reported increase in LC3-II with age (401). These results would signify a greater capacity for autophagy, and although this may be true, interpreting such findings is challenging as these data could also indicate blunted autophagic breakdown. In contrast to these studies, others have failed

to report an increase in Beclin1 or Atg7 in humans (402) or LC3-II/I and p62 protein in aged mice (378), which would signify no changes in autophagy in aged muscle. The age-induced autophagy execution may be fiber-type specific, as in young, healthy muscle, oxidative muscle has greater basal autophagy flux than predominantly fast muscle (75), a phenomenon that requires investigation in aged muscle. Importantly, two independent reports by Baehr et al., and Carter et al., which utilized colchicine to assess autophagy flux in Fisher344BN rats, show enhanced autophagy flux in the aged cohort vs young counterparts (313, 403). Thus, it appears that autophagy flux is elevated in muscle with age, at least up until the point of cargo delivery to lysosomes.

2.4.2.3. Lysosomes in Aged Muscle

Within aging tissue, there is a progressive increase in "the age pigment", scientifically termed lipofuscin. These granules are composed of indigestible material of lysosome origin and are commonly observed in post-mitotic tissue (404, 405). Lipofuscin occurs when oxidized lipids, carbohydrates and proteins become resistant to lysosomal hydrolysis. This phenomenon is linked, at least in part to the mitochondria in what is termed the "Lysosomal Theory of Aging". In this theory, dysfunctional lysosomes prevent the terminal degradation of autophagic substrates, and thus, dysfunctional, ROS-producing mitochondria accumulate, and lead to the hyper-oxidation of proteins, which then accumulate within the tissue, in a feedforward mechanism (404, 405). It is hypothesized that these harmful substances can accelerate cell death via apoptosis. Importantly, skeletal muscle is not exempt from such changes, as these lipofuscin granules are visible in both rodent (313, 399) and human (406) skeletal muscle. Thus, reports of increased lysosome content in aged muscle (313, 407) may not be indicative of enhanced lysosome function, but rather an accumulation of dysfunctional organelles. In support of this hypothesis, there is evidence of

reduced lysosome-related transcript in aged muscle (395). Furthermore, apoptosis, and myonuclear degeneration is observed in the muscle of aged rodents (408), and these apoptotic sites are localized in regions where mitochondrial degeneration is present (409), further linking lysosome dysfunction to mitochondria and ultimately sarcopenia. It has also recently been proposed that lysosome-dysfunction and the ensuing release of cathepsins can promote apoptosis (410), a phenomenon which remains unclear in skeletal muscle aging. Furthermore, as discussed earlier in this review of literature, the role of Tfeb in aged muscle remains relatively unexplored, and more work is necessary to determine how Tfeb impacts aged skeletal muscle. With these points in mind, some important questions remain: 1) whether the functional lysosomes that exist within muscle are sufficient to degrade autophagic substrates; 2) whether upregulating lysosome content/function can enhance autophagic/mitophagic capacity and improve the function of the tissue; and 3) whether the presence of lipofuscin perturbs autophagosome degradation in skeletal muscle.

2.4.3. MITOCHONDRIA IN AGED SKELETAL MUSCLE

Mitochondria play an integral role in age-related muscle wasting. Alterations in mitochondrial content, structure and function are evident in aged skeletal muscle. Specifically, mitochondrial content, as measured by enzymatic activity, protein markers and mtDNA, is reduced in old skeletal muscle (411–415). Electron micrographs provide visual evidence that IMF mitochondria have diminished size and SS-mitochondria have reduced depth (416). Furthermore, mitochondria appear swollen and fragmented (178, 414, 416) with cristae disruption (399). Functionally, mitochondria are impaired within aging muscle. These changes include reduced mitochondrial respiration (241, 269, 313, 417, 418), deficits in maximal ATP production rate (350, 413), uncoupling of oxygen consumption from ATP synthesis (350, 419, 420), and loss of

membrane potential (421). It remains controversial if this is due to age or activity level differences between young and old (422). Beyond the respiratory deficits observed in aged muscle, mitochondrial ROS, in single fibers (421), as well as in SS and IMF subfractions (423) is elevated. Further, there are greater indices of oxidative stress in aged muscle (424, 425). Since the mitochondrial targeted antioxidant SS31 prevents aging-induced mitochondrial ROS production and oxidative damage (421), one could assume that mitochondrial ROS are contributing to age-related sarcopenia. However, this remains controversial as other sources of ROS may be promoting such changes. Nonetheless, elevated damage can lead to SR abnormalities (discussed in Chapter 2), and NMJ instability, ultimately impacting the quality of aged muscle (426).

Importantly, mitochondrial dysfunction is theorized to contribute aging because of a gradual accumulation of organellar damage from ROS. Further, mtDNA lack histones and DNA repair mechanisms. Thus, this proximity to ROS generation makes mtDNA susceptible to damage. This perpetuates a vicious cycle of forming faulty ETC complexes, which produce more ROS, thereby damaging cellular components (i.e., proteins, genomic DNA). Supporting this theory, overexpression of mitochondrial catalase extends lifespan in mice (427). Regarding muscle, regions of fibers that exhibit mitochondrial dysfunction have the greatest mtDNA damage and muscle atrophy with age (162, 428–430). Further, mitochondria play an integral role in mediating apoptosis through enhancing mtPTP pore opening and release of pro-apoptotic proteins. Ultimately, this can lead to myonuclear decay and loss of a cytoplasmic domain, resulting in fiber atrophy. In fact, indices of apoptosis are enhanced with age (162, 411, 413, 414, 423, 431–433), which may be more pronounced in fast-twitch muscle (141). Overall, mitochondrial abnormalities perpetuate damage and promote apoptosis, which ultimately contribute to muscle atrophy.

2.4.3.1. Mitochondrial Biogenesis in Aged Muscle

The diminished content of mitochondria in aged muscle is due to, at least in part, reduced expression of PGC-1α mRNA and protein (241, 411, 413, 423, 435, 436). These changes have commonly been observed in both slow and fast muscle. Very recently it was shown that these reductions may be explained by reduced PGC-1a transcriptional activity and mRNA stability (241). In addition, nuclear PGC-1α is lower in aged skeletal muscle (411, 437). Importantly overexpression of PGC-1α in mice preserves muscle integrity with age (438). In fact, these mice retain many characteristics of young mice (438), pointing to the importance of this regulator in muscular longevity. Alternatively, lack of PGC-1α hinders aged muscle from adapting to exercise (439). In contrast to PGC-1α, Tfam is elevated in aged muscle, even with reduced mitochondrial content (436, 440, 441), which may lead to mito-nuclear imbalance.

Although these regulators have been characterized, very few studies have clarified the upstream regulatory mechanisms involved. For example, as mentioned above, there may be reduced baseline AMPK activity in aged muscle, and this would provide a probable explanation for reduced PGC-1α activity. Various stimuli have been used to activate AMPK in aged muscle and the response is blunted (241, 386–388), which over the course of time may impair mitochondrial biogenesis. Furthermore, lower basal NAD+ and Sirt1 protein are reported in aged muscle (415, 437, 442). This acts to downregulate signaling toward organelle biogenesis through hindered Sirt1 activity. In fact, restoration of NAD+ through caloric restriction or the NAD+ precursor, NMN, restore mitochondrial homeostasis (415), highlighting the importance of NAD+ in age-related mitochondrial dysregulation. Furthermore, since markers of oxidative stress and Ca^{2+} are elevated in muscle, one would expect p38-MAPK and CaMK-II activation to be higher,

yet this is not the case in aged muscle (386). The implications of this remain unclear in the regulation of mitochondrial biogenesis in aged muscle.

2.4.3.2. Mitochondrial Dynamics in Aged Muscle

Although controversial (443), an overwhelming number of studies have reported a greater abundance of mitochondrial fission, relative to fusion proteins in aged skeletal muscle (398, 399, 416, 436, 444). Importantly, in these reports' inconsistencies have been found regarding the absolute change in the expression of fusion and fission proteins. Overall, however, this imbalance in organellar dynamics would explain the commonly observed mitochondrial fragmentation described above. It is important to note that this effect may be fiber-type specific, as the pro-fusion protein, Mfn2 is reduced to a larger extent in the tonic soleus muscle versus the predominantly fast-twitch TA muscle (178). If this pattern holds true, whereby there are fiber-type dependent changes in dynamics with age favoring fragmentation in slow muscle, then the ramifications on mitophagy would be vast, likely priming the mitochondria for a greater rate of basal mitophagy. Overall, as mitochondrial dysfunction is apparent in aged muscle, and as fission precedes mitophagy, it is not surprising that there is evidence of fragmented mitochondria in aged muscle, which may prime this organellar pool for mitophagy.

2.4.3.3. Mitophagy in Aged Muscle

As with measurements of autophagy, there are inconsistencies within the literature on whether mitophagy is in fact up- or down- regulated in aged skeletal muscle. Specifically, in examining Pink1-Parkin-mediatied mitophagy, we and others have reported decreases in Parkin protein in both whole muscle (270) and isolated mitochondria (269) in 18-month-old mice. Alternatively, others have reported, in older mice (24 mo) and rats (36 mo) elevations in Pink1,

Parkin and Ubiquitin (398, 399). These data together may implicate an age-specific mitophagic response regarding Pink1-Parkin-mediated mitophagy. With respect to Bnip3 and Nix, studies have failed to measure any change in these mitophagy receptors (398, 402, 445), however, phosphorylation of these proteins would clarify their involvement in mitophagy within aged muscle.

Work that has been published in recent years from our lab has measured increased LC3-II (399) and p62 (399, 446) in isolated mitochondrial fractions from aged rodents. These data would suggest either enhanced rate of targeting and degradation or perturbed efficiency of mitophagic breakdown. Utilizing a colchicine-flux-assay, we have uncovered that mitophagy flux is enhanced in aged rodent muscle (269, 313). However, the remaining presence of impaired organelles suggests that the production of mitochondrial dysfunction is greater than the rate of removal. This may contribute to the propagation of further dysfunction. Thus, restoring mitophagy in aged muscle may hold therapeutic benefit in slowing age-related sarcopenia.

2.4.4. IMPLICATIONS OF EXERCISE IN AGED MUSCLE

Physical activity and exercise have a dramatic impact on whole body health for aging individuals. For example, regular, moderate exercise can reduce age-induced inflammation (447, 448), improve whole body metabolism (449) and cardiovascular fitness (450). All these changes may have positive consequences in aged skeletal muscle. Focusing on skeletal muscle specifically, exercise is a stimulus that acts to remodel skeletal muscle. As discussed in more detail below, the ability of aged muscle to adapt to exercise is hindered. Thus, understanding the mechanistic differences responsible is important in developing novel treatments for age-related sarcopenia.

As discussed in Chapter 3.3, endurance exercise simulates mitochondrial biogenesis and induces quality control mechanisms. Over the course of a training regime, these changes enhance the quality of the organellar pool and creates a more metabolically adept tissue. This seems to be the case within aged muscle as well as lifelong physical activity improves mitochondrial integrity and aerobic performance that are attenuated with age (451, 452). Importantly, there is reduced adaptive plasticity in response to acute contractile activity in aged muscle due to an attenuation of kinase signaling (AMPK, p38, CaMK-II) that converge on mitochondrial biogenesis (241, 386–388). Yet, contractile-activity induced enhancement of PGC-1α promoter activity is no different in young and aged muscle (241).. Supportive of these acute differences in mitochondrial biogenesis, there is evidence of a diminished response with chronic activity in comparison to young (386, 453). However, although the response is blunted, training in aged muscle upregulates upstream kinases, PGC-1α protein, PGC-1α nuclear localization and ultimately mitochondrial content to that of young muscle (411, 436). Unfortunately, few studies have investigated protein import in aging muscle, a requirement for biogenesis. However, one investigation found that with chronic contractile activity, protein import machinery was not enhanced, unlike in young muscle. Further, enhanced import of the matrix protein OCT was blunted (414).

Mitochondrial quality control mechanisms are also altered with exercise training. For example, the ratio of fusion:fission proteins are normalized with endurance training in rodents (436). Further, in human, physical activity increase fusion protein levels (401). This likely facilitates the formation of a more reticular organellar network. With regard to mitophagy, acute exercise fails to elicit the same level of mitophagic breakdown to that young muscle (269). However, chronic contractile activity was able to reduce mitophagy flux to the same extent as young muscle (313), suggestive of an overall enhancement of these organelles and their quality

control in aged muscle with training. Importantly, chronic contractile activity and endurance exercise programs have been shown to normalize myonuclear decay, increase anti-apoptotic proteins and slow protein release from mitochondria, which ultimately reduce age-related DNA fragmentation (395, 414, 434, 454, 455). This change likely preserves myonuclear content and domain size, thereby slowing atrophy in aged muscle.

In young muscle, contradictory findings have been observed in the regulation of autophagic breakdown in muscle in response to acute exercise, but most reports suggest elevated autophagy (456–458). However, utilizing appropriate flux measures, it has been uncovered that one bout of exercise does in fact stimulate autophagic breakdown in young muscle (294, 459). It remains to be seen if autophagy flux changes in aged muscle with acute endurance-style exercise, and thus work of this kind would be valuable to the field. However, since kinase signaling is attenuated in exercised old muscle, one would presume that exercise-stimulated autophagy would be blunted. Supportively, with fasting, there is perturbed AKT and mTORC1 pathway inactivation, and ultimately lower activation of Ulk1 versus young-exercised counterparts (381). Similarly, in response to one bout of electrical activity there is blunted mTORC1 activation (460). Cumulatively, these findings may implicate a blunted autophagy potential in aged muscle following acute exercise.

With exercise training, in young animals, there are increases in autophagy in fast, but not slow muscle (75). Further, in humans, indices of autophagy are greater following training (401). However, Carter et al., failed to measure any changes in LC3-II autophagy flux with chronic contractile activity. With aging, exercise training increases static measures of autophagy and mature autophagosomes in rodents (378, 395, 456, 461). Furthermore, physically active elderly individuals have increased autophagy-related mRNA (451, 462). This upregulation of autophagy

may stimulate improved removal of damaged cellular constituents. However, this area requires clarification, and modern flux measurements will allow for us to better understand how exercise training influences autophagy flux rates within aging muscle.

Lysosomes also undergo adaptation to exercise training in young animals. In an acute exercise setting, both Tfeb promoter activity and nuclear localization are enhanced (463). It is unknown if acute excise stimulates lysosome biosynthesis in aged muscle, a fundamental process worth investigating. These acute regulatory changes in lysosome biosynthetic pathways in young animals explain the elevated lysosome content following chronic contractile activity (65, 155, 156). With age however, this response is blunted, whereby not all lysosome proteins increase (313). This may have significant ramifications on the ability of aged muscle to sufficiently degrade autophagic substrates. Therefore, future studies should aim to examine aging-related alterations in the lysosomal system in skeletal muscle with exercise. These findings may lead to a possible pharmaceutical target for improving aging-related muscle dysregulation.

2.5. Skeletal Muscle Atrophy:

Atrophy is simply defined the reduction in tissue size as a result of a loss of cytoplasmic volume. This deficit entails a loss of proteins and organelles. Although atrophy is commonly observed in various conditions such as with starvation, diabetes, cachexia, sarcopenia and more, the objective of this chapter is to address muscle atrophy regulation in disuse and denervation. Ultimately, the goal of a developed understanding of the molecular process that govern atrophy is for the development of novel therapeutic targets that prevent or slow muscle wasting.

2.5.1. PHENOTYPIC CHANGES IN ATROPHYING MUSCLE

Atrophying skeletal muscle undergoes a shift toward reliance on glycolytic metabolism. This is in part due to changes in mitochondrial architecture, as discussed further below in Chapter 2.5.4. Sarcomere structure is concomitantly altered, characterized by z-line streaming in both denervation and disuse models (464, 465). There is also an apparent fiber-type-specific atrophy, whereby Type I fibers are more sensitive to denervation and disuse atrophy (466–468). This contrasts the predominant Type II atrophy observed in multifactorial wasting model (i.e., sarcopenia and cachexia). The basis for this selectivity in fiber type atrophy remains unresolved, but it is nonetheless clear that force production is lost in denervation and disuse atrophy (469). In denervation, muscle atrophy is biphasic, whereby there is a rapid decline in muscle mass over the first two weeks followed by a more gradual reduction in the rate of loss (470–472). Immobilization is similar, with deficits in muscle mass as early as 2-days following disuse in humans (473). Further, the rate of muscle loss is greatest in the first 7 days (474). Importantly, the overall rate of change is greater in denervation models of atrophy (475). As highlighted in Chapter 2.5.4, this bi-phasic atrophy is correlated with mitochondrial volume loss, implicating these organelles in mediating some aspects of the degree of disuse-atrophy.

2.5.2. PROTEIN DEGREDATION IN MUSCLE ATROPHY

Muscle mass is regulated by two opposing processes, the synthesis of proteins and organelles, and their degradation. It is an imbalance in these fundamental processes that ultimately promotes hypertrophy or atrophy of the tissue. Protein synthesis is largely mediated by growth factors such as IGF-1 and insulin, which stimulate intracellular signaling cascades that converge on AKT and mTOR to promote the synthesis of proteins (476–478). Simultaneously, this series of events impedes protein breakdown by indirectly inhibiting FoxO transcription factors (476, 477).

In response to prolonged inactivity, there is a net loss of proteins, resulting in atrophy (479, 480). Although decrements in protein synthesis have typically been hypothesized to produce this change (481), in various atrophic conditions the mTORC1 pathway activity is enhanced (479, 482–485). This staggering finding suggests that protein degradation pathways have a greater contribution to muscle atrophy, which will be detailed within this chapter. Several proteolytic systems converge, acting as a cohesive unit to produce atrophy of muscle with prolonged disuse and denervation (486). These include the ubiquitin-proteasome system (UPS) and the autophagy-lysosome system, calpains and caspases.

The UPS requires the targeting of proteins via the addition of polyubiquitin chains followed by docking at the multiunit proteasome and subsequent degradation (79, 487). Ubiquitination requires an E1 ubiquitin activating enzyme which primes ubiquitin (Ub). Next, an E2 conjugating enzyme will receive the Ub and with the help of an E3 ubiquitin ligase, thus Ub will be transferred to the target protein. It is these E3 ligases that create specificity (488). Muscle ring finger 1 (MuRF1) and muscle atrophy F-box (Atrogin1/MAFbx) are the most characterized E3-ub-ligases in skeletal muscle due to their exclusive expression in this tissue (488, 489). Other more recently identified E3 ligases that play a role in atrophy include Trim32, TRAF6, MUSA1, SMART and Nedd4-1 (488, 489). Not surprisingly, an overwhelming number of studies have reported increases in the expression of these E3-ligases and proteasome-related content in denervation or muscle inactivity (34, 35, 40, 41, 43, 116, 390, 472, 490–499). One study did also note a correlation between the phases of muscle loss and expression of atrogenes, whereby the upregulation of these genes is most pronounced at periods associated with rapid muscle atrophy (i.e., early post-denervation), followed by a normalization during a period where atrophy is slowed (i.e., late post-denervation) (472). Finally, the UPS has been shown to be vital for the atrophy process, since mice

deficient in MuRF1, MAFbx or TRAF6 are protected against muscular inactivity-induces loss of muscle mass (500–502).

Activation of UPS-related gene expression is mediated by multiple factors. For example, inflammatory cytokines such as TNFsα, TWEAK or IL-1 converge to activate the NF-κβ pathway, stimulating expression of atrogenes (489). Further, ROS can promote NF-κβ and FoxO expression (503). Importantly, these cytokines are enhanced with denervation (494, 496, 504), and muscle disuse (505) and likely promotes activation of the UPS-program. Furthermore, IGF-1 signaling cascades activate AKT, leading to repression of FoxO3. Thus, if IGF-1 is lessened, which seems to be the case with muscle disuse (506–509) and denervation (509–512), and insulin resistance develops, this may also contribute to atrophy. The pro-inflammatory cytokine IL-6 is also upregulated in denervation (494) and disuse atrophy (513) and is implicated in the control of signal transducers and activators of transcription 3 (STAT3) to promote atrophy-related gene expression. Finally, the AKT inhibiting cytokine TGF-β is upregulated in denervation atrophy (475, 514) and hindlimb unloading (515), but not immobilization (475). This molecule signals via Smad proteins. Ultimately, this pathway can regulate FoxO3 activity and UPS activation. Based on the premise that inflammation is a major contributor to disuse-induced atrophy, the group of Hualin Sun has recently published a series of studies, whereby they found that targeting these pathways pharmacologically blunts denervation-atrophy (359, 494–496, 516). As discussed in Chapter 4.5.4., perturbations in mitochondrial homeostasis are also implicated in the induction of atrophy with chronic disuse, and these systems may be co-regulated.

Calpains are Ca^{2+}-induced cysteine proteases, cleaving proteins, thereby priming the segments for degradation by other proteolytic systems. Importantly, these substrates consist of myofibril proteins and apoptotic factors (517). Calpains also mediate inflammatory signaling (NF-

κβ activation and TNF-α expression) (518, 519), and are implicated in the inactivation of AKT (520), both of which may perpetuate atrophy in skeletal muscle, as addressed above. Since ROS promote Ca^{2+} overload in muscle, mitochondrial dysfunction is implicated in the activation of calpains (see Chapter 2.5.4.). Of the many Calpains that exist in eukaryotic cells, calpains 1 and 2 are implicated in skeletal muscle (517). Calpains are activated with hindlimb casting and unloading. Importantly, both pharmacologic (521) and genetic inhibition (522, 523) of calains perturb the atrophy of muscle. These effects are more pronounced in slow muscle, likely a product of the accelerated muscle atrophy in these muscle types (522, 523). Similarity, caspases are Ca^{2+}-induced proteases, and are typically thought of for their role in apoptosis. Caspases cleave proteins which can alter their function or target them for breakdown. For example, in muscle, caspase 3 cleaves myofilament proteins for degradation by the UPS (524). It has been documented that activation of caspase occurs with both immobilization (521) and denervation (525, 526). Caspase inhibition attenuates atrophy (521, 525), however this seems to be due to an effect on apoptosis rather than actin cleavage and degradation (525).

These proteolytic mechanisms are implicated in the degradation of a wide array of proteins. However, they alone cannot degrade all long-lived proteins, aggregates, or organelles. Thus, these systems are coordinated with the autophagy lysosome system to promote atrophy, likely through the simultaneous induction of their genetic programs through shared upstream signaling mechanism.

2.5.3 THE AUTOPHAGY LYSOSOME SYSTEM IN ATROPHY

As highlighted in Chapter 2.2, the autophagy process is responsible for the degradation of long-lived organelles and protein aggregates via the lysosomes. Regarding its involvement in muscle atrophy, early reports by Dr. Stefano Schiaffino and colleagues found, via electron

microscopy, that in response to denervation there is increased presence of autophagic vacuoles (527).Work since this time has focused on the regulation of autophagy in a variety of conditions. Importantly, as addressed in Chapter 2.2., perturbations in autophagy alone are capable of eliciting muscle atrophy. Earlier work showed that activating autophagy via genetic manipulation (i.e., constituently active FoxO3) promotes atrophy (34). However, silencing LC3 prevented this atrophy, implying that blocking autophagy may help preserve muscle mass in atrophy conditions (528). Thus, studies have explored the merit of blocking autophagy in muscle wasting, such as denervation. Contrary to what was expected, blocking autophagy via genetic manipulation (i.e., TSC1/2, Atg7 knockout) in denervation models led to defective muscle performance and the accumulation of damaged/dysfunctional constituents, which ultimately accelerates muscle wasting (22, 529). Thus, balanced autophagy is required for muscle mass maintenance and the merit of targeting autophagy in slowing atrophy is an avenue commonly explored.

2.5.3.1. Upstream Autophagic Signaling

As discussed extensively in Chapter 2.2, autophagy is fine-tuned via interactions of kinases and their associated signaling pathways, which ultimately leads to activation of 1) genetic programs that produce proteins required enhanced autophagic capacity, 2) upstream autophagy (i.e., formation of autophagosomal membranes) and 3) autophagic degradation. This section is intended to detail the divergent responses regarding autophagy in denervation and disuse-atrophy.

In both denervation and immobilized muscle there is evidence of increases in FoxO3 transcript and protein (40, 43, 490–492). These changes likely support autophagy-related, and proteasomal gene expression. The importance of FoxO3 in promoting atrophy has been observed, whereby its inhibition reduced the extent of muscle atrophy in denervation and disuse models (41,

43, 383, 493, 530). This is at least in part due to a normalization of autophagy, leading to preserved muscle mass and function.

AKT is a core negative regulator of FoxO3 activity in skeletal muscle. Based on a variety of reports, it seems that AKT activity is reduced early in the denervation-response and is then progressively activated (39, 112, 475, 529, 531). This would presumably lead to early activation of FoxO3, through alleviation of its repression. However, phosphorylation on the inhibitory FoxO3 sites do not match these AKT activity changes (112, 475, 494), thus, other mechanisms may regulate FoxO3 in denervation. Despite these observations, nuclear FoxO3 content is upregulated following 3 days of denervation (40), which may serve to upregulate in autophagy gene expression. In contrast to denervation-atrophy, immobilization studies indicate that AKT activity is reduced as early as 1 day-post immobilization (499) and is sustained at lower levels in more prolonged interventions (116, 475, 497, 532, 533). This correlates with reduced inhibitory FoxO3 phosphorylation and enhanced nuclear FoxO3 at 3-days post-immobilization (43). Thus, AKT activity and its impact on FoxO3 appears to be stimulus dependent.

AMPK is another core regulator of both FoxO3 and Ulk1 activity. In denervated muscle, there is a time-dependent activation of AMPK whereby it is decreased early post-denervation (6-24hr) (491) and is then enhanced and sustained after 3 days (36, 112, 531). Correspondingly, these changes are coupled with increased AMPK-mediated phosphorylation of FoxO3 at 3 days post-denervation (31), as well as Ulk1 activating phosphorylation (36, 529, 531, 534). This would be indicative of 1) sustained autophagy activation and 2) inhibition of mTORC1 to preserve muscle mass. Like denervation, short-term disuse (i.e., 24 hr hindlimb suspension) reduces AMPK activity (499, 535). However, it remains unclear whether prolonged inactivity enhances (490, 536) or reduces (492, 537) AMPK. Nonetheless, AMPK-mediated Ulk1 activation and Atg13 are

increased following 6 and 12 hours of hindlimb suspension (538), but not with prolonged disuse (539), suggesting an early activation of autophagy.

Another core regulator of muscle size is mTORC1. As with the above signaling molecules, there are divergent responses in the regulation of mTORC1 activity with denervation and disuse models. In the denervation literature, enhanced mTORC1 activity is evident as early as 24-hours post-nerve transection and is sustained for at least 28 days (39, 111, 475). This correlates with elevated Ulk1 inactivating phosphorylation (529, 531), a mechanism which may serve to preserve muscle mass with denervation. This effect was only observed in fast muscle, and this may explain the greater autophagy and atrophy in slow muscle with denervation (111). Alternatively, with prolonged disuse, mTORC1 activation is reduced in slow muscle (116, 537), but remains unchanged in fast muscle (116, 475). This finding also supports the greater atrophy in slow muscle with disuse. Similarly, in humans no change in mTORC1 activity was measured following 2-weeks of immobilization (539, 540). As no changes in mTORC1 are measured in these studies, it is not surprising that many have failed to report changes in mTORC1-inactivating Ulk1 phosphorylation in disuse models (390, 475, 539).

2.5.3.2. Autophagic Clearance

The upstream processes discussed above are important and contribute to the upregulation of autophagy-related mRNA and protein in denervation (34–36, 359, 399, 475, 493–496, 531, 534, 541) and disuse models (41, 390, 490, 497, 498, 542–544). This upregulation in autophagic proteins likely support an enhanced capacity for autophagy. However, they are not necessarily indicative of changes in autophagic resolution. Thus, measurements of autophagosomal content (i.e., LC3-II) and flux have been made. Our group has shown decrements in both LC3-II and p62 flux following 7-days of denervation in the mouse tibialis anterior muscle (541). Similarly, Castets

et al., uncovered decreases in LC3-II flux at 7-days post denervation, but these investigators report elevations at 14 days onwards (529). The lower autophagy flux at 7-days may be mechanism to preserve muscle prior to the accumulation of damage that requires autophagic breakdown, or that the endogenous autophagy machinery is insufficient to support breakdown early post-denervation. More work is required to understand the early time-dependent changes in autophagy flux (i.e., prior to 7 days), as therapeutic treatments may vary based on time post-nerve injury.

Following short-term 3-day immobilization, autophagy flux, as assessed by both an LC3-II colchicine assay and mRFP-GFP-LC3 assay was found to be reduced (390). In another report utilizing colchicine, LC3-II flux was increased whereas p62 flux was decreased following 10 days of immobilization (532). As p62 and LC3-II are not mutually exclusive, these findings may suggest differential control of autophagic breakdown in muscle with disuse.

As highlighted in Chapter 2.2., autophagy flux in response to caloric restriction and exercise is greater in fast muscle, and this fiber type difference may influence autophagy in denervation and disuse models. In this vein, muscle specific deletion of the autophagy inhibitor TSC, accelerates muscle loss in slow muscle in the late stages of denervation (i.e., 28 days) (529). Alternatively, in fast muscle, TSC deletion accelerated muscle loss early in the denervation time course (i.e., 7 days) (529). These results indicate a differential regulation of autophagy in the progression of atrophy in slow versus fast muscle. Ultimately, with advancing scientific methodologies, more work is required to fully understand the impact of immobilization/disuse/denervation on autophagy flux, and to delineate the time-dependent changes in these disuse models.

2.5.3.3. Lysosomal Regulation

It has long been known that skeletal muscle disuse is matched with elevations in lysosomal content and proteolysis (545–548). However, as the molecular underpinnings of the autophagy-lysosome system have been uncovered, a budding interest in the investigation into lysosomes and muscle disuse has ensued. A variety of the methods used to assess disuse have cumulatively displayed results showing enhanced lysosome content, however future work must investigate the function of these lysosomes, as there have been indications of autophagy impairments in some of these models, as discussed above. For example, following 9-days of hindlimb suspension in rats, the soleus muscle contains elevated cathepsin mRNA (93). Further, 7 days of unilateral hindlimb immobilization led to elevated transcripts encoding LAMP2 in both the gastrocnemius and tibialis anterior muscles (543). Others have shown that 7 days of hindlimb casting increases cathepsin L transcript in the soleus and plantaris muscles of rats (116), and 14 days of casting elevated cathepsin L activity in the gastrocnemius muscle of mice (549). In mechanical ventilation models of muscle disuse, the diaphragm muscle exhibited elevated Cathepsin L and Cathepsin B mRNA and Cathepsin L activity (41, 498). Work from our group has reported that in muscle from 7 day denervated mice, there are accumulations in lysosomal protein (541), which could be explained by the increased total Tfeb protein that we observed (541). As such, there may be an increased drive for lysosome biogenesis to meet the denervation-induced autophagic demands placed on the muscle. However, we and others have also reported lysosomal impairments in 7-and-14-day denervated muscle, evident by the presence of lipofuscin (359, 399). These results suggest hindered lysosome function. Thus, the accumulation of lysosomal proteins could be explained by the build-up of dysfunctional organelles. As addressed in Chapter 2.4, lysosome impairment can lead to membrane instability, swelling and ultimately apoptosis through the release of cathepsins

(410). Thus, in denervation/disuse atrophy, if lysosome function is indeed impaired, these organelles may contribute to myonuclear apoptosis both directly, and indirectly through a lack of mitochondrial degradation (see mitochondrial apoptosis in Chapter 2.3.1.3). Thus, it is evident that functional assessment of lysosomes in disuse/denervated muscle is necessary. Ultimately, this work will allow us to explore the vitality of treating muscle wasting with lysosome-based therapies.

Further work is also required to understand the transcriptional control of lysosome biosynthetic pathways in disuse/denervation models. No direct assessments have been made measuring the signaling mechanisms discussed above (i.e., AMPK, mTORC1, AKT etc…) in denervation/disuse models. Further, as discussed above, ROS and associated damage is elevated in denervation (550–552) and disuse models of atrophy (116, 553, 554), and this is associated with high concentrations of cytosolic Ca^{2+} (555, 556). Both can act as signaling mechanisms that can promote Tfeb/3-mediated lysosome biogenesis. Thus, future work should aim to explore the requirement of these upstream signaling molecules and kinases in lysosome biosynthesis, and their role in the atrophy process.

2.5.4. MITOCHONDRIA IN MUSCLE ATROPHY

Contrary to chronic exercise, prolonged disuse is characterized by a reduction in mitochondrial content, ultimately shifting the metabolic phenotype of muscle toward that of a more glycolytic fiber (26,39). Just as muscle atrophy is biphasic, so too are the declines in mitochondrial content. Specifically, there is a rapid deficit in mitochondrial content over the first 5 days, followed by a more gradual loss through to 42 days of denervation (470). Importantly, loss in muscle mass is preceded by changes in mitochondrial content (557), suggesting that mitochondrial dysregulation may play a role the atrophy program in inactive muscle.

As discussed in more detail below, even with these decrements, the remaining mitochondrial pool is fragmented, and ROS production and ROS-induced damage are enhanced in disuse models (470, 552, 558–561). It is worth noting that these studies explored ROS production in isolated mitochondria preparations, indicating that these organelles contribute to disuse/denervation-induced oxidative stress, but may not account for the full oxidative phenotype in disuse/denervated muscle. Nonetheless, the bioproduct of sustained ROS production is vast, including 1) loss of mitochondrial membrane stability (562), 2) opening of the mitochondrial permeability transition pore (mPTP) (470, 563), 3) loss of membrane potential (561), and 4) damage to membranes, proteins, organelles, and nucleic acids (564–566). In light of this, indices of apoptosis including the increased expression of apoptotic proteins, upregulation the Bax:Bcl-2 ratio, cytochrome c release, AIF release and faster mtPTP kinetics are observed in denervation and disuse models (470, 526, 561, 563, 567, 568). Furthermore, it is these damaging effects that are thought to contribute to induction of the atrophy program through activation of proteolytic pathways. Thus, targeting mitochondrial dysfunction may provide therapeutic benefit in slowing atrophy.

Since oxidative stress can promote atrophy via impairing protein synthesis and activating proteolysis in muscle through autophagy, UPS, calpains, caspases and apoptosis (569, 570), multiple studies have investigated whether targeting mitochondrial ROS can slow / prevent muscle wasting in disuse models. For example, preconditioning and treatment with the antioxidant resveratrol reduced the extent of atrophy with hindlimb immobilization (571). Similarly, vitamin E reduced soleus muscle atrophy following 14 days of hindlimb unloading through blunting of caspase activity, calpain activity and UPS induction (572). However, these results were not reproduced when an antioxidant cocktail containing vitamin E was used (573). Furthermore,

Trolox, a vitamin E derivative did not prevent denervation atrophy (574) and n-acetyl cysteine (NAC) did not prevent disuse atrophy (575). These results must be interpreted carefully, as these compounds are not mitochondrial-specific, and have widescale system effects. However, the importance of mitochondrial ROS and the utility of targeting it has been shown in a series of studies where SS31 was used. For example, treatment with SS31 prevented atrophy following 7-day of casting (116). This was due to normalization of indices of autophagy, atrogene expression, and calpain activity (116). Furthermore, SS31 treatment normalized AKT signaling (116), which has implications on FoxO3 and Tfeb/3 activation. Similar effects were seen in the soleus and plantaris muscles with 14-days of casting in mice (559). Overall, there is strong evidence that specifically targeting mitochondrial oxidant production may be protective in atrophy.

2.5.4.1. Mitochondrial Biogenesis in Atrophying Muscle

During chronic disuse, loss of muscle mass is closely associated with declines in mitochondrial content. Research into alterations in mitochondrial biogenesis have developed an understanding of how atrophy stimuli promote a downregulation in mitochondrial volume. Early reports have shown rapid 80% reductions in PGC-1α transcript at 1-day post-denervation (472). We and others have also documented rapid declines in the levels of the PGC-1α and Tfam in the first 3-5-day of denervation (470, 576). Recent transcriptomic analysis confirmed deficits in the expression of mitochondrial genes in both denervation (577) and hindlimb suspension (578). Not only do fewer mitochondrial proteins get made, but the import machinery (579, 580) responsible for NuGEMP incorporation, and the rate of import (558) are reduced with chronic disuse. These changes ultimately result in the reduced mitochondrial content (166, 382, 581, 582).

PGC-1α also plays an integral role in regulation in muscle atrophy pathways. For example, PGC-1α overexpression attenuates muscle atrophy due to both increases in mitochondrial biogenesis, and inhibition of the FoxO3 and the UPS (583). More recently, Vainshtein et al., reported a similar blunting of denervation-atrophy in PGC-1α transgenic mice, but unlike the UPS measurements in the previous report, this study measured greater elevations in autophagy-lysosome proteins (541). In this same study, it was reported that lack of PGC-1α attenuated autophagic signaling and autophagy flux in denervated muscle (541). Furthermore, in hindlimb-unloading models of muscle inactivity, PGC1-α overexpression prevented atrophy, due to a blunted induction of the UPS, autophagy and mitochondrial fragmentation (584, 585). Cumulatively, this implies that PGC-1α regulates muscle atrophy beyond its role in mitochondrial biogenesis. Finally, PGC-1α also controls the expression of cardiolipin (CL) biosynthetic enzymes. CL is integral phospholipid that is integral in mitochondrial membrane stability and protein import. As such, chronic muscle disuse downregulates CL content in muscle (579, 580), leading to poor ETC performance and the production of ROS (586), which can perpetuate more muscle damage.

2.5.4.2. Mitochondrial Dynamics in Atrophying Muscle

The mitochondrial pool in inactive muscle, whether induced via disuse or denervation, becomes not only lessened, but increasingly dysfunctional. Dissimilar to the aging literature, there is far more consensus on the impact of disuse and denervation on changes in organelle dynamics. With denervation for example, there are decreases in the fusion:fission regulatory protein ratio (134), including reports of enhanced fission protein content (Drp1, Fis1) and of decreased fusion proteins (Mfn1 and Opa1) (531, 567), promoting a fragmented phenotype. Similarly, in

immobilization models, there is a substantial decrease in fusion proteins after 3 days of immobilization (135) and a moderate decrease in pro-fusion Mfn2 protein over the course of 3 weeks, whereas the pro-fission protein Fis1 doubled by 2-weeks (542). These protein changes may be due, in part, due to the transcriptional control of PGC-1α Mfn2 (587). Cumulatively, these results suggest that mitochondrial dynamics are altered in a time-dependent manner, resulting in a fragmented organellar pool that may potentiate mitophagy in disuse and denervation chronic muscle disuse. Uniquely, mitochondrial dynamics may be a therapeutic target in denervation-atrophy. This reasoning comes from multiple reports that show overexpression of the fusion proteins Mfn1 (567) and Opa1 (136) preserved mitochondrial and muscle homoeostasis. Furthermore, activating mitochondrial fission alone induces muscle atrophy (177), thus, the fragmentation observed in chronic disuse models may be causative in muscle wasting.

2.5.4.3. Mitophagy in Atrophying Muscle

This enhanced organelle fission signature in skeletal muscle atrophy would likely support mitophagy. In fact, in both fast and slow muscle there are reports of elevated Parkin mRNA and protein at 7- (94, 137) and 14-days post-denervation (359, 494–496, 534). Although one study failed to measure any denervation-induced change in mitochondrial Parkin (137), there are multiple reports of increased Pink1 and Parkin in isolated mitochondria from denervated animals (399, 531, 567). In addition, p62 (399, 531, 541), an adaptor protein specific to Pink1/Parkin mitophagy, and ubiquitin (541) are present in isolated mitochondria from denervated rodents. These results suggest increased capacity for Pink1/Parkin-mediated mitophagy with denervation. In fact, Pink1/Parkin-mediated mitophagy may contribute to atrophy, as Parkin null mice retain soleus mass after denervation, even with higher indices of mitochondrial dysfunction (137). In contrast, there is scare literature with respect to mitophagy receptors in denervation, apart from

observed increases in whole muscle BNIP3 protein by the group of Dr. Hualin Sun (494–496). Cumulatively, these data indicate that mitochondria are tagged for degradation during denervation, however more work is required to determine localization of mitophagy receptors with denervation, and their role in the contribution of denervation-atrophy. In isolated mitochondria from denervated animals, there is evidence of increased LC3-II (399, 531, 541) suggestive of autophagosomal engulfment. When flux was assessed via colchicine, Vainshtein et al., observed enhanced mitophagy flux at 7 days post-denervation (541), whereas Tamura et al., measure reduced LC3-II flux in 10 day denervated muscle (531). Thus, the regulation of mitophagic targeting and flux differ throughout the course of denervation. More research is required to investigate the immediate-early response of muscle mitophagy to denervation.

In contrast, with disuse atrophy there is far more controversy surrounding the regulation of mitophagy. For example, one report measured elevated gene expression and protein levels of mitophagy receptors Bnip3 and Nix, but not Fundc1 or Pink1/Parkin with 3 days of hindlimb suspension (590). Alternatively, 7-days of unilateral immobilization increased the protein levels of Bnip3, Nix and Fundc1 in the gastrocnemius muscle, but only Nix in the TA muscle (543). Furthermore, Kang et al., measured mitophagy receptors over the course of 1-3 weeks of hindlimb immobilization and found decreases in whole muscle Bnip3 after 1 week of immobilization, which was sustained at a later, 3-week timepoint (542). Furthermore, in isolated mitochondria there were declines in Pink1 at 3-weeks of immobilization, whereas mitochondrial-Parkin was elevated in the first 2 weeks of immobilization and reduced to control levels at 3-weeks (542). Recently, it was also reported that 28 days of hindlimb suspension in rats had no impact on Pink1, Parkin or Bnip3 protein (544). Furthermore, 12 hours of mechanical ventilation, used as a model muscle disuse, led to increases in Pink1, Bnip3 and Nix mRNA(41, 498). In many of these studies, the lack of

appropriate mitophagy flux measures fails to encapsulate the dynamics of this process. However, the trend in the data referred to above seems to suggest that mitophagy is enhanced.

2.6. References

1. **Janssen I**, **Heymsfield SB**, **Wang Z**, **Ross R**. Skeletal muscle mass and distribution in 468 men and women aged 18–88 yr. *Journal of Applied Physiology* 89: 81–88, 2000. doi: 10.1152/JAPPL.2000.89.1.81.

2. **Argilés JM**, **Campos N**, **Lopez-Pedrosa JM**, **Rueda R**, **Rodriguez-Mañas L**. Skeletal Muscle Regulates Metabolism via Interorgan Crosstalk: Roles in Health and Disease. *Journal of the American Medical Directors Association* 17: 789–796, 2016. doi: 10.1016/J.JAMDA.2016.04.019.

3. **Gotti C**, **Sensini A**, **Zucchelli A**, **Carloni R**, **Focarete ML**. Hierarchical fibrous structures for muscle-inspired soft-actuators: A review. *Applied Materials Today* 20: 100772, 2020. doi: 10.1016/J.APMT.2020.100772.

4. **Shishmarev D**. Excitation-contraction coupling in skeletal muscle: recent progress and unanswered questions. *Biophysical Reviews 2020 12:1* 12: 143–153, 2020. doi: 10.1007/S12551-020-00610-X.

5. **Calderón JC**, **Bolaños P**, **Caputo C**. The excitation–contraction coupling mechanism in skeletal muscle. *Biophysical Reviews* 6: 133, 2014. doi: 10.1007/S12551-013-0135-X.

6. **Tupling AR**. The decay phase of Ca2+ transients in skeletal muscle: regulation and physiology. *Applied Physiology, Nutrition and Metabolism* 34: 373–376, 2009. doi: 10.1139/H09-033.

7. **Pette D**, **Vrbová G**. Invited review: Neural control of phenotypic expression in mammalian muscle fibers. *Muscle & Nerve* 8: 676–689, 1985. doi: 10.1002/MUS.880080810.

8. **Nemeth PM**, **Pette D**, **Vrbová G**. Comparison of enzyme activities among single muscle fibres within defined motor units. *The Journal of Physiology* 311: 489, 1981. doi: 10.1113/JPHYSIOL.1981.SP013600.

9. **Mendell LM**. The size principle: a rule describing the recruitment of motoneurons. *Journal of Neurophysiology* 93: 3024–3026, 2005. doi: 10.1152/CLASSICESSAYS.00025.2005.

10. **Bawa PNS**, **Jones KE**, **Stein RB**. Assessment of size ordered recruitment. *Frontiers in Human Neuroscience* 8, 2014. doi: 10.3389/FNHUM.2014.00532.

11. **Guimarães-Ferreira L**. Role of the phosphocreatine system on energetic homeostasis in skeletal and cardiac muscles. *Einstein* 12: 126, 2014. doi: 10.1590/S1679-45082014RB2741.

12. **Hargreaves M**, **Spriet LL**. Skeletal muscle energy metabolism during exercise. *Nature Metabolism 2020 2:9* 2: 817–828, 2020. doi: 10.1038/s42255-020-0251-4.

13. **Baker JS**, **McCormick MC**, **Robergs RA**. Interaction among skeletal muscle metabolic energy systems during intense exercise. *Journal of Nutrition and Metabolism* 2010, 2010. doi: 10.1155/2010/905612.

14. **Schiaffino S**, **Reggiani C**. Fiber Types in Mammalian Skeletal Muscles. *Physiological Reviews* 91: 1447–1531, 2011. doi: 10.1152/PHYSREV.00031.2010.

15. **Tsukada M**, **Ohsumi Y**. Isolation and characterization of autophagy-defective mutants of Saccharomyces cerevisiae. *FEBS Letters* 333: 169–174, 1993. doi: 10.1016/0014-5793(93)80398-E.

16. **Takeshige K**, **Baba M**, **Tsuboi S**, **Noda T**, **Ohsumi Y**. Autophagy in Yeast Demonstrated with Proteinase-deficient Mutants and Conditions for its Induction. *Journal of Cell Biology* 119: 301–311, 1992. doi: 10.1083/jcb.119.2.301.

17. **Ohsumi Y**. Historical landmarks of autophagy research. *Cell Research* 24: 9–23, 2014. doi: 10.1038/CR.2013.169.

18. **Mijaljica D**, **Prescott M**, **Devenish RJ**. Microautophagy in mammalian cells: Revisiting a 40-year-old conundrum. *Autophagy* 7: 673–682, 2011. doi: 10.4161/AUTO.7.7.14733.

19. **Kaushik S**, **Cuervo AM**. Chaperone-mediated autophagy: a unique way to enter the lysosome world. *Trends in Cell Biology* 22: 407, 2012. doi: 10.1016/J.TCB.2012.05.006.

20. **Das G**, **Shravage B v.**, **Baehrecke EH**. Regulation and function of autophagy during cell survival and cell death. *Cold Spring Harbor Perspectives in Biology* 4: 1–14, 2012. doi: 10.1101/cshperspect.a008813.

21. **Raben N**, **Hill V**, **Shea L**, **Takikita S**, **Baum R**, **Mizushima N**, **Ralston E**, **Plotz P**. Suppression of autophagy in skeletal muscle uncovers the accumulation of ubiquitinated proteins and their potential role in muscle damage in Pompe disease. *Human Molecular Genetics* 17: 3897–908, 2008. doi: 10.1093/hmg/ddn292.

22. **Masiero E**, **Agatea L**, **Mammucari C**, **Blaauw B**, **Loro E**, **Komatsu M**, **Metzger D**, **Reggiani C**, **Schiaffino S**, **Sandri M**. Autophagy Is Required to Maintain Muscle Mass. *Cell Metabolism* 10: 507–515, 2009. doi: 10.1016/j.cmet.2009.10.008.

23. **Carnio S**, **LoVerso F**, **Baraibar MA**, **Longa E**, **Khan MM**, **Maffei M**, **Reischl M**, **Canepari M**, **Loefler S**, **Kern H**, **Blaauw B**, **Friguet B**, **Bottinelli R**, **Rudolf R**, **Sandri M**. Autophagy Impairment in Muscle Induces Neuromuscular Junction Degeneration and Precocious Aging. *Cell Reports* 8: 1509–1521, 2014. doi: 10.1016/j.celrep.2014.07.061.

24. **Paré MF**, **Baechler BL**, **Fajardo VA**, **Earl E**, **Wong E**, **Campbell TL**, **Tupling AR**, **Quadrilatero J**. Effect of acute and chronic autophagy deficiency on skeletal muscle apoptotic signaling, morphology, and function. *Biochimica et Biophysica Acta - Molecular Cell Research* 1864: 708–718, 2017. doi: 10.1016/j.bbamcr.2016.12.015.

25. **Nemazanyy I**, **Blaauw B**, **Paolini C**, **Caillaud C**, **Protasi F**, **Mueller A**, **Proikas-Cezanne T**, **Russell RC**, **Guan KL**, **Nishino I**, **Sandri M**, **Pende M**, **Panasyuk G**. Defects of Vps15 in skeletal muscles lead to autophagic vacuolar myopathy and lysosomal disease. *EMBO Molecular Medicine* 5: 870–890, 2013. doi: 10.1002/emmm.201202057.

26. **Triolo M**, **Hood DA**. Mitochondrial breakdown in skeletal muscle and the emerging role of the lysosomes. *Archives of Biochemistry and Biophysics* 661, 2019. doi: 10.1016/j.abb.2018.11.004.

27. **VanderVeen BN**, **Fix DK**, **Carson JA**. Disrupted Skeletal Muscle Mitochondrial Dynamics, Mitophagy, and Biogenesis during Cancer Cachexia: A Role for Inflammation. *Oxidative Medicine and Cellular Longevity* 2017: 1–13, 2017. doi: 10.1155/2017/3292087.

28. **Moore TM**, **Lin AJ**, **Strumwasser AR**, **Cory K**, **Whitney K**, **Ho T**, **Ho T**, **Lee JL**, **Rucker DH**, **Nguyen CQ**, **Yackly A**, **Mahata SK**, **Wanagat J**, **Stiles L**, **Turcotte LP**, **Crosbie RH**, **Zhou Z**. Mitochondrial Dysfunction Is an Early Consequence of Partial or Complete Dystrophin Loss in mdx Mice. *Frontiers in Physiology* 11, 2020. doi: 10.3389/FPHYS.2020.00690.

29. **Penna F**, **Ballarò R**, **Martinez-Cristobal P**, **Sala D**, **Sebastian D**, **Busquets S**, **Muscaritoli M**, **Argilés JM**, **Costelli P**, **Zorzano A**. Autophagy Exacerbates Muscle Wasting in Cancer Cachexia

and Impairs Mitochondrial Function. *Journal of Molecular Biology* 431: 2674–2686, 2019. doi: 10.1016/J.JMB.2019.05.032.

30. **Pauly M**, **Daussin F**, **Burelle Y**, **Li T**, **Godin R**, **Fauconnier J**, **Koechlin-Ramonatxo C**, **Hugon G**, **Lacampagne A**, **Coisy-Quivy M**, **Liang F**, **Hussain S**, **Matecki S**, **Petrof BJ**. AMPK Activation Stimulates Autophagy and Ameliorates Muscular Dystrophy in the mdx Mouse Diaphragm. *The American Journal of Pathology* 181: 583–592, 2012. doi: 10.1016/J.AJPATH.2012.04.004.

31. **Ballarò R**, **Beltrà M**, **Lucia S de**, **Pin F**, **Ranjbar K**, **Hulmi JJ**, **Costelli P**, **Penna F**. Moderate exercise in mice improves cancer plus chemotherapy-induced muscle wasting and mitochondrial alterations. *The FASEB Journal* 33: 5482–5494, 2019. doi: 10.1096/FJ.201801862R.

32. **Aversa Z**, **Pin F**, **Lucia S**, **Penna F**, **Verzaro R**, **Fazi M**, **Colasante G**, **Tirone A**, **Fanelli FR**, **Ramaccini C**, **Costelli P**, **Muscaritoli M**. Autophagy is induced in the skeletal muscle of cachectic cancer patients. *Scientific Reports* 6: 30340, 2016. doi: 10.1038/srep30340.

33. **Sandri M**, **Sandri C**, **Gilbert A**, **Skurk C**, **Calabria E**, **Picard A**, **Walsh K**, **Schiaffino S**, **Lecker SH**, **Goldberg AL**. Foxo transcription factors induce the atrophy-related ubiquitin ligase atrogin-1 and cause skeletal muscle atrophy. *Cell* 117: 399–412, 2004. doi: 10.1016/S0092-8674(04)00400-3.

34. **Zhao J**, **Brault JJ**, **Schild A**, **Cao P**, **Sandri M**, **Schiaffino S**, **Lecker SH**, **Goldberg AL**. FoxO3 Coordinately Activates Protein Degradation by the Autophagic/Lysosomal and Proteasomal Pathways in Atrophying Muscle Cells. *Cell Metabolism* 6: 472–483, 2007. doi: 10.1016/j.cmet.2007.11.004.

35. **Mammucari C**, **Milan G**, **Romanello V**, **Masiero E**, **Rudolf R**, **del Piccolo P**, **Burden SJ**, **di Lisi R**, **Sandri C**, **Zhao J**, **Goldberg AL**, **Schiaffino S**, **Sandri M**. FoxO3 Controls Autophagy in Skeletal Muscle In Vivo. *Cell Metabolism* 6: 458–471, 2007. doi: 10.1016/j.cmet.2007.11.001.

36. **Stouth DW**, **vanLieshout TL**, **Ng SY**, **Webb EK**, **Manta A**, **Moll Z**, **Ljubicic V**. CARM1 Regulates AMPK Signaling in Skeletal Muscle. *iScience* 23: 101755, 2020. doi: 10.1016/j.isci.2020.101755.

37. **Liu Y**, **Li J**, **Shang Y**, **Guo Y**, **Li Z**. CARM1 contributes to skeletal muscle wasting by mediating FoxO3 activity and promoting myofiber autophagy. *Experimental Cell Research* 374: 198–209, 2019. doi: 10.1016/j.yexcr.2018.11.024.

38. **Lee D**, **Goldberg AL**. SIRT1 protein, by blocking the activities of transcription factors FoxO1 and FoxO3, inhibits muscle atrophy and promotes muscle growth. *Journal of Biological Chemistry* 288: 30515–30526, 2013. doi: 10.1074/jbc.M113.489716.

39. **Tang H**, **Inoki K**, **Lee M**, **Wright E**, **Khuong A**, **Khuong A**, **Sugiarto S**, **Garner M**, **Paik J**, **DePinho RA**, **Goldman D**, **Guan KL**, **Shrager JB**. MTORC1 promotes denervation-induced muscle atrophy through a mechanism involving the activation of FoxO and E3 ubiquitin ligases. *Science Signaling* 7, 2014. doi: 10.1126/scisignal.2004809.

40. **Bertaggia E**, **Coletto L**, **Sandri M**. Posttranslational modifications control FoxO3 activity during denervation. *American Journal of Physiology - Cell Physiology* 302: 587–596, 2012. doi: 10.1152/ajpcell.00142.2011.

41. **Smuder AJ**, **Sollanek KJ**, **Min K**, **Nelson WB**, **Powers SK**. Inhibition of forkhead BoxO-specific transcription prevents mechanical ventilation-induced diaphragm dysfunction. *Critical Care Medicine* 43: e133–e142, 2015. doi: 10.1097/CCM.0000000000000928.

42. **Reed SA**, **Sandesara PB**, **Senf SM**, **Judge AR**. Inhibition of FoxO transcriptional activity prevents muscle fiber atrophy during cachexia and induces hypertrophy. *The FASEB Journal* 26: 987, 2012. doi: 10.1096/FJ.11-189977.

43. **Senf SM**, **Dodd SL**, **Judge AR**. FOXO signaling is required for disuse muscle atrophy and is directly regulated by Hsp70. *American Journal of Physiology - Cell Physiology* 298: C38, 2010. doi: 10.1152/ajpcell.00315.2009.

44. **Sanchez AMJ**, **Candau RB**, **Bernardi H**. FoxO transcription factors: their roles in the maintenance of skeletal muscle homeostasis. *Cellular and Molecular Life Sciences 2013 71:9* 71: 1657–1671, 2013. doi: 10.1007/S00018-013-1513-Z.

45. **Martina JA**, **Diab HI**, **Li H**, **Puertollano R**. Novel roles for the MiTF/TFE family of transcription factors in organelle biogenesis, nutrient sensing, and energy homeostasis. *Cellular and Molecular Life Sciences* 71: 2483–97, 2014. doi: 10.1007/s00018-014-1565-8.

46. **Palmieri M**, **Impey S**, **Kang H**, **Ronza A**, **Pelz C**, **Sardiello M**, **Ballabio A**. Characterization of the CLEAR network reveals an integrated control of cellular clearance pathways. 20: 3852–3866, 2011. doi: 10.1093/hmg/ddr306.

47. **Martina JA**, **Diab HI**, **Lishu L**, **Jeong-A L**, **Patange S**, **Raben N**, **Puertollano R**. The nutrient-responsive transcription factor TFE3 promotes autophagy, lysosomal biogenesis, and clearance of cellular debris. *Science Signaling* 7, 2014. doi: 10.1126/scisignal.2004754.

48. **Settembre C**, **Polito VA**, **Garcia M**, **Vetrini F**, **Erdin S**, **Erdin SU**, **Huynh T**, **Medina D**, **Colella P**, **Sardiello M**, **Rubinsztein DC**, **Ballabio A**. TFEB Links Autophagy to Lysosomal Biogenesis. 332: 1429–1433, 2013. doi: 10.1126/science.1204592.TFEB.

49. **Sardiello M**, **Palmieri M**, **di Ronza A**, **Medina DL**, **Valenza M**, **Gennarino VA**, **di Malta C**, **Donaudy F**, **Embrione V**, **Polishchuk RS**, **Banfi S**, **Parenti G**, **Cattaneo E**, **Ballabio A**. A gene network regulating lysosomal biogenesis and function. *Science (New York, NY)* 325: 473–7, 2009. doi: 10.1126/science.1174447.

50. **Ploper D**, **de Robertis EM**. The MITF family of transcription factors: Role in endolysosomal biogenesis, Wnt signaling, and oncogenesis. *Pharmacological Research* 99: 36–43, 2015. doi: 10.1016/J.PHRS.2015.04.006.

51. **Slade L**, **Pulinilkunnil T**. The MiTF/TFE family of transcription factors: Master regulators of organelle signaling, metabolism, and stress adaptation. *Molecular Cancer Research* 15: 1637–1643, 2017.

52. **Mansueto G**, **Armani A**, **Viscomi C**, **Zeviani M**, **Sandri M**, **Ballabio A**, **Mansueto G**, **Armani A**, **Viscomi C**, **Orsi LD**, **Cegli R de**, **Polishchuk E v**, **Lamperti C**, **Meo I di**, **Romanello V**, **Marchet S**, **Saha PK**, **Zong H**. Transcription factor EB controls metabolic flexibility during exercise. *Cell Metabolism* 25: 182–196, 2017. doi: 10.1016/j.cmet.2016.11.003.

53. **Hosokawa N**, **Sasaki T**, **Iemura SI**, **Natsume T**, **Hara T**, **Mizushima N**. Atg101, a novel mammalian autophagy protein interacting with Atg13. *Autophagy* 5: 973–979, 2009. doi: 10.4161/auto.5.7.9296.

54. **Mercer CA**, **Kaliappan A**, **Dennis PB**. A novel, human Atg13 binding protein, Atg101, interacts with ULK1 and is essential for macroautophagy. *Autophagy* 5: 649–662, 2009. doi: 10.4161/auto.5.5.8249.

55. **Noda NN**, **Mizushima N**. Atg101: Not just an accessory subunit in the autophagy-initiation complex. *Cell Structure and Function* 41: 13–20, 2016.

56. **Hara T**, **Mizushima N**. Role of ULK-FIP200 complex in mammalian autophagy: FIP200, a counterpart of yeast Atg17? *Autophagy* 5: 85–87, 2009. doi: 10.4161/auto.5.1.7180.

57. **Hara T**, **Takamura A**, **Kishi C**, **Iemura SI**, **Natsume T**, **Guan JL**, **Mizushima N**. FIP200, a ULK-interacting protein, is required for autophagosome formation in mammalian cells. *Journal of Cell Biology* 181: 497–510, 2008. doi: 10.1083/jcb.200712064.

58. **Chang YY**, **Neufeld TP**. An Atg1/Atg13 complex with multiple roles in TOR-mediated autophagy regulation. *Molecular Biology of the Cell* 20: 2004–2014, 2009. doi: 10.1091/mbc.E08-12-1250.

59. **Alers S**, **Loffler AS**, **Wesselborg S**, **Stork B**. Role of AMPK-mTOR-Ulk1/2 in the Regulation of Autophagy: Cross Talk, Shortcuts, and Feedbacks. *Molecular and Cellular Biology* 32: 2–11, 2012. doi: 10.1128/mcb.06159-11.

60. **Egan D**, **Kim J**, **Shaw RJ**, **Guan K-L**. The autophagy initiating kinase ULK1 is regulated via opposing phosphorylation by AMPK and mTOR. *Autophagy* 7: 643–4, 2011. doi: 10.4161/AUTO.7.6.15123.

61. **Kim Joungmok, Kundu Mondira, Viollet Benoit GK-L**. AMPK and mTOR regulate autophagy through direct phosphorylation of Ulk1. 48: 1–6, 2010. doi: 10.1097/MPG.0b013e3181a15ae8.Screening.

62. **Nichenko AS**, **Sorensen JR**, **Southern WM**, **Qualls AE**, **Schifino AG**, **McFaline-Figueroa J**, **Blum JE**, **Tehrani KF**, **Yin H**, **Mortensen LJ**, **Thalacker-Mercer AE**, **Greising SM**, **Call JA**. Lifelong Ulk1-Mediated Autophagy Deficiency in Muscle Induces Mitochondrial Dysfunction and Contractile Weakness. *International Journal of Molecular Sciences* 22: 1937, 2021. doi: 10.3390/ijms22041937.

63. **Fuqua JD**, **Mere CP**, **Kronemberger A**, **Blomme J**, **Bae D**, **Turner KD**, **Harris MP**, **Scudese E**, **Edwards M**, **Ebert SM**, **Sousa LGO de**, **Bodine SC**, **Yang L**, **Adams CM**, **Lira VA**. ULK2 is essential for degradation of ubiquitinated protein aggregates and homeostasis in skeletal muscle. *The FASEB Journal* 33: 11735, 2019. doi: 10.1096/FJ.201900766R.

64. **di Bartolomeo S**, **Corazzari M**, **Nazio F**, **Oliverio S**, **Lisi G**, **Antonioli M**, **Pagliarini V**, **Matteoni S**, **Fuoco C**, **Giunta L**, **D'Amelio M**, **Nardacci R**, **Romagnoli A**, **Piacentini M**, **Cecconi F**, **Fimia GM**. The dynamic interaction of AMBRA1 with the dynein motor complex regulates mammalian autophagy. *Journal of Cell Biology* 191: 155–168, 2010. doi: 10.1083/jcb.201002100.

65. **Backer JM**. The intricate regulation and complex functions of the Class III phosphoinositide 3-kinase Vps34. *Biochemical Journal* 473: 2251–2271, 2016.

66. **Yue Z**, **Zhong Y**. From a global view to focused examination: Understanding cellular function of lipid kinase VPS34-Beclin 1 complex in autophagy. *Journal of Molecular Cell Biology* 2: 305–307, 2010. doi: 10.1093/jmcb/mjq028.

67. **Russell RC**, **Tian Y**, **Yuan H**, **Park HW**, **Chang YY**, **Kim J**, **Kim H**, **Neufeld TP**, **Dillin A**, **Guan KL**. ULK1 induces autophagy by phosphorylating Beclin-1 and activating VPS34 lipid kinase. *Nature Cell Biology* 15: 741–750, 2013. doi: 10.1038/ncb2757.

68. **Park J-M**, **Seo M**, **Jung CH**, **Grunwald D**, **Stone M**, **Otto NM**, **Toso E**, **Ahn Y**, **Kyba M**, **Griffin TJ**, **Higgins L**, **Kim D-H**. ULK1 phosphorylates Ser30 of BECN1 in association with ATG14 to stimulate autophagy induction. *Autophagy* 14: 584, 2018. doi: 10.1080/15548627.2017.1422851.

69. **Wei Y**, **Liu M**, **Li X**, **Liu J**, **Li H**. Origin of the Autophagosome Membrane in Mammals. *BioMed Research International* 2018, 2018. doi: 10.1155/2018/1012789.

70. **Orsi A**, **Razi M**, **Dooley HC**, **Robinson D**, **Weston AE**, **Collinson LM**, **Tooze SA**. Dynamic and transient interactions of Atg9 with autophagosomes, but not membrane integration, are required for autophagy. *Molecular Biology of the Cell* 23: 1860, 2012. doi: 10.1091/MBC.E11-09-0746.

71. **Parzych KR**, **Klionsky DJ**. An overview of autophagy: Morphology, mechanism, and regulation. *Antioxidants and Redox Signaling* 20: 460–473, 2014.

72. **Kabeya Y**, **Mizushima N**, **Ueno T**, **Yamamoto A**, **Kirisako T**, **Noda T**, **Kominami E**, **Ohsumi Y**, **Yoshimori T**. LC3, a mammalian homologue of yeast Apg8p, is localized in autophagosome membranes after processing. *EMBO Journal* 19: 5720–5728, 2000. doi: 10.1093/emboj/19.21.5720.

73. **Hemelaar J**, **Lelyveld VS**, **Kessler BM**, **Ploegh HL**. A Single Protease, Apg4B, Is Specific for the Autophagy-related Ubiquitin-like Proteins GATE-16, MAP1-LC3, GABARAP, and Apg8L. *Journal of Biological Chemistry* 278: 51841–51850, 2003. doi: 10.1074/jbc.M308762200.

74. **Weidberg H**, **Shvets E**, **Shpilka T**, **Shimron F**, **Shinder V**, **Elazar Z**. LC3 and GATE-16/GABARAP subfamilies are both essential yet act differently in autophagosome biogenesis. *EMBO Journal* 29: 1792–1802, 2010. doi: 10.1038/emboj.2010.74.

75. **Lira VA**, **Okutsu M**, **Zhang M**, **Greene NP**, **Laker RC**, **Breen DS**, **Hoehn KL**, **Yan Z**. Autophagy is required for exercise training-induced skeletal muscle adaptation and improvement of physical performance. *FASEB journal : official publication of the Federation of American Societies for Experimental Biology* 27: 4184–93, 2013. doi: 10.1096/fj.13-228486.

76. **Mofarrahi M**, **Guo Y**, **Haspel J a**, **Choi AMK**, **Davis EC**, **Gouspillou G**, **Hepple RT**, **Godin R**, **Burelle Y**, **Hussain SN a**. Autophagic flux and oxidative capacity of skeletal muscles during acute starvation. *Autophagy* 9: 1604–1620, 2013. doi: 10.4161/auto.25955.

77. **Mizushima N**, **Yamamoto A**, **Matsui M**, **Yoshimori T**, **Ohsumi Y**. In Vivo Analysis of Autophagy in Response to Nutrient Starvation Using Transgenic Mice Expressing a Fluorescent Autophagosome Marker. *Molecular Biology of the Cell* 15: 1101, 2004. doi: 10.1091/MBC.E03-09-0704.

78. **Khaminets A**, **Behl C**, **Dikic I**. Ubiquitin-Dependent And Independent Signals In Selective Autophagy. *Trends in Cell Biology* 26: 6–16, 2016.

79. **Pohl C**, **Dikic I**. Cellular quality control by the ubiquitin-proteasome system and autophagy. *Science* 366: 818–822, 2019.

80. **Lippai M**, **Lőw P**. The Role of the Selective Adaptor p62 and Ubiquitin-Like Proteins in Autophagy. *BioMed Research International* 2014, 2014.

81. **Pankiv S**, **Clausen TH**, **Lamark T**, **Brech A**, **Bruun J-A**, **Outzen H**, **Øvervatn A**, **Bjørkøy G**, **Johansen T**. p62/SQSTM1 binds directly to Atg8/LC3 to facilitate degradation of ubiquitinated protein aggregates by autophagy. *The Journal of Biological Chemistry* 282: 24131–45, 2007. doi: 10.1074/jbc.M702824200.

82. **Kirkin V**, **Lamark T**, **Sou YS**, **Bjørkøy G**, **Nunn JL**, **Bruun JA**, **Shvets E**, **McEwan DG**, **Clausen TH**, **Wild P**, **Bilusic I**, **Theurillat JP**, **Øvervatn A**, **Ishii T**, **Elazar Z**, **Komatsu M**, **Dikic I**, **Johansen T**. A Role for NBR1 in Autophagosomal Degradation of Ubiquitinated Substrates. *Molecular Cell* 33: 505–516, 2009. doi: 10.1016/j.molcel.2009.01.020.

83. **Wild P**, **Farhan H**, **McEwan DG**, **Wagner S**, **Rogov V v.**, **Brady NR**, **Richter B**, **Korac J**, **Waidmann O**, **Choudhary C**, **Dötsch V**, **Bumann D**, **Dikic I**. Phosphorylation of the autophagy receptor optineurin restricts Salmonella growth. *Science* 333: 228–233, 2011. doi: 10.1126/science.1205405.

84. **Ying H**, **Yue BYJT**. Optineurin: The autophagy connection. *Experimental Eye Research* 144: 73–80, 2016.

85. **Lu K**, **Psakhye I**, **Jentsch S**. Autophagic clearance of PolyQ proteins mediated by ubiquitin-Atg8 adaptors of the conserved CUET protein family. *Cell* 158: 549–563, 2014. doi: 10.1016/j.cell.2014.05.048.

86. **Birgisdottir ÅB**, **Lamark T**, **Johansen T**. The LIR motif - crucial for selective autophagy. *Journal of Cell Science* 126: 3237–47, 2013. doi: 10.1242/jcs.126128.

87. **Johansen T**, **Lamark T**. Selective autophagy mediated by autophagic adapter proteins. *Autophagy* 7: 279–96, 2011. doi: 10.4161/AUTO.7.3.14487.

88. **Noda T**, **Fujita N**, **Yoshimori T**. The late stages of autophagy: How does the end begin? *Cell Death and Differentiation* 16: 984–990, 2009.

89. **Monastyrska I**, **Rieter E**, **Klionsky DJ**, **Reggiori F**. Multiple roles of the cytoskeleton in autophagy. *Biological Reviews* 84: 431–448, 2009.

90. **Ju J-S**, **Varadhachary AS**, **Miller SE**, **Weihl CC**. Quantitation of autophagic flux in mature skeletal muscle. *Autophagy* 6: 929–35, 2010. doi: 10.4161/auto.6.7.12785.

91. **Ching JK**, **Ju JS**, **Pittman SK**, **Margeta M**, **Weihl CC**. Increased autophagy accelerates colchicine-induced muscle toxicity. *Autophagy* 9: 2115–2125, 2013. doi: 10.4161/AUTO.26150.

92. **Mindell JA**. Lysosomal Acidification Mechanisms. *Annual Review of Physiology* 74: 69–86, 2012. doi: 10.1146/annurev-physiol-012110-142317.

93. **Bechet D**, **Tassa A**, **Taillandier D**, **Combaret L**, **Attaix D**. Lysosomal proteolysis in skeletal muscle. *International Journal of Biochemistry and Cell Biology* 37: 2098–2114, 2005.

94. **Ballabio A**, **Bonifacino JS**. Lysosomes as dynamic regulators of cell and organismal homeostasis. *Nature Reviews Molecular Cell Biology* 21: 101–118, 2020.

95. **Lawrence RE**, **Zoncu R**. The lysosome as a cellular centre for signalling, metabolism and quality control. *Nature Cell Biology* 21: 133–142, 2019.

96. **Todkar K**, **Ilamathi HS**, **Germain M**. Mitochondria and Lysosomes: Discovering Bonds. *Frontiers in Cell and Developmental Biology* 0: 106, 2017. doi: 10.3389/FCELL.2017.00106.

97. **Ramachandran P v.**, **Savini M**, **Folick AK**, **Hu K**, **Masand R**, **Graham BH**, **Wang MC**. Lysosomal Signaling Promotes Longevity through Adjusting Mitochondrial Activity. *Developmental cell* 48: 685, 2019. doi: 10.1016/J.DEVCEL.2018.12.022.

98. **Demers-Lamarche J**, **Guillebaud G**, **Tlili M**, **Todkar K**, **Bélanger N**, **Grondin M**, **Nguyen AP**, **Michel J**, **Germain M**. Loss of mitochondrial function impairs lysosomes. *The Journal of Biological Chemistry* 291: 10263–76, 2016. doi: 10.1074/jbc.M115.695825.

99. **Saftig P**, **Klumperman J**. Lysosome biogenesis and lysosomal membrane proteins: Trafficking meets function. *Nature Reviews Molecular Cell Biology* 10: 623–635, 2009. doi: 10.1038/nrm2745.

100. **Wang X**, **Hu S**, **Liu L**. Phosphorylation and acetylation modifications of FOXO3a: Independently or synergistically? *Oncology Letters* 13: 2867, 2017. doi: 10.3892/OL.2017.5851.

101. **Palmieri M**, **Pal R**, **Nelvagal HR**, **Lotfi P**, **Stinnett GR**, **Seymour ML**, **Chaudhury A**, **Bajaj L**, **Bondar V v.**, **Bremner L**, **Saleem U**, **Tse DY**, **Sanagasetti D**, **Wu SM**, **Neilson JR**, **Pereira FA**, **Pautler RG**, **Rodney GG**, **Cooper JD**, **Sardiello M**. mTORC1-independent TFEB activation via Akt inhibition promotes cellular clearance in neurodegenerative storage diseases. *Nature Communications 2017 8:1* 8: 1–19, 2017. doi: 10.1038/ncomms14338.

102. **Martina JA**, **Chen Y**, **Gucek M**, **Puertollano R**. MTORC1 functions as a transcriptional regulator of autophagy by preventing nuclear transport of TFEB. *Autophagy* 8: 903–14, 2012. doi: 10.4161/auto.19653.

103. **Xu Y**, **Ren J**, **He X**, **Chen H**, **Wei T**, **Feng W**. YWHA/14-3-3 proteins recognize phosphorylated TFEB by a noncanonical mode for controlling TFEB cytoplasmic localization. *Autophagy* 15: 1017–1030, 2019. doi: 10.1080/15548627.2019.1569928.

104. **Settembre C**, **Zoncu R**, **Medina DL**, **Vetrini F**, **Erdin S**, **Erdin S**, **Huynh T**, **Ferron M**, **Karsenty G**, **Vellard MC**, **Facchinetti V**, **Sabatini DM**, **Ballabio A**. A lysosome-to-nucleus signalling mechanism senses and regulates the lysosome via mTOR and TFEB. *EMBO* 31: 1095–108, 2012. doi: 10.1038/emboj.2012.32.

105. **Hosokawa N**, **Hara T**, **Kaizuka T**, **Kishi C**, **Takamura A**, **Miura Y**, **Iemura S**, **Natsume T**, **Takehana K**, **Yamada N**, **Guan J-L**, **Oshiro N**, **Mizushima N**. Nutrient-dependent mTORC1 Association with the ULK1–Atg13–FIP200 Complex Required for Autophagy. *Molecular Biology of the Cell* 20: 1981–1991, 2009. doi: 10.1091/MBC.E08-12-1248.

106. **Greer EL**, **Oskoui PR**, **Banko MR**, **Maniar JM**, **Gygi MP**, **Gygi SP**, **Brunet A**. The energy sensor AMP-activated protein kinase directly regulates the mammalian FOXO3 transcription factor. *Journal of Biological Chemistry* 282: 30107–30119, 2007. doi: 10.1074/jbc.M705325200.

107. **Sanchez AM**, **Csibi A**, **Raibon A**, **Cornille K**, **Gay S**, **Bernardi H**, **Candau R**. AMPK promotes skeletal muscle autophagy through activation of forkhead FoxO3a and interaction with Ulk1. *Journal of Cellular Biochemistry* 113: 695–710, 2012. doi: 10.1002/jcb.23399.

108. **Paquette M**, **El-Houjeiri L**, **Zirden LC**, **Puustinen P**, **Blanchette P**, **Jeong H**, **Dejgaard K**, **Siegel PM**, **Pause A**. AMPK-dependent phosphorylation is required for transcriptional activation of TFEB and TFE3. *Autophagy* Epub: 1–19, 2021. doi: 10.1080/15548627.2021.1898748.

109. **Roach PJ**. AMPK -> ULK1 -> Autophagy. *Molecular and Cellular Biology* 31: 3082–3084, 2011. doi: 10.1128/mcb.05565-11.

110. **Gonzá Lez A**, **Hall MN**, **Lin S-C**, **Grahame Hardie D**. Cell Metabolism Review AMPK and TOR: The Yin and Yang of Cellular Nutrient Sensing and Growth Control. *Cell Metabolism* 31: 472–492, 2020. doi: 10.1016/j.cmet.2020.01.015.

111. **Castets P**, **Lin S**, **Rion N**, **di Fulvio S**, **Romanino K**, **Guridi M**, **Frank S**, **Tintignac LA**, **Sinnreich M**, **Rüegg MA**. Sustained Activation of mTORC1 in Skeletal Muscle Inhibits Constitutive and Starvation-Induced Autophagy and Causes a Severe, Late-Onset Myopathy. *Cell Metabolism* 17: 731–744, 2013. doi: 10.1016/J.CMET.2013.03.015.

112. **Guo Y**, **Meng J**, **Tang Y**, **Wang T**, **Wei B**, **Feng R**, **Gong B**, **Wang H**, **Ji G**, **Lu Z**. AMP-activated kinase α2 deficiency protects mice from denervation-induced skeletal muscle atrophy. *Archives of Biochemistry and Biophysics* 600: 56–60, 2016. doi: 10.1016/J.ABB.2016.04.015.

113. **Egawa T**, **Goto A**, **Ohno Y**, **Yokoyama S**, **Ikuta A**, **Suzuki M**, **Sugiura T**, **Ohira Y**, **Yoshioka T**, **Hayashi T**, **Goto K**. Involvement of AMPK in regulating slow-twitch muscle atrophy during hindlimb unloading in mice. *American Journal of Physiology - Endocrinology and Metabolism* 309: E651–E662, 2015. doi: 10.1152/AJPENDO.00165.2015.

114. **Irrcher I**, **Ljubicic V**, **Hood DA**. Interactions between ROS and AMP kinase activity in the regulation of PGC-1alpha transcription in skeletal muscle cells. *American Journal of Physiology - Cell Physiology* 296: C116–C123, 2009. doi: 10.1152/ajpcell.00267.2007.

115. **Rahman M**, **Mofarrahi M**, **Kristof AS**, **Nkengfac B**, **Harel S**, **Hussain S**. Reactive oxygen species regulation of autophagy in skeletal muscles. *Antioxidants and Redox Signaling* 20: 443–459, 2014. doi: 10.1089/ars.2013.5410.

116. **Talbert EE**, **Smuder AJ**, **Min K**, **Kwon OS**, **Szeto HH**, **Powers SK**. Immobilization-induced activation of key proteolytic systems in skeletal muscles is prevented by a mitochondria-targeted antioxidant. *Journal of Applied Physiology* 115: 529–538, 2013. doi: 10.1152/japplphysiol.00471.2013.

117. **Wang H**, **Wang N**, **Xu D**, **Ma Q**, **Chen Y**, **Xu S**, **Xia Q**, **Zhang Y**, **Prehn JHM**, **Wang G**, **Ying Z**. Oxidation of multiple MiT/TFE transcription factors links oxidative stress to transcriptional control of autophagy and lysosome biogenesis. *Autophagy* 16: 1683–1696, 2020. doi: 10.1080/15548627.2019.1704104.

118. **Zhang X**, **Cheng X**, **Yu L**, **Yang J**, **Calvo R**, **Patnaik S**, **Hu X**, **Gao Q**, **Yang M**, **Lawas M**, **Delling M**, **Marugan J**, **Ferrer M**, **Xu H**. MCOLN1 is a ROS sensor in lysosomes that regulates autophagy. *Nature Communications* 7: 12109, 2016. doi: 10.1038/ncomms12109.

119. **Andersson DC**, **Betzenhauser MJ**, **Reiken S**, **Meli AC**, **Umanskaya A**, **Xie W**, **Shiomi T**, **Zalk R**, **Lacampagne A**, **Marks AR**. Ryanodine receptor oxidation causes intracellular calcium leak and muscle weakness in aging. *Cell Metabolism* 14: 196–207, 2011. doi: 10.1016/j.cmet.2011.05.014.

120. **Medina DL**, **Paola S di**, **Peluso I**, **Armani A**, **Stefani D de**, **Venditti R**, **Montefusco S**, **Scotto-rosato A**, **Prezioso C**, **Forrester A**, **Settembre C**, **Wang W**, **Gao Q**, **Xu H**, **Sandri M**, **Rizzuto R**, **Matteis MA de**. Lysosomal calcium signalling regulates autophagy through calcineurin and TFEB. 17, 2015. doi: 10.1038/ncb3114.

121. **Martina JA**, **Diab HI**, **Brady OA**, **Puertollano R**. TFEB and TFE3 are novel components of the integrated stress response. *The EMBO Journal* 35: 479–495, 2016. doi: 10.15252/embj.201593428.

122. **Moulis M**, **Vindis C**. Methods for Measuring Autophagy in Mice. *Cells* 6: 14, 2017. doi: 10.3390/CELLS6020014.

123. **Klionsky DJ**, **Abdelmohsen K**, **Abe A**, **Abedin MJ**, **Abeliovich H**, **Al E**. Guidelines for the use and interpretation of assays for monitoring autophagy (3rd edition). *Autophagy* 12: 1, 2016. doi: 10.1080/15548627.2015.1100356.

124. **Lopez A**, **Fleming A**, **Rubinsztein DC**. Seeing is believing: methods to monitor vertebrate autophagy in vivo. *Royal Society Open Biology* 8, 2018. doi: 10.1098/RSOB.180106.

125. **Terada M**, **Nobori K**, **Munehisa Y**, **Kakizaki M**, **Ohba T**, **Takahashi Y**, **Koyama T**, **Terata Y**, **Ishida M**, **Iino K**, **Kosaka T**, **Watanabe H**, **Hasegawa H**, **Ito H**. Double Transgenic Mice Crossed GFP-LC3 Transgenic Mice With αMyHC-mCherry-LC3 Transgenic Mice Are a New and

Useful Tool to Examine the Role of Autophagy in the Heart. *Circulation Journal* 74: 203–206, 2010. doi: 10.1253/CIRCJ.CJ-09-0589.

126. **Kimura S**, **Noda T**, **Yoshimori T**. Dissection of the autophagosome maturation process by a novel reporter protein, tandem fluorescent-tagged LC3. *Autophagy* 3: 452–460, 2007. doi: 10.4161/AUTO.4451.

127. **Li L**, **Wang Z v.**, **Hill JA**, **Lin F**. New Autophagy Reporter Mice Reveal Dynamics of Proximal Tubular Autophagy. *Journal of the American Society of Nephrology* 25: 305, 2014. doi: 10.1681/ASN.2013040374.

128. **Hariharan N**, **Zhai P**, **Sadoshima J**. Oxidative Stress Stimulates Autophagic Flux During Ischemia/Reperfusion. *Antioxidants & Redox Signaling* 14: 2179, 2011. doi: 10.1089/ARS.2010.3488.

129. **Katayama H**, **Kogure T**, **Mizushima N**, **Yoshimori T**, **Miyawaki A**. A Sensitive and Quantitative Technique for Detecting Autophagic Events Based on Lysosomal Delivery. *Chemistry & Biology* 18: 1042–1052, 2011. doi: 10.1016/J.CHEMBIOL.2011.05.013.

130. **Sun N**, **Yun J**, **Liu J**, **Malide D**, **Liu C**, **Rovira II**, **Holmström KM**, **Fergusson MM**, **Yoo YH**, **Combs CA**, **Finkel T**. Measuring in vivo mitophagy. *Molecular Cell* 60: 685–696, 2015. doi: 10.1016/j.molcel.2015.10.009.

131. **Sun N**, **Malide D**, **Liu J**, **Rovira II**, **Combs CA**, **Finkel T**. A fluorescence-based imaging method to measure in vitro and in vivo mitophagy using mt-Keima. *Nature Protocols* 12: 1576–1587, 2017. doi: 10.1038/nprot.2017.060.

132. **Boncompagni S**, **Rossi AE**, **Micaroni M**, **Beznoussenko G v**, **Polishchuk RS**, **Dirksen RT**, **Protasi F**. Mitochondria Are Linked to Calcium Stores in Striated Muscle by Developmentally Regulated Tethering Structures. *Molecular Biology of the Cell* 20: 1058–1067, 2009. doi: 10.1091/mbc.E08.

133. **Bleck CKE**, **Kim Y**, **Willingham TB**, **Glancy B**. Subcellular connectomic analyses of energy networks in striated muscle. *Nature Communications* 9, 2018. doi: 10.1038/S41467-018-07676-Y.

134. **Ogata T**, **Yamasaki Y**. Scanning electron-microscopic studies on the three-dimensional structure of mitochondria in the mammalian red, white and intermediate muscle fibers. *Cell and Tissue Research* 241: 251–256, 1985. doi: 10.1007/BF00217168.

135. **Ogata T**, **Yamasaki Y**. Ultra-high-resolution scanning electron microscopy of mitochondria and sarcoplasmic reticulum arrangement in human red, white, and intermediate muscle fibers. *Anatomical Record* 248: 214–23, 1997. doi: 10.1002/(SICI)1097-0185(199706)248:2<214::AID-AR8>3.0.CO;2-S.

136. **Hoppeler H**. Exercise-induced ultrastructural changes in skeletal muscle. *International Journal of Sports Medicine* 07: 187–204, 1986. doi: 10.1055/s-2008-1025758.

137. **Ogata T**, **Yamasaki Y**. Scanning electron-microscopic studies on the three-dimensional structure of sarcoplasmic reticulum in the mammalian red, white and intermediate muscle fibers. *Cell and Tissue Research* 242: 461–467, 1985. doi: 10.1007/BF00225410.

138. **Müller W**. Subsarcolemmal mitochondria and capillarization of soleus muscle fibers in young rats subjected to an endurance training. *Cell and Tissue Research* 174: 367–389, 1976. doi: 10.1007/BF00220682.

139. **Picard M**, **White K**, **Turnbull DM**. Mitochondrial morphology, topology, and membrane interactions in skeletal muscle: a quantitative three-dimensional electron microscopy study. *Journal of Applied Physiology* 114: 161–171, 2013. doi: 10.1152/japplphysiol.01096.2012.

140. **Vincent AE**, **White K**, **Davey T**, **Philips J**, **Ogden RT**, **Lawless C**, **Warren C**, **Hall MG**, **Ng YS**, **Falkous G**, **Holden T**, **Deehan D**, **Taylor RW**, **Turnbull DM**, **Picard M**. Quantitative 3D mapping of the human skeletal muscle mitochondrial network. *Cell Reports* 26: 996–1009, 2019. doi: 10.1016/j.celrep.2019.01.010.

141. **Glancy B**, **Hsu LY**, **Dao L**, **Bakalar M**, **French S**, **Chess DJ**, **Taylor JL**, **Picard M**, **Aponte A**, **Daniels MP**, **Esfahani S**, **Cushman S**, **Balaban RS**. In Vivo microscopy reveals extensive embedding of capillaries within the sarcolemma of skeletal muscle fibers. *Microcirculation* 21: 131–147, 2014. doi: 10.1111/micc.12098.

142. **Kirkwood SP**, **Munn EA**, **Brooks GA**. Mitochondrial reticulum in limb skeletal muscle. *The American Journal of Physiology - Cell Physiology* 251: C395-402, 1986. doi: 10.1152/ajpcell.1986.251.3.C395.

143. **Kirkwood SP**, **Packer L**, **Brooks GA**. Effects of Endurance Training on a Mitochondrial Reticulum in Limb Skeletal Muscle. *Archives of Biochemistry and Biophysics* 255: 80–88, 1987. doi: 10.1016/0003-9861(87)90296-7.

144. **Adhihetty PJ**, **Ljubicic V**, **Menzies KJ**, **Hood DA**, **Peter J**, **Ljubicic V**, **Menzies KJ**, **Hood DA**. Differential susceptibility of subsarcolemmal and intermyofibrillar mitochondria to apoptotic stimuli. *American Journal of Physiology - Cell Physiology* 3: 994–1001, 2005. doi: 10.1152/ajpcell.00031.2005.

145. **Cogswell AM**, **Stevens RJ**, **Hood DA**. Properties of skeletal muscle mitochondria from subsarcolemmal and intermyofibrillar isolated regions. *The American Journal of Physiology - Cell Physiology* 264: C383-389, 1993. doi: 10.1152/ajpcell.1993.264.2.C383.

146. **Krieger DA**, **Tate CA**, **McMillan-Wood J**, **Booth FW**. Populations of rat skeletal muscle mitochondria after exercise and immobilization. *Journal of Applied Physiology* 48: 23–8, 1980. doi: 10.1152/jappl.1980.48.1.23.

147. **Takahashi M**, **Hood DA**. Protein Import into Subsarcolemmal and Intermyofibrillar Skeletal Muscle Mitochondria. *Journal of Biological Chemistry* 271: 27285–27291, 1996. doi: doi.org/10.1074/jbc.271.44.27285.

148. **Padrão AI**, **Ferreira R**, **Amado F**, **Vitorino R**, **Duarte JA**. Uncovering the exercise-related proteome signature in skeletal muscle. *Proteomics* 16: 816–830, 2016. doi: 10.1002/pmic.201500382.

149. **Makrecka-Kuka M**, **Krumschnabel G**, **Gnaiger E**. High-Resolution Respirometry for Simultaneous Measurement of Oxygen and Hydrogen Peroxide Fluxes in Permeabilized Cells, Tissue Homogenate and Isolated Mitochondria. *Biomolecules* 5: 1319, 2015. doi: 10.3390/BIOM5031319.

150. **Silva AM**, **Oliveira PJ**. Evaluation of respiration with clark type electrode in isolated mitochondria and permeabilized animal cells. *Methods in Molecular Biology* 810: 7–24, 2012. doi: 10.1007/978-1-61779-382-0_2.

151. **Li Z**, **Graham BH**. Measurement of mitochondrial oxygen consumption using a Clark electrode. *Methods in Molecular Biology* 837: 63–72, 2012. doi: 10.1007/978-1-61779-504-6_5.

152. **Mailloux RJ**. Teaching the fundamentals of electron transfer reactions in mitochondria and the production and detection of reactive oxygen species. *Redox Biology* 4: 381, 2015. doi: 10.1016/J.REDOX.2015.02.001.

153. **Murphy MP**. How mitochondria produce reactive oxygen species. *Biochemical Journal* 417: 1, 2009. doi: 10.1042/BJ20081386.

154. **Liochev SI**, **Fridovich I**. The effects of superoxide dismutase on H2O2 formation. *Free Radical Biology and Medicine* 42: 1465–1469, 2007. doi: 10.1016/J.FREERADBIOMED.2007.02.015.

155. **Bienert GP**, **Chaumont F**. Aquaporin-facilitated transmembrane diffusion of hydrogen peroxide. *Biochimica et Biophysica Acta (BBA)* 1840: 1596–1604, 2014. doi: 10.1016/J.BBAGEN.2013.09.017.

156. **Bienert GP**, **Schjoerring JK**, **Jahn TP**. Membrane transport of hydrogen peroxide. *Biochimica et Biophysica Acta (BBA) - Biomembranes* 1758: 994–1003, 2006. doi: 10.1016/J.BBAMEM.2006.02.015.

157. **Ristow M**. Unraveling the Truth About Antioxidants: Mitohormesis explains ROS-induced health benefits. *Nature Medicine* 20: 709–711, 2014. doi: doi: 10.1038/nm.3624.

158. **Powers SK**, **Talbert EE**, **Adhihetty PJ**. Reactive oxygen and nitrogen species as intracellular signals in skeletal muscle. *The Journal of Physiology* 589: 2129, 2011. doi: 10.1113/JPHYSIOL.2010.201327.

159. **Pastor R**, **Tur JA**. Antioxidant Supplementation and Adaptive Response to Training: A Systematic Review. *Current Pharmaceutical Design* 25: 1889–1912, 2019. doi: 10.2174/1381612825666190701164923.

160. **Ziada AS**, **Smith M-SR**, **Côté HCF**. Updating the Free Radical Theory of Aging. *Frontiers in Cell and Developmental Biology* 0: 908, 2020. doi: 10.3389/FCELL.2020.575645.

161. **Xiong S**, **Mu T**, **Wang G**, **Jiang X**. Mitochondria-mediated apoptosis in mammals. *Protein & Cell* 5: 737, 2014. doi: 10.1007/S13238-014-0089-1.

162. **Cheema N**, **Herbst A**, **McKenzie D**, **Aiken JM**. Apoptosis and necrosis mediate skeletal muscle fiber loss in age-induced mitochondrial enzymatic abnormalities. *Aging Cell* 14: 1085–1093, 2015. doi: 10.1111/ACEL.12399.

163. **Dupont-Versteegden EE**. Apoptosis in skeletal muscle and its relevance to atrophy. *World Journal of Gastroenterology* 12: 7463, 2006. doi: 10.3748/WJG.V12.I46.7463.

164. **Schwartz LM**. Skeletal Muscles Do Not Undergo Apoptosis During Either Atrophy or Programmed Cell Death-Revisiting the Myonuclear Domain Hypothesis. *Frontiers in Physiology* 0: 1887, 2019. doi: 10.3389/FPHYS.2018.01887.

165. **Marzetti E**, **Calvani R**, **Cesari M**, **Buford TW**, **Lorenzi M**, **Behnke BJ**, **Leeuwenburgh C**. Mitochondrial dysfunction and sarcopenia of aging: From signaling pathways to clinical trials. *International Journal of Biochemistry and Cell Biology* 45: 2288–2301, 2013. doi: 10.1016/j.biocel.2013.06.024.

166. **Hood DA**, **Memme JM**, **Oliveira AN**, **Triolo M**. Maintenance of skeletal muscle mitochondria in health, exercise, and aging. *Annual Review of Physiology* 81: 19–41, 2019. doi: 10.1146/annurev-physiol-020518-114310.

167. **Kim Y**, **Triolo M**, **Hood DA**. Impact of Aging and Exercise on Mitochondrial Quality Control in Skeletal Muscle. *Oxidative Medicine and Cellular Longevity* 2017, 2017. doi: 10.1155/2017/3165396.

168. **Glancy B**, **Hartnell LM**, **Combs CA**, **Fenmou A**, **Sun J**, **Murphy E**, **Subramaniam S**, **Balaban RS**. Power grid protection of the muscle mitochondrial reticulum. *Cell Reports* 19: 487–496, 2017. doi: 10.1016/j.celrep.2017.03.063.

169. **Glancy B**, **Hartnell LM**, **Malide D**, **Yu ZX**, **Combs CA**, **Connelly PS**, **Subramaniam S**, **Balaban RS**. Mitochondrial reticulum for cellular energy distribution in muscle. *Nature* 523: 617–620, 2015. doi: 10.1038/nature14614.

170. **Giacomello M**, **Pyakurel A**, **Glytsou C**, **Scorrano L**. The cell biology of mitochondrial membrane dynamics. *Nature Reviews Molecular Cell Biology 2020 21:4* 21: 204–224, 2020. doi: 10.1038/s41580-020-0210-7.

171. **Pickles S**, **Vigié P**, **Youle RJ**. Mitophagy and quality control mechanisms in mitochondrial maintenance. *Current Biology* 28: R170–R185, 2018. doi: 10.1016/J.CUB.2018.01.004.

172. **Iqbal S**, **Hood DA**. The role of mitochondrial fusion and fission in skeletal muscle function and dysfunction. *Frontiers in Bioscience* 20: 157–172, 2015. doi: 10.2741/4303.

173. **Twig G**, **Elorza A**, **Molina AJA**, **Mohamed H**, **Wikstrom JD**, **Walzer G**, **Stiles L**, **Haigh SE**, **Katz S**, **Las G**, **Alroy J**, **Wu M**, **Py BF**, **Yuan J**, **Deeney JT**, **Corkey BE**, **Shirihai OS**. Fission and selective fusion govern mitochondrial segregation and elimination by autophagy. *The EMBO journal* 27: 433–46, 2008. doi: 10.1038/sj.emboj.7601963.

174. **Zhang Z**, **Sliter DA**, **Bleck CKE**, **Ding S**. Fis1 deficiencies differentially affect mitochondrial quality in skeletal muscle. *Mitochondrion* 49: 217–226, 2019. doi: 10.1016/J.MITO.2019.09.005.

175. **Dulac M**, **Leduc-Gaudet J-P**, **Reynaud O**, **Ayoub M-B**, **Guérin A**, **Finkelchtein M**, **Hussain SN**, **Gouspillou G**. Drp1 knockdown induces severe muscle atrophy and remodelling, mitochondrial dysfunction, autophagy impairment and denervation. *The Journal of Physiology* 598: 3691–3710, 2020. doi: 10.1113/JP279802.

176. **Favaro G**, **Romanello V**, **Varanita T**, **Andrea Desbats M**, **Morbidoni V**, **Tezze C**, **Albiero M**, **Canato M**, **Gherardi G**, **de Stefani D**, **Mammucari C**, **Blaauw B**, **Boncompagni S**, **Protasi F**, **Reggiani C**, **Scorrano L**, **Salviati L**, **Sandri M**. DRP1-mediated mitochondrial shape controls calcium homeostasis and muscle mass. *Nature Communications 2019 10:1* 10: 1–17, 2019. doi: 10.1038/s41467-019-10226-9.

177. **Romanello V**, **Guadagnin E**, **Gomes L**, **Roder I**, **Sandri C**, **Petersen Y**, **Milan G**, **Masiero E**, **del Piccolo P**, **Foretz M**, **Scorrano L**, **Rudolf R**, **Sandri M**. Mitochondrial fission and remodelling contributes to muscle atrophy. *EMBO Journal* 29: 1774–1785, 2010. doi: 10.1038/emboj.2010.60.

178. **Sebastián D**, **Sorianello E**, **Segalés J**, **Irazoki A**, **Ruiz-Bonilla V**, **Sala D**, **Planet E**, **Berenguer-Llergo A**, **Muñoz JP**, **Sánchez-Feutrie M**, **Plana N**, **Hernández-Álvarez MI**, **Serrano AL**, **Palacín M**, **Zorzano A**. Mfn2 deficiency links age-related sarcopenia and impaired autophagy to activation of an adaptive mitophagy pathway. *The EMBO Journal* 35: 1677–1693, 2016. doi: 10.15252/embj.201593084.

179. **Sebastián D**, **Hernández-Alvarez MI**, **Segalés J**, **Sorianello E**, **Muñoz JP**, **Sala D**, **Waget A**, **Liesa M**, **Paz JC**, **Gopalacharyulu P**, **Orešič M**, **Pich S**, **Burcelin R**, **Palacín M**, **Zorzano A**. Mitofusin 2 (Mfn2) links mitochondrial and endoplasmic reticulum function with insulin signaling

and is essential for normal glucose homeostasis. *Proceedings of the National Academy of Sciences* 109: 5523–5528, 2012. doi: 10.1073/PNAS.1108220109.

180. **Tezze C**, **Romanello V**, **Desbats MA**, **Fadini GP**, **Albiero M**, **Favaro G**, **Ciciliot S**, **Soriano ME**, **Morbidoni V**, **Cerqua C**, **Loefler S**, **Kern H**, **Franceschi C**, **Salvioli S**, **Conte M**, **Blaauw B**, **Zampieri S**, **Salviati L**, **Scorrano L**, **Sandri M**. Age-Associated Loss of OPA1 in Muscle Impacts Muscle Mass, Metabolic Homeostasis, Systemic Inflammation, and Epithelial Senescence. *Cell Metabolism* 25: 1374, 2017. doi: 10.1016/J.CMET.2017.04.021.

181. **Anderson S**, **Bankier AT**, **Barrell BG**, **de Bruijn MH**, **Coulson AR**, **Drouin J**, **Eperon IC**, **Nierlich DP**, **Roe BA**, **Sanger F**, **Schreier PH**, **Smith AJ**, **Staden R**, **Young IG**. Sequence and organization of the human mitochondrial genome. *Nature* 290: 457–465, 1981. doi: 10.1038/290457a0.

182. **Taanman J-W**. The mitochondrial genome: structure, transcription, translation and replication. *Biochimica et Biophysica Acta (BBA) - Bioenergetics* 1410: 103–123, 1999. doi: 10.1016/S0005-2728(98)00161-3.

183. **Vega RB**, **Huss JM**, **Kelly DP**. The Coactivator PGC-1 Cooperates with Peroxisome Proliferator-Activated Receptor alpha in Transcriptional Control of Nuclear Genes Encoding Mitochondrial Fatty Acid Oxidation Enzymes. *Molecular and Cellular Biology* 20: 1868–1876, 2000. doi: 10.1128/MCB.20.5.1868-1876.2000.

184. **Schreiber SN**, **Knutti D**, **Brogli K**, **Uhlmann T**, **Kralli A**. The transcriptional coactivator PGC-1 regulates the expression and activity of the orphan nuclear receptor estrogen-related receptor alpha (ERRalpha). *The Journal of Biological Chemistry* 278: 9013–8, 2003. doi: 10.1074/jbc.M212923200.

185. **Schreiber SN**, **Emter R**, **Hock MB**, **Knutti D**, **Cardenas J**, **Podvinec M**, **Oakeley EJ**, **Kralli A**. The estrogen-related receptor alpha (ERRalpha) functions in PPARgamma coactivator 1alpha (PGC-1alpha)-induced mitochondrial biogenesis. *Proceedings of the National Academy of Sciences of the United States of America* 101: 6472–7, 2004. doi: 10.1073/pnas.0308686101.

186. **Puigserver P**, **Adelmant G**, **Wu Z**, **Fan M**, **Xu J**, **O'Malley B**, **Spiegelman BM**. Activation of PPARgamma coactivator-1 through transcription factor docking. *Science* 286: 1368–71, 1999.

187. **Puigserver P**, **Wu Z**, **Park CW**, **Graves R**, **Wright M**, **Spiegelman BM**. A Cold-Inducible Coactivator of Nuclear Receptors Linked to Adaptive Thermogenesis. *Cell* 92: 829–839, 1998. doi: 10.1016/S0092-8674(00)81410-5.

188. **Mortensen OH**, **Frandsen L**, **Schjerling P**, **Nishimura E**, **Grunnet N**. PGC-1α and PGC-1β have both similar and distinct effects on myofiber switching toward an oxidative phenotype. *American Journal of Physiology-Endocrinology and Metabolism* 291: E807–E816, 2006. doi: 10.1152/ajpendo.00591.2005.

189. **Lin J**, **Wu H**, **Tarr PT**, **Zhang C-Y**, **Wu Z**, **Boss O**, **Michael LF**, **Puigserver P**, **Isotani E**, **Olson EN**, **Lowell BB**, **Bassel-Duby R**, **Spiegelman BM**. Transcriptional co-activator PGC-1 alpha drives the formation of slow-twitch muscle fibres. *Nature* 418: 797–801, 2002. doi: 10.1038/nature00904.

190. **Leone TC**, **Lehman JJ**, **Finck BN**, **Schaeffer PJ**, **Wende AR**, **Boudina S**, **Courtois M**, **Wozniak DF**, **Sambandam N**, **Bernal-Mizrachi C**, **Chen Z**, **Holloszy JO**, **Medeiros DM**, **Schmidt RE**, **Saffitz JE**, **Abel ED**, **Semenkovich CF**, **Kelly DP**. PGC-1alpha deficiency causes multi-system energy metabolic derangements: muscle dysfunction, abnormal weight control and hepatic steatosis. *PLoS biology* 3: e101, 2005. doi: 10.1371/journal.pbio.0030101.

191. **Zechner C**, **Lai L**, **Zechner JF**, **Geng T**, **Yan Z**, **Rumsey JW**, **Collia D**, **Chen Z**, **Wozniak DF**, **Leone TC**, **Kelly DP**. Total skeletal muscle PGC-1 deficiency uncouples mitochondrial derangements from fiber type determination and insulin sensitivity. *Cell metabolism* 12: 633–42, 2010. doi: 10.1016/j.cmet.2010.11.008.

192. **Finley LWS**, **Lee J**, **Souza A**, **Desquiret-Dumas V**, **Bullock K**, **Rowe GC**, **Procaccio V**, **Clish CB**, **Arany Z**, **Haigis MC**. Skeletal muscle transcriptional coactivator PGC-1α mediates mitochondrial, but not metabolic, changes during calorie restriction. *Proceedings of the National Academy of Sciences of the United States of America* 109: 2931–6, 2012. doi: 10.1073/pnas.1115813109.

193. **Handschin C**, **Cheol SC**, **Chin S**, **Kim S**, **Kawamori D**, **Kurpad AJ**, **Neubauer N**, **Hu J**, **Mootha VK**, **Kim YB**, **Kulkarni RN**, **Shulman GI**, **Spiegelman BM**. Abnormal glucose homeostasis in skeletal muscle-specific PGC-1α knockout mice reveals skeletal muscle-pancreatic β cell crosstalk. *Journal of Clinical Investigation* 117: 3463–3474, 2007. doi: 10.1172/JCI31785.

194. **Handschin C**, **Chin S**, **Li P**, **Liu F**, **Maratos-Flier E**, **LeBrasseur NK**, **Yan Z**, **Spiegelman BM**. Skeletal muscle fiber-type switching, exercise intolerance, and myopathy in PGC-1α muscle-specific knock-out animals. *Journal of Biological Chemistry* 282: 30014–30021, 2007. doi: 10.1074/jbc.M704817200.

195. **Hood DA**, **Memme JM**, **Oliveira AN**, **Triolo M**. Maintenance of skeletal muscle mitochondria in health, exercise, and aging. *Annual Review of Physiology* 81: 19–41, 2019. doi: 10.1146/annurev-physiol-020518-114310.

196. **Hood DA**, **Tryon LD**, **Carter HN**, **Kim Y**, **Chen CCW**. Unravelling the mechanisms regulating muscle mitochondrial biogenesis. *Biochem J* 473: 2295–2314, 2016. doi: 10.1042/BCJ20160009.

197. **Virbasius J v**, **Scarpulla RC**. Activation of the human mitochondrial transcription factor A gene by nuclear respiratory factors: a potential regulatory link between nuclear and mitochondrial gene expression in organelle biogenesis. *Proceedings of the National Academy of Sciences of the United States of America* 91: 1309–13, 1994. doi: 10.1073/pnas.91.4.1309.

198. **Falkenberg M**, **Larsson N-G**, **Gustafsson CM**. DNA Replication and Transcription in Mammalian Mitochondria. *Annual Review of Biochemistry* 76: 679–699, 2007. doi: 10.1146/annurev.biochem.76.060305.152028.

199. **Arnold JJ**, **Smidansky ED**, **Moustafa IM**, **Cameron CE**. Human mitochondrial RNA polymerase: Structure–function, mechanism and inhibition. *Biochimica et Biophysica Acta (BBA) - Gene Regulatory Mechanisms* 1819: 948–960, 2012. doi: 10.1016/J.BBAGRM.2012.04.002.

200. **Ngo HB**, **Kaiser JT**, **Chan DC**. The mitochondrial transcription and packaging factor Tfam imposes a U-turn on mitochondrial DNA. *Nature Structural and Molecular Biology* 18: 1290–1296, 2011. doi: 10.1038/nsmb.2159.

201. **Rubio-Cosials A**, **Sidow JF**, **Jiménez-Menéndez N**, **Fernández-Millán P**, **Montoya J**, **Jacobs HT**, **Coll M**, **Bernadó P**, **Solà M**. Human mitochondrial transcription factor A induces a U-turn structure in the light strand promoter. *Nature Structural and Molecular Biology* 18: 1281–1289, 2011. doi: 10.1038/nsmb.2160.

202. **Carter HN**, **Hood DA**. Contractile activity-induced mitochondrial biogenesis and mTORC1. *American Journal of Physiology - Cell Physiology* 303: C540–C547, 2012. doi: 10.1152/ajpcell.00156.2012.

203. **Gordon JW**, **Rungi AA**, **Inagaki H**, **Hood DA**. Effects of contractile activity on mitochondrial transcription factor A expression in skeletal muscle. *Journal of Applied Physiology* 90: 389–396, 2001. doi: 10.1152/jappl.2001.90.1.389.

204. **Lai RYJ**, **Ljubicic V**, **D'souza D**, **Hood DA**. Effect of chronic contractile activity on mRNA stability in skeletal muscle. *American Journal of Physiology Cell physiology* 299: C155--163, 2010. doi: 10.1152/ajpcell.00523.2009.

205. **Pilegaard H**, **Saltin B**, **Neufer PD**. Exercise induces transient transcriptional activation of the PGC-1α gene in human skeletal muscle. *The Journal of Physiology* 546: 851–858, 2003. doi: 10.1113/jphysiol.2002.034850.

206. **Uguccioni G**, **Hood DA**. The importance of PGC-1α in contractile activity-induced mitochondrial adaptations. *American Journal of Physiology Endocrinology and Metabolism* 300: E361–E371, 2011. doi: 10.1152/ajpendo.00292.2010.

207. **Beyfuss K**, **Hood DA**. A systematic review of p53 regulation of oxidative stress in skeletal muscle. *Redox Report* 23: 100–117, 2018. doi: 10.1080/13510002.2017.1416773.

208. **Ngo HB**, **Lovely GA**, **Phillips R**, **Chan DC**. Distinct structural features of TFAM drive mitochondrial DNA packaging versus transcriptional activation. *Nature communications* 5: 3077, 2014. doi: 10.1038/ncomms4077.

209. **Bogenhagen DF**. Mitochondrial DNA nucleoid structure. *Biochimica et Biophysica Acta (BBA) - Gene Regulatory Mechanisms* 1819: 914–920, 2012. doi: 10.1016/J.BBAGRM.2011.11.005.

210. **Winder WW**, **Holmes BF**, **Rubink DS**, **Jensen EB**, **Chen M**, **Holloszy JO**. Activation of AMP-activated protein kinase increases mitochondrial enzymes in skeletal muscle. *Journal of Applied Physiology* 88: 2219–2226, 2000. doi: 10.1152/jappl.2000.88.6.2219.

211. **Bergeron R**, **Ren JM**, **Cadman KS**, **Moore IK**, **Perret P**, **Pypaert M**, **Young LH**, **Semenkovich CF**, **Shulman GI**. Chronic activation of AMP kinase results in NRF-1 activation and mitochondrial biogenesis. *American Journal of Physiology - Endocrinology and Metabolism* 281, 2001. doi: 10.1152/ajpendo.2001.281.6.e1340.

212. **Cantó C**, **Houtkooper RH**, **Pirinen E**, **Youn DY**, **Oosterveer MH**, **Cen Y**, **Fernandez-Marcos PJ**, **Yamamoto H**, **Andreux PA**, **Cettour-Rose P**, **Gademann K**, **Rinsch C**, **Schoonjans K**, **Sauve AA**, **Auwerx J**. The NAD+ precursor nicotinamide riboside enhances oxidative metabolism and protects against high-fat diet-induced obesity. *Cell Metabolism* 15: 838–847, 2012. doi: 10.1016/j.cmet.2012.04.022.

213. **Khan NA**, **Auranen M**, **Paetau I**, **Pirinen E**, **Euro L**, **Forsström S**, **Pasila L**, **Velagapudi V**, **Carroll CJ**, **Auwerx J**, **Suomalainen A**. Effective treatment of mitochondrial myopathy by nicotinamide riboside, a vitamin B3. *EMBO Molecular Medicine* 6: 721–731, 2014. doi: 10.1002/emmm.201403943.

214. **van de Weijer T**, **Phielix E**, **Bilet L**, **Williams EG**, **Ropelle ER**, **Bierwagen A**, **Livingstone R**, **Nowotny P**, **Sparks LM**, **Paglialunga S**, **Szendroedi J**, **Havekes B**, **Moullan N**, **Pirinen E**, **Hwang JH**, **Schrauwen-Hinderling VB**, **Hesselink MKC**, **Auwerx J**, **Roden M**, **Schrauwen P**. Evidence for a direct effect of the NAD+ precursor acipimox on muscle mitochondrial function in humans. *Diabetes* 64: 1193–1201, 2015. doi: 10.2337/db14-0667.

215. **Jäger S**, **Handschin C**, **St-Pierre J**, **Spiegelman BM**. AMP-activated protein kinase (AMPK) action in skeletal muscle via direct phosphorylation of PGC-1alpha. *Proceedings of the National*

Academy of Sciences of the United States of America 104: 12017–12022, 2007. doi: 10.1073/pnas.0705070104.

216. **Irrcher I**, **Ljubicic V**, **Kirwan AF**, **Hood DA**. AMP-Activated Protein Kinase-Regulated Activation of the PGC-1α Promoter in Skeletal Muscle Cells. *PLoS ONE* 3: e3614, 2008. doi: 10.1371/journal.pone.0003614.

217. **Gerhart-Hines Z**, **Rodgers JT**, **Bare O**, **Lerin C**, **Kim S-H**, **Mostoslavsky R**, **Alt FW**, **Wu Z**, **Puigserver P**. Metabolic control of muscle mitochondrial function and fatty acid oxidation through SIRT1/PGC-1alpha. *The EMBO journal* 26: 1913–23, 2007. doi: 10.1038/sj.emboj.7601633.

218. **Gurd BJ**. Deacetylation of PGC-1α by SIRT1: importance for skeletal muscle function and exercise-induced mitochondrial biogenesis. *Applied Physiology, Nutrition, and Metabolism* 36: 589–597, 2011. doi: 10.1139/h11-070.

219. **Cantó C**, **Auwerx J**. PGC-1alpha, SIRT1 and AMPK, an energy sensing network that controls energy expenditure. *Current Opinion in Lipidology* 20: 98–105, 2009. doi: 10.1097/MOL.0b013e328328d0a4.

220. **O'Neill HM**, **Maarbjerg SJ**, **Crane JD**, **Jeppesen J**, **Jørgensen SB**, **Schertzer JD**, **Shyroka O**, **Kiens B**, **van Denderen BJ**, **Tarnopolsky MA**, **Kemp BE**, **Richter EA**, **Steinberg GR**. AMP-activated protein kinase (AMPK) beta1beta2 muscle null mice reveal an essential role for AMPK in maintaining mitochondrial content and glucose uptake during exercise. *Proceedings of the National Academy of Sciences of the United States of America* 108: 16092–7, 2011. doi: 10.1073/pnas.1105062108.

221. **Zong H**, **Ren JM**, **Young LH**, **Pypaert M**, **Mu J**, **Birnbaum MJ**, **Shulman GI**. AMP kinase is required for mitochondrial biogenesis in skeletal muscle in response to chronic energy deprivation. *Proceedings of the National Academy of Sciences of the United States of America* 99: 15983–15987, 2002. doi: 10.1073/pnas.252625599.

222. **Zhang Y**, **Uguccioni G**, **Ljubicic V**, **Irrcher I**, **Iqbal S**, **Singh K**, **Ding S**, **Hood DA**. Multiple signaling pathways regulate contractile activity mediated PGC-1α gene expression and activity in skeletal muscle cells. *Physiological Reports* 2, 2014. doi: 10.14814/phy2.12008.

223. **Chalkiadaki A**, **Igarashi M**, **Nasamu AS**, **Knezevic J**, **Guarente L**. Muscle-Specific SIRT1 Gain-of-Function Increases Slow-Twitch Fibers and Ameliorates Pathophysiology in a Mouse Model of Duchenne Muscular Dystrophy. *PLoS Genetics* 10, 2014. doi: 10.1371/journal.pgen.1004490.

224. **Ojuka EO**, **Jones TE**, **Han D-H**, **Chen M**, **Wamhoff BR**, **Sturek M**, **Holloszy JO**. Intermittent increases in cytosolic Ca $^{2+}$ stimulate mitochondrial biogenesis in muscle cells. *American Journal of Physiology-Endocrinology and Metabolism* 283: E1040–E1045, 2002. doi: 10.1152/ajpendo.00242.2002.

225. **Freyssenet D**, **Irrcher I**, **Connor MK**, **di Carlo M**, **Hood DA**. Calcium-regulated changes in mitochondrial phenotype in skeletal muscle cells. *American Journal of Physiology Cell Physiology* 286: C1053–C1061, 2004. doi: 10.1152/ajpcell.00418.2003.

226. **Connor MK**, **Irrcher I**, **Hood DA**. Contractile activity-induced transcriptional activation of cytochrome C involves Sp1 and is proportional to mitochondrial ATP synthesis in C2C12 muscle cells. *The Journal of Biological Chemistry* 276: 15898–15904, 2001. doi: 10.1074/jbc.M100272200.

227. **Ojuka EO**, **Jones TE**, **Han D-H**, **Chen M**, **Holloszy JO**. Raising Ca2+ in L6 myotubes mimics effects of exercise on mitochondrial biogenesis in muscle. *Federation of American Societies for Experimental Biology* 17: 675–681, 2003. doi: 10.1096/fj.02-0951com.

228. **Wu H**, **Kanatous SB**, **Thurmond FA**, **Gallardo T**, **Isotani E**, **Bassel-Duby R**, **Williams RS**. Regulation of mitochondrial biogenesis in skeletal muscle by CaMK. *Science (New York, NY)* 296: 349–52, 2002. doi: 10.1126/science.1071163.

229. **Freyssenet D**, **di Carlo M**, **Hood DA**. Calcium-dependent regulation of cytochrome c gene expression in skeletal muscle cells. Identification of a protein kinase c-dependent pathway. 274: 9305–9311, 1999. doi: 10.1074/jbc.274.14.9305.

230. **Rose AJ**, **Hargreaves M**. Exercise increases Ca2+-calmodulin-dependent protein kinase II activity in human skeletal muscle. *Journal of Physiology* 553: 303–309, 2003. doi: 10.1113/jphysiol.2003.054171.

231. **Zhang Y**, **Uguccioni G**, **Ljubicic V**, **Irrcher I**, **Iqbal S**, **Singh K**, **Ding S**, **Hood DA**. Multiple signaling pathways regulate contractile activity-mediated PGC-1 gene expression and activity in skeletal muscle cells. *Physiological Reports* 2: e12008, 2014. doi: 10.14814/phy2.12008.

232. **Handschin C**, **Rhee J**, **Lin J**, **Tarr PT**, **Spiegelman BM**. An autoregulatory loop controls peroxisome proliferator-activated receptor gamma coactivator 1alpha expression in muscle. *Proceedings of the National Academy of Sciences of the United States of America* 100: 7111–6, 2003. doi: 10.1073/pnas.1232352100.

233. **Wright DC**, **Geiger PC**, **Han DH**, **Jones TE**, **Holloszy JO**. Calcium induces increases in peroxisome proliferator-activated receptor gamma coactivator-1alpha and mitochondrial biogenesis by a pathway leading to p38 mitogen-activated protein kinase activation. *The Journal of Biological Chemistry* 282: 18793–18799, 2007. doi: 10.1074/jbc.M611252200.

234. **Yoboue ED**, **Devin A**. Reactive Oxygen Species-Mediated Control of Mitochondrial Biogenesis. *International Journal of Cell Biology* 2012: 1–8, 2012. doi: 10.1155/2012/403870.

235. **Bouchez C**, **Devin A**. Mitochondrial Biogenesis and Mitochondrial Reactive Oxygen Species (ROS): A Complex Relationship Regulated by the cAMP/PKA Signaling Pathway. *Cells* 8, 2019. doi: 10.3390/cells8040287.

236. **Fan M**, **Rhee J**, **St-Pierre J**, **Handschin C**, **Puigserver P**, **Lin J**, **Jäeger S**, **Erdjument-Bromage H**, **Tempst P**, **Spiegelman BM**. Suppression of mitochondrial respiration through recruitment of p160 myb binding protein to PGC-1α: Modulation by p38 MAPK. *Genes and Development* 18: 278–289, 2004. doi: 10.1101/gad.1152204.

237. **Puigserver P**, **Rhee J**, **Lin J**, **Wu Z**, **Yoon JC**, **Zhang C**, **Krauss S**, **Mootha VK**, **Lowell BB**, **Spiegelman BM**. Cytokine stimulation of energy expenditure through p38 MAP kinase activation of PPARgamma coactivator-1. *Molecular Cell* 8: 971–982, 2001. doi: 10.1016/s1097-2765(01)00390-2.

238. **Barger PM**, **Browning AC**, **Garner AN**, **Kelly DP**. p38 mitogen-activated protein kinase activates peroxisome proliferator-activated receptor alpha: a potential role in the cardiac metabolic stress response. *The Journal of Biological Chemistry* 276: 44495–501, 2001. doi: 10.1074/jbc.M105945200.

239. **Zhao M**, **New L**, **Kravchenko V v**, **Kato Y**, **Gram H**, **di Padova F**, **Olson EN**, **Ulevitch RJ**, **Han J**. Regulation of the MEF2 family of transcription factors by p38. *Molecular and Cellular Biology* 19: 21–30, 1999. doi: 10.1128/mcb.19.1.21.

240. **Cao W**, **Daniel KW**, **Robidoux J**, **Puigserver P**, **Medvedev A v**, **Bai X**, **Floering LM**, **Spiegelman BM**, **Collins S**. p38 mitogen-activated protein kinase is the central regulator of cyclic AMP-dependent transcription of the brown fat uncoupling protein 1 gene. *Molecular and Cellular Biology* 24: 3057–67, 2004. doi: 10.1128/mcb.24.7.3057-3067.2004.

241. **Carter HN**, **Pauly M**, **Tryon LD**, **Hood DA**. Effect of contractile activity on PGC-1 transcription in young and aged skeletal muscle. *Journal of Applied Physiology* 124: 1605–1615, 2018. doi: 10.1152/japplphysiol.01110.2017.

242. **Combes A**, **Dekerle J**, **Webborn N**, **Watt P**, **Bougault V**, **Daussin FN**. Exercise-induced metabolic fluctuations influence AMPK, p38-MAPK and CaMKII phosphorylation in human skeletal muscle. *Physiological Reports* 3, 2015. doi: 10.14814/phy2.12462.

243. **Parker L**, **Trewin A**, **Levinger I**, **Shaw CS**, **Stepto NK**. The effect of exercise-intensity on Skeletal muscle stress kinase and insulin protein signaling. *PLoS ONE* 12, 2017. doi: 10.1371/journal.pone.0171613.

244. **Akimoto T**, **Pohnert SC**, **Li P**, **Zhang M**, **Gumbs C**, **Rosenberg PB**, **Williams RS**, **Yan Z**. Exercise stimulates Pgc-1alpha transcription in skeletal muscle through activation of the p38 MAPK pathway. *The Journal of Biological Chemistry* 280: 19587–93, 2005. doi: 10.1074/jbc.M408862200.

245. **Thomas RE**, **Andrews LA**, **Burman JL**, **Lin W-Y**, **Pallanck LJ**. PINK1-Parkin Pathway Activity Is Regulated by Degradation of PINK1 in the Mitochondrial Matrix. *PLoS Genetics* 10: e1004279, 2014. doi: 10.1371/journal.pgen.1004279.

246. **Jin SM**, **Lazarou M**, **Wang C**, **Kane LA**, **Narendra DP**, **Youle RJ**. Mitochondrial membrane potential regulates PINK1 import and proteolytic destabilization by PARL. *The Journal of Cell Biology* 191: 933–42, 2010. doi: 10.1083/jcb.201008084.

247. **Yamano K**, **Youle RJ**. PINK1 is degraded through the N-end rule pathway. *Autophagy* 9: 1758–1769, 2013. doi: 10.4161/auto.24633.

248. **Jin SM**, **Youle RJ**. The accumulation of misfolded proteins in the mitochondrial matrix is sensed by PINK1 to induce PARK2/Parkin-mediated mitophagy of polarized mitochondria. *Autophagy* 9: 1750–1757, 2013. doi: 10.4161/auto.26122.

249. **Narendra DP**, **Jin SM**, **Tanaka A**, **Suen DF**, **Gautier CA**, **Shen J**, **Cookson MR**, **Youle RJ**. PINK1 is selectively stabilized on impaired mitochondria to activate Parkin. *PLoS Biology* 8, 2010. doi: 10.1371/journal.pbio.1000298.

250. **Kondapalli C**, **Kazlauskaite A**, **Zhang N**, **Woodroof HI**, **Campbell DG**, **Gourlay R**, **Burchell L**, **Walden H**, **Macartney TJ**, **Deak M**, **Knebel A**, **Alessi DR**, **Muqit MMK**. PINK1 is activated by mitochondrial membrane potential depolarization and stimulates Parkin E3 ligase activity by phosphorylating Serine 65. *Open Biology* 2: 120080, 2012. doi: 10.1098/rsob.120080.

251. **Matsuda N**, **Sato S**, **Shiba K**, **Okatsu K**, **Saisho K**, **Gautier CA**, **Sou YS**, **Saiki S**, **Kawajiri S**, **Sato F**, **Kimura M**, **Komatsu M**, **Hattori N**, **Tanaka K**. PINK1 stabilized by mitochondrial depolarization recruits Parkin to damaged mitochondria and activates latent Parkin for mitophagy. *Journal of Cell Biology* 189: 211–221, 2010. doi: 10.1083/jcb.200910140.

252. **Okatsu K**, **Oka T**, **Iguchi M**, **Imamura K**, **Kosako H**, **Tani N**, **Kimura M**, **Go E**, **Koyano F**, **Funayama M**, **Shiba-Fukushima K**, **Sato S**, **Shimizu H**, **Fukunaga Y**, **Taniguchi H**, **Komatsu M**, **Hattori N**, **Mihara K**, **Tanaka K**, **Matsuda N**. PINK1 autophosphorylation upon membrane

potential dissipation is essential for Parkin recruitment to damaged mitochondria. *Nature Communications* 3: 1–10, 2012. doi: 10.1038/ncomms2016.

253. **Shiba-Fukushima K**, **Imai Y**, **Yoshida S**, **Ishihama Y**, **Kanao T**, **Sato S**, **Hattori N**. PINK1-mediated phosphorylation of the Parkin ubiquitin-like domain primes mitochondrial translocation of Parkin and regulates mitophagy. *Scientific Reports* 2: 1002, 2012. doi: 10.1038/srep01002.

254. **Kane LA**, **Lazarou M**, **Fogel AI**, **Li Y**, **Yamano K**, **Sarraf SA**, **Banerjee S**, **Youle RJ**. PINK1 phosphorylates ubiquitin to activate Parkin E3 ubiquitin ligase activity. *The Journal of Cell Biology* 205: 143–53, 2014. doi: 10.1083/jcb.201402104.

255. **Kazlauskaite A**, **Kondapalli C**, **Gourlay R**, **Campbell DG**, **Ritorto MS**, **Hofmann K**, **Alessi DR**, **Knebel A**, **Trost M**, **Muqit MMK**. Parkin is activated by PINK1-dependent phosphorylation of ubiquitin at Ser65. *The Biochemical Journal* 460: 127–39, 2014. doi: 10.1042/BJ20140334.

256. **Koyano F**, **Okatsu K**, **Kosako H**, **Tamura Y**, **Go E**, **Kimura M**, **Kimura Y**, **Tsuchiya H**, **Yoshihara H**, **Hirokawa T**, **Endo T**, **Fon EA**, **Trempe J-F**, **Saeki Y**, **Tanaka K**, **Matsuda N**. Ubiquitin is phosphorylated by PINK1 to activate parkin. *Nature* 510: 162–166, 2014. doi: 10.1038/nature13392.

257. **Okatsu K**, **Koyano F**, **Kimura M**, **Kosako H**, **Saeki Y**, **Tanaka K**, **Matsuda N**. Phosphorylated ubiquitin chain is the genuine Parkin receptor. *The Journal of Cell Biology* 209: 111–28, 2015. doi: 10.1083/jcb.201410050.

258. **Sarraf SA**, **Raman M**, **Guarani-Pereira V**, **Sowa ME**, **Huttlin EL**, **Gygi SP**, **Harper JW**. Landscape of the PARKIN-dependent ubiquitylome in response to mitochondrial depolarization. *Nature* 496: 372–6, 2013. doi: 10.1038/nature12043.

259. **Gegg ME**, **Cooper JM**, **Chau KY**, **Rojo M**, **Schapira AHV**, **Taanman JW**. Mitofusin 1 and mitofusin 2 are ubiquitinated in a PINK1/parkin-dependent manner upon induction of mitophagy. *Human Molecular Genetics* 19: 4861–4870, 2010. doi: 10.1093/hmg/ddq419.

260. **Tanaka A**, **Cleland MM**, **Xu S**, **Narendra DP**, **Suen DF**, **Karbowski M**, **Youle RJ**. Proteasome and p97 mediate mitophagy and degradation of mitofusins induced by Parkin. *Journal of Cell Biology* 191: 1367–1380, 2010. doi: 10.1083/jcb.201007013.

261. **Geisler S**, **Holmström KM**, **Skujat D**, **Fiesel FC**, **Rothfuss OC**, **Kahle PJ**, **Springer W**. PINK1/Parkin-mediated mitophagy is dependent on VDAC1 and p62/SQSTM1. *Nature Cell Biology* 12: 119–131, 2010. doi: 10.1038/ncb2012.

262. **Wong YC**, **Holzbaur ELF**. Optineurin is an autophagy receptor for damaged mitochondria in parkin-mediated mitophagy that is disrupted by an ALS-linked mutation. *Proceedings of the National Academy of Sciences of the United States of America* 111: E4439-48, 2014. doi: 10.1073/pnas.1405752111.

263. **Lazarou M**, **Sliter DA**, **Kane LA**, **Sarraf SA**, **Wang C**, **Burman JL**, **Sideris DP**, **Fogel AI**, **Youle RJ**. The ubiquitin kinase PINK1 recruits autophagy receptors to induce mitophagy. *Nature 2015 524:7565* 524: 309–314, 2015. doi: 10.1038/nature14893.

264. **Greene JC**, **Whitworth AJ**, **Kuo I**, **Andrews LA**, **Feany MB**, **Pallanck LJ**. Mitochondrial pathology and apoptotic muscle degeneration in Drosophila parkin mutants. *Proceedings of the National Academy of Sciences* 100: 4078–4083, 2003. doi: 10.1073/pnas.0737556100.

265. **Drew BG**, **Ribas V**, **Le JA**, **Henstridge DC**, **Phun J**, **Zhou Z**, **Soleymani T**, **Daraei P**, **Sitz D**, **Vergnes L**, **Wanagat J**, **Reue K**, **Febbraio MA**, **Hevener AL**. HSP72 Is a Mitochondrial Stress

Sensor Critical for Parkin Action, Oxidative Metabolism, and Insulin Sensitivity in Skeletal Muscle. *Diabetes* 63: 1488, 2014. doi: 10.2337/DB13-0665.

266. **Rosen KM**, **Veereshwarayya V**, **Moussa CE**, **Fu Q**, **Goldberg MS**, **Schlossmacher MG**, **Shen J**, **Querfurth HW**. Parkin protects against mitochondrial toxins and beta-amyloid accumulation in skeletal muscle cells. *Journal of Biological Chemistry* 281: 12809–12816, 2006. doi: 10.1074/jbc.M512649200.

267. **Gouspillou G**, **Godin R**, **Piquereau J**, **Picard M**, **Mofarrahi M**, **Mathew J**, **Purves-Smith FM**, **Sgarioto N**, **Hepple RT**, **Burelle Y**, **Hussain SNA**. Protective role of Parkin in skeletal muscle contractile and mitochondrial function. *Journal of Physiology* 596: 2565–2579, 2018. doi: 10.1113/JP275604.

268. **Chen CC**, **Erlich AT**, **Hood DA**. Role of Parkin and endurance training on mitochondrial turnover in skeletal muscle. *Skeletal Muscle* 8: 1–14, 2018. doi: 10.1186/s13395-018-0157-y.

269. **Chen CCW**, **Erlich AT**, **Crilly MJ**, **Hood DA**. Parkin is required for exercise-induced mitophagy in muscle: impact of aging. *American Journal of Physiology-Endocrinology and Metabolism* 315: E404–E415, 2018. doi: 10.1152/ajpendo.00391.2017.

270. **Leduc-Gaudet JP**, **Reynaud O**, **Hussain SN**, **Gouspillou G**. Parkin overexpression protects from ageing-related loss of muscle mass and strength. *Journal of Physiology* 597: 1975–1991, 2019. doi: 10.1113/JP277157.

271. **Liu L**, **Feng D**, **Chen G**, **Chen M**, **Zheng Q**, **Song P**, **Ma Q**, **Zhu C**, **Wang R**, **Qi W**, **Huang L**, **Xue P**, **Li B**, **Wang X**, **Jin H**, **Wang J**, **Yang F**, **Liu P**, **Zhu Y**, **Sui S**, **Chen Q**. Mitochondrial outer-membrane protein FUNDC1 mediates hypoxia-induced mitophagy in mammalian cells. *Nature Cell Biology* 14: 177–185, 2012. doi: 10.1038/ncb2422.

272. **Quinsay MN**, **Thomas RL**, **Lee Y**, **Gustafsson AB**. Bnip3-mediated mitochondrial autophagy is independent of the mitochondrial permeability transition pore. *Autophagy* 6: 855–62, 2010. doi: 10.4161/AUTO.6.7.13005.

273. **Hamacher-Brady A**, **Brady NR**, **Logue SE**, **Sayen MR**, **Jinno M**, **Kirshenbaum LA**, **Gottlieb RA**, **Gustafsson ÅB**. Response to myocardial ischemia/reperfusion injury involves Bnip3 and autophagy. *Cell Death and Differentiation* 14: 146–157, 2007. doi: 10.1038/sj.cdd.4401936.

274. **Chen G**, **Cizeau J**, **Velde C vande**, **Park JH**, **Bozek G**, **Bolton J**, **Shi L**, **Dubik D**, **Greenberg A**. Nix and Nip3 Form a Subfamily of Pro-apoptotic Mitochondrial Proteins. *Journal of Biological Chemistry* 274: 7–10, 1999. doi: 10.1074/JBC.274.1.7.

275. **Zhu Y**, **Massen S**, **Terenzio M**, **Lang V**, **Chen-Lindner S**, **Eils R**, **Novak I**, **Dikic I**, **Hamacher-Brady A**, **Brady NR**. Modulation of serines 17 and 24 in the LC3-interacting region of Bnip3 determines pro-survival mitophagy versus apoptosis. *The Journal of Biological Chemistry* 288: 1099–113, 2013. doi: 10.1074/jbc.M112.399345.

276. **Rogov V v.**, **Suzuki H**, **Marinković M**, **Lang V**, **Kato R**, **Kawasaki M**, **Buljubašić M**, **Šprung M**, **Rogova N**, **Wakatsuki S**, **Hamacher-Brady A**, **Dötsch V**, **Dikic I**, **Brady NR**, **Novak I**. Phosphorylation of the mitochondrial autophagy receptor Nix enhances its interaction with LC3 proteins. *Scientific Reports 2017 7:1* 7: 1–12, 2017. doi: 10.1038/s41598-017-01258-6.

277. **Hanna RA**, **Quinsay MN**, **Orogo AM**, **Giang K**, **Rikka S**, **Gustafsson ÅB**. Microtubule-associated protein 1 light chain 3 (LC3) interacts with Bnip3 protein to selectively remove endoplasmic reticulum and mitochondria via autophagy. *The Journal of Biological Chemistry* 287: 19094–104, 2012. doi: 10.1074/jbc.M111.322933.

278. **Zhang H**, **Bosch-Marce M**, **Shimoda LA**, **Tan YS**, **Baek JH**, **Wesley JB**, **Gonzalez FJ**, **Semenza GL**. Mitochondrial autophagy is an HIF-1-dependent adaptive metabolic response to hypoxia. *The Journal of Biological Chemistry* 283: 10892–903, 2008. doi: 10.1074/jbc.M800102200.

279. **Rikka S**, **Quinsay MN**, **Thomas RL**, **Kubli DA**, **Zhang X**, **Murphy AN**, **Gustafsson ÅB**. Bnip3 impairs mitochondrial bioenergetics and stimulates mitochondrial turnover. *Cell Death and Differentiation* 18: 721–31, 2011. doi: 10.1038/cdd.2010.146.

280. **Novak I**, **Kirkin V**, **McEwan DG**, **Zhang J**, **Wild P**, **Rozenknop A**, **Rogov V**, **Löhr F**, **Popovic D**, **Occhipinti A**, **Reichert AS**, **Terzic J**, **Dötsch V**, **Ney PA**, **Dikic I**. Nix is a selective autophagy receptor for mitochondrial clearance. *EMBO reports* 11: 45–51, 2010. doi: 10.1038/embor.2009.256.

281. **Schweers RL**, **Zhang J**, **Randall MS**, **Loyd MR**, **Li W**, **Dorsey FC**, **Kundu M**, **Opferman JT**, **Cleveland JL**, **Miller JL**, **Ney PA**. NIX is required for programmed mitochondrial clearance during reticulocyte maturation. *Proceedings of the National Academy of Sciences of the United States of America* 104: 19500–19505, 2007. doi: 10.1073/pnas.0708818104.

282. **Wu W**, **Tian W**, **Hu Z**, **Chen G**, **Huang L**, **Li W**, **Zhang X**, **Xue P**, **Zhou C**, **Liu L**, **Zhu Y**, **Zhang X**, **Li L**, **Zhang L**, **Sui S**, **Zhao B**, **Feng D**. ULK1 translocates to mitochondria and phosphorylates FUNDC1 to regulate mitophagy. *EMBO reports* 15: 566–75, 2014. doi: 10.1002/embr.201438501.

283. **Lee Y**, **Lee H-Y**, **Hanna R**, **Gustafsson A**. Mitochondrial autophagy by Bnip3 involves Drp1-mediated mitochondrial fission and recruitment of Parkin in cardiac myocytes. *AJP: Heart and Circulatory Physiology* 301: H1924–H1931, 2011. doi: 10.1152/ajpheart.00368.2011.

284. **Ding W-X**, **Ni H-M**, **Li M**, **Liao Y**, **Chen X**, **Stolz DB**, **Dorn GW**, **Yin X-M**, **Yin X-M**. Nix is critical to two distinct phases of mitophagy, reactive oxygen species-mediated autophagy induction and Parkin-ubiquitin-p62-mediated mitochondrial priming. *The Journal of Biological Chemistry* 285: 27879–90, 2010. doi: 10.1074/jbc.M110.119537.

285. **Simpson CL**, **Tokito MK**, **Uppala R**, **Sarkar MK**, **Gudjonsson JE**, **Holzbaur ELF**. NIX initiates mitochondrial fragmentation via DRP1 to drive epidermal differentiation. *Cell Reports* 34: 108689, 2021. doi: 10.1016/J.CELREP.2021.108689.

286. **Baechler BL**, **Bloemberg D**, **Quadrilatero J**. Mitophagy regulates mitochondrial network signaling, oxidative stress, and apoptosis during myoblast differentiation. *Autophagy* 15: 1606–1619, 2019. doi: 10.1080/15548627.2019.1591672.

287. **Lampert MA**, **Orogo AM**, **Najor RH**, **Hammerling BC**, **Leon LJ**, **Wang BJ**, **Kim T**, **Sussman MA**, **Gustafsson Åsa B.** BNIP3L/NIX and FUNDC1-mediated mitophagy is required for mitochondrial network remodeling during cardiac progenitor cell differentiation. *Autophagy* 15: 1182, 2019. doi: 10.1080/15548627.2019.1580095.

288. **Fu T**, **Xu Z**, **Liu L**, **Guo Q**, **Wu H**, **Liang X**, **Zhou D**, **Xiao L**, **Liu L**, **Liu Y**, **Zhu M-S**, **Chen Q**, **Gan Z**. Mitophagy Directs Muscle-Adipose Crosstalk to Alleviate Dietary Obesity. *Cell Reports* 23: 1357–1372, 2018. doi: 10.1016/j.celrep.2018.03.127.

289. **Gao J**, **Yu L**, **Wang Z**, **Wang R**, **Liu X**. Induction of mitophagy in C2C12 cells by electrical pulse stimulation involves increasing the level of the mitochondrial receptor FUNDC1 through the AMPK-ULK1 pathway. *American Journal of Translational Research* 12: 6879–6894, 2020.

290. **Terada S**, **Goto M**, **Kato M**, **Kawanaka K**, **Shimokawa T**, **Tabata I**. Effects of low-intensity prolonged exercise on PGC-1 mRNA expression in rat epitrochlearis muscle. *Biochemical and Biophysical Research Communications* 296: 350–354, 2002. doi: 10.1016/S0006-291X(02)00881-1.

291. **Wright DC**, **Han D**, **Garcia-roves PM**, **Geiger PC**, **Jones TE**, **Holloszy JO**. Exercise-induced Mitochondrial Biogenesis Begins before the Increase in Muscle PGC-1alpha Expression. *Journal of Biological Chemistry* 282: 194–199, 2007. doi: 10.1074/jbc.M606116200.

292. **Herzig S**, **Shaw RJ**. AMPK: guardian of metabolism and mitochondrial homeostasis. *Nature Reviews Molecular Cell Biology* 19: 121–135, 2018. doi: 10.1038/nrm.2017.95.

293. **Irrcher I**, **Adhihetty PJ**, **Sheehan T**, **Joseph AM**, **Hood DA**. PPARγ coactivator-1α expression during thyroid hormone- and contractile activity-induced mitochondrial adaptations. *American Journal of Physiology - Cell Physiology* 284, 2003. doi: 10.1152/ajpcell.00409.2002.

294. **Vainshtein A**, **Tryon LD**, **Pauly M**, **Hood DA**. Role of PGC-1α during acute exercise-induced autophagy and mitophagy in skeletal muscle. *American Journal of Physiology Cell Physiology* 308: C710-9, 2015. doi: 10.1152/ajpcell.00380.2014.

295. **Kjøbsted R**, **Hingst JR**, **Fentz J**, **Foretz M**, **Sanz MN**, **Pehmøller C**, **Shum M**, **Marette A**, **Mounier R**, **Treebak JT**, **Wojtaszewski JFP**, **Viollet B**, **Lantier L**. AMPK in skeletal muscle function and metabolism. *FASEB Journal* 32: 1741–1777, 2018. doi: 10.1096/fj.201700442R.

296. **Cantó C**, **Jiang LQ**, **Deshmukh AS**, **Mataki C**, **Coste A**, **Lagouge M**, **Zierath JR**, **Auwerx J**. Interdependence of AMPK and SIRT1 for metabolic adaptation to fasting and exercise in skeletal muscle. *Cell Metabolism* 11: 213–9, 2010. doi: 10.1016/j.cmet.2010.02.006.

297. **Gurd BJ**, **Yoshida Y**, **McFarlan JT**, **Holloway GP**, **Moyes CD**, **Heigenhauser GJF**, **Spriet L**, **Bonen A**. Nuclear SIRT1 activity, but not protein content, regulates mitochondrial biogenesis in rat and human skeletal muscle. *American Journal of Physiology - Regulatory Integrative and Comparative Physiology* 301, 2011. doi: 10.1152/ajpregu.00417.2010.

298. **Vargas-Ortiz K**, **Pérez-Vázquez V**, **Macías-Cervantes MH**. Exercise and sirtuins: A way to mitochondrial health in skeletal muscle. *International Journal of Molecular Sciences* 20, 2019. doi: 10.3390/ijms20112717.

299. **Powers SK**, **Deminice R**, **Ozdemir M**, **Yoshihara T**, **Bomkamp MP**, **Hyatt H**. Exercise-induced oxidative stress: Friend or foe? *Journal of Sport and Health Science* 9: 415, 2020. doi: 10.1016/J.JSHS.2020.04.001.

300. **Takahashi M**, **Chesley A**, **Freyssenet D**, **Hood DA**. Contractile activity-induced adaptations in the mitochondrial protein import system. *The American Journal of Physiology* 274: C1380-7, 1998. doi: 10.1152/ajpcell.1998.274.5.C1380.

301. **Joseph A**, **Hood DA**. Plasticity of TOM complex assembly in skeletal muscle mitochondria in response to chronic contractile activity. *Mitochondrion* 12: 305–312, 2012. doi: 10.1016/j.mito.2011.11.005.

302. **Holloszy JO**. Biochemical Adaptations in Muscle. *The Journal of Biological Chemistry* 242: 2278–2282, 1967.

303. **Holloszy JO**, **Booth FW**. Biochemical adaptations to endurance exercise in muscle. *Annual Review of Physiology* 38: 273–291, 1976. doi: 10.1146/annurev.ph.38.030176.001421.

304. **Kim Y**, **Hood DA**. Regulation of the autophagy system during chronic contractile activity-induced muscle adaptations. *Physiological Reports* 5, 2017. doi: 10.14814/phy2.13307.

305. **Kim Y**, **Triolo M**, **Erlich AT**, **Hood DA**. Regulation of autophagic and mitophagic flux during chronic contractile activity-induced muscle adaptations. *Pflugers Archiv* 471: 431–440, 2019. doi: 10.1007/s00424-018-2225-x.

306. **Oliveira AN**, **Hood DA**. Exercise is mitochondrial medicine for muscle. *Sports Medicine and Health Science* 1: 11–18, 2019. doi: 10.1016/J.SMHS.2019.08.008.

307. **Chen CCW**, **Erlich AT**, **Hood DA**. Role of Parkin and endurance training on mitochondrial turnover in skeletal muscle. *Skeletal Muscle* 8: 1–14, 2018. doi: 10.1186/s13395-018-0157-y.

308. **Brandt N**, **Gunnarsson TP**, **Bangsbo J**, **Pilegaard H**. Exercise and exercise training-induced increase in autophagy markers in human skeletal muscle. *Physiological Reports* 6: e13651, 2018. doi: 10.14814/phy2.13651.

309. **lo Verso F**, **Carnio S**, **Vainshtein A**, **Sandri M**. Autophagy is not required to sustain exercise and PRKAA1/AMPK activity but is important to prevent mitochondrial damage during physical activity. *Autophagy* 10: 1883–1894, 2014. doi: 10.4161/auto.32154.

310. **Yoo S-Z**, **No M-H**, **Heo J-W**, **Park D-H**, **Kang J-H**, **Kim J-H**, **Seo D-Y**, **Han J**, **Jung S-J**, **Kwak H-B**. Effects of Acute Exercise on Mitochondrial Function, Dynamics, and Mitophagy in Rat Cardiac and Skeletal Muscles. *International Neurourology Journal* 23: S22-31, 2019. doi: 10.5213/inj.1938038.019.

311. **Shang H**, **Xia Z**, **Bai S**, **Zhang HE**, **Gu B**, **Wang R**. Downhill Running Acutely Elicits Mitophagy in Rat Soleus Muscle. *Medicine and Science in Sports and Exercise* 51: 1396–1403, 2019. doi: 10.1249/MSS.0000000000001906.

312. **Drake JC**, **Laker RC**, **Wilson RJ**, **Zhang M**, **Yan Z**. Exercise-induced mitophagy in skeletal muscle occurs in the absence of stabilization of Pink1 on mitochondria. *Cell Cycle* 18: 1–6, 2018. doi: 10.1080/15384101.2018.1559556.

313. **Carter HN**, **Kim Y**, **Erlich AT**, **Zarrin-khat D**, **Hood DA**. Autophagy and mitophagy flux in young and aged skeletal muscle following chronic contractile activity. *Journal of Physiology* 596: 3568–3584, 2018. doi: 10.1113/JP275998.

314. **Ju J-S**, **Jeon S-I**, **Park J-Y**, **Lee J-Y**, **Lee S-C**, **Cho K-J**, **Jeong J-M**. Autophagy plays a role in skeletal muscle mitochondrial biogenesis in an endurance exercise-trained condition. *Journal of Physiological Sciences* 66: 417–430, 2016. doi: 10.1007/s12576-016-0440-9.

315. **Schwalm C**, **Deldicque L**, **Francaux M**. Lack of Activation of Mitophagy during Endurance Exercise in Human. *Medicine and Science in Sports and Exercise* 49: 1552–1561, 2017. doi: 10.1249/MSS.0000000000001256.

316. **Canada S**. 2016 Census of Population. 2017.

317. **Rejeski WJ**, **Mihalko SL**. Physical Activity and Quality of Life in Older Adults. *The Journals of Gerontology Series A: Biological Sciences and Medical Sciences* 56: 23–35, 2001. doi: 10.1093/gerona/56.suppl_2.23.

318. **Janssen I**, **Heymsfield SB**, **Ross R**. Low relative skeletal muscle mass (sarcopenia) in older persons is associated with functional impairment and physical disability. *Journal of the American Geriatrics Society* 50: 889–96, 2002.

319. **Santilli V**, **Bernetti A**, **Mangone M**, **Paoloni M**. Clinical definition of sarcopenia. *Clinical Cases in Mineral and Bone Metabolism* 11: 177–80, 2014.

320. **Larsson L**, **Degens H**, **Li M**, **Salviati L**, **Lee Y il**, **Thompson W**, **Kirkland JL**, **Sandri M**. Sarcopenia: Aging-Related Loss of Muscle Mass and Function. *Physiological Reviews* 99: 427, 2019. doi: 10.1152/PHYSREV.00061.2017.

321. **III LJM**, **Khosla S**, **Crowson CS**, **O'Connor MK**, **O'Fallon WM**, **Riggs BL**. Epidemiology of Sarcopenia. *Journal of the American Geriatrics Society* 48: 625–630, 2000. doi: 10.1111/J.1532-5415.2000.TB04719.X.

322. **Kim TN**, **Choi KM**. Sarcopenia: Definition, Epidemiology, and Pathophysiology. *Journal of Bone Metabolism* 20: 1, 2013. doi: 10.11005/JBM.2013.20.1.1.

323. **Tay L**, **Ding YY**, **Leung BP**, **Ismail NH**, **Yeo A**, **Yew S**, **Tay KS**, **Tan CH**, **Chong MS**. Sex-specific differences in risk factors for sarcopenia amongst community-dwelling older adults. *Age* 37: 1–12, 2015. doi: 10.1007/S11357-015-9860-3.

324. **Du Y**, **Wang X**, **Xie H**, **Zheng S**, **Wu X**, **Zhu X**, **Zhang X**, **Xue S**, **Li H**, **Hong W**, **Tang W**, **Chen M**, **Cheng Q**, **Sun J**. Sex differences in the prevalence and adverse outcomes of sarcopenia and sarcopenic obesity in community dwelling elderly in East China using the AWGS criteria. *BMC Endocrine Disorders 2019 19:1* 19: 1–11, 2019. doi: 10.1186/S12902-019-0432-X.

325. **Iannuzzi-Sucich M**, **Prestwood KM**, **Kenny AM**. Prevalence of Sarcopenia and Predictors of Skeletal Muscle Mass in Healthy, Older Men and Women. *The Journals of Gerontology: Series A* 57: M772–M777, 2002. doi: 10.1093/GERONA/57.12.M772.

326. **Janssen I**, **Heymsfield SB**, **Wang Z**, **Ross R**. Skeletal muscle mass and distribution in 468 men and women aged 18–88 yr. *Journal of Applied Physiology* 89: 81–88, 2000. doi: 10.1152/JAPPL.2000.89.1.81.

327. **di Monaco M**, **Castiglioni C**, **Vallero F**, **di Monaco R**, **Tappero R**. Sarcopenia is more prevalent in men than in women after hip fracture: A cross-sectional study of 591 inpatients. *Archives of Gerontology and Geriatrics* 55: e48–e52, 2012. doi: 10.1016/J.ARCHGER.2012.05.002.

328. **Bodine SC**. Disuse-induced muscle wasting. *The Iternational Journal of Biochemistry & Cell Biology* 45: 2200–8, 2013. doi: 10.1016/j.biocel.2013.06.011.

329. **Knight JA**. Physical inactivity: associated diseases and disorders. *Annals of Clinical and Laboratory Science* 42: 320–37, 2012.

330. **Goodpaster BH**, **Chomentowski P**, **Ward BK**, **Rossi A**, **Glynn NW**, **Delmonico MJ**, **Kritchevsky SB**, **Pahor M**, **Newman AB**. Effects of physical activity on strength and skeletal muscle fat infiltration in older adults: a randomized controlled trial. *Journal of Applied Physiology* 105: 1498–1503, 2008. doi: 10.1152/japplphysiol.90425.2008.

331. **Larsson L**, **Yu F**, **Höök P**, **Ramamurthy B**, **Marx JO**, **Pircher P**. Effects of Aging on Regulation of Muscle Contraction at the Motor Unit, Muscle Cell, and Molecular Levels. *International Journal of Sport Nutrition and Exercise Metabolism* 11: S28–S43, 2001. doi: 10.1123/IJSNEM.11.S1.S28.

332. **Frontera WR**, **Suh D**, **Krivickas LS**, **Hughes VA**, **Goldstein R**, **Roubenoff R**. Skeletal muscle fiber quality in older men and women. *American Journal of Physiology - Cell Physiology* 279, 2000. doi: 10.1152/AJPCELL.2000.279.3.C611.

333. **Lexell J**, **Henriksson-Larsén K**, **Winblad B**, **Sjöström M**. Distribution of different fiber types in human skeletal muscles: Effects of aging studied in whole muscle cross sections. *Muscle & Nerve* 6: 588–595, 1983. doi: 10.1002/MUS.880060809.

334. **Brocca L**, **McPhee JS**, **Longa E**, **Canepari M**, **Seynnes O**, **Vito G de**, **Pellegrino MA**, **Narici M**, **Bottinelli R**. Structure and function of human muscle fibres and muscle proteome in physically active older men. *The Journal of Physiology* 595: 4823, 2017. doi: 10.1113/JP274148.

335. **Miljkovic N**, **Lim J-Y**, **Miljkovic I**, **Frontera WR**. Aging of Skeletal Muscle Fibers. *Annals of Rehabilitation Medicine* 39: 155, 2015. doi: 10.5535/ARM.2015.39.2.155.

336. **Volpi E**, **Nazemi R**, **Fujita S**. Muscle tissue changes with aging. *Current Opinion in Clinical Nutrition and Metabolic Care* 7: 405–410, 2004.

337. **Purves-Smith FM**, **Solbak NM**, **Rowan SL**, **Hepple RT**. Severe atrophy of slow myofibers in aging muscle is concealed by myosin heavy chain co-expression. *Experimental Gerontology* 47: 913–918, 2012. doi: 10.1016/J.EXGER.2012.07.013.

338. **Liu W**, **Klose A**, **Forman S**, **Paris ND**, **Wei-LaPierre L**, **Cortés-Lopéz M**, **Tan A**, **Flaherty M**, **Miura P**, **Dirksen RT**, **Chakkalakal J v**. Loss of adult skeletal muscle stem cells drives age-related neuromuscular junction degeneration. *eLife* 6, 2017. doi: 10.7554/ELIFE.26464.

339. **Khosa S**, **Trikamji B**, **Khosa GS**, **Khanli HM**, **Mishra SK**. An Overview of Neuromuscular Junction Aging Findings in Human and Animal Studies. *Current Aging Science* 12: 28, 2019. doi: 10.2174/1874609812666190603165746.

340. **Renganathan M**, **Messi ML**, **Delbono O**. Dihydropyridine Receptor-Ryanodine Receptor Uncoupling in Aged Skeletal Muscle. *The Journal of Membrane Biology 1997 157 :3* 157: 247–253, 1997. doi: 10.1007/S002329900233.

341. **Anderson AA**, **Altafaj X**, **Zheng Z**, **Wang Z-M**, **Delbono O**, **Ronjat M**, **Treves S**, **Zorzato F**. The junctional SR protein JP-45 affects the functional expression of the voltage-dependent Ca2+ channel Cav1.1. *Journal of Cell Science* 119: 2145, 2006. doi: 10.1242/JCS.02935.

342. **Russ DW**, **Grandy JS**, **Toma K**, **Ward CW**. Ageing, but not yet senescent, rats exhibit reduced muscle quality and sarcoplasmic reticulum function. *Acta Physiologica* 201: 391–403, 2011. doi: 10.1111/J.1748-1716.2010.02191.X.

343. **Larsson L**, **Salviati G**. Effects of age on calcium transport activity of sarcoplasmic reticulum in fast- and slow-twitch rat muscle fibres. *The Journal of Physiology* 419: 253, 1989. doi: 10.1113/JPHYSIOL.1989.SP017872.

344. **Jiménez-Moreno R**, **Wang Z-M**, **Gerring RC**, **Delbono O**. Sarcoplasmic Reticulum Ca2+ Release Declines in Muscle Fibers from Aging Mice. *Biophysical Journal* 94: 3178, 2008. doi: 10.1529/BIOPHYSJ.107.118786.

345. **González E**, **Messi ML**, **Zheng Z**, **Delbono O**. Insulin-like growth factor-1 prevents age-related decrease in specific force and intracellular Ca2+ in single intact muscle fibres from transgenic mice. *The Journal of Physiology* 552: 833, 2003. doi: 10.1113/JPHYSIOL.2003.048165.

346. **Miller MS**, **Toth MJ**. Myofilament Protein Alterations Promote Physical Disability in Aging and Disease. *Exercise and Sport Sciences Reviews* 41: 93, 2013. doi: 10.1097/JES.0B013E31828BBCD8.

347. **Ochala J**, **Frontera WR**, **Dorer DJ**, **Hoecke J van**, **Krivickas LS**. Single Skeletal Muscle Fiber Elastic and Contractile Characteristics in Young and Older Men. *The Journals of Gerontology: Series A* 62: 375–381, 2007. doi: 10.1093/GERONA/62.4.375.

348. **Correa-de-Araujo R**, **Addison O**, **Miljkovic I**, **Goodpaster BH**, **Bergman BC**, **Clark R v.**, **Elena JW**, **Esser KA**, **Ferrucci L**, **Harris-Love MO**, **Kritchevsky SB**, **Lorbergs A**, **Shepherd JA**, **Shulman GI**, **Rosen CJ**. Myosteatosis in the Context of Skeletal Muscle Function Deficit: An Interdisciplinary Workshop at the National Institute on Aging. *Frontiers in Physiology* 0: 963, 2020. doi: 10.3389/FPHYS.2020.00963.

349. **Rivas DA**, **McDonald DJ**, **Rice NP**, **Haran PH**, **Dolnikowski GG**, **Fielding RA**. Diminished anabolic signaling response to insulin induced by intramuscular lipid accumulation is associated with inflammation in aging but not obesity. *American Journal of Physiology - Regulatory, Integrative and Comparative Physiology* 310: R561, 2016. doi: 10.1152/AJPREGU.00198.2015.

350. **Johannsen DL**, **Conley KE**, **Bajpeyi S**, **Punyanitya M**, **Gallagher D**, **Zhang Z**, **Covington J**, **Smith SR**, **Ravussin E**. Ectopic Lipid Accumulation and Reduced Glucose Tolerance in Elderly Adults Are Accompanied by Altered Skeletal Muscle Mitochondrial Activity. *The Journal of Clinical Endocrinology and Metabolism* 97: 242, 2012. doi: 10.1210/JC.2011-1798.

351. **Shou J**, **Chen P-J**, **Xiao W-H**. Mechanism of increased risk of insulin resistance in aging skeletal muscle. *Diabetology & Metabolic Syndrome 2020 12:1* 12: 1–10, 2020. doi: 10.1186/S13098-020-0523-X.

352. **Alnaqeeb MA**, **Zaid NS al**, **Goldspink G**. Connective tissue changes and physical properties of developing and ageing skeletal muscle. *Journal of Anatomy* 139: 677, 1984.

353. **Imamura K**, **Ashida H**, **Ishikawa T**, **Fujii M**. Human major psoas muscle and sacrospinalis muscle in relation to age: a study by computed tomography. *Journal of Gerontology* 38: 678–681, 1983. doi: 10.1093/GERONJ/38.6.678.

354. **Kovanen V**, **Suominen H**, **Peltonen L**. Effects of aging and life-long physical training on collagen in slow and fast skeletal muscle in rats. A morphometric and immuno-histochemical study. *Cell and Tissue Research* 248: 247–255, 1987. doi: 10.1007/BF00218191.

355. **Reid MB**, **Li Y-P**. Tumor necrosis factor-α and muscle wasting: a cellular perspective. *Respiratory Research* 2: 269, 2001. doi: 10.1186/RR67.

356. **Wang DT**, **Yin Y**, **Yang YJ**, **Lv PJ**, **Shi Y**, **Lu L**, **Wei LB**. Resveratrol prevents TNF-α-induced muscle atrophy via regulation of Akt/mTOR/FoxO1 signaling in C2C12 myotubes. *International Immunopharmacology* 19: 206–213, 2014. doi: 10.1016/J.INTIMP.2014.02.002.

357. **White JP**, **Puppa MJ**, **Gao S**, **Sato S**, **Welle SL**, **Carson JA**. Muscle mTORC1 suppression by IL-6 during cancer cachexia: a role for AMPK. *American Journal of Physiology - Endocrinology and Metabolism* 304: 1042–1052, 2013. doi: 10.1152/AJPENDO.00410.2012.

358. **Haddad F**, **Zaldivar F**, **Cooper DM**, **Adams GR**. IL-6-induced skeletal muscle atrophy. *Journal of Applied Physiology* 98: 911–917, 2005. doi: 10.1152/JAPPLPHYSIOL.01026.2004.

359. **Huang Z**, **Zhong L**, **Zhu J**, **Xu H**, **Ma W**, **Zhang L**, **Shen Y**, **Law BY-K**, **Ding F**, **Gu X**, **Sun H**. Inhibition of IL-6/JAK/STAT3 pathway rescues denervation-induced skeletal muscle atrophy. *Annals of Translational Medicine* 8: 1681–1681, 2020. doi: 10.21037/ATM-20-7269.

360. **Wang J**, **Leung K-S**, **Chow SK-H**, **Cheung W-H**. Inflammation and age-associated skeletal muscle deterioration (sarcopaenia). *Journal of Orthopaedic Translation* 10: 94, 2017. doi: 10.1016/J.JOT.2017.05.006.

361. **Marzetti E**, **Carter CS**, **Wohlgemuth SE**, **Lees HA**, **Giovannini S**, **Anderson B**, **Quinn LS**, **Leeuwenburgh C**. Changes in IL-15 expression and death-receptor apoptotic signaling in rat gastrocnemius muscle with aging and life-long calorie restriction. *Mechanisms of Ageing and Development* 130: 272, 2009. doi: 10.1016/J.MAD.2008.12.008.

362. **Perrini S**, **Laviola L**, **Carreira MC**, **Cignarelli A**, **Natalicchio A**, **Giorgino F**. The GH/IGF1 axis and signaling pathways in the muscle and bone: mechanisms underlying age-related skeletal muscle wasting and osteoporosis. *Journal of Endocrinology* 205: 201–210, 2010. doi: 10.1677/JOE-09-0431.

363. **O'connor KG**, **Tobin JD**, **Harman SM**, **Plato CC**, **Roy TA**, **Sherman SS**, **Blackman MR**. Serum Levels of Insulin-like Growth Factor-I Are Related to Age and Not to Body Composition in Healthy Women and Men. *Journal of Gerontology: Medical Science* 53: 176–82, 1998. doi: 10.1093/gerona/53a.3.m176.

364. **Gharahdaghi N**, **Phillips BE**, **Szewczyk NJ**, **Smith K**, **Wilkinson DJ**, **Atherton PJ**. Links Between Testosterone, Oestrogen, and the Growth Hormone/Insulin-Like Growth Factor Axis and Resistance Exercise Muscle Adaptations. *Frontiers in Physiology* 0: 1814, 2021. doi: 10.3389/FPHYS.2020.621226.

365. **Chidi-Ogbolu N**, **Baar K**. Effect of Estrogen on Musculoskeletal Performance and Injury Risk. *Frontiers in Physiology* 0: 1834, 2019. doi: 10.3389/FPHYS.2018.01834.

366. **White TA**, **LeBrasseur NK**. Myostatin and Sarcopenia: Opportunities and Challenges - A Mini-Review. *Gerontology* 60: 289–293, 2014. doi: 10.1159/000356740.

367. **Etienne J**, **Liu C**, **Skinner CM**, **Conboy MJ**, **Conboy IM**. Skeletal muscle as an experimental model of choice to study tissue aging and rejuvenation. *Skeletal Muscle 2020 10:1* 10: 1–16, 2020. doi: 10.1186/S13395-020-0222-1.

368. **Verdijk LB**, **Koopman R**, **Schaart G**, **Meijer K**, **Savelberg HHCM**, **Loon LJC van**. Satellite cell content is specifically reduced in type II skeletal muscle fibers in the elderly. *American Journal of Physiology - Endocrinology and Metabolism* 292: 151–157, 2007. doi: 10.1152/AJPENDO.00278.2006.

369. **Rasmussen BB**, **Fujita S**, **Wolfe RR**, **Mittendorfer B**, **Roy M**, **Rowe VL**, **Volpi E**. Insulin resistance of muscle protein metabolism in aging. *The FASEB Journal* 20: 768, 2006. doi: 10.1096/FJ.05-4607FJE.

370. **Paulussen KJM**, **McKenna CF**, **Beals JW**, **Wilund KR**, **Salvador AF**, **Burd NA**. Anabolic Resistance of Muscle Protein Turnover Comes in Various Shapes and Sizes. *Frontiers in Nutrition* 0: 115, 2021. doi: 10.3389/FNUT.2021.615849.

371. **Endo Y**, **Nourmahnad A**, **Sinha I**. Optimizing Skeletal Muscle Anabolic Response to Resistance Training in Aging. *Frontiers in Physiology* 0: 874, 2020. doi: 10.3389/FPHYS.2020.00874.

372. **Samengo G**, **Avik A**, **Fedor B**, **Whittaker D**, **Myung KH**, **Wehling-Henricks M**, **Tidball JG**. Age-related loss of nitric oxide synthase in skeletal muscle causes reductions in calpain Snitrosylation that increase myofibril degradation and sarcopenia. *Aging Cell* 11: 1036–1045, 2012. doi: 10.1111/ACEL.12003.

373. **Altun M**, **Besche HC**, **Overkleeft HS**, **Piccirillo R**, **Edelmann MJ**, **Kessler BM**, **Goldberg AL**, **Ulfhake B**. Muscle Wasting in Aged, Sarcopenic Rats Is Associated with Enhanced Activity of the Ubiquitin Proteasome Pathway. *Journal of Biological Chemistry* 285: 39597–39608, 2010. doi: 10.1074/jbc.M110.129718.

374. **Mikkelsen UR**, **Agergaard J**, **Couppé C**, **Grosset JF**, **Karlsen A**, **Magnusson SP**, **Schjerling P**, **Kjaer M**, **Mackey AL**. Skeletal muscle morphology and regulatory signalling in endurance-trained and sedentary individuals: The influence of ageing. *Experimental Gerontology* 93: 54–67, 2017. doi: 10.1016/j.exger.2017.04.001.

375. **Stefanetti RJ**, **Zacharewicz E**, **Gatta P della**, **Garnham A**, **Russell AP**, **Lamon S**. Ageing has no effect on the regulation of the ubiquitin proteasome-related genes and proteins following resistance exercise. *Frontiers in Physiology* 5, 2014. doi: 10.3389/fphys.2014.00030.

376. **Wagatsuma A**, **Shiozuka M**, **Takayama Y**, **Hoshino T**, **Mabuchi K**, **Matsuda R**. Effects of ageing on expression of the muscle-specific E3 ubiquitin ligases and Akt-dependent regulation of Foxo transcription factors in skeletal muscle. *Molecular and Cellular Biochemistry* 412: 59–72, 2016. doi: 10.1007/s11010-015-2608-7.

377. **Léger B**, **Derave W**, **de Bock K**, **Hespel P**, **Russell AP**. Human Sarcopenia Reveals an Increase in SOCS-3 and Myostatin and a Reduced Efficiency of Akt Phosphorylation. *Rejuvenation Research* 11: 163–175, 2008. doi: 10.1089/rej.2007.0588.

378. **White Z**, **Terrill J**, **White RB**, **McMahon C**, **Sheard P**, **Grounds MD**, **Shavlakadze T**. Voluntary resistance wheel exercise from mid-life prevents sarcopenia and increases markers of mitochondrial function and autophagy in muscles of old male and female C57BL/6J mice. *Skeletal Muscle 2016 6:1* 6: 1–21, 2016. doi: 10.1186/S13395-016-0117-3.

379. **Paturi S**, **Gutta AK**, **Katta A**, **Kakarla SK**, **Arvapalli RK**, **Gadde MK**, **Nalabotu SK**, **Rice KM**, **Wu M**, **Blough E**. Effects of aging and gender on muscle mass and regulation of Akt-mTOR-p70s6k related signaling in the F344BN rat model. *Mechanisms of Ageing and Development* 131: 202–209, 2010. doi: 10.1016/j.mad.2010.01.008.

380. **Paturi S**, **Gutta AK**, **Katta A**, **Kakarla SK**, **Arvapalli RK**, **Gadde MK**, **Nalabotu SK**, **Rice KM**, **Wu M**, **Blough E**. Effects of aging and gender on muscle mass and regulation of Akt-mTOR-p70s6k related signaling in the F344BN rat model. *Mechanisms of Ageing and Development* 131: 202–209, 2010. doi: 10.1016/J.MAD.2010.01.008.

381. **White Z**, **White RB**, **McMahon C**, **Grounds MD**, **Shavlakadze T**. High mTORC1 signaling is maintained, while protein degradation pathways are perturbed in old murine skeletal muscles in the fasted state. *International Journal of Biochemistry and Cell Biology* 78: 10–21, 2016. doi: 10.1016/j.biocel.2016.06.012.

382. **Stefanetti RJ**, **Voisin S**, **Russell A**, **Lamon S**. Recent advances in understanding the role of FOXO3. *F1000Research* 7, 2018. doi: 10.12688/f1000research.15258.1.

383. **Beharry AW**, **Sandesara PB**, **Roberts BM**, **Ferreira LF**, **Senf SM**, **Judge AR**. HDAC1 activates FoxO and is both sufficient and required for skeletal muscle atrophy. *Journal of Cell Science* 127: 1441–1453, 2014. doi: 10.1242/jcs.136390.

384. **Kim KW**, **Cho H-J**, **Khaliq SA**, **Son KH**, **Yoon M-S**. Comparative Analyses of mTOR/Akt and Muscle Atrophy-Related Signaling in Aged Respiratory and Gastrocnemius Muscles. *International Journal of Molecular Sciences* 21, 2020. doi: 10.3390/IJMS21082862.

385. **Koltai E**, **Hart N**, **Taylor AW**, **Goto S**, **Ngo JK**, **Davies KJA**, **Radak Z**. Integrative and Translational Physiology: Integrative Aspects of Energy Homeostasis and Metabolic Diseases: Age-associated declines in mitochondrial biogenesis and protein quality control factors are minimized by exercise training. *American Journal of Physiology - Regulatory, Integrative and Comparative Physiology* 303: R127, 2012. doi: 10.1152/AJPREGU.00337.2011.

386. **Ljubicic V**, **Hood DA**. Diminished contraction-induced intracellular signaling towards mitochondrial biogenesis in aged skeletal muscle. *Aging Cell* 8: 394–404, 2009. doi: 10.1111/j.1474-9726.2009.00483.x.

387. **Hardman SE**, **Hall DE**, **Cabrera AJ**, **Hancock CR**, **Thomson DM**. The effects of age and muscle contraction on AMPK activity and heterotrimer composition. *Experimental Gerontology* 55: 120–128, 2014. doi: 10.1016/j.exger.2014.04.007.

388. **Reznick RM**, **Zong H**, **Li J**, **Morino K**, **Moore IK**, **Yu HJ**, **Liu ZX**, **Dong J**, **Mustard KJ**, **Hawley SA**, **Befroy D**, **Pypaert M**, **Hardie DG**, **Young LH**, **Shulman GI**. Aging-Associated Reductions in AMP-Activated Protein Kinase Activity and Mitochondrial Biogenesis. *Cell Metabolism* 5: 151–156, 2007. doi: 10.1016/j.cmet.2007.01.008.

389. **Parkington JD**, **LeBrasseur NK**, **Siebert AP**, **Fielding RA**. Contraction-mediated mTOR, p70S6k, and ERK1/2 phosphorylation in aged skeletal muscle. *Journal of Applied Physiology* 97: 243–248, 2004. doi: 10.1152/JAPPLPHYSIOL.01383.2003.

390. **Segalés J**, **Perdiguero E**, **Serrano AL**, **Sousa-Victor P**, **Ortet L**, **Jardí M**, **Budanov A v.**, **Garcia-Prat L**, **Sandri M**, **Thomson DM**, **Karin M**, **Hee Lee J**, **Muñoz-Cánoves P**. Sestrin prevents atrophy of disused and aging muscles by integrating anabolic and catabolic signals. *Nature Communications* 11: 1–13, 2020. doi: 10.1038/s41467-019-13832-9.

391. **Fodor J**, **Al-Gaadi D**, **Czirják T**, **Oláh T**, **Dienes B**, **Csernoch L**, **Szentesi P**. Improved Calcium Homeostasis and Force by Selenium Treatment and Training in Aged Mouse Skeletal Muscle. *Scientific Reports* 10: 1–14, 2020. doi: 10.1038/s41598-020-58500-x.

392. **Ziaaldini MM**, **Marzetti E**, **Picca A**, **Murlasits Z**. Biochemical pathways of sarcopenia and their modulation by physical exercise: A narrative review. *Frontiers in Medicine* 4, 2017. doi: 10.3389/fmed.2017.00167.

393. **Fraysse B**, **Desaphy JF**, **Rolland JF**, **Pierno S**, **Liantonio A**, **Giannuzzi V**, **Camerino C**, **Didonna MP**, **Cocchi D**, **de Luca A**, **Conte Camerino D**. Fiber type-related changes in rat skeletal muscle calcium homeostasis during aging and restoration by growth hormone. *Neurobiology of Disease* 21: 372–380, 2006. doi: 10.1016/j.nbd.2005.07.012.

394. **Damiano S**, **Muscariello E**, **la Rosa G**, **di Maro M**, **Mondola P**, **Santillo M**. Dual role of reactive oxygen species in muscle function: Can antioxidant dietary supplements counteract age-related sarcopenia? *International Journal of Molecular Sciences* 20, 2019. doi: 10.3390/ijms20153815.

395. **Wohlgemuth SE**, **Seo AY**, **Marzetti E**, **Lees HA**, **Leeuwenburgh C**. Skeletal muscle autophagy and apoptosis during aging: Effects of calorie restriction and life-long exercise. *Experimental Gerontology* 45: 138–148, 2010. doi: 10.1016/j.exger.2009.11.002.

396. **Fritzen AM**, **Frøsig C**, **Jeppesen J**, **Jensen TE**, **Lundsgaard AM**, **Serup AK**, **Schjerling P**, **Proud CG**, **Richter EA**, **Kiens B**. Role of AMPK in regulation of LC3 lipidation as a marker of autophagy in skeletal muscle. *Cellular Signalling* 28: 663–674, 2016. doi: 10.1016/J.CELLSIG.2016.03.005.

397. **Sakuma K**, **Kinoshita M**, **Ito Y**, **Aizawa M**, **Aoi W**, **Yamaguchi A**. p62/SQSTM1 but not LC3 is accumulated in sarcopenic muscle of mice. *Journal of Cachexia, Sarcopenia and Muscle* 7: 204–212, 2016. doi: 10.1002/jcsm.12045.

398. **Yeo D**, **Kang C**, **Gomez-Cabrera MC**, **Vina J**, **Ji LL**. Intensified mitophagy in skeletal muscle with aging is downregulated by PGC-1alpha overexpression in vivo. *Free Radical Biology and Medicine* 130: 361–368, 2018. doi: 10.1016/j.freeradbiomed.2018.10.456.

399. **O'Leary MF**, **Vainshtein A**, **Iqbal S**, **Ostojic O**, **Hood DA**. Adaptive plasticity of autophagic proteins to denervation in aging skeletal muscle. *American Journal of Physiology-Cell Physiology* 304: C422–C430, 2013. doi: 10.1152/ajpcell.00240.2012.

400. **Fry CS**, **Drummond MJ**, **Glynn EL**, **Dickinson JM**, **Gundermann DM**, **Timmerman KL**, **Walker DK**, **Volpi E**, **Rasmussen BB**. Skeletal muscle autophagy and protein breakdown following resistance exercise are similar in younger and older adults. *Journals of Gerontology - Series A Biological Sciences and Medical Sciences* 68: 599–607, 2013. doi: 10.1093/gerona/gls209.

401. **Balan E**, **Schwalm C**, **Naslain D**, **Nielens H**, **Francaux M**, **Deldicque L**. Regular Endurance Exercise Promotes Fission, Mitophagy, and Oxidative Phosphorylation in Human Skeletal Muscle Independently of Age. *Frontiers in Physiology* 0: 1088, 2019. doi: 10.3389/FPHYS.2019.01088.

402. **Distefano G**, **Standley RA**, **Dubé JJ**, **Carnero EA**, **Ritov VB**, **Stefanovic-Racic M**, **Toledo FGS**, **Piva SR**, **Goodpaster BH**, **Coen PM**. Chronological Age Does not Influence Ex-vivo Mitochondrial Respiration and Quality Control in Skeletal Muscle. *The Journals of Gerontology: Series A* 72: 535–542, 2017. doi: 10.1093/GERONA/GLW102.

403. **Baehr LM**, **West DWD**, **Marcotte G**, **Marshall AG**, **de Sousa LG**, **Baar K**, **Bodine SC**. Age-related deficits in skeletal muscle recovery following disuse are associated with neuromuscular junction instability and ER stress, not impaired protein synthesis. *Aging* 8: 127–146, 2016. doi: 10.18632/aging.100879.

404. **Brunk UT**, **Terman A**. The mitochondrial-lysosomal axis theory of aging. *European Journal of Biochemistry* 269: 1996–2002, 2002. doi: 10.1046/j.1432-1033.2002.02869.x.

405. **Terman A**, **Kurz T**, **Navratil M**, **Arriaga EA**, **Brunk UT**. Mitochondrial Turnover and aging of long-lived postmitotic cells: The mitochondrial-lysosomal axis theory of aging. *Antioxidants and Redox Signaling* 12: 503–535, 2010. doi: 10.1089/ars.2009.2598.

406. **Hütter E**, **Skovbro M**, **Lener B**, **Prats C**, **Rabøl R**, **Dela F**, **Jansen-Dürr P**. Oxidative stress and mitochondrial impairment can be separated from lipofuscin accumulation in aged human skeletal muscle. *Aging Cell* 6: 245–256, 2007. doi: 10.1111/j.1474-9726.2007.00282.x.

407. **Fernando R**, **Castro JP**, **Flore T**, **Deubel S**, **Grune T**, **Ott C**. Age-Related Maintenance of the Autophagy-Lysosomal System Is Dependent on Skeletal Muscle Type. *Oxidative Medicine and Cellular Longevity* 2020, 2020. doi: 10.1155/2020/4908162.

408. **Marzetti E**, **Leeuwenburgh C**. Skeletal muscle apoptosis, sarcopenia and frailty at old age. *Experimental Gerontology* 41: 1234–1238, 2006. doi: 10.1016/J.EXGER.2006.08.011.

409. **Cheema N**, **Herbst A**, **Mckenzie D**, **Aiken JM**. Apoptosis and necrosis mediate skeletal muscle fiber loss in age-induced mitochondrial enzymatic abnormalities. *Aging Cell* 14: 1085–1093, 2015. doi: 10.1111/acel.12399.

410. **Wang F**, **Gómez-Sintes R**, **Boya P**. Lysosomal membrane permeabilization and cell death. *Traffic* 19: 918–931, 2018. doi: 10.1111/tra.12613.

411. **Kang C**, **Chung E**, **Diffee G**, **Ji LL**. Exercise training attenuates aging-associated mitochondrial dysfunction in rat skeletal muscle: Role of PGC-1α. *Experimental Gerontology* 48: 1343–1350, 2013. doi: 10.1016/J.EXGER.2013.08.004.

412. **Welle S**, **Bhatt K**, **Shah B**, **Needler N**, **Delehanty JM**, **Thornton CA**. Reduced amount of mitochondrial DNA in aged human muscle. *https://doi.org/101152/japplphysiol010612002* 94: 1479–1484, 2003. doi: 10.1152/JAPPLPHYSIOL.01061.2002.

413. **Short KR**, **Bigelow ML**, **Kahl J**, **Singh R**, **Coenen-Schimke J**, **Raghavakaimal S**, **Nair KS**. Decline in skeletal muscle mitochondrial function with aging in humans. *Proceedings of the National Academy of Sciences of the United States of America* 102: 5618–23, 2005. doi: 10.1073/pnas.0501559102.

414. **Ljubicic V**, **Joseph AM**, **Adhihetty PJ**, **Huang JH**, **Saleem A**, **Uguccioni G**, **Hood DA**. Molecular basis for an attenuated mitochondrial adaptive plasticity in aged skeletal muscle. *Aging* 1: 818–830, 2009. doi: 10.18632/aging.100083.

415. **Gomes AP**, **Price NL**, **Ling AJY**, **Moslehi JJ**, **Montgomery MK**, **Rajman L**, **White JP**, **Teodoro JS**, **Wrann CD**, **Hubbard BP**, **Mercken EM**, **Palmeira CM**, **Cabo R de**, **Rolo AP**, **Turner N**, **Bell EL**, **Sinclair DA**. Declining NAD+ Induces a Pseudohypoxic State Disrupting Nuclear-Mitochondrial Communication during Aging. *Cell* 155: 1624, 2013. doi: 10.1016/J.CELL.2013.11.037.

416. **Iqbal S**, **Ostojic O**, **Singh K**, **Joseph A-M**, **Hood DA**. Expression of mitochondrial fission and fusion regulatory proteins in skeletal muscle during chronic use and disuse. *Muscle & Nerve* 48: 963–970, 2013. doi: 10.1002/mus.23838.

417. **Boffoli D**, **Scacco SC**, **Vergari R**, **Solarino G**, **Santacroce G**, **Papa S**. Decline with age of the respiratory chain activity in human skeletal muscle. *Biochimica et Biophysica Acta (BBA) - Molecular Basis of Disease* 1226: 73–82, 1994. doi: 10.1016/0925-4439(94)90061-2.

418. **Trounce I**, **Byrne E**, **Marzuki S**. Decline in Skeletal Muscle Mitochondrial Respiratory Chain Function: Possible Factor in Ageing. *The Lancet* 333: 637–639, 1989. doi: 10.1016/S0140-6736(89)92143-0.

419. **Conley KE**, **Jubrias SA**, **Esselman PC**. Oxidative capacity and ageing in human muscle. *The Journal of Physiology* 526: 203–210, 2000. doi: 10.1111/J.1469-7793.2000.T01-1-00203.X.

420. **Marcinek DJ**, **Schenkman KA**, **Ciesielski WA**, **Lee D**, **Conley KE**. Reduced mitochondrial coupling in vivo alters cellular energetics in aged mouse skeletal muscle. *The Journal of Physiology* 569: 467–473, 2005. doi: 10.1113/JPHYSIOL.2005.097782.

421. **Sakellariou GK**, **Pearson T**, **Lightfoot AP**, **Nye GA**, **Wells N**, **Giakoumaki II**, **Vasilaki A**, **Griffiths RD**, **Jackson MJ**, **McArdle A**. Mitochondrial ROS regulate oxidative damage and mitophagy but not age-related muscle fiber atrophy. *Scientific Reports 2016 6:1* 6: 1–15, 2016. doi: 10.1038/srep33944.

422. **Carter HN**, **Chen CCW**, **Hood DA**. Mitochondria, muscle health, and exercise with advancing age. *Physiology* 30: 208–223, 2015. doi: 10.1152/physiol.00039.2014.

423. **Chabi B**, **Ljubicic V**, **Menzies KJ**, **Huang JH**, **Saleem A**, **Hood DA**. Mitochondrial function and apoptotic susceptibility in aging skeletal muscle. *Aging Cell* 7: 2–12, 2008. doi: 10.1111/j.1474-9726.2007.00347.x.

424. **Mecocci P**, **Fanó G**, **Fulle S**, **MacGarvey U**, **Shinobu L**, **Polidori MC**, **Cherubini A**, **Vecchiet J**, **Senin U**, **Beal MF**. Age-dependent increases in oxidative damage to DNA, lipids, and proteins in human skeletal muscle. *Free Radical Biology and Medicine* 26: 303–308, 1999. doi: 10.1016/S0891-5849(98)00208-1.

425. **Melov S**, **Shoffner JM**, **Kaufman A**, **Wallace DC**. Marked increase in the number and variety of mitochondrial DNA rearrangements in aging human skeletal muscle. *Nucleic Acids Research* 23: 4122, 1995. doi: 10.1093/NAR/23.20.4122.

426. **Ivannikov M v.**, **Remmen H van**. Sod1 gene ablation in adult mice leads to physiological changes at the neuromuscular junction similar to changes that occur in old wild type mice. *Free Radical Biology & Medicine* 84: 254–275, 2015. doi: 10.1016/J.FREERADBIOMED.2015.03.021.

427. **Schriner SE**, **Linford NJ**, **Martin GM**, **Treuting P**, **Ogburn CE**, **Emond M**, **Coskun PE**, **Ladiges W**, **Wolf N**, **van Remmen H**, **Wallace DC**, **Rabinovitch PS**. Extension of murine life span by overexpression of catalase targeted to mitochondria. *Science* 308: 1909–1911, 2005. doi: 10.1126/science.1106653.

428. **Bua EA**, **McKiernan SH**, **Wanagat J**, **McKenzie D**, **Aiken JM**. Mitochondrial abnormalities are more frequent in muscles undergoing sarcopenia. *Journal of Applied Physiology* 92: 2617–2624, 2002. doi: 10.1152/japplphysiol.01102.2001.

429. **Cheema NJ**, **Herbst A**, **McKenzie D**, **Aiken JM**. Apoptosis and necrosis mediate skeletal muscle fiber loss in age-induced mitochondrial enzymatic abnormalities. *Aging Cell* 14: 1085–1093, 2015. doi: 10.1111/acel.12399.

430. **Herbst A**, **Widjaja K**, **Nguy B**, **Lushaj EB**, **Moore TM**, **Hevener AL**, **McKenzie D**, **Aiken JM**, **Wanagat J**. Digital PCR Quantitation of Muscle Mitochondrial DNA: Age, Fiber Type, and Mutation-Induced Changes. *Journals of Gerontology - Series A Biological Sciences and Medical Sciences* 72: 1327–1333, 2017. doi: 10.1093/gerona/glx058.

431. **Dirks A**, **Leeuwenburgh C**. Apoptosis in skeletal muscle with aging. *American Journal of Physiology - Regulatory Integrative and Comparative Physiology* 282: R519-527, 2002. doi: 10.1152/AJPREGU.00458.2001.

432. **Dirks AJ**, **Leeuwenburgh C**. Aging and lifelong calorie restriction result in adaptations of skeletal muscle apoptosis repressor, apoptosis-inducing factor, X-linked inhibitor of apoptosis, caspase-3, and caspase-12. *Free Radical Biology and Medicine* 36: 27–39, 2004. doi: 10.1016/j.freeradbiomed.2003.10.003.

433. **Gouspillou G**, **Sgarioto N**, **Kapchinsky S**, **Purves-Smith F**, **Norris B**, **Pion CH**, **Barbat-Artigas S**, **Lemieux F**, **Taivassalo T**, **Morais JA**, **Aubertin-Leheudre M**, **Hepple RT**. Increased sensitivity to mitochondrial permeability transition and myonuclear translocation of endonuclease G in atrophied muscle of physically active older humans. *The FASEB Journal* 28: 1621–1633, 2014. doi: 10.1096/FJ.13-242750.

434. **Marzetti E**, **Groban L**, **Wohlgemuth SE**, **Lees HA**, **Lin M**, **Jobe H**, **Giovannini S**, **Leeuwenburgh C**, **Carter CS**. Effects of short-term GH supplementation and treadmill exercise training on physical performance and skeletal muscle apoptosis in old rats. *American Journal of Physiology - Regulatory Integrative and Comparative Physiology* 294: 558–567, 2008. doi: 10.1152/AJPREGU.00620.2007.

435. **Conley KE**, **Marcinek DJ**, **Villarin J**. Mitochondrial dysfunction and age. *Current Opinion in Clinical Nutrition and Metabolic Care* 10: 688–92, 2007. doi: 10.1097/MCO.0b013e3282f0dbfb.

436. **Koltai E**, **Hart N**, **Taylor AW**, **Goto S**, **Ngo JK**, **Davies KJA**, **Radak Z**. Age-associated declines in mitochondrial biogenesis and protein quality control factors are minimized by exercise training. *American Journal of Physiology-Regulatory, Integrative and Comparative Physiology* 303: R127–R134, 2012. doi: 10.1152/ajpregu.00337.2011.

437. **Pugh TD**, **Conklin MW**, **Evans TD**, **Polewski MA**, **Barbian HJ**, **Pass R**, **Anderson BD**, **Colman RJ**, **Eliceiri KW**, **Keely PJ**, **Weindruch R**, **Beasley TM**, **Anderson RM**. A shift in energy metabolism anticipates the onset of sarcopenia in rhesus monkeys. *Aging Cell* 12: 672, 2013. doi: 10.1111/ACEL.12091.

438. **Wenz T**, **Rossi SG**, **Rotundo RL**, **Spiegelman BM**, **Moraes CT**. Increased muscle PGC-1α expression protects from sarcopenia and metabolic disease during aging. *Proceedings of the National Academy of Sciences of the United States of America* 106: 20405, 2009. doi: 10.1073/PNAS.0911570106.

439. **Leick L**, **Lyngby SS**, **Wojtasewski JF**, **Pilegaard H**. PGC-1α is required for training-induced prevention of age-associated decline in mitochondrial enzymes in mouse skeletal muscle. *Experimental Gerontology* 45: 336–342, 2010. doi: 10.1016/J.EXGER.2010.01.011.

440. **Pesce V**, **Cormio A**, **Fracasso F**, **Lezza AMS**, **Cantatore P**, **Gadaleta MN**. Age-Related Changes of Mitochondrial DNA Content and Mitochondrial Genotypic and Phenotypic Alterations in Rat Hind-Limb Skeletal Muscles. *The Journals of Gerontology: Series A* 60: 715–723, 2005. doi: 10.1093/GERONA/60.6.715.

441. **Lezza AMS**, **Pesce V**, **Cormio A**, **Fracasso F**, **Vecchiet J**, **Felzani G**, **Cantatore P**, **Gadaleta MN**. Increased expression of mitochondrial transcription factor A and nuclear respiratory factor-1 in skeletal muscle from aged human subjects. *FEBS Letters* 501: 74–78, 2001. doi: 10.1016/S0014-5793(01)02628-X.

442. **Camacho-Pereira J**, **Tarragó MG**, **Chini CCS**, **Nin V**, **Escande C**, **Warner GM**, **Puranik AS**, **Schoon RA**, **Reid JM**, **Galina A**, **Chini EN**. CD38 dictates age-related NAD decline and mitochondrial dysfunction through a SIRT3-dependent mechanism. *Cell Metabolism* 23: 1127, 2016. doi: 10.1016/J.CMET.2016.05.006.

443. **Leduc-Gaudet J-P**, **Picard M**, **Pelletier FS-J**, **Sgarioto N**, **Auger M-J**, **Vallée J**, **Robitaille R**, **St-Pierre DH**, **Gouspillou G**. Mitochondrial morphology is altered in atrophied skeletal muscle of aged mice. *Oncotarget* 6: 17923–17937, 2015. doi: 10.18632/ONCOTARGET.4235.

444. **Joseph AM**, **Adhihetty PJ**, **Buford TW**, **Wohlgemuth SE**, **Lees HA**, **Nguyen LMD**, **Aranda JM**, **Sandesara BD**, **Pahor M**, **Manini TM**, **Marzetti E**, **Leeuwenburgh C**. The impact of aging on mitochondrial function and biogenesis pathways in skeletal muscle of sedentary high- and low-functioning elderly individuals. *Aging Cell* 11: 801–9, 2012. doi: 10.1111/j.1474-9726.2012.00844.x.

445. **Ogborn DI**, **McKay BR**, **Crane JD**, **Safdar A**, **Akhtar M**, **Parise G**, **Tarnopolsky MA**. Effects of age and unaccustomed resistance exercise on mitochondrial transcript and protein abundance in skeletal muscle of men. *American Journal of Physiology-Regulatory, Integrative and Comparative Physiology* 308: R734–R741, 2015. doi: 10.1152/ajpregu.00005.2014.

446. **Carter HN**, **Kim Y**, **Erlich AT**, **Zarrin-khat D**, **Hood DA**. Autophagy and mitophagy flux in young and aged skeletal muscle following chronic contractile activity. *The Journal of Physiology* 596: 3567–3584, 2018. doi: 10.1113/JP275998.

447. **Zheng G**, **Qiu P**, **Xia R**, **Lin H**, **Ye B**, **Tao J**, **Chen L**. Effect of Aerobic Exercise on Inflammatory Markers in Healthy Middle-Aged and Older Adults: A Systematic Review and Meta-Analysis of Randomized Controlled Trials. *Frontiers in Aging Neuroscience* 0: 98, 2019. doi: 10.3389/FNAGI.2019.00098.

448. **Woods JA**, **Wilund KR**, **Martin SA**, **Kistler BM**. Exercise, Inflammation and Aging. *Aging and Disease* 3: 130–140, 2012.

449. **Ryan AS**. Exercise in aging: its important role in mortality, obesity and insulin resistance. *Aging Health* 6: 551, 2010. doi: 10.2217/AHE.10.46.

450. **Roh J**, **Rhee J**, **Chaudhari V**, **Rosenzweig A**. The Role of Exercise in Cardiac Aging: From Physiology to Molecular Mechanisms. *Circulation Research* 118: 279, 2016. doi: 10.1161/CIRCRESAHA.115.305250.

451. **Zampieri S**, **Pietrangelo L**, **Loefler S**, **Fruhmann H**, **Vogelauer M**, **Burggraf S**, **Pond A**, **Grim-Stieger M**, **Cvecka J**, **Sedliak M**, **Tirpakova V**, **Mayr W**, **Sarabon N**, **Rossini K**, **Barberi L**, **de Rossi M**, **Romanello V**, **Boncompagni S**, **Musaro A**, **Sandri M**, **Protasi F**, **Carraro U**, **Kern H**. Lifelong Physical Exercise Delays Age-Associated Skeletal Muscle Decline. *The Journals of Gerontology Series A: Biological Sciences and Medical Sciences* 70: 163–173, 2015. doi: 10.1093/gerona/glu006.

452. **Garcia-Valles R**, **Gomez-Cabrera M**, **Rodriguez-Mañas L**, **Garcia-Garcia FJ**, **Diaz A**, **Noguera I**, **Olaso-Gonzalez G**, **Viña J**. Life-long spontaneous exercise does not prolong lifespan but improves health span in mice. *Longevity & Healthspan* 2: 14, 2013. doi: 10.1186/2046-2395-2-14.

453. **Betik AC**, **Thomas MM**, **Wright KJ**, **Riel CD**, **Hepple RT**. Exercise training from late middle age until senescence does not attenuate the declines in skeletal muscle aerobic function. *American Journal of Physiology - Regulatory Integrative and Comparative Physiology* 297: 744–755, 2009. doi: 10.1152/AJPREGU.90959.2008.

454. **Adhihetty PJ**, **Ljubicic V**, **Hood DA**. Effect of chronic contractile activity on SS and IMF mitochondrial apoptotic susceptibility in skeletal muscle. *American Journal of Physiology - Endocrinology and Metabolism* 292: 748–755, 2007. doi: 10.1152/ajpendo.00311.2006.

455. **Song W**, **Kwak H-B**, **Lawler JM**. Exercise Training Attenuates Age-Induced Changes in Apoptotic Signaling in Rat Skeletal Muscle. *Antioxidants and Redox Signaling* 8: 517–528, 2006. doi: 10.1089/ARS.2006.8.517.

456. **Kim YA**, **Kim YS**, **Oh SL**, **Kim HJ**, **Song W**. Autophagic response to exercise training in skeletal muscle with age. *Journal of Physiology and Biochemistry* 69: 697–705, 2013. doi: 10.1007/s13105-013-0246-7.

457. **Schwalm C**, **Jamart C**, **Benoit N**, **Naslain D**, **Prémont C**, **Prévet J**, **van Thienen R**, **Deldicque L**, **Francaux M**. Activation of autophagy in human skeletal muscle is dependent on exercise intensity and AMPK activation. *The FASEB Journal* 29: 3515–3526, 2015. doi: 10.1096/fj.14-267187.

458. **Grumati P**, **Coletto L**, **Schiavinato A**, **Castagnaro S**, **Bertaggia E**, **Sandri M**, **Bonaldo P**. Physical exercise stimulates autophagy in normal skeletal muscles but is detrimental for collagen VI-deficient muscles. *Autophagy* 7: 1415–23, 2011. doi: 10.4161/AUTO.7.12.17877.

459. **He C**, **Bassik MC**, **Moresi V**, **Sun K**, **Wei Y**, **Zou Z**, **An Z**, **Loh J**, **Fisher J**, **Sun Q**, **Korsmeyer S**, **Packer M**, **May HI**, **Hill JA**, **Virgin HW**, **Gilpin C**, **Xiao G**, **Bassel-Duby R**, **Scherer PE**, **Levine B**. Exercise-induced BCL2-regulated autophagy is required for muscle glucose homeostasis. *Nature* 481: 511–515, 2012. doi: 10.1038/nature10758.

460. **Funai K**, **Parkington JD**, **Carambula S**, **Fielding RA**. Age-associated decrease in contraction-induced activation of downstream targets of Akt/mTor signaling in skeletal muscle. *American Journal of Physiology - Regulatory Integrative and Comparative Physiology* 290: 1080–1086, 2006. doi: 10.1152/AJPREGU.00277.2005.

461. **Garvey SM**, **Russ DW**, **Skelding MB**, **Dugle JE**, **Edens NK**. Molecular and metabolomic effects of voluntary running wheel activity on skeletal muscle in late middle-aged rats. *Physiological Reports* 3, 2015. doi: 10.14814/PHY2.12319.

462. **Drummond MJ**, **Addison O**, **Brunker L**, **Hopkins PN**, **McClain DA**, **LaStayo PC**, **Marcus RL**. Downregulation of E3 ubiquitin ligases and mitophagy-related genes in skeletal muscle of physically inactive, frail older women: a cross-sectional comparison. *The Journals of Gerontology Series A, Biological Sciences and Medical Sciences* 69: 1040–1048, 2014. doi: 10.1093/gerona/glu004.

463. **Erlich AT**, **Brownlee DM**, **Beyfuss K**, **Hood DA**. Exercise induces TFEB expression and activity in skeletal muscle in a PGC-1α-dependent manner. *American Journal of Physiology-Cell Physiology* 314: C62–C72, 2018. doi: 10.1152/ajpcell.00162.2017.

464. **Riley DA**, **Slocum GR**, **Bain JL**, **Sedlak FR**, **Sowa TE**, **Mellender JW**. Rat hindlimb unloading: soleus histochemistry, ultrastructure, and electromyography. *Journal of Applied Physiology* 69: 58–66, 1990. doi: 10.1152/JAPPL.1990.69.1.58.

465. **Boncompagni S**, **Kern H**, **Rossini K**, **Hofer C**, **Mayr W**, **Carraro U**, **Protasi F**. Structural differentiation of skeletal muscle fibers in the absence of innervation in humans. *Proceedings of the National Academy of Sciences of the United States of America* 104: 19339, 2007. doi: 10.1073/PNAS.0709061104.

466. **Wang Y**, **Pessin JE**. Mechanisms for fiber-type specificity of skeletal muscle atrophy. *Current Opinion in Clinical Nutrition and Metabolic Care* 16: 243, 2013. doi: 10.1097/MCO.0B013E328360272D.

467. **Macpherson PCD**, **Wang X**, **Goldman D**. Myogenin Regulates Denervation-Dependent Muscle Atrophy in Mouse Soleus Muscle. *Journal of Cellular Biochemistry* 112: 2149, 2011. doi: 10.1002/JCB.23136.

468. **Walden F von**, **Jakobsson F**, **EdstrÖm L**, **Nader GA**. Altered autophagy gene expression and persistent atrophy suggest impaired remodeling in chronic hemiplegic human skeletal muscle. *Muscle & Nerve* 46: 785–792, 2012. doi: 10.1002/MUS.23387.

469. **Wu P**, **Chawla A**, **Spinner RJ**, **Yu C**, **Yaszemski MJ**, **Windebank AJ**, **Wang H**. Key changes in denervated muscles and their impact on regeneration and reinnervation. *Neural Regeneration Research* 9: 1796, 2014. doi: 10.4103/1673-5374.143424.

470. **Adhihetty PJ**, **O'Leary MFN**, **Chabi B**, **Wicks KL**, **Hood DA**. Effect of denervation on mitochondrially mediated apoptosis in skeletal muscle. *Journal of Applied Physiology* 102: 1143–1151, 2007. doi: 10.1152/japplphysiol.00768.2006.

471. **O′Leary MFN**, **Vainshtein A**, **Carter HN**, **Zhang Y**, **Hood DA**. Denervation-induced mitochondrial dysfunction and autophagy in skeletal muscle of apoptosis-deficient animals. *American Journal of Physiology-Cell Physiology* 303: C447–C454, 2012. doi: 10.1152/ajpcell.00451.2011.

472. **Sacheck JM**, **Hyatt J-PK**, **Raffaello A**, **Jagoe RT**, **Roy RR**, **Edgerton VR**, **Lecker SH**, **Goldberg AL**. Rapid disuse and denervation atrophy involve transcriptional changes similar to those of muscle wasting during systemic diseases. *The FASEB Journal* 21: 140–155, 2007. doi: 10.1096/FJ.06-6604COM.

473. **Kilroe SP**, **Fulford J**, **Jackman SR**, **van Loon LJC**, **Wall BT**. Temporal Muscle-specific Disuse Atrophy during One Week of Leg Immobilization. *Medicine and Science in Sports and Exercise* 52: 944–954, 2020. doi: 10.1249/MSS.0000000000002200.

474. **Chacon-Cabrera A**, **Lund-Palau H**, **Gea J**, **Barreiro E**. Time-Course of Muscle Mass Loss, Damage, and Proteolysis in Gastrocnemius following Unloading and Reloading: Implications in Chronic Diseases. *PLOS ONE* 11: e0164951, 2016. doi: 10.1371/JOURNAL.PONE.0164951.

475. **MacDonald EM**, **Andres-Mateos E**, **Mejias R**, **Simmers JL**, **Mi R**, **Park JS**, **Ying S**, **Hoke A**, **Lee SJ**, **Cohn RD**. Denervation atrophy is independent from Akt and mTOR activation and is not rescued by myostatin inhibition. *DMM Disease Models and Mechanisms* 7: 471–481, 2014. doi: 10.1242/dmm.014126.

476. **Parr MK**, **Müller-Schöll A**, **Parr MK**, **Müller-Schöll A**. Pharmacology of doping agents—mechanisms promoting muscle hypertrophy. *AIMS Molecular Science 2018 2:131* 5: 131–159, 2018. doi: 10.3934/MOLSCI.2018.2.131.

477. **Schiaffino S**, **Mammucari C**. Regulation of skeletal muscle growth by the IGF1-Akt/PKB pathway: insights from genetic models. *Skeletal Muscle 2011 1:1* 1: 1–14, 2011. doi: 10.1186/2044-5040-1-4.

478. **Rommel C**, **Bodine SC**, **Clarke BA**, **Rossman R**, **Nunez L**, **Stitt TN**, **Yancopoulos GD**, **Glass DJ**. Mediation of IGF-1-induced skeletal myotube hypertrophy by PI(3)K/Akt/mTOR and PI(3)K/Akt/GSK3 pathways. *Nature Cell Biology 2001 3:11* 3: 1009–1013, 2001. doi: 10.1038/ncb1101-1009.

479. **Argadine HM**, **Hellyer NJ**, **Mantilla CB**, **Zhan W-Z**, **Sieck GC**. The effect of denervation on protein synthesis and degradation in adult rat diaphragm muscle. *Journal of Applied Physiology* 107: 438, 2009. doi: 10.1152/JAPPLPHYSIOL.91247.2008.

480. **Eley HL**, **Tisdale MJ**. Skeletal Muscle Atrophy, a Link between Depression of Protein Synthesis and Increase in Degradation. *Journal of Biological Chemistry* 282: 7087–7097, 2007. doi: 10.1074/JBC.M610378200.

481. **Atherton PJ**, **Greenhaff PL**, **Phillips SM**, **Bodine SC**, **Adams CM**, **Lang CH**. Control of skeletal muscle atrophy in response to disuse: clinical/preclinical contentions and fallacies of evidence. *American Journal of Physiology - Endocrinology and Metabolism* 311: E594, 2016. doi: 10.1152/AJPENDO.00257.2016.

482. **Goldspink DF**. The effects of denervation on protein turnover of rat skeletal muscle. *Biochemical Journal* 156: 71, 1976. doi: 10.1042/BJ1560071.

483. **Langer HT**, **Senden JMG**, **Gijsen AP**, **Kempa S**, **van Loon LJC**, **Spuler S**. Muscle Atrophy Due to Nerve Damage Is Accompanied by Elevated Myofibrillar Protein Synthesis Rates. *Frontiers in Physiology* 0: 1220, 2018. doi: 10.3389/FPHYS.2018.01220.

484. **You J-S**, **Kim K**, **Steinert ND**, **Chen J**, **Hornberger TA**. mTORC1 mediates fiber type-specific regulation of protein synthesis and muscle size during denervation. *Cell Death Discovery 2021 7:1* 7: 1–7, 2021. doi: 10.1038/s41420-021-00460-w.

485. **Tokinoya K**, **Shirai T**, **Ota Y**, **Takemasa T**, **Takekoshi K**. Denervation-induced muscle atrophy suppression in renalase-deficient mice via increased protein synthesis. *Physiological Reports* 8: e14475, 2020. doi: 10.14814/PHY2.14475.

486. **Tryon LD**, **Vainshtein A**, **Memme JM**, **Crilly MJ**, **Hood DA**. Recent advances in mitochondrial turnover during chronic muscle disuse. *Integrative Medicine Research* 3: 161, 2014. doi: 10.1016/J.IMR.2014.09.001.

487. **Ji CH**, **Kwon YT**. Crosstalk and Interplay between the Ubiquitin-Proteasome System and Autophagy. *Molecules and Cells* 40: 441, 2017. doi: 10.14348/MOLCELLS.2017.0115.

488. **Taillandier D**, **Polge C**. Skeletal muscle atrogenes: From rodent models to human pathologies. *Biochimie* 166: 251–269, 2019. doi: 10.1016/J.BIOCHI.2019.07.014.

489. **Egerman MA**, **Glass DJ**. Signaling pathways controlling skeletal muscle mass. *Critical Reviews in Biochemistry and Molecular Biology* 49: 59, 2014. doi: 10.3109/10409238.2013.857291.

490. **Zhang S-F**, **Zhang Y**, **Li B**, **Chen N**. Physical inactivity induces the atrophy of skeletal muscle of rats through activating AMPK/FoxO3 signal pathway. *European Review for Medical and Pharmacological Sciences* 22: 199–209, 2018. doi: 10.26355/eurrev_201801_14118.

491. **Stouth DW**, **Manta A**, **Ljubicic V**. Protein arginine methyltransferase expression, localization, and activity during disuse-induced skeletal muscle plasticity. *American Journal of Physiology - Cell Physiology* 314: C177–C190, 2018. doi: 10.1152/AJPCELL.00174.2017.

492. **Liu J**, **Peng Y**, **Cui Z**, **Wu Z**, **Qian A**, **Shang P**, **Qu L**, **Li Y**, **Liu J**, **Long J**. Depressed mitochondrial biogenesis and dynamic remodeling in mouse tibialis anterior and gastrocnemius induced by 4-week hindlimb unloading. *IUBMB Life* 64: 901–910, 2012. doi: 10.1002/iub.1087.

493. **Milan G**, **Romanello V**, **Pescatore F**, **Armani A**, **Paik J-H**, **Frasson L**, **Seydel A**, **Zhao J**, **Abraham R**, **Goldberg AL**, **Blaauw B**, **DePinho RA**, **Sandri M**. Regulation of autophagy and the ubiquitin–proteasome system by the FoxO transcriptional network during muscle atrophy. *Nature Communications 2015 6:1* 6: 1–14, 2015. doi: 10.1038/ncomms7670.

494. **Huang Z**, **Fang Q**, **Ma W**, **Zhang Q**, **Qiu J**, **Gu X**, **Yang H**, **Sun H**. Skeletal muscle atrophy was alleviated by salidroside through suppressing oxidative stress and inflammation during denervation. *Frontiers in Pharmacology* 10: 997, 2019. doi: 10.3389/fphar.2019.00997.

495. **Shen Y**, **Zhang Q**, **Huang Z**, **Zhu J**, **Qiu J**, **Ma W**, **Yang X**, **Ding F**, **Sun H**. Isoquercitrin Delays Denervated Soleus Muscle Atrophy by Inhibiting Oxidative Stress and Inflammation. *Frontiers in Physiology* 11, 2020. doi: 10.3389/FPHYS.2020.00988.

496. **Wan Q**, **Zhang L**, **Huang Z**, **Zhang H**, **Gu J**, **Xu H**, **Yang X**, **Shen Y**, **Law BY-K**, **Zhu J**, **Sun H**. Aspirin alleviates denervation-induced muscle atrophy via regulating the Sirt1/PGC-1α axis and STAT3 signaling. *Annals of Translational Medicine* 8: 1524–1524, 2020. doi: 10.21037/ATM-20-5460.

497. **Suetta C**, **Frandsen U**, **Jensen L**, **Jensen MM**, **Jespersen JG**, **Hvid LG**, **Bayer M**, **Petersson SJ**, **Schrøder HD**, **Andersen JL**, **Heinemeier KM**, **Aagaard P**, **Schjerling P**, **Kjaer M**. Aging Affects the Transcriptional Regulation of Human Skeletal Muscle Disuse Atrophy. *PLoS ONE* 7: e51238, 2012. doi: 10.1371/journal.pone.0051238.

498. **Smuder AJ**, **Sollanek KJ**, **Nelson WB**, **Min K**, **Talbert EE**, **Kavazis AN**, **Hudson MB**, **Sandri M**, **Szeto HH**, **Powers SK**. Crosstalk between autophagy and oxidative stress regulates proteolysis in the diaphragm during mechanical ventilation. *Free Radical Biology and Medicine* 115: 179–190, 2018. doi: 10.1016/j.freeradbiomed.2017.11.025.

499. **Belova SP**, **Vilchinskaya NA**, **Mochalova EP**, **Mirzoev TM**, **Nemirovskaya TL**, **Shenkman BS**. Elevated p70S6K phosphorylation in rat soleus muscle during the early stage of unloading:

Causes and consequences. *Archives of Biochemistry and Biophysics* 674: 108105, 2019. doi: 10.1016/J.ABB.2019.108105.

500. **Bodine SC**, **Latres E**, **Baumhueter S**, **Lai VKM**, **Nunez L**, **Clarke BA**, **Poueymirou WT**, **Panaro FJ**, **Erqian Na**, **Dharmarajan K**, **Pan ZQ**, **Valenzuela DM**, **Dechiara TM**, **Stitt TN**, **Yancopoulos GD**, **Glass DJ**. Identification of ubiquitin ligases required for skeletal Muscle Atrophy. *Science* 294: 1704–1708, 2001. doi: 10.1126/science.1065874.

501. **Cadena SM**, **Zhang Y**, **Fang J**, **Brachat S**, **Kuss P**, **Giorgetti E**, **Stodieck LS**, **Kneissel M**, **Glass DJ**. Skeletal muscle in MuRF1 null mice is not spared in low-gravity conditions, indicating atrophy proceeds by unique mechanisms in space. *Scientific Reports 2019 9:1* 9: 1–11, 2019. doi: 10.1038/s41598-019-45821-9.

502. **Paul PK**, **Gupta SK**, **Bhatnagar S**, **Panguluri SK**, **Darnay BG**, **Choi Y**, **Kumar A**. Targeted ablation of TRAF6 inhibits skeletal muscle wasting in mice. *The Journal of Cell Biology* 191: 1395, 2010. doi: 10.1083/JCB.201006098.

503. **Dodd SL**, **Gagnon BJ**, **Senf SM**, **Hain BA**, **Judge AR**. ROS-mediated activation of NF-κB and Foxo during muscle disuse. *Muscle & Nerve* 41: 110, 2010. doi: 10.1002/MUS.21526.

504. **Ruohonen S**, **Khademi M**, **Jagodic M**, **Taskinen H-S**, **Olsson T**, **Röyttä M**. Cytokine responses during chronic denervation. *Journal of Neuroinflammation 2005 2:1* 2: 1–11, 2005. doi: 10.1186/1742-2094-2-26.

505. **Bryndina IG**, **Ovchinina NG**, **Protopopov VA**, **Shalagina MN**, **Ovchinina NN**, **Sekunov A v**. TNFa is Involved in the Development of Disuse Muscle Atrophy Through the Acid Sphingomyelinase/ Ceramide Up-Regulation and Pro-Oxidant Signaling. *Research Square* 1, 2020. doi: 10.21203/rs.3.rs-111015/v1.

506. **Richter EA**, **Kiens B**, **Mizuno M**, **Strange S**. Insulin action in human thighs after one-legged immobilization. *Journal of Applied Physiology* 67: 19–23, 1989. doi: 10.1152/JAPPL.1989.67.1.19.

507. **Stuart CA**, **Shangraw RE**, **Prince MJ**, **Peters EJ**, **Wolfe RR**. Bed-rest-induced insulin resistance occurs primarily in muscle. *Metabolism - Clinical and Experimental* 37: 802–806, 1988. doi: 10.1016/0026-0495(88)90018-2.

508. **Allen DL**, **Linderman JK**, **Roy RR**, **Grindeland RE**, **Mukku V**, **Edgerton VR**. Growth hormone/IGF-I and/or resistive exercise maintains myonuclear number in hindlimb unweighted muscles. *Journal of Applied Physiology* 83: 1857–1861, 1997. doi: 10.1152/JAPPL.1997.83.6.1857.

509. **Henriksen EJ**, **Rodnick K**, **Mondon C**, **James D**, **Holloszy JO**. Effect of denervation or unweighting on GLUT-4 protein in rat soleus muscle. *Journal of Applied Physiology* 70: 2322–2327, 1991. doi: 10.1152/JAPPL.1991.70.5.2322.

510. **McMillin SL**, **Stanley EC**, **Weyrauch LA**, **Brault JJ**, **Kahn BB**, **Witczak CA**. Insulin Resistance Is Not Sustained Following Denervation in Glycolytic Skeletal Muscle. *International Journal of Molecular Sciences* 22, 2021. doi: 10.3390/IJMS22094913.

511. **Wilkes JJ**, **Bonen A**. Reduced insulin-stimulated glucose transport in denervated muscle is associated with impaired Akt-α activation. *American Journal of Physiology - Endocrinology and Metabolism* 279: 42, 2000. doi: 10.1152/AJPENDO.2000.279.4.E912.

512. **Turinsky J**, **Damrau-Abney A**, **Loegering D**. Blood flow and glucose uptake in denervated, insulin-resistant muscles. *American Journal of Physiology - Regulatory Integrative and Comparative Physiology* 274: R311-317, 1998. doi: 10.1152/AJPREGU.1998.274.2.R311.

513. **Yakabe M**, **Ogawa S**, **Ota H**, **Iijima K**, **Eto M**, **Ouchi Y**, **Akishita M**. Inhibition of interleukin-6 decreases atrogene expression and ameliorates tail suspension-induced skeletal muscle atrophy. *PLoS ONE* 13, 2018. doi: 10.1371/JOURNAL.PONE.0191318.

514. **Yang X**, **Xue P**, **Liu X**, **Xu X**, **Chen Z**. HMGB1/autophagy pathway mediates the atrophic effect of TGF-β1 in denervated skeletal muscle. *Cell Communication and Signaling* 16: 97, 2018. doi: 10.1186/S12964-018-0310-6.

515. **Wang J**, **Wang F**, **Zhang P**, **Liu H**, **He J**, **Zhang C**, **Fan M**, **Chen X**. PGC-1α over-expression suppresses the skeletal muscle atrophy and myofiber-type composition during hindlimb unloading. *Bioscience, Biotechnology, and Biochemistry* 81: 500–513, 2017. doi: 10.1080/09168451.2016.1254531.

516. **Ma W**, **Zhang R**, **Huang Z**, **Zhang Q**, **Xie X**, **Yang X**, **Zhang Q**, **Liu H**, **Ding F**, **Zhu J**, **Sun H**. PQQ ameliorates skeletal muscle atrophy, mitophagy and fiber type transition induced by denervation via inhibition of the inflammatory signaling pathways. *Annals of Translational Medicine* 7: 440–440, 2019. doi: 10.21037/ATM.2019.08.101.

517. **Hyatt HW**, **Powers SK**. The Role of Calpains in Skeletal Muscle Remodeling with Exercise and Inactivity-induced Atrophy. *International Journal of Sports Medicine* 41: 994–1008, 2020. doi: 10.1055/A-1199-7662.

518. **Liu ZQ**, **Kunimatsu M**, **Yang JP**, **Ozaki Y**, **Sasaki M**, **Okamoto T**. Proteolytic processing of nuclear factor κB by calpain in vitro. *FEBS Letters* 385: 109–113, 1996. doi: 10.1016/0014-5793(96)00360-2.

519. **Li X**, **Luo R**, **Chen R**, **Song L**, **Zhang S**, **Hua W**, **Chen H**. Cleavage of IκBα by calpain induces myocardial NF-κB activation, TNF-α expression, and cardiac dysfunction in septic mice. *American Journal of Physiology - Heart and Circulatory Physiology* 306: H833-843, 2014. doi: 10.1152/AJPHEART.00893.2012.

520. **Smith IJ**, **Dodd SL**. Calpain activation causes a proteasome-dependent increase in protein degradation and inhibits the Akt signalling pathway in rat diaphragm muscle. *Experimental Physiology* 92: 561–573, 2007. doi: 10.1113/EXPPHYSIOL.2006.035790.

521. **Talbert EE**, **Smuder AJ**, **Min K**, **Kwon OS**, **Powers SK**. Calpain and caspase-3 play required roles in immobilization-induced limb muscle atrophy. *Journal of Applied Physiology* 114: 1482–1489, 2013. doi: 10.1152/JAPPLPHYSIOL.00925.2012.

522. **Tidball JG**, **Spencer MJ**. Expression of a calpastatin transgene slows muscle wasting and obviates changes in myosin isoform expression during murine muscle disuse. *The Journal of Physiology* 545: 819, 2002. doi: 10.1113/JPHYSIOL.2002.024935.

523. **Salazar JJ**, **Michele DE**, **Brooks S v.** Inhibition of calpain prevents muscle weakness and disruption of sarcomere structure during hindlimb suspension. *Journal of Applied Physiology* 108: 120, 2010. doi: 10.1152/JAPPLPHYSIOL.01080.2009.

524. **Du J**, **Wang X**, **Miereles C**, **Bailey JL**, **Debigare R**, **Zheng B**, **Price SR**, **Mitch WE**. Activation of caspase-3 is an initial step triggering accelerated muscle proteolysis in catabolic conditions. *The Journal of Clinical Investigation* 113: 115, 2004. doi: 10.1172/JCI200418330.

525. **Plant PJ**, **Bain JR**, **Correa JE**, **Woo M**, **Batt J**. Absence of caspase-3 protects against denervation-induced skeletal muscle atrophy. *Journal of Applied Physiology* 107: 224–234, 2009. doi: 10.1152/JAPPLPHYSIOL.90932.2008.

526. **Siu PM**, **Alway SE**. Mitochondria-associated apoptotic signalling in denervated rat skeletal muscle. *The Journal of Physiology* 565: 309, 2005. doi: 10.1113/JPHYSIOL.2004.081083.

527. **Schiaffino S**, **Hanzlíková V**. Studies on the effect of denervation in developing muscle. II. The lysosomal system. *Journal of Ultrastructure Research* 39: 1–14, 1972. doi: 10.1016/S0022-5320(72)80002-9.

528. **Dobrowolny G**, **Aucello M**, **Rizzuto E**, **Beccafico S**, **Mammucari C**, **Boncompagni S**, **Belia S**, **Wannenes F**, **Nicoletti C**, **del Prete Z**, **Rosenthal N**, **Molinaro M**, **Protasi F**, **Fanò G**, **Sandri M**, **Musarò A**. Skeletal Muscle Is a Primary Target of SOD1G93A-Mediated Toxicity. *Cell Metabolism* 8: 425–436, 2008. doi: 10.1016/J.CMET.2008.09.002.

529. **Castets P**, **Rion N**, **Théodore M**, **Falcetta D**, **Lin S**, **Reischl M**, **Wild F**, **Guérard L**, **Eickhorst C**, **Brockhoff M**, **Guridi M**, **Ibebunjo C**, **Cruz J**, **Sinnreich M**, **Rudolf R**, **Glass DJ**, **Rüegg MA**. mTORC1 and PKB/Akt control the muscle response to denervation by regulating autophagy and HDAC4. *Nature Communications* 10: 1–16, 2019. doi: 10.1038/s41467-019-11227-4.

530. **Senf SM**, **Dodd SL**, **McClung JM**, **Judge AR**. Hsp70 overexpression inhibits NF-κB and Foxo3a transcriptional activities and prevents skeletal muscle atrophy. *The FASEB Journal* 22: 3836, 2008. doi: 10.1096/FJ.08-110163.

531. **Tamura Y**, **Kitaoka Y**, **Matsunaga Y**, **Hoshino D**, **Hatta H**. Daily heat stress treatment rescues denervation-activated mitochondrial clearance and atrophy in skeletal muscle. *The Journal of Physiology* 593: 2707–20, 2015. doi: 10.1113/JP270093.

532. **Foresto CS**, **Paula-Gomes S**, **Silveira WA**, **Graça FA**, **Kettelhut I do C**, **Gonçalves DAP**, **Mattiello-Sverzut AC**. Morphological and molecular aspects of immobilization-induced muscle atrophy in rats at different stages of postnatal development: the role of autophagy. *Journal of Applied Physiology* 121: 646–660, 2016. doi: 10.1152/japplphysiol.00687.2015.

533. **Sugiura T**, **Abe N**, **Nagano M**, **Goto K**, **Sakuma K**, **Naito H**, **Yoshioka T**, **Powers SK**. Changes in PKB/Akt and calcineurin signaling during recovery in atrophied soleus muscle induced by unloading. *American Journal of Physiology - Regulatory Integrative and Comparative Physiology* 288: 1273–1278, 2005. doi: 10.1152/AJPREGU.00688.2004.

534. **Graham ZA**, **Harlow L**, **Bauman WA**, **Cardozo CP**. Alterations in mitochondrial fission, fusion, and mitophagic protein expression in the gastrocnemius of mice after a sciatic nerve transection. *Muscle & Nerve* 58: 592–599, 2018. doi: 10.1002/MUS.26197.

535. **Mirzoev T**, **Tyganov S**, **Vilchinskaya N**, **Lomonosova Y**, **Shenkman B**. Key Markers of mTORC1-Dependent and mTORC1-Independent Signaling Pathways Regulating Protein Synthesis in Rat Soleus Muscle During Early Stages of Hindlimb Unloading. *Cellular Physiology and Biochemistry* 39: 1011–1020, 2016. doi: 10.1159/000447808.

536. **Hilder TL**, **Baer LA**, **Fuller PM**, **Fuller CA**, **Grindeland RE**, **Wade CE**, **Graves LM**. Insulin-independent pathways mediating glucose uptake in hindlimb-suspended skeletal muscle. *Journal of Applied Physiology* 99: 2181–2188, 2005. doi: 10.1152/JAPPLPHYSIOL.00743.2005.

537. **Han B**, **Zhu MJ**, **Ma C**, **Du M**. Rat hindlimb unloading down-regulates insulin like growth factor-1 signaling and AMP-activated protein kinase, and leads to severe atrophy of the soleus

muscle. *Applied Physiology, Nutrition and Metabolism* 32: 1115–1123, 2007. doi: 10.1139/H07-102.

538. **Chibalin A v**, **Benziane B**, **Zakyrjanova GF**, **Kravtsova V v**, **Krivoi II**. Early endplate remodeling and skeletal muscle signaling events following rat hindlimb suspension. *Journal of Cellular Physiology* 233: 6329–6336, 2018. doi: 10.1002/jcp.26594.

539. **Møller AB**, **Vendelbo MH**, **Schjerling P**, **Couppé C**, **Møller N**, **Kjær M**, **Hansen M**, **Jessen N**. Immobilization Decreases FOXO3a Phosphorylation and Increases Autophagy-Related Gene and Protein Expression in Human Skeletal Muscle. *Frontiers in Physiology* 10: 736, 2019. doi: 10.3389/fphys.2019.00736.

540. **Wall BT**, **Snijders T**, **Senden JMG**, **Ottenbros CLP**, **Gijsen AP**, **Verdijk LB**, **van Loon LJC**. Disuse Impairs the Muscle Protein Synthetic Response to Protein Ingestion in Healthy Men. *The Journal of Clinical Endocrinology & Metabolism* 98: 4872–4881, 2013. doi: 10.1210/jc.2013-2098.

541. **Vainshtein A**, **Desjardins EM**, **Armani A**, **Sandri M**, **Hood DA**. PGC-1α modulates denervation-induced mitophagy in skeletal muscle. *Skeletal muscle* 5: 9, 2015. doi: 10.1186/s13395-015-0033-y.

542. **Kang C**, **Yeo D**, **Ji LL**. Muscle immobilization activates mitophagy and disrupts mitochondrial dynamics in mice. *Acta Physiologica* 218: 188–197, 2016. doi: 10.1111/apha.12690.

543. **Deval C**, **Calonne J**, **Coudy-Gandilhon C**, **Vazeille E**, **Bechet D**, **Polge C**, **Taillandier D**, **Attaix D**, **Combaret L**. Mitophagy and mitochondria biogenesis are differentially induced in rat skeletal muscles during immobilization and/or remobilization. *International Journal of Molecular Sciences* 21, 2020. doi: 10.3390/ijms21103691.

544. **Rosa-Caldwell ME**, **Brown JL**, **Perry RA**, **Shimkus KL**, **Shirazi-Fard Y**, **Brown LA**, **Hogan HA**, **Fluckey JD**, **Washington TA**, **Wiggs MP**, **Greene NP**. Regulation of mitochondrial quality following repeated bouts of hindlimb unloading. *Applied Physiology, Nutrition and Metabolism* 45: 264–274, 2020. doi: 10.1139/apnm-2019-0218.

545. **Weinstein RB**, **Slentz MJ**, **Webster K**, **Takeuchi JA**, **Tischler ME**. Lysosomal proteolysis in distally or proximally denervated rat soleus muscle. *American Journal of Physiology - Regulatory Integrative and Comparative Physiology* 273, 1997. doi: 10.1152/ajpregu.1997.273.4.r1562.

546. **Tischler ME**, **Rosenberg S**, **Satarug S**, **Henriksen EJ**, **Kirby CR**, **Tome M**, **Chase P**. Different mechanisms of increased proteolysis in atrophy induced by denervation or unweighting of rat soleus muscle. *Metabolism* 39: 756–763, 1990. doi: 10.1016/0026-0495(90)90113-Q.

547. **Max SR**, **Mayer RF**, **Vogelsang L**. Lysosomes and disuse atrophy of skeletal muscle. *Archives of Biochemistry and Biophysics* 146: 227–232, 1971. doi: 10.1016/S0003-9861(71)80059-0.

548. **Taillandier D**, **Aurousseau E**, **Meynial-Denis D**, **Bechet D**, **Ferrara M**, **Cottin P**, **Ducastaing A**, **Bigard X**, **Guezennec CY**, **Schmid HP**, **Attaix D**. Coordinate activation of lysosomal, Ca2+-activated and ATP-ubiquitin-dependent proteinases in the unweighted rat soleus muscle. *Biochemical Journal* 316: 65–72, 1996. doi: 10.1042/bj3160065.

549. **Bialek P**, **Morris C**, **Parkington J**, **st. Andre M**, **Owens J**, **Yaworsky P**, **Seeherman H**, **Jelinsky SA**. Distinct protein degradation profiles are induced by different disuse models of skeletal muscle atrophy. *Physiological Genomics* 43: 1075–1085, 2011. doi: 10.1152/physiolgenomics.00247.2010.

550. **Singh K**, **Hood DA**. Effect of denervation-induced muscle disuse on mitochondrial protein import. *American Journal of Physiology - Cell physiology* 300: C138–C145, 2011. doi: 10.1152/ajpcell.00181.2010.

551. **Karam C**, **Yi J**, **Xiao Y**, **Dhakal K**, **Zhang L**, **Li X**, **Manno C**, **Xu J**, **Li K**, **Cheng H**, **Ma J**, **Zhou J**. Absence of physiological Ca2+ transients is an initial trigger for mitochondrial dysfunction in skeletal muscle following denervation. *Skeletal Muscle* 7, 2017. doi: 10.1186/s13395-017-0123-0.

552. **Muller FL**, **Song W**, **Jang YC**, **Liu Y**, **Sabia M**, **Richardson A**, **van Remmen H**. Denervation-induced skeletal muscle atrophy is associated with increased mitochondrial ROS production. *American Journal of Physiology-Regulatory, Integrative and Comparative Physiology* 293: R1159–R1168, 2007. doi: 10.1152/ajpregu.00767.2006.

553. **Powers SK**, **Ji LL**, **Kavazis AN**, **Jackson MJ**. Reactive Oxygen Species: Impact on Skeletal Muscle. *Compr Physiol* 1: 941–969, 2011. doi: 10.1002/cphy.c100054.REACTIVE.

554. **Powers SK**, **Ozdemir M**, **Hyatt H**. Redox Control of Proteolysis During Inactivity-Induced Skeletal Muscle Atrophy. *Antioxidants & Redox Signaling* 33: 559–569, 2020. doi: 10.1089/ars.2019.8000.

555. **Kourie JI**. Interaction of reactive oxygen species with ion transport mechanisms. *American Journal of Physiology - Cell Physiology* 275 American Physiological Society: 1998.

556. **Ingalls CP**, **Warren GL**, **Armstrong RB**. Intracellular Ca2+ transients in mouse soleus muscle after hindlimb unloading and reloading. *Journal of Applied Physiology* 87: 386–390, 1999. doi: 10.1152/jappl.1999.87.1.386.

557. **Cartee GD**, **Hepple RT**, **Bamman MM**, **Zierath JR**. Exercise Promotes Healthy Aging of Skeletal Muscle. *Cell Metabolism* 23: 1034–1047, 2016. doi: 10.1016/j.cmet.2016.05.007.

558. **Singh K**, **Hood DA**. Effect of denervation-induced muscle disuse on mitochondrial protein import. *American Journal of Physiology - Cell physiology* 300: C138-145, 2011. doi: 10.1152/ajpcell.00181.2010.

559. **Min K**, **Smuder AJ**, **Kwon O**, **Kavazis AN**, **Szeto HH**, **Powers SK**. Mitochondrial-targeted antioxidants protect skeletal muscle against immobilization-induced muscle atrophy. *Journal of Applied Physiology* 111: 1459–1466, 2011. doi: 10.1152/japplphysiol.00591.2011.

560. **Min K**, **Smuder AJ**, **Kwon O-S**, **Kavazis AN**, **Szeto HH**, **Powers SK**. Mitochondrial-targeted antioxidants protect skeletal muscle against immobilization-induced muscle atrophy. *Journal of Applied Physiology* 111: 1459–1466, 2011. doi: 10.1152/japplphysiol.00591.2011.

561. **Yang X**, **Xue P**, **Yuan M**, **Xu X**, **Wang C**, **Li W**, **Machens H-G**, **Chen Z**. SESN2 protects against denervated muscle atrophy through unfolded protein response and mitophagy. *Cell Death & Disease 2021 12:9* 12: 1–13, 2021. doi: 10.1038/s41419-021-04094-9.

562. **Guo C**, **Sun L**, **Chen X**, **Zhang D**. Oxidative stress, mitochondrial damage and neurodegenerative diseases. *Neural Regeneration Research* 8: 2003, 2013. doi: 10.3969/J.ISSN.1673-5374.2013.21.009.

563. **Csukly K**, **Ascah A**, **Matas J**, **Gardiner PF**, **Fontaine E**, **Burelle Y**. Muscle denervation promotes opening of the permeability transition pore and increases the expression of cyclophilin D. *Journal of Physiology* 574: 319–327, 2006. doi: 10.1113/jphysiol.2006.109702.

564. **Cooke MS**, **Evans MD**, **Dizdaroglu M**, **Lunec J**. Oxidative DNA damage: mechanisms, mutation, and disease. *The FASEB Journal* 17: 1195–1214, 2003. doi: 10.1096/FJ.02-0752REV.

565. **Davies KJ**. Protein damage and degradation by oxygen radicals. I. general aspects. *Journal of Biological Chemistry* 262: 9895–9901, 1987. doi: 10.1016/S0021-9258(18)48018-0.

566. **Kowalska M**, **Piekut T**, **Prendecki M**, **Sodel A**, **Kozubski W**, **Dorszewska J**. Mitochondrial and Nuclear DNA Oxidative Damage in Physiological and Pathological Aging. *DNA and Cell Biology* 39: 1410–1420, 2020. doi: 10.1089/DNA.2019.5347.

567. **Yang X**, **Xue P**, **Chen H**, **Yuan M**, **Kang Y**, **Duscher D**, **Machens H-G**, **Chen Z**. Denervation drives skeletal muscle atrophy and induces mitochondrial dysfunction, mitophagy and apoptosis via miR-142a-5p/MFN1 axis. *Theranostics* 10: 1415, 2020. doi: 10.7150/THNO.40857.

568. **Siu PM**, **Alway SE**. Deficiency of the Bax gene attenuates denervation-induced apoptosis. *Apoptosis* 11: 967, 2006. doi: 10.1007/S10495-006-6315-4.

569. **Powers SK**. Can antioxidants protect against disuse muscle atrophy? *Sports Medicine* 44: S155--65, 2014. doi: 10.1007/s40279-014-0255-x.

570. **Hyatt HW**, **Powers SK**. Mitochondrial Dysfunction Is a Common Denominator Linking Skeletal Muscle Wasting Due to Disease, Aging, and Prolonged Inactivity. *Antioxidants* 10, 2021. doi: 10.3390/ANTIOX10040588.

571. **Momken I**, **Stevens L**, **Bergouignan A**, **Desplanches D**, **Rudwill F**, **Chery I**, **Zahariev A**, **Zahn S**, **Stein TP**, **Sebedio JL**, **Pujos-Guillot E**, **Falempin M**, **Simon C**, **Coxam V**, **Andrianjafiniony T**, **Gauquelin-Koch G**, **Picquet F**, **Blanc S**. Resveratrol prevents the wasting disorders of mechanical unloading by acting as a physical exercise mimetic in the rat. *The FASEB Journal* 25: 3646–3660, 2011. doi: 10.1096/FJ.10-177295.

572. **Servais S**, **Letexier D**, **Favier R**, **Duchamp C**, **Desplanches D**. Prevention of unloading-induced atrophy by vitamin E supplementation: links between oxidative stress and soleus muscle proteolysis? *Free Radical Biology & Medicine* 42: 627, 2007. doi: 10.1016/J.FREERADBIOMED.2006.12.001.

573. **Koesterer TJ**, **Dodd SL**, **Powers S**. Increased antioxidant capacity does not attenuate muscle atrophy caused by unweighting. *Journal of Applied Physiology* 93: 1959–1965, 2002. doi: 10.1152/JAPPLPHYSIOL.00511.2002.

574. **Pigna E**, **Greco E**, **Morozzi G**, **Grottelli S**, **Rotini A**, **Minelli A**, **Fulle S**, **Adamo S**, **Mancinelli R**, **Bellezza I**, **Moresi V**. Denervation does not Induce Muscle Atrophy Through Oxidative Stress. *European Journal of Translational Myology* 27: 43–50, 2017. doi: 10.4081/EJTM.2017.6406.

575. **Farid M**, **Reid MB**, **Li Y-P**, **Gerken E**, **Durham WJ**. Effects of dietary curcumin or N-acetylcysteine on NF-κB activity and contractile performance in ambulatory and unloaded murine soleus. *Nutrition & Metabolism 2005 2:1* 2: 1–8, 2005. doi: 10.1186/1743-7075-2-20.

576. **Sandri M**, **Lin J**, **Handschin C**, **Yang W**, **Arany ZP**, **Lecker SH**, **Goldberg AL**, **Spiegelman BM**. PGC-1alpha protects skeletal muscle from atrophy by suppressing FoxO3 action and atrophy-specific gene transcription. *Proceedings of the National Academy of Sciences of the United States of America* 103: 16260–16265, 2006. doi: 10.1073/pnas.0607795103.

577. **Chen X**, **Li M**, **Chen B**, **Wang W**, **Zhang L**, **Ji Y**, **Chen Z**, **Ni X**, **Shen Y**, **Sun H**. Transcriptome sequencing and analysis reveals the molecular mechanism of skeletal muscle atrophy induced by denervation. *Annals of Translational Medicine* 9: 697–697, 2021. doi: 10.21037/ATM-21-1230.

578. **Cui Q**, **Yang H**, **Gu Y**, **Zong C**, **Chen X**, **Lin Y**, **Sun H**, **Shen Y**, **Zhu J**. RNA sequencing (RNA-seq) analysis of gene expression provides new insights into hindlimb unloading-induced skeletal muscle atrophy. *Annals of Translational Medicine* 8: 1595–1595, 2020. doi: 10.21037/ATM-20-7400.

579. **Wicks KL**, **Hood DA**. Mitochondrial adaptations in denervated muscle: relationship to muscle performance. *American Journal of Physiology - Cell Physiology* 260, 1991. doi: 10.1152/ajpcell.1991.260.4.c841.

580. **Ostojic O**, **O'Leary MFN**, **Singh K**, **Menzies KJ**, **Vainshtein A**, **Hood DA**. The effects of chronic muscle use and disuse on cardiolipin metabolism. *Journal of Applied Physiology* 114: 444–452, 2013. doi: 10.1152/japplphysiol.01312.2012.

581. **Powers SK**, **Kavazis AN**, **DeRuisseau KC**. Mechanisms of disuse muscle atrophy: role of oxidative stress. *American Journal of Physiology - Regulatory Integrative and Comparative Physiology* 288: R337-344, 2005. doi: 10.1152/ajpregu.00469.2004.

582. **Powers SK**, **Wiggs MP**, **Duarte JA**, **Zergeroglu AM**, **Demirel HA**. Mitochondrial signaling contributes to disuse muscle atrophy. *American Journal of Physiology Endocrinology and Metabolism* 303: E31-9, 2012. doi: 10.1152/ajpendo.00609.2011.

583. **Brault JJ**, **Jespersen JG**, **Goldberg AL**. Peroxisome proliferator-activated receptor gamma coactivator 1alpha or 1beta overexpression inhibits muscle protein degradation, induction of ubiquitin ligases, and disuse atrophy. *The Journal of Biological Chemistry* 285: 19460–19471, 2010. doi: 10.1074/jbc.M110.113092.

584. **Cannavino J**, **Brocca L**, **Sandri M**, **Grassi B**, **Bottinelli R**, **Pellegrino MA**. The role of alterations in mitochondrial dynamics and PGC-1α over-expression in fast muscle atrophy following hindlimb unloading. *Journal of Physiology* 593: 1981–1995, 2015. doi: 10.1113/jphysiol.2014.286740.

585. **Rosa-Caldwell ME**, **Lim S**, **Haynie WS**, **Jansen LT**, **Westervelt LC**, **Amos MG**, **Washington TA**, **Greene NP**. Altering aspects of mitochondrial quality to improve musculoskeletal outcomes in disuse atrophy. *Journal of Applied Physiology* 129: 1290–1303, 2020. doi: 10.1152/JAPPLPHYSIOL.00407.2020.

586. **Petrosillo G**, **Ruggiero FM**, **Paradies G**. Role of reactive oxygen species and cardiolipin in the release of cytochrome c from mitochondria. *FASEB journal : official publication of the Federation of American Societies for Experimental Biology* 17: 2202–2208, 2003. doi: 10.1096/fj.03-0012com.

587. **Soriano FX**, **Liesa M**, **Bach D**, **Chan DC**, **Palacín M**, **Zorzano A**. Evidence for a Mitochondrial Regulatory Pathway Defined by Peroxisome Proliferator–Activated Receptor-γ Coactivator-1α, Estrogen-Related Receptor-α, and Mitofusin 2. *Diabetes* 55: 1783–1791, 2006. doi: 10.2337/DB05-0509.

588. **Varanita T**, **Soriano ME**, **Romanello V**, **Zaglia T**, **Quintana-Cabrera R**, **Semenzato M**, **Menabò R**, **Costa V**, **Civiletto G**, **Pesce P**, **Viscomi C**, **Zeviani M**, **Di Lisa F**, **Mongillo M**, **Sandri M**, **Scorrano L**. The Opa1-Dependent Mitochondrial Cristae Remodeling Pathway Controls Atrophic, Apoptotic, and Ischemic Tissue Damage. *Cell Metabolism* 21: 834, 2015. doi: 10.1016/J.CMET.2015.05.007.

589. **Furuya N**, **Ikeda SI**, **Sato S**, **Soma S**, **Ezaki J**, **Trejo JAO**, **Takeda-Ezaki M**, **Fujimura T**, **Arikawa-Hirasawa E**, **Tada N**, **Komatsu M**, **Tanaka K**, **Kominami E**, **Hattori N**, **Ueno T**. PARK2/Parkin-mediated mitochondrial clearance contributes to proteasome activation during

slow-twitch muscle atrophy via NFE2L1 nuclear translocation. *Autophagy* 10: 631–641, 2014. doi: 10.4161/auto.27785.

590. **Leermakers PA**, **Kneppers AEM**, **Schols AMWJ**, **Kelders MCJM**, **de Theije CC**, **Verdijk LB**, **van Loon LJC**, **Langen RCJ**, **Gosker HR**. Skeletal muscle unloading results in increased mitophagy and decreased mitochondrial biogenesis regulation. *Muscle and Nerve* 60: 769–778, 2019. doi: 10.1002/mus.26702.

Chapter Three: PhD Objectives and Hypotheses

Based on the review of literature it can be concluded that autophagy, mitophagy and lysosomes are essential for the maintenance of skeletal muscle quality. With both chronic disuse and advancing age there are deficits in mitochondrial quality and perturbations in the regulation of autophagy in skeletal muscle. However, multiple facets of these molecular mechanisms remain undefined in these contexts. Further, the influence of biological sex on these processes is not yet determined. With many remaining questions, the purpose this dissertation was to investigate the mechanisms that regulated impairments in mitochondrial quality and autophagy in both denervation and advanced age, and how acute exercise can enhance these processes. Based on the rationale presented above, my thesis will have the following objectives:

OBJECTIVE #1:

To determine the temporal regulation of autophagic and mitophagic flux in SS and IMF mitochondria and regulation of lysosomes in response denervation.

Hypotheses:

1) Autophagy and mitophagy flux will be enhanced in denervated skeletal muscle as decrements in mitochondrial content are observed with denervation;
2) Indicators of lysosome biosynthesis will be upregulated with denervation to assist with the increased autophagic demand;
3) Lysosome dysfunction will be apparent in denervated skeletal muscle.

OBJECTIVE #2:

To assess whether young male and female mice exhibit a differential regulation of autophagy, mitophagy and lysosome biogenesis in skeletal muscle in a basal state and with exercise. Further, we wanted to explore the influence of age and biological sex on these pathways, and if the exercise-stimulated pathways differed amongst groups.

Hypotheses:

1) No differences in mitochondrial content decay will be observed between aged male and female mice;
2) Female mice will have greater levels of autophagy and mitophagy than male mice, irrespective of age;
3) Exercise will stimulate autophagic clearance and lysosome biogenesis in young muscle, but the absolute level of activation will be lower in aged skeletal muscle, irrespective of biological sex.

Chapter 4:

Time-dependent changes in autophagy, mitophagy and lysosomes in skeletal muscle during denervation-induced disuse

Authors: Matthew Triolo[1,2], Mikhaela Slavin[1,2], Neushaw Moradi[1,2], David A. Hood[1,2]

Affiliations: [1] Muscle Health Research Centre, York University, Toronto, Ontario, Canada M3J 1P3

[2] School of Kinesiology and Health Science, York University, Toronto, Ontario, Canada M3J 1P3

Running Title: Regulation of mitophagy and lysosomes with muscle denervation

Corresponding Author: David A Hood, PhD
School of Kinesiology and Health Science
Muscle Health Research Centre
York University, Toronto, ON
M3J 1P3, Canada
Tel: (416) 736-2100 ext. 66640
Email: dhood@yorku.ca

Table of Contents Category: Muscle

Key Words: mitochondrial dysfunction, reactive oxygen species, atrophy, TFEB, lysosome dysfunction, autophagy, mitophagy

This manuscript has been submitted to The Journal of Physiology (July 2021). Revised manuscript submitted (November 2021).

Key Point Summary:

-Denervation is an experimental model of peripheral neuropathies as well as muscle disuse, and it helps us understand some aspects of the sarcopenia of aging.

-Muscle disuse is associated with reduced mitochondrial content and function, leading to metabolic impairments within the tissue. Although the processes that regulate mitochondrial biogenesis are understood, those that govern mitochondrial breakdown (i.e., mitophagy) are not well characterized in this context.

-Autophagy and mitophagy flux up to the point of the lysosome were increased in the early stages of denervation, along with mitochondrial dysfunction, but were reduced at later time points when the degree of muscle atrophy was highest.

-Denervation led to progressive increases in lysosomal proteins to accommodate mitophagy flux, yet evidence for lysosomal impairment at later stages may limit the removal of dysfunctional mitochondria, stimulate reactive oxygen species signaling, and reduce muscle health as denervation time progresses.

Abstract:

Deficits in skeletal muscle mitochondrial content and quality are observed following denervation-atrophy. This is due to alterations in the biogenesis of new mitochondria as well as the degradation of dysfunctional organelles via mitophagy. The regulation of autophagy and mitophagy over the course of denervation (Den) remains unknown. Further, the time-dependent changes in lysosome content, the end-stage organelle for mitophagy, remains unexplored. Here, we studied autophagic as well as mitophagic flux in subsarcolemmal (SS) and intermyofibrillar (IMF) mitochondria from rat muscle subjected to Den for 1, 3, or 7 days. We also assessed flux at 1-day post-denervation in transgenic mt-keima mice. Markers of mitochondrial content were reduced at 7 days following Den, and Den further resulted in rapid decrements in mitochondrial respiration, along with increased ROS emission. Autophagy flux was upregulated at 1- and 3-days post-Den but was reduced compared to time-matched sham-operated controls at 7-days post-Den. Mitophagy flux was enhanced in SS mitochondria as early as 1- and 3-days of Den but decreased in both SS and IMF subfractions following 7 days of Den. Lysosome protein content and transcriptional regulators TFEB and TFE3 were progressively enhanced with Den, an adaptation designed to enhance autophagic capacity. However, evidence for lysosome dysfunction was apparent by 7 days, which may limit degradation capacity. This may contribute to an inability to clear dysfunctional mitochondria and increased ROS signaling, thereby accelerating muscle atrophy. Thus, therapeutic targeting of lysosome function may help to maintain autophagic flux and muscle health during conditions of muscle disuse or denervation.

Introduction:

Skeletal muscle is a large organ system, making up approximately 40% of body mass in lean individuals. Primarily thought of for its role in locomotion, muscle is also responsible for determining whole body metabolic rate. In a unique way, muscle displays a high degree of adaptive plasticity to meet the metabolic demands placed upon it. This is due to the extensive malleability of mitochondria within muscle. The volume of these organelles is regulated by a balance of opposing processes of organelle synthesis (i.e., biogenesis) and degradation (i.e., mitophagy). Mitochondrial biogenesis is an intricate process, largely mediated by the enhanced transcription of genes in both the nuclear and mitochondrial genomes, followed by the assembly of these gene products into functional complexes within the organelle (1, 2). In opposition, mitophagy requires the removal of damaged mitochondrial segments produced by the fission of dysfunctional mitochondria (3). These mitochondrial fragments are tagged for removal via the autophagy-lysosome system (3, 4). This occurs through either Pink1-Parkin-mediated mechanisms, or via receptor-mediated pathways (i.e., BNIP3, NIX) that act to tether the mitochondria to autophagosomes for engulfment and subsequent degradation by the lysosomes (4). Therefore, mitophagy contributes to both the loss of mitochondrial volume, as well as the maintenance of organelle quality (2). This is best exemplified when mitophagy in inhibited, wherein dysfunctional organelles accumulate to the detriment of cellular health (5), leading to an inability to preserve muscle mass and contractile function (6).

It has long been known that mitochondria within skeletal muscle reside in two geographically distinct regions (7). The mitochondria that populate the area beneath the sarcolemma are termed subsarcolemmal (SS). This fraction of the organelle pool is thought to provide energy for membrane and nuclear events and represent 10-20% of total mitochondrial

volume in muscle (7, 8). In contrast, intermyofibrillar (IMF) mitochondria are far more abundant and exist in a reticulum (7–9). IMF mitochondria are essential for providing energy to support contraction. These two populations of mitochondria also possess distinct biochemical properties, (10), and divergent responses to stimuli such as exercise and disuse. Specifically, the SS subfraction are thought to be more labile compared to the IMF organelles (11–14). Although much is known about the regulation of biogenesis in these two mitochondrial fractions, their response to denervation remains unexplored in the context of mitophagy.

Chronic muscle disuse leads to a loss of muscle mass (i.e., atrophy), accompanied by weakness and metabolic inefficiency (15–17). This is propagated, in part, by the accumulation of dysfunctional mitochondria (18, 19). Following prolonged periods of muscle disuse, there is evidence of suppressed mitochondrial biogenesis (20–23) and organellar fragmentation (24–27). Concomitantly, there are accumulations of mitophagic proteins in both denervation and disuse models (25, 28). Although informative, these latter studies cannot provide insight into whether changes in mitophagy protein content are due to 1) the upregulation of mitochondrial targeting to the autophagosome, 2) the accumulation of tagged mitochondria without terminal breakdown at the lysosomes (i.e., reduced flux), or 3) the tagging and subsequent clearance of mitochondria at the lysosome level (i.e., enhanced flux). Additionally, there is little knowledge regarding the time course of mitophagy changes that occur during the atrophy process.

Lysosomes act as an end-stage organelle for the autophagy pathway, and dysfunction within the lysosomal system hinders autophagosomal degradation (29, 30). As mitochondria rely on lysosomal proteolysis, alterations in lysosome health have profound implications for mitophagy. The regulation of lysosomal and autophagy genes is mediated transcriptionally by the MiTF/TFE family of proteins, specifically transcription factor EB (TFEB) (31–34). We have

previously reported that denervation-induced atrophy leads to the accumulation of TFEB and lysosomal proteins in mouse muscle, which is accompanied by reduced autophagy flux (35). This is suggestive of an impaired ability to clear cellular debris. Therefore, the terminal degradation of mitochondria in the lysosomes may represent the limiting factor in the preservation of mitochondrial quality.

The purpose of this study was to examine the time-dependent changes in the regulation of autophagy and mitophagy flux during denervation-induced muscle disuse, as well as the role that the lysosomes have in mediating these changes. To provide a clear indication of autophagy and mitophagy flux, we used a rat model of muscle denervation and employed treatment with saline or colchicine. To further assessed mitophagy in a non-inhibited state, we utilized transgenic mt-keima mice. We hypothesized that mitochondrial dysfunction and elevated mitophagy flux would precede decrements in mitochondrial content. Further, we hypothesized that these changes would occur concomitantly with an upregulated lysosome protein content to meet the increasing demands of autophagy.

Materials and Methods:

Animals and Denervation

All animal procedures were conducted in accordance with the standards set by the Canadian Council on Animal Care and were approved by the York University Animal Care Committee (Protocol # 2017-23). Adult Sprague-Dawley (350-450g, 3-4 months old) rats were obtained from Charles River Laboratories (St. Constant, QC, Canada). Animals were provided chow and water *ad libitum*. Rats underwent surgical procedures to induce denervation (Den) of the tibialis anterior (TA) and extensor digitorum longus (EDL) muscles. Briefly, following isoflurane anesthetization, the common the peroneal nerve was exposed and transected in the left hindlimb, whereas the right served as a sham operated internal control. After administration of sterile ampicillin, the incision was sutured, and the skin was closed with metal clips. Animals were given amoxicillin in their drinking water (0.3mg/L for up to 7 days) and Meloxicam (2mg/kg Day 1, 1mg/kg Day 2, 0.5mg/kg Day 3) subcutaneously for pain management, following the surgery rats were randomly assigned to Den for 1, 3, or 7 days, respectively. At each of these time points, animals were held under anesthesia, and the TA and EDL muscle were excised from the denervated and contralateral limb to be used for various biochemical analysis. Animals were then euthanized via cardiotomy.

Autophagy and Mitophagy Flux

To determine autophagy and mitophagy flux, sterile colchicine (COLCH; 0.4mg/kg/day; Sigma, Oakville, ON, Canada) or vehicle (SAL; 0.9%saline) were administered via intraperitoneal injections 24 and 48 hours prior to sacrifice, which is sufficient to inhibit autophagy for the measurement of flux (36). Animals were randomly assigned to the treatment groups. To determine flux, western blotting of LC3-II was performed in whole muscle extracts or isolated SS or IMF

mitochondrial subfractions (as described below). Protein abundance was quantified using Image J and values were corrected for the corresponding loading controls. To determine flux, the SAL values were subtracted from the mean COLCH value for the corresponding time point (i.e., Mean $CON_{COLCH} - CON_{SAL}$).

Whole Muscle Protein Extracts

The proximal one third of the TA muscle was snap frozen in liquid nitrogen following excision from the animal and stored at -80ºC. The tissue was pulverized to a fine powder at the temperature of liquid nitrogen. Protein extracts were made by diluting (10x) a small amount of powder (~15-20mg) in Sakamoto buffer (20mM HEPES, 2mM EGTA, 1% Triton X-100, 50% Glycerol, 50 mM ß-Glycerophosphate) containing both phosphatase (Sigma) and protease (Roche Mississauga, ON, Canada) inhibitors and rotated end-over-end for 1 hour at 4ºC. Samples were then sonicated on ice (3 seconds x 3 times) and centrifuged (14,000g) for 15 minutes at 4ºC. The supernatant fraction was collected and stored at -80ºC until further analysis.

Quantitative PCR

Total RNA was isolated from frozen, whole muscle TA. Briefly, TRIzol® reagent was added to frozen TA muscle samples (~25mg) and mixed with chloroform using a Qiagen TissueLyser II. Samples were centrifuged at 4°C at 16,000 g for 15 min. The upper aqueous phase of the sample was transferred to a new tube along with isopropanol and left for 1 hour at −80°C to precipitate. Samples were thawed and centrifuged at 4°C at 16,000 g for 10 min. The resultant supernate was discarded, and the pellet was resuspended in 30 µl of molecular-grade sterile H_2O (Wisent Bio Products, Saint-Jean-Baptiste, QC, Canada). The concentration and purity of the RNA were measured using a NanoDrop 2000. SuperScript III reverse transcriptase (Invitrogen, Carlsbad, CA)

was used to reverse-transcribe 1.5 μg of total RNA into cDNA in a 20 μL reaction. Forward and reverse primers for the genes of interest were created and optimized for specificity and concentration (Table 1). mRNA expression was measured with SYBR Green chemistry (PerfeCTa SYBR Green SuperMix, ROX, Quanta BioSciences, Gaithersburg, MD). Each well of a 96-well plate contained SYBR Green SuperMix, forward and reverse primers (20 μM), sterile H_2O, and 10ng of cDNA. All real-time PCR amplification was detected using a StepOnePlus Real-Time PCR System (Applied Biosystems, Foster City, CA) and a final reaction volume of each well was 25μl. Samples were run in duplicates to ensure accuracy and negative control wells contained H_2O in place of cDNA. Gene expression was normalized to both GAPDH and S12 and then quantitated utilizing the $2^{-\Delta\Delta CT}$ method relative to time matched controls.

Mitochondrial Isolation

To isolate subsarcolemmal (SS) and intermyofibrillar (IMF) mitochondrial subfractions, the distal 2/3 of the muscle (~500-600mg) was minced, homogenized mechanically, and underwent differential centrifugation as previously described (10, 37, 38). The final mitochondrial pellets were resuspended in ice-cold buffer (100 mm KCl, 10 mm MOPS, 0.2% BSA). Fresh mitochondria were utilized for assessment of respiration and ROS production. The remaining mitochondrial samples were supplemented with phosphatase inhibitor cocktails as well as protease inhibitors and stored at –80°C for Western blotting procedures.

Mitochondrial Respiration

To assess mitochondrial respiration (O_2/min/mg), SS and IMF subfractions were incubated in a Clark Oxygen Electrode system (Strathkelvin Instruments, North Lanakshire, UK) with 250uL of VO2 Buffer (250mM sucrose, 50mM KCl, 25mM Tris-HCl, 10mM K2HPO4, 0.2% BSA, pH=7.4)

at 30ºC. Following background respiration, Complex-I supported basal respiration (state 4) was measured with the addition of 10mM glutamate. Subsequently, Complex-I supported active respiration (state 3) was measured following the addition of 0.44mM ADP. Finally, NADH was added to the chamber to test mitochondrial integrity. All values were corrected for background respiration within the chamber (i.e., following the addition of mitochondria, but prior to the addition of glutamate).

Mitochondrial ROS Production

To assess mitochondrial reactive oxygen ROS production, 50mg of freshly isolated SS and IMF mitochondria were incubated in VO2 buffer supplemented with 50mM H_2DCFDA (D399, Thermo Fisher Scientific) in a white polystyrene 96-well plate. Fluorescent emission (480-520nm) was measured for 30 minutes at 37ºC in a Synergy HT microplate reader (Biotek, Winooski, VT). ROS production was assessed with the addition of 10mM glutamate in the absence (state 4) or presence (state 3) of 0.44mM ADP. Data were analyzed with KC4 software V3.0 and normalized to the corresponding respiration.

High Resolution Respiration and ROS Emission

High-resolution respirometry (Oroboros O2k, Austria) was used to measure oxygen consumption in permeabilized muscle fibers from the distal-lateral portion of the TA muscle of rats that underwent 1 day of denervation. Briefly, the muscle was excised, and fibers were mechanically separated in ice cold BIOPS buffer (2.77mM CaK2EGTA, 7.23mM K2EGTA, 7.55mM Na2ATP, 6.56mM MgCl26H2O, 20mM Taurine, 15mM Na2Phosphocreatine, 20mM Imidazole, 0.5mM Dithiothreitol, 50mM MES-Hydrate, pH 7.1). Subsequently, the fibers were permeabilized in BIOPS supplemented with 40ug/uL saponin at 4ºC for 30 minutes with gentle rocking and washed

in Buffer-Z (105mM K-MES, 30mM KCl, 10mM KH2PO4, 5mM MgCl2•6H2O, 1mM EGTA, 5mg/ml BSA) with gentle rocking. Fibers were then incubated in the chamber with oxygenated Buffer-Z supplemented. with 10μM Amplex-Red to simultaneously measure ROS-production, as well as 1μM Blebbistatin to prevent tetanus of the muscle (39), 25U/ml Cu/Zn SOD1 to convert O2- to H2O2 and 2mM EGTA. Following oxygenation and measurement of background values, substrates were titrated to assess respiration and ROS production simultaneously. Substrates were titrated as follows: 5mM glutamate + 2mM malate (Complex I – State 4/Basal), 5mM ADP (Complex I – State 3/Active), and 10mM succinate (Complex I+II – State 3/Active). To test for mitochondrial membrane integrity, cytochrome c was added to the chamber. Any increase in respiration following its addition was indicative of damaged mitochondria, and the samples were excluded from the data set. Respiratory function was determined by oxygen flux rates (pmol/s·ml) minus background rates and corrected to fiber mass (pmol/s·ml/mg). ROS-emission was calculated by taking the rate of ROS-emission (pmol/s) and correcting it by the weight (mg) of tissue and subsequently, the corresponding respiration rate.

Cytosolic and Nuclear Fractionation

Nuclear and cytosolic fractions from fresh TA muscles of rats that underwent 1 day of denervation were obtained using the NE-PER extraction reagents (38835, Thermo Scientific Scientific) with minor modifications. Briefly, 50~100 mg of the TA muscle was minced on ice and homogenized using a Dounce homogenizer in cytosolic extraction reagent (CER) I. Homogenates were then vortexed and let to stand on ice for 10 minutes. Following the addition of CER II solution, samples were briefly vortexed and centrifuged (16,000g) for 10 min. The cytosolic fractions (supernates) were then collected. The remaining pellets, containing nuclei and cellular debris, were washed in cold 3 times in 1×PBS and subsequently resuspended in nuclear extraction buffer (NER). Nuclear

fractions were then sonicated for 3 seconds x 3 times, and incubated on ice for 40 min. These samples were vortexed every 10 min during the incubation, and subsequently underwent centrifugation (16,000g) for 10 min. The resulting supernatant nuclear fractions were collected. Both the cytosolic and nuclear fractions were stored at -80°C until further analysis.

Western Blotting

All protein concentrations were determined using the Bradford method. Equal amounts of protein (~20-30μg) were loaded and separated via SDS-PAGE and transferred onto nitrocellulose membranes (Bio-Rad, Mississauga, ON, Canada). Membranes were blocked with wash buffer (0.12% Tris-HCl, 0.585% NaCl, 0.1% Tween, pH 7.5) supplemented with 5% skim milk (w/v) at room temperature for 1 hour with gentle agitation. Membranes were then incubated with primary antibodies overnight at 4°C. The following day, membranes were washed 3x5minutes in wash buffer and incubated for 1 hour at room temperature with the appropriate HRP-conjugated secondary antibody and subsequently washed 3x5 minutes in wash buffer. The protein density was visualized using enhanced chemiluminescence (1705061, Bio-Rad) with an ImageStation 4000MM Pro (Carestream, Concord, ON, Canada). Band densities were quantified by ImageJ software (NIH) and normalized to corresponding loading controls. Antibodies are detailed in Table 2.

mt-Keima Mice to Assess Acute Changes in Mitophagy Using Confocal Microscopy

Mice overexpressing mt-Keima, a mitochondrial-targeted probe that fluoresces green when exposed to the pH of the cytosol, and red when exposed to the pH of the lysosomes, were used to further assess acute changes in mitophagy flux, (40, 41). Increases in the red:green fluorescence are indicative of mitophagy flux (40, 41). These mice were a generous gift from Dr. Toren Finkel

and Dr. Nuo Sun and bred in-house according to standard procedures. At ~4 months old, mice underwent unilateral sciatic denervation for 1 day and the contralateral limb was sham operated and served as an internal control. Following 24 hours, images were captured using confocal microscopy. Briefly, mice were held under anesthetic (isoflurane), and the TA muscle from the sham-operated or denervated limb was excised and placed in ice cold 1xPBS, cut longitudinally, and a portion was placed on a cover slip, dampened with 1xPBS. The muscle was then visualized and imaged at 20x magnification using an inverted Nikon Eclipse TE2000-U Fluorescence microscope coupled to a Nikon C2 confocal microscope. Images were taken via sequential excitation of 488nm (green) and 561nm (red) and emission of 500-550nm or 575-625nm for green and red, respectively. Settings for all images and quantifications were consistent throughout the study. The individual green and red channels were exported and quantified on a pixel-by-pixel basis using ImageJ software (NIH). Red pixels were quantified as a fraction of total red and green pixels. For each of 4 biological replicates, 8 images were taken at random resulting in 32 data points/group.

Electron Microscopy of Vacuolar Inclusions

Muscle cubes (~2 mm^2) from three saline-treated 7-day sham operated and 7-day denervated TA muscles were placed in a 2% glutaraldehyde solution in 0.1 mm sodium cacodylate, pH 7.3 and stored at 4^oC until further use. Samples were embedded, stained and cut the samples using standardized procedures at the Advanced Imaging Centre at The Hospital for Sick Children. Images were captured on a FEI Tecnai 20 transmission electron microscope. Briefly, for each biological replicate, 3 myofibrils were selected at random, and 3 images were taken per myofibril at 9600x magnification. Thus, each data point represents one of these images quantified (Figure 6B and C). Vacuolar inclusions were selected by the presence of a membrane surrounding a

heterogenous electron-lucent and electron-dense region. To analyze the vacuolar inclusions, ImageJ was utilized. Specifically, sample images were calibrated using the embedded scale bar. Subsequently, the "Freehand Section" tool was utilized to trace each inclusion. The number of inclusions and area (nm^2) of each was recorded and normalized to the area of the entire image (μm^2). To ensure no experimenter bias, the quantifier was blinded to the random selection of images from each group.

Statistical Analysis

Statistics were assessed using GraphPad Prism Software (Version 9). In saline-conditions, the impact of denervation over the course of 1-, 3- or 7-days values for figures was represented as Den/Sham at each timepoint. To assess the independent and combined effects of denervation and time, statistics were run on raw values, which are found in the Statistical Summary Table. To assess the independent and combined effects of denervation and time in the autophagy and mitophagy flux data, sham and denervated values were plotted over the course of 1, 3 and 7 days. All time-course data were analyzed by a repeated measures two-way ANOVA with a subsequent Fisher LSD post-hoc test comparing time-matched Sham and Den values. # represents a significant effect of time, † represents a significant effect of denervation and ¶ represents the interaction of time and denervation at $p<0.05$. A Fisher LSD post-hoc test was used to compare time-matched control and denervated values, with significance represented by * at $p<0.05$. In Figures 5 and 7, each quantified data point was not paired, thus a Students' unpaired t-test was utilized, and * represents a significant difference. All data are shown as Means ± SD.

Results:

Denervation leads to time-dependent changes in muscle mass.

In the both the tibialis anterior (TA) (time: $p<0.0001$, denervation: $p<0.0001$, interaction: $p<0.0001$; Fig 1A) and extensor digitorum longus (EDL) (time: $p<0.0001$, denervation: $p<0.0001$, interaction: $p<0.0001$; Fig 1B) main effects of time, denervation, and an interaction of the two variables were observed. Den for 3 days elicited significant (5%) reductions in both TA ($p=0.0004$) and EDL ($p=0.0054$) mass in comparison to time-matched sham. 7 days of Den reduced the mass of both muscles by ~25% ($p<0.0001$)

Denervation promotes reductions in mitochondrial content within muscle.

To determine the time-dependent changes in mitochondrial content with Den, we quantified the levels of various mitochondrial proteins derived from the expression of both the nuclear and mitochondrial genomes (Figs. 2A, B). An interaction between time and Den was found for the mitochondrial-encoded COX subunit I (COX-I) ($p=0.0012$), the nuclear-encoded COX subunit IV (COXI-IV) ($p=0.0055$) and the nuclear-encoded Complex III subunit UQCRC2 ($p=0.0054$). Main effects of time were uncovered for both UQCRC2 ($p=0.0394$) and the Krebs' Cycle enzyme Citrate Synthase ($p=0.0265$). No difference was observed in these proteins at 1- or 3-days post-Den, however, all proteins were reduced by 15-40% at 7-days post-Den in comparison to time-matched sham tissues (COX-I: $p<0.0001$, COX-IV: $p=0.0010$, UQCRC2: $p=0.0004$, Citrate Synthase: $p=0.0671$).

Denervation leads to functional deficits in skeletal muscle mitochondria.

To determine if these changes in mitochondrial content were matched with alterations in the function of these organelles, we assessed respiration (Fig. 2C) and ROS-production (Fig. 2D)

in isolated subsarcolemmal (SS) and intermyofibrillar (IMF) mitochondria. In SS mitochondria, Complex-I supported State 4 (basal) and State 3 (active) respiration underwent denervation-induced reductions (State 4: p=0.0034, State 3: p=0.0007) that were influenced by time (State 4: p=0.0241, State 3: p=0.0034). Post-hoc analysis revealed 53% reductions in State 4 (p=0.0036) and 27% decrease in State 3 (p=0.0506) as early as 3 days of Den. This deficit was more pronounced at 7 days of Den with 34% and 60% reductions in basal (p=0.0091) and active (p<0.0001) respiration. State 4 (basal) and State 3 (active) ROS-emission in SS mitochondria underwent denervation-induced reductions (State 4: p<0.0001, State 3: p=0.0011). Furthermore, time influenced the magnitude of the denervation response (State 4: p=0.0061, State 3: p=0.0263). State 4 ROS-emission in SS mitochondria was not altered at 1 day, but underwent a significant, 3.2-fold increase following 3-days of Den (p<0.0001), which was sustained at 7 days (p=0.0016). State 3 ROS-emission in SS mitochondria was significantly upregulated by 2.6-fold following 3-days of Den (p=0.0271) and further by 5.7-fold following 7-days of Den (p=0.0007).

In IMF mitochondria, both State 4 (p=0.0483) and State 3 (p=0.0027) respiration were reduced by denervation. Post-hoc analysis revealed a trend for decrease in State 4 respiration at 7-days post-Den (p=0.0598). Significant 30% reductions were observed in State 3 respiration at 1 (p=0.0139) and 7 (p=0.0249) days of Den in comparison to time-matched Sham controls. Overall, State 4 (p=0.0350) and State 3 (p=0.0004) ROS-emission were enhanced with Den. Post-hoc analysis of Den versus time-matched Sham animals exposed a significant 2.1-fold increase in State 4 ROS-emission at 3 days (p=0.0085), a 1.8-fold increase in State 3 ROS-emission at 1 day (p=0.0280) and a 2.0-fold increase at 7 days (p=0.0029).

To further understand the alterations in mitochondrial ROS signaling observed as early as 1-day post-Den in isolated mitochondria, we also assessed respiration and H_2O_2 production in

permeabilized fibers from 1-day Sham and Den TA muscle. No changes in respiration (Statistical Summary Table) between Sham and Den fibers were observed, but our data revealed a significant 2.2-fold increase in ROS emission per mg of muscle in ADP-stimulated, Complex-I supported respiration ($p=0.0133$; Fig. 2E).

Autophagy-related protein expression is elevated with denervation.

To evaluate how denervation affected the autophagy-lysosome system, we measured autophagy proteins in whole muscle TA samples (Figs. 3A-D). Main effects of Den and interactions of Den and time were uncovered in the upstream autophagy regulators Beclin1 (Den: $p<0.0001$, Interaction: $p<0.0001$) and ATG-7 (Den: $p<0.0001$, Interaction: $p=0.0011$) and the autophagy adapter protein p62 (Den: $p<0.0001$, Interaction: $p<0.0001$) (Figs. 3A, B). At 3 days post-Den, Beclin1 was significantly upregulated 1.2-fold ($p=0.0182$), and further elevated by 2.0-fold by 7 days post-Den ($p<0.0001$). ATG-7 protein content underwent a 1.3-fold increase at 3 days ($p=0.0106$) and a further 1.8-fold increase following 7 days of Den ($p<0.0001$). p62 was significantly enhanced by 3.4-fold at 3 days ($p<0.0001$), and by 2.3-fold following 7 days of Den ($p<0.0001$) in comparison to the time-matched Sham condition.

In saline-injected animals we assessed LC3-I, II, II/I and total LC3 protein from sham-operated and Den TA muscle (Fig 3C, D). A significant impact of denervation ($p<0.0001$), time ($p=0.0186$) and an interaction of the two variable ($p<0.0001$) was measured in autophagosomal precursor protein, LC3-I. Specifically, LC3-I was reduced by 20% below control levels following 1 day of Den ($p=0.0346$) and was then subsequently elevated to 2.9-fold of control at 7-days of Den ($p<0.0001$). Mature LC3-II underwent denervation-induced increases ($p<0.0001$) that were time-dependent ($p=0.0002$). A trend for a 1.5-fold increase in LC3-II was measured at 3 days ($p=0.0521$), whereas 7 days of Den significantly upregulated protein levels by 2.1-fold ($p<0.0001$).

A time dependent decrease in LC3-II/I with denervation was measured ($p=0.0086$). One day of Den elevated LC3-II/I by 1.5-fold ($p=0.0247$), indicative of increased mature:immature autophagosomes, but this was reduced below control by 21% at 7-days post-Den (p=00241). Total LC3 protein underwent independent denervation- ($p<0.0001$) and time- ($p<0.0341$) induced changes, and an interaction of the two variables was observed ($p<0.0001$). Specifically, LC3 protein was gradually elevated with Den, and significantly increased by 2.5-fold at 7-days ($p<0.0001$) in comparison to sham-operated controls.

To determine if some of these changes could be explained by alterations in gene expression, we measured *Lc3* and *p62* mRNA (Fig. 3F). Both *Lc3* (Den: $p=0.0108$, Interaction: p=0,0332) and *p62* underwent denervation-induced increases that were dependent on time (Den: $p<0.0001$, Time: $p=0.0004$, Interaction $p<0.0001$). *p62* was 1.6-fold greater in 1-day Den muscle ($p=0.0036$), and further increased to 3.8-fold greater in 3 ($p<0.0001$) and 7-day ($p<0.0001$) Den muscle when compared to time-matched sham-operated control. *Lc3* was elevated 65% at 7-days post-denervation ($p=0.0002$) but was unchanged at earlier time points.

Skeletal muscle autophagy flux is altered with denervation.

To evaluate autophagy flux, we examined the levels of LC3-II protein in the TA muscles of saline- and colchicine-treated animals subjected to 1, 3 or 7 days of Den (Fig. 3C, E). Significant time-dependent changes in autophagy flux were observed in response to denervation (time: $p<0.0001$, interaction: $p=0.0005$). Post-hoc analyses revealed a significant 1.3- and 1.5-fold increases in autophagy flux following 1 ($p=0.0333$) and 3 ($p=0.0111$) days of Den, respectively. Flux was reduced by 28% following 7 days of Den, relative to sham muscle ($p=0.0121$).

Mitophagy in SS and IMF subfractions is altered during denervation.

To determine if the functional changes observed in mitochondria coincided with changes in mitophagy, we assessed the autophagosomal marker LC3-II in isolated SS (Figs. 4A, B) and IMF mitochondria (Figs. 4D, E). In both the SS (Den: $p<0.0001$, Time: $p=0.0030$, Interaction: $p=0.0046$) and IMF (Den: $p<0.0001$, Time: $p=0.0042$, Interaction: $p=0.0009$) subfractions, a time-dependent increase in LC3-II accumulation with denervation was observed in saline-treated animals. There was no change in LC3-II protein at the early 1-day Den timepoint. In the SS subfraction there was 1.9-fold more LC3-II at 3-day Den ($p=0.0419$), and a 3.3-fold increase was found at 7-day Den ($p=0.0091$). In the IMF subfraction, there was a 2.2-fold increase at 3-day Den ($p=0.0139$) and 2.5-fold increase at 7-day Den ($p=0.0007$).

To evaluate mitophagy flux, we examined the levels of LC3-II protein in these isolated mitochondria, in saline- and colchicine-treated animals subjected to 1, 3 or 7 days of Den (Figs. 4 C, F). Colchicine treatment successfully increased LC3-II accumulation in both SS and IMF mitochondria (See Statistical Summary Table). A time-dependent denervation effect was observed in SS (Den: $p=0.0008$, Time: $p<0.0001$, Interaction $p<0.0001$) and IMF (Den: $p<0.0001$, Time: $p<0.0001$, Interaction: $p<0.0001$) mitochondria. In SS mitochondria post-hoc analysis revealed an 20% increase in mitophagy flux at 1-day post-Den ($p=0.0450$) and a 40% increase at 3 days post-Den ($p<0.0001$). This was followed by a 20% reduction in mitophagy flux at 7 days ($p=0.0123$). In contrast, the IMF subfraction flux remained unchanged at earlier time-points, and only showed significant 55% reductions in flux at 7 days post-Den ($p<0.0001$).

Mitophagy flux assessed via mt-keima is upregulated after 1-day of denervation.

To further evaluate transient, early changes in mitophagy flux, transgenic mt-keima mice were utilized and underwent sciatic nerve denervation for 24-hours, with the contralateral limb

acting as a sham-operated control (Fig. 5A, B). Representative images are depicted in Figure 5A. We observed a 1.3-fold increase in red fluorescence (i.e. mitolysosomes) ($p=0.0176$), indicative of upregulated mitophagy flux

Lysosomal protein markers are enhanced with denervation.

To assess the end-stage of the autophagy pathway, we evaluated lysosomal protein content (Figs 6A, B). The protein levels of vesicular ATPase (V-ATPase), a H+ pump that help maintain the acidic pH of the lysosomes, and lysosome-associated membrane proteins (Lamp)-1 and -2 all increased as a product of denervation (V-ATPase: $p<0.0001$, Lamp1: $p=0.0110$, Lamp2: $p<0.0001$). This response was significantly influenced by time for Lamp1 ($p=0.0045$), and a trend toward an interaction was measured in V-ATPase ($p=0.0779$) and Lamp2 ($p=0.0909$). Post-hoc analysis revealed increases in V-ATPase by 1.6-1.7-fold at both 3 ($p=0.0046$) and 7 ($p=0.0002$) days post-Den. Lamp 2 increased similarly at 3 ($p=0.0031$) and 7 days ($p=0.0004$). The increase in LAMP-1 was significant following 7 days of Den ($p=0.0003$).To understand the basis for the upregulation of these lysosomal proteins we measured the levels of TFEB and TFE3, two transcription factors that are primarily responsible for the transcription of lysosomal genes (Fig 6C, D). Both proteins increased with Den as a main effect (TFEB: $p=0.0017$, TFE3: $p<0.0001$). TFEB protein was upregulated by 1.4-fold following 3 days of Den ($p=0.0332$) and 2.3-fold following 7-days of Den ($p=0.0046$) . TFE3 protein was increased as early as 1-day post-Den ($p=0.0471$) and which was sustained at 1.7-fold of control at day 3 ($p=0.0015$), and further increased by 2.1-fold by 7 days of Den ($p<0.0001$). A trend for an increase in nuclear (active) TFEB by 1.2-fold as early as 1-day post-Den was measured ($p=0.0710$, Fig 6E, F).

Lysosomal dysfunction is evident in 7 day denervated muscle.

We sought evidence for the functionality of lysosomes by using TEM to measure the presence of vacuolar inclusions in 7-day sham and Den muscle. Representative images are depicted in Figure 7A. Following 7 days of Den there was a 3.8-fold increase in area of inclusions ($p<0.0001$; Fig. 7B), as well as a 2.3-fold increase in their number ($p<0.0001$; Fig. 7C) compared to sham-operated control.

Discussion:

Skeletal muscle inactivity promotes a concomitant loss of mass and function. Denervation (Den) is a commonly utilized model to mimic disuse-atrophy (42) and it recapitulates, in a time-compressed manner, age-related neuromuscular denervation (43, 44). Within the first week of Den there is an accelerated loss of mitochondrial volume, followed by a more gradual rate of loss in organelle content with prolonged Den (42, 45). Since mitochondrial content is regulated by the opposing processes of biogenesis and mitophagy, organelle decay could be due to either decrements in biogenesis and/or elevations in mitophagy. In the case of denervation-induced atrophy, it is well established that mitochondrial biogenesis is reduced (22), yet far less is known about the regulation of mitophagy. Thus, the primary goal of this study was to investigate the time-dependent influence of denervation on mitophagy, and how the lysosomes, which act as end-stage organelles, are impacted. We hypothesized that mitophagy signaling would be enhanced throughout the course of denervation, prior to the alterations in mitochondrial content, and that lysosomal proteins would be elevated to meet these demands.

Since mitophagy is activated by signals that alter mitochondrial function (2, 46), our first objective was to look towards the chronological effects of Den-induced adaptations in organelle function that accompanied the progressive loss in muscle mass observed. Utilizing isolated subsarcolemmal (SS) and intermyofibrillar (IMF) mitochondria allowed us to determine if these two distinct populations undergo similar or differential changes. Our results indicate that IMF mitochondria display respiratory dysfunction as early as 1 day following Den, and further that both organellar subfractions display impairments at 3 days following Den, which was maintained at 7 days. These respiratory changes occurred concomitant with elevated ROS-emission as early as 1-day post-Den in IMF mitochondria. This early dysfunction observed in isolated organelles was

surprising, so we wanted to recapitulate these findings in an experimental system that does not remove mitochondria from their cellular environment. Therefore, we measured H_2O_2 emission using Amplex Red oxidation in permeabilized muscle fibers. Similarly, we found that H_2O_2 emission was elevated in complex-I supported active respiration at 1-day post-Den. Interestingly, these deficits in mitochondrial function preceded any loss of mitochondrial protein content observed at 7-days post Den. This finding is suggestive of a time-dependent inability of the muscle to efficiently clear the dysfunctional organelles following the onset of denervation.

Since mitochondria are removed through mitophagy, the organelle-specific degradation pathway of the autophagy-lysosome system, we first measured autophagy-related protein content over the course of denervation. We show an increase in upstream autophagy-related proteins such as Beclin-1 and Atg-7 as early as 3-days post-Den. We also measured an upregulation of LC3-II (47), and p62, the autophagosome adaptor protein (47–49), as early as 3-days post-Den. At 7-days post-Den there was a further increase in these proteins, along with LC3-I. This result at 7-days is similar to previously published studies (25, 35, 50).

The LC3-II/I ratio is commonly used as an indicator of the ratio of mature:immature autophagosomes (51). Here we report a decrease in LC3-I at 1 day of Den, without change in LC3-II. This ultimately elevated the LC3-II/I ratio. In corroboration with the lack of change in p62 protein, but elevations in its transcript, we interpret this as enhanced autophagosome clearance at the early 1-day timepoint. Further, our observed time-dependent decrease in LC3-II/I below control levels at 7-days post-Den, in conjunction with elevations in p62 at 3- and 7-days post-Den would suggest that the early enhancement in autophagy was followed by a later decrement. To assess this directly via flux measurements, we administered the microtubule destabilizer colchicine to a subset of animals for 2-days prior to sacrifice to inhibit autophagosomal breakdown. This is a

commonly utilized method to assess flux in rodent muscle (36). Colchicine treatment led to the accumulation of LC3-II protein levels in whole muscle samples, confirming that flux was inhibited in all conditions. Interestingly, although LC3-II flux was enhanced following 1 day, and further at 3 days of Den, flux fell below control by 30% at 7 days post-Den. These data at 7-days corroborate previous findings in Den mouse TA muscle (35). Thus, our interpretation based on the static measures (LC3-II/I ratio, p62) reflect a similar result as our flux data. Based on our findings, autophagy is dynamic over the course of denervation and this catabolic pathway may form part of the initial signaling stages of muscle atrophy.

Previous work has demonstrated elevated mitophagy signaling following both denervation (25, 35), and immobilization (28, 52).We similarly observe a greater abundance of LC3-II in both SS and IMF subfractions by 3 and 7 days of Den. Although informative, these previous findings fail to provide a clear indication of flux. Thus, we also assessed LC3-II mitophagy flux in both SS and IMF mitochondria. Our results suggest a differential regulation of mitophagy in these two subfractions in the early (i.e., 1 and 3 day) Den response. Specifically, SS mitochondria from denervated muscle exhibited greater flux than sham-operated control, whereas this was not observed in the IMF subfraction. These observations support the notion that SS mitochondria are more labile in response to both exercise (11–14) and disuse (12, 19).

A limitation of assessing both autophagy and mitophagy flux with colchicine is that it dissociates autophagosome transport to the lysosome, overlooking the importance of lysosomes in regulating this degradation process. To overcome these issues, transgenic models have been developed, such as the mt-Keima mouse, to evaluate mitophagy flux *in vivo* (40, 41). This method is highly sensitive to transient changes in mitophagy. Thus, we utilized these transgenic animals to verify our short-term (1 day) measures of mitophagy flux using the colchicine method in our rat

model. We observed an increase in red:green fluorescence following 1 day of denervation, matching our mitophagy flux data measured in SS mitochondria at the same time point.

Since lysosomes act as the end stage for autophagosome-bound substrate degradation, it is plausible that these organelles undergo alterations in response to Den. In this study we show evidence of an adaptive increase in the lysosomal protein content early as 3 days post-Den (v-ATPase and LAMP2), whereas all lysosomal proteins measured (v-ATPase, LAMP1, LAMP2) were elevated by 7 days post-Den. The transcription factors TFEB and TFE3 regulate lysosomal content in skeletal muscle and other tissues (31–34). We observed elevations in these proteins within denervated skeletal muscle as early as day 1-day post-Den, which were sustained throughout our time course. Further, we noted enhanced nuclear localization of TFEB as early as 1-day post-Den, which may provide a transcriptional explanation for the elevations in lysosomal abundance. We interpret this upregulation in lysosome protein as an adaptation to increase the capacity for autophagosomal degradation. However, the perturbation in both auto- and mitophagy "flux" at 7-days, leads us to believe that the lysosomes are not functioning normally.

We have previously reported evidence of lipofuscin, non-digested lysosomal contents, in electron micrographs following denervation (25), suggestive of organellar impairments. Thus, we wanted to quantify the presence of vacuolar inclusions as an index of lysosome function. The increase we quantified in both inclusion area and number at 7 days of Den suggest that the end-stage of the autophagy system is, in fact, impaired in Den muscle. While we understand that this is not a complete indicator of lysosome function, the presence of these inclusions, which are not apparent in sham-operated muscle, are suggestive of impaired autophagic breakdown at the lysosomes. Cumulatively, these observations indicate that denervated skeletal muscle accrues defective lysosomes which may not be able to meet the demands placed upon them by the

elevations in autophagy-bound substrates, such as mitochondria. We believe that this provides and explanation for the presence of mitochondria that have reduced respiratory capacity and more ROS generation as denervation ensues.

Notably, these findings are different from aged skeletal muscle, wherein mitophagy flux is enhanced, concomitant with lysosomal abundance (27). These data indicate a differential response to natural aging and denervation-induced muscle atrophy with respect to the autophagy pathway. The etiology of musculoskeletal aging is multi-factorial (53). Thus, the denervation model utilized may not sufficiently recapitulate the aging process leading to sarcopenia. Despite this, neuromuscular denervation and remodeling is considered an important aspect of muscular aging. Therefore, findings from our report may more accurately resemble fibers from regions of muscle that undergo denervation with age. Future work aiming to understand the functional alterations in lysosomes under conditions of muscle disuse brought about by Den and aging seems warranted.

As summarized in Figure 8, the results of the present study support our hypothesis that mitochondrial dysfunction and elevations in mitophagy flux precede decrements in mitochondrial content and occur simultaneously with the upregulation in lysosomal protein abundance. Furthermore, the early mitochondrial dysfunction likely contributes to the signaling involved in driving muscle wasting during disuse (18, 19). However, contrary to our initial hypothesis, auto- and mitophagy flux were downregulated as Den-induced atrophy progressed. This finding, in corroboration with the observed lysosome irregularities, suggests that enhancing lysosome function may provide substantial benefits in ameliorating denervation-induced atrophy. Further studies in other models of muscle disuse will be helpful to delineate the effects of inactivity on the autophagy-lysosome system, and its impact on muscle health.

Figure Legends:

Figure 1. Muscle mass over the course of denervation.

A. Tibialis anterior (TA) muscle mass corrected for body mass at 1-, 3- and 7-days post-denervation. Data are presented as Den/Sham (1/3/7 days, N=13/9/13). A Two-Way ANOVA was performed on saline-data, # represents a time effect, † represents a denervation effect, and ¶ represents an interaction effect at $p<0.05$. A Fisher LSD post-hoc test was performed and * represents a significant difference between time matched Sham and Den muscle.

B. Extensor digitorum longus (EDL) muscle mass corrected for body mass at 1-, 3- and 7-days post-denervation. Data are presented as Den/Sham (1/3/7 days, N=9/9/13). A Two-Way ANOVA was performed on saline-data, # represents a time effect, † represents a denervation effect, and ¶ represents an interaction effect at $p<0.05$. A Fisher LSD post-hoc test was performed and * represents a significant difference between time matched Sham and Den muscle.

Figure 2. Mitochondrial content and function over the course of denervation.

A. Western blot images for mitochondrial protein targets in 1, 3- and 7-day sham and denervated TA muscle. GAPDH was used as a loading control.

B. Quantification of COX-I, COX-IV, UQCRC2 and Citrate Synthase protein in Sham and Den TA muscle. Data are represented as Den/Sham (COX-I; 1/3/7 days, N=7), (COX-IV; 1/3/7 days, N=9), (UQCRC2; 1/3/7 days, N=7), (Citrate synthase; 1/3/7, N=7). A Two-Way ANOVA was performed on saline-data, # represents a time effect, † represents a denervation effect, and ¶ represents an interaction effect at $p<0.05$. A Fisher LSD post-hoc test was performed and * represents a significant difference between time matched Sham and Den muscle.

C. Basal (State 4) and active (State 3) respiration in isolated subsarcolemmal (SS) and intermyofibrillar (IMF) mitochondria. Data are represented as Den/Sham (SS State 4; 1/3/7 days, N=7/7/6), (SS State 3; 1/3/7 days, N=7/7/6), (IMF State 4; 1/3/7, N=6), (IMF State 3; 1/3/7, N=6). A Two-Way ANOVA was performed on saline-data, # represents a time effect, † represents a denervation effect, and ¶ represents an interaction effect at $p<0.05$. A Fisher LSD post-hoc test was performed and * represents a significant difference between time matched Sham and Den muscle.

D. Basal (State 4) and active (State 3) reactive oxygen species emission (ROS) in isolated subsarcolemmal (SS) and intermyofibrillar (IMF) mitochondria. Data are represented as Den/Sham (SS State 4; 1/3/7 days, N=7/7/6), (SS State 3; 1/3/7 days, N=7/7/6), (IMF State 4; 1/3/7, N=6), (IMF State 3; 1/3/7, N=6). A Two-Way ANOVA was performed on saline-data, # represents a time effect, † represents a denervation effect, and ¶ represents an interaction effect at $p<0.05$. A Fisher LSD post-hoc test was performed and * represents a significant difference between time matched Sham and Den muscle.

E. H_2O_2 emission in 1 day sham and denervated permeabilized muscle fibers following titration of Pyruvate/Malate (+Pyr/Mal), ADP (+ADP), and Succinate (+Succ) (n=6). A Student's paired t-test was performed for raw time-matched Sham vs Den values, $*p<0.05$.

Figure 3. Autophagic protein expression and flux over the course of denervation.

A. Western blot images for autophagy protein targets in 1, 3- and 7-day Sham and denervated TA muscle. GAPDH was used as a loading control.

B. Quantification of Beclin1, Atg-7 and p62 in Sham and Den TA muscle. Data are represented as Den/Sham (Beclin-1; 1/3/7 days, N=11), (Atg-7; 1/3/7 days, N=10), (p62; 1/3/7 days, N=7/7/10).

A Two-Way ANOVA was performed on saline-data, # represents a time effect, † represents a denervation effect, and ¶ represents an interaction effect at $p<0.05$. A Fisher LSD post-hoc test was performed and * represents a significant difference between time matched Sham and Den muscle.

C. Western blot images for the autophagy protein LC3-II in 1, 3- and 7-day Sham and Den TA muscle from saline and colchicine treated animals. Aciculin was used as a loading control.

D. Quantification of LC3-I, LC3-II, LC3-II/I and Total LC3 in Sham and Den TA muscle from saline treated animals. Data are represented as Den/Sham (All Markers; 1/3/7 days, N=10/10/14). A Two-Way ANOVA was performed on saline-data, # represents a time effect, † represents a denervation effect, and ¶ represents an interaction effect at $p<0.05$. A Fisher LSD post-hoc test was performed and * represents a significant difference between time matched Sham and Den muscle.

E. Quantification of LC3-II autophagy flux in Sham and Den TA muscle from sham and denervated animals (1/3/7 days, N=7/7/11). A Two-Way ANOVA was performed, # represents a time effect, and ¶ represents an interaction effect at $p<0.05$. A Fisher LSD post-hoc test was performed and * represents a significant difference between time matched Sham and Den muscle.

F. Fold mRNA change in *p62* and *lc3*. Data are represented as 2^{-DDCT} (All Markers; 1/3/7 days, N=5). A Two-Way ANOVA was performed on saline-data, # represents a time effect, † represents a denervation effect, and ¶ represents an interaction effect at $p<0.05$. A Fisher LSD post-hoc test was performed and * represents a significant difference between time matched Sham and Den muscle.

Figure 4. Mitophagy flux in subsarcolemmal and intermyofibrillar mitochondria over the course of denervation.

A. Western blot images for LC3-II in isolated subsarcolemmal (SS) mitochondria in 1, 3- and 7-day sham and denervated TA muscle from saline and colchicine treated animals.

B. Quantification of LC3-II protein in isolated SS mitochondria. Raw values are represented (Saline; 1/3/7-day, N=7/7/7) (Colchicine; 1/3/7 Day, N=7/7/6). A three-way ANOVA was performed for raw data to test for independent and combined effects of colchicine, denervation and time (see statistical summary for details). A Two-Way ANOVA was performed on saline-data, # represents a time effect, † represents a denervation effect, and ¶ represents an interaction effect at $p<0.05$. * represents a significant difference between time matched Sham and Den muscle.

C. Quantification of LC3-II mitophagy flux in SS mitochondria from sham and denervated animals (1/3/7 days, N=7/7/7). A Two-Way ANOVA was performed, # represents a time effect, † represents a denervation effect, and ¶ represents an interaction effect at $p<0.05$. A Fisher LSD post-hoc test was performed, and ∗ represents a significant difference between time matched Sham and Den muscle.

D. Western blot images for LC3-II in isolated intermyofibrillar (IMF) mitochondria in 1, 3- and 7-day sham and denervated TA muscle from saline and colchicine treated animals.

E. Quantification of LC3-II protein in isolated IMF mitochondria. Raw values are represented (Saline; 1/3/7-day, N=6/6/7) (Colchicine; 1/3/7 Day, N=6/6/6). A three-way ANOVA was performed for raw data to test for independent and combined effects of colchicine, denervation and time (see statistical summary for details). A Two-Way ANOVA was performed on saline-data,

represents a time effect, † represents a denervation effect, and ¶ represents an interaction effect at $p<0.05$. * represents a significant difference between time matched Sham and Den muscle.

F. Quantification of LC3-II mitophagy flux in IMF mitochondria from sham and denervated animals (1/3/7 days, N=7/7/7). A Two-Way ANOVA was performed, # represents a time effect, † represents a denervation effect, and ¶ represents an interaction effect at $p<0.05$. A Fisher LSD post-hoc test was performed, and * represents a significant difference between time matched Sham and Den muscle.

Figure 5. Mitophagy flux following 1 day of denervation in mt-keima mice.

A. Representative mt-keima images for sham-operated and 1-day denervated TA muscle.

B. Mitophagy index as calculated by red:green fluorescence. Each data point represents the quantification from one image taken with a 20x objective from a region within the TA muscle. 4 biological replicates were used, and 8 images were taken per replicate (n=32). A student's unpaired t-test was performed for raw time matched Sham vs Den values, * represents a significant effect at $p<0.05$.

Figure 6. Lysosome protein expression and TFEB localization over the course of denervation.

A. Western blot images for lysosomal protein targets in 1, 3- and 7-day sham and denervated TA muscle.

B. Quantification of Lamp1, Lamp2, and v-ATPase in Sham and Den TA muscle. Data are represented as Den/Sham (Lamp1; 1/3/7 days, N=5), (Lamp2; 1/3/7 days, N=7), (v-ATPase; 1/3/7 days, N=6). A Two-Way ANOVA was performed on saline-data, # represents a time effect, † represents a denervation effect, and ¶ represents an interaction effect at $p<0.05$. A Fisher LSD

post-hoc test was performed and * represents a significant difference between time matched Sham and Den muscle.

C. Western blot images of the autophagy lysosome transcription factors TFEB and TEF3 in 1, 3- and 7-day sham and denervated TA muscle.

D. Quantification of TFEB and TFE3 in Sham and Den TA muscle. Data are represented as Den/Con (TFEB; 1/3/7 days, N=9), (TFE3; 1/3/7 days, N=7). A one-way ANOVA was performed, # represents a time effect at $p<0.05$. A Two-Way ANOVA was performed on saline-data, # represents a time effect, † represents a denervation effect, and ¶ represents an interaction effect at $p<0.05$. A Fisher LSD post-hoc test was performed and * represents a significant difference between time matched Sham and Den muscle.

E. Western blot images of TFEB in nuclear and cytosolic fractions of TA muscle following 1 day of denervation.

F. Nuclear TFEB Protein in sham and 1-day denervated TA muscle. Data are represented as a % of total TFEB protein. A student's paired t-test was performed.

Figure 7. Vacuolar inclusions in saline injected animals following 7-day of sham-operation or denervation TA muscle.

A. Represented TEM images from each group. The presence of inclusions is denoted by the white arrowhead.

B. Quantification of the area of inclusions in each group. Each data point represents the quantification from one image at 9600x magnification from a region within a myofibril. 3 biological replicates were used, and 3 myofibrils were imaged per replicate (n=9). A student's

unpaired t-test was performed for raw time matched Sham vs Den values, * represents a significant effect at $p<0.05$.

C. Quantification of the number of inclusions in each group. For the saline groups, 3 biological replicates were used, and 3 myofibrils were imaged per replicate (n=9). A student's unpaired t-test was performed for raw time matched Sham vs Den values, * represents a significant effect at $p<0.05$.

Figure 8. Summary of the temporal changes that occur with denervation.

Surgical nerve transection leads to time-dependent changes in mitochondrial, autophagic, and lysosomal homeostasis. At the early stages of denervation-atrophy, mitochondrial function is reduced, concomitant with an upregulation in auto/mitophagy flux. No changes in mitochondrial or lysosome content are apparent. At the intermediate stages of denervation, mitochondrial function is greater, and auto/mitophagy flux are enhanced further. The onset of enhancement in lysosome content is apparent. No changes in mitochondrial content are yet detected. When denervation is prolonged, deficits in mitochondrial content and function are observed. Auto/mitophagy flux are reduced, and lysosome protein levels are further upregulated. Arrow direction denotes up or down regulation; arrow thickness denotes relative extent of the change; "=" denotes unchanged values; "?" denotes unknown.

Tables:

Table 1: List of forward and reverse primers.

	Forward Primer	**Reverse Primer**
p62	5'-GATAAGAGTGGTACTCAGCCAA -3'	5'-GTTATCCGACTCCATCAGTT-3'
lc3	5'-GCACAGCATGGTGAGTGTAT-3'	5'-AGGTTTCTTGGGAGGCATAGA-3'
Gapdh	5'-CTCTCTGCTCCTCCCTGTTCT-3'	5'-GGTAACCAGGCGTCCGATAC-3'
S12	5'-ATGGACGTCAACACTGCTCT-3'	5'-ATGCAAGCACGCAGAGAT-3'

Table 2: List of antibodies.

Antibody	**Manufacturer**	**Product #**	**Lot #**	**Primary Dilution**	**Exposure Time (min)**
COX-I	Abcam	Ab1405	GR3338268-8	1:1000	3
COX-IV	Abcam	Ab14744	GR3319143-9	1:1000	1
UCQRC2	Abcam	Ab14745	GR3216455-3	1:1000	1
Citrate Synthase	Abcam	Ab96600	GR3183619-6	1:1000	1
Beclin 1	Cell Signaling	3738	3	1:1000	3
Atg-7	Sigma	A2856	078M4843V	1:1000	3
p62	Abcam	Ab56416	GR3285986-1	1:2500	2
LC3-I/II	Cell Signaling	4108	3	1:1000	5
VDAC	Abcam	Ab14734	GR3391163-2	1:3000	1
Lamp1	Abcam	Ab24170	GR3235632-1	1:1000	5
Lamp2	Abcam	Ab13524	GR228675-1	1:1000	5
V-ATPase B1/2	SantaCruz	sc-55544	I1018	1:1000	3
TFEB	Bethyl	A303-673A	7	1:1000	7
TFE3	Sigma	HPA023881	000010514	1:500	7
GAPDH	Abacm	ab8254	GR3317834-1	1:100,000	0.5
Aciculin	Gift			1:5000	1
a-tubulin	Calbiochem	CP06	D00175772	1:5000	1
H2B	Cell Signaling	2934	4	1:500	5

Figures:

Figure 1:

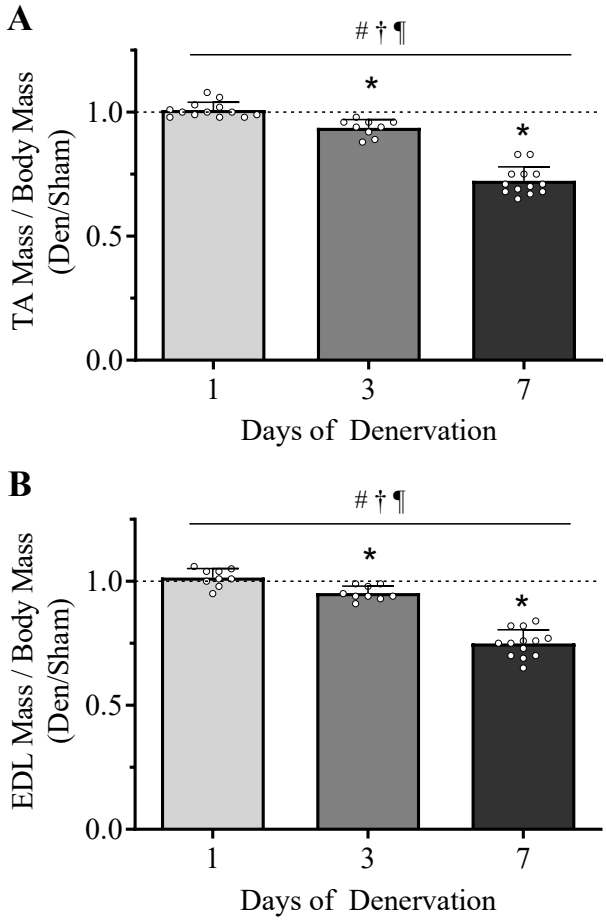

Figure 2:

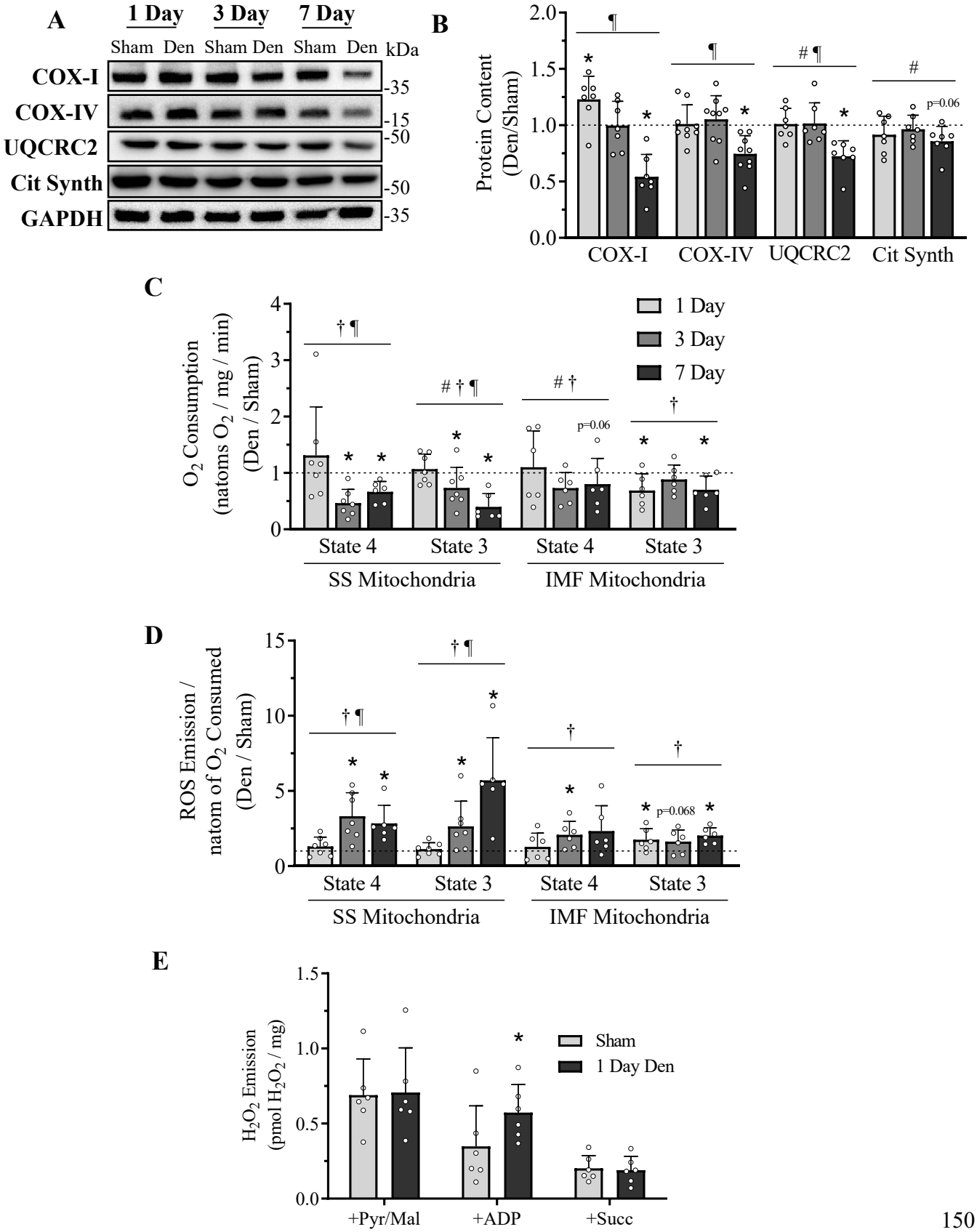
A
1 Day
3 Day
7 Day
Sham Den Sham Den Sham Den kDa
COX-I
COX-IV
UQCRC2
Cit Synth
GAPDH
-35
-15
-50
-50
-35
B
Protein Content (Den/Sham)
COX-I
COX-IV
UQCRC2
Cit Synth
p=0.06
C
O2 Consumption (natoms O2 / mg / min) (Den / Sham)
1 Day
3 Day
7 Day
State 4
State 3
State 4
State 3
SS Mitochondria
IMF Mitochondria
p=0.06
D
ROS Emission / natom of O2 Consumed (Den / Sham)
State 4
State 3
State 4
State 3
SS Mitochondria
IMF Mitochondria
p=0.068
E
H2O2 Emission (pmol H2O2 / mg)
Sham
1 Day Den
+Pyr/Mal
+ADP
+Succ

Figure 3:

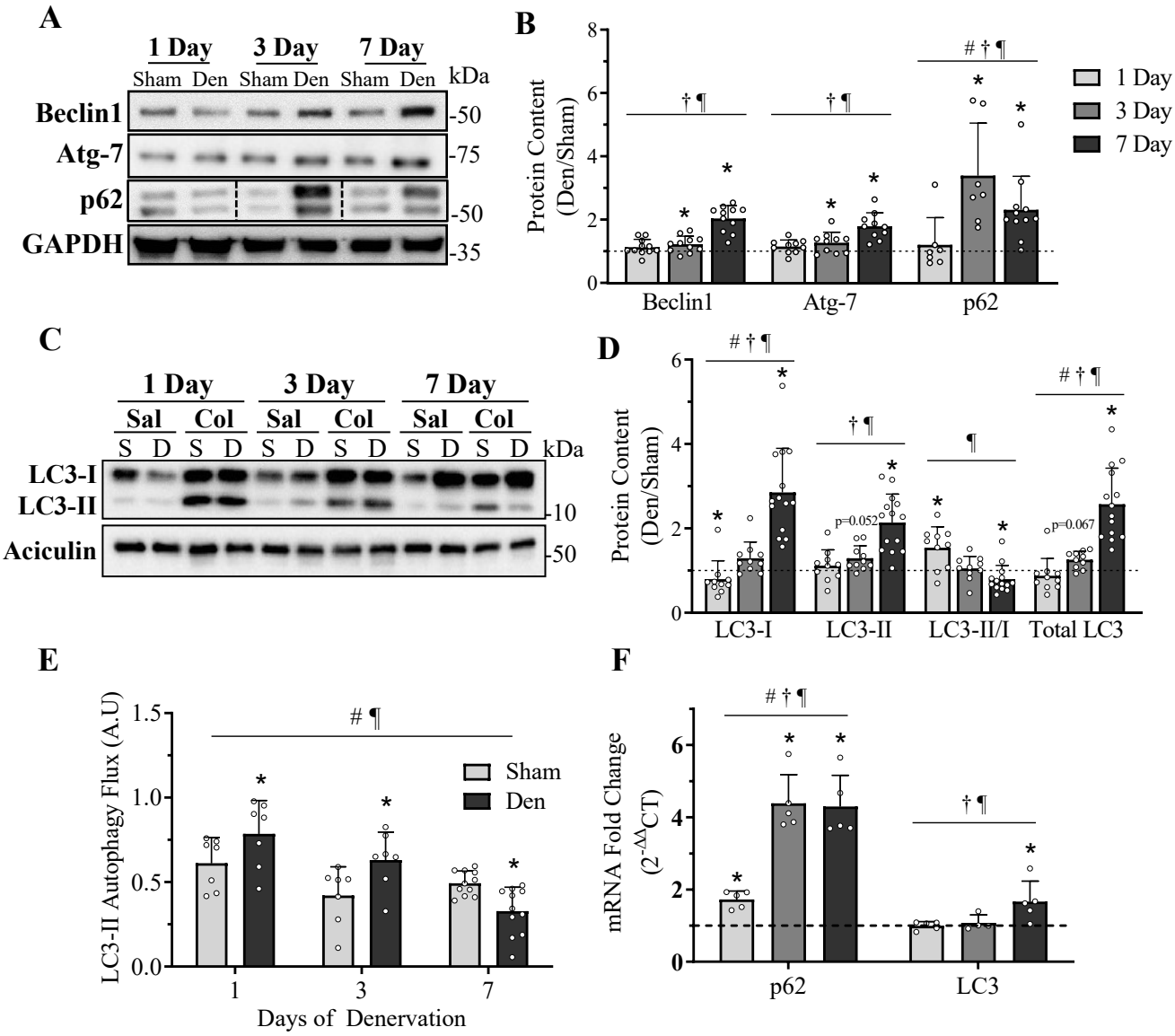
A
1 Day
3 Day
7 Day
Sham Den Sham Den Sham Den kDa
Beclin1
Atg-7
p62
GAPDH
-50
-75
-50
-35
B
Protein Content (Den/Sham)
1 Day
3 Day
7 Day
Beclin1
Atg-7
p62
C
1 Day
3 Day
7 Day
Sal Col Sal Col Sal Col
S D S D S D S D S D S D kDa
LC3-I
LC3-II
Aciculin
-10
-50
D
Protein Content (Den/Sham)
p=0.052
p=0.067
LC3-I
LC3-II
LC3-II/I
Total LC3
E
LC3-II Autophagy Flux (A.U)
Sham
Den
Days of Denervation
F
mRNA Fold Change (2^-ΔΔCT)
p62
LC3

Figure 4:

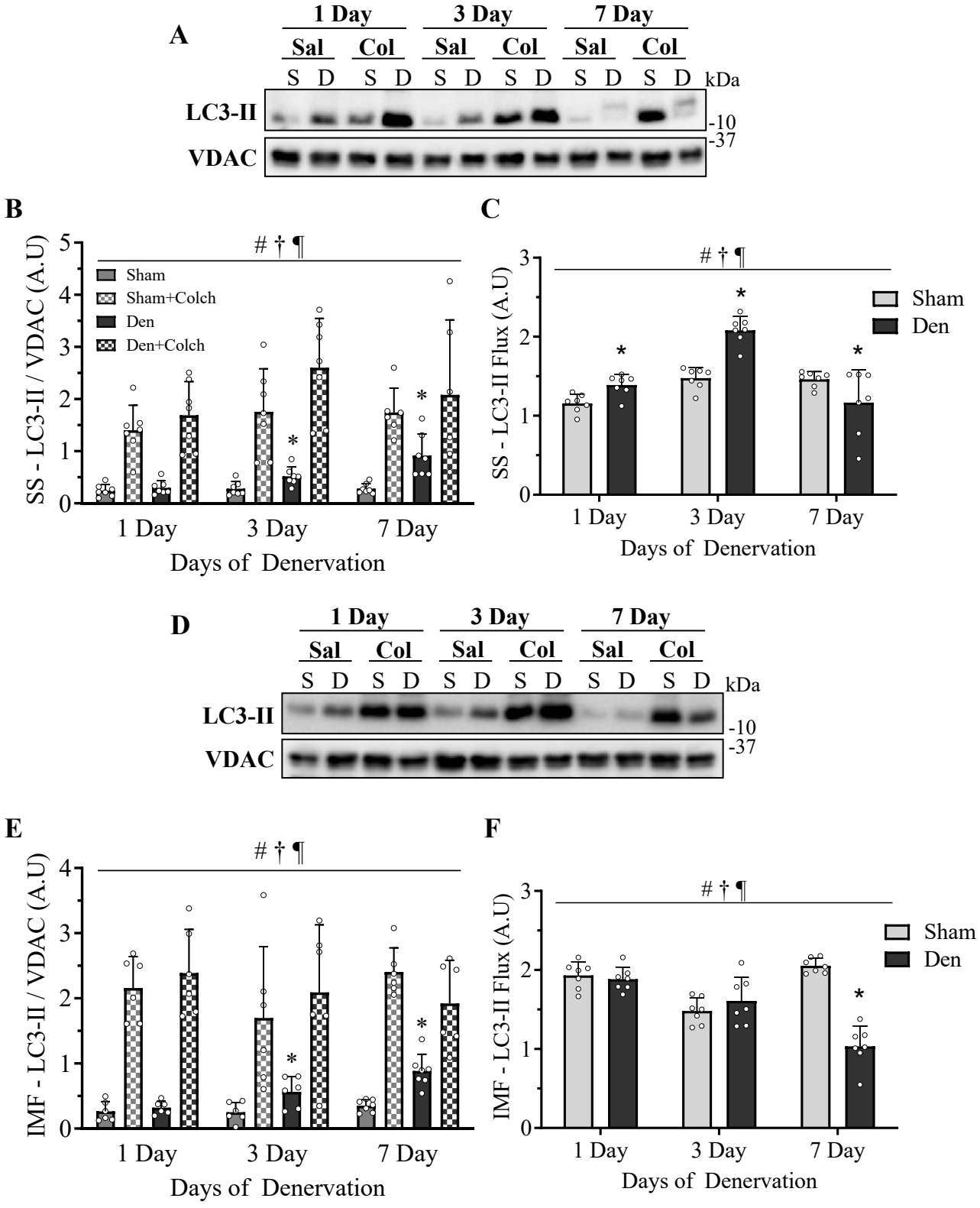
A
1 Day
3 Day
7 Day
Sal
Col
S D
kDa
LC3-II
VDAC
-10
-37
B
SS - LC3-II / VDAC (A.U)
Sham
Sham+Colch
Den
Den+Colch
Days of Denervation
C
SS - LC3-II Flux (A.U)
Sham
Den
D
E
IMF - LC3-II / VDAC (A.U)
F
IMF - LC3-II Flux (A.U)

Figure 5:

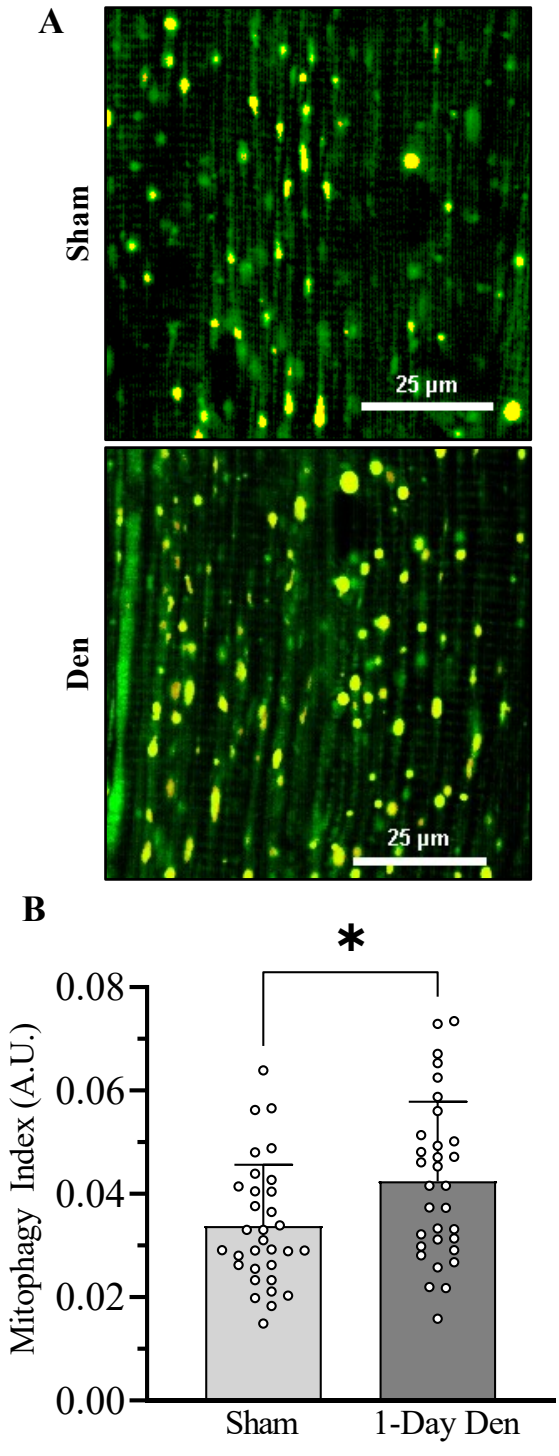
A
Sham
25 µm
Den
25 µm
B
*
Mitophagy Index (A.U.)
0.08
0.06
0.04
0.02
0.00
Sham
1-Day Den

Figure 6:

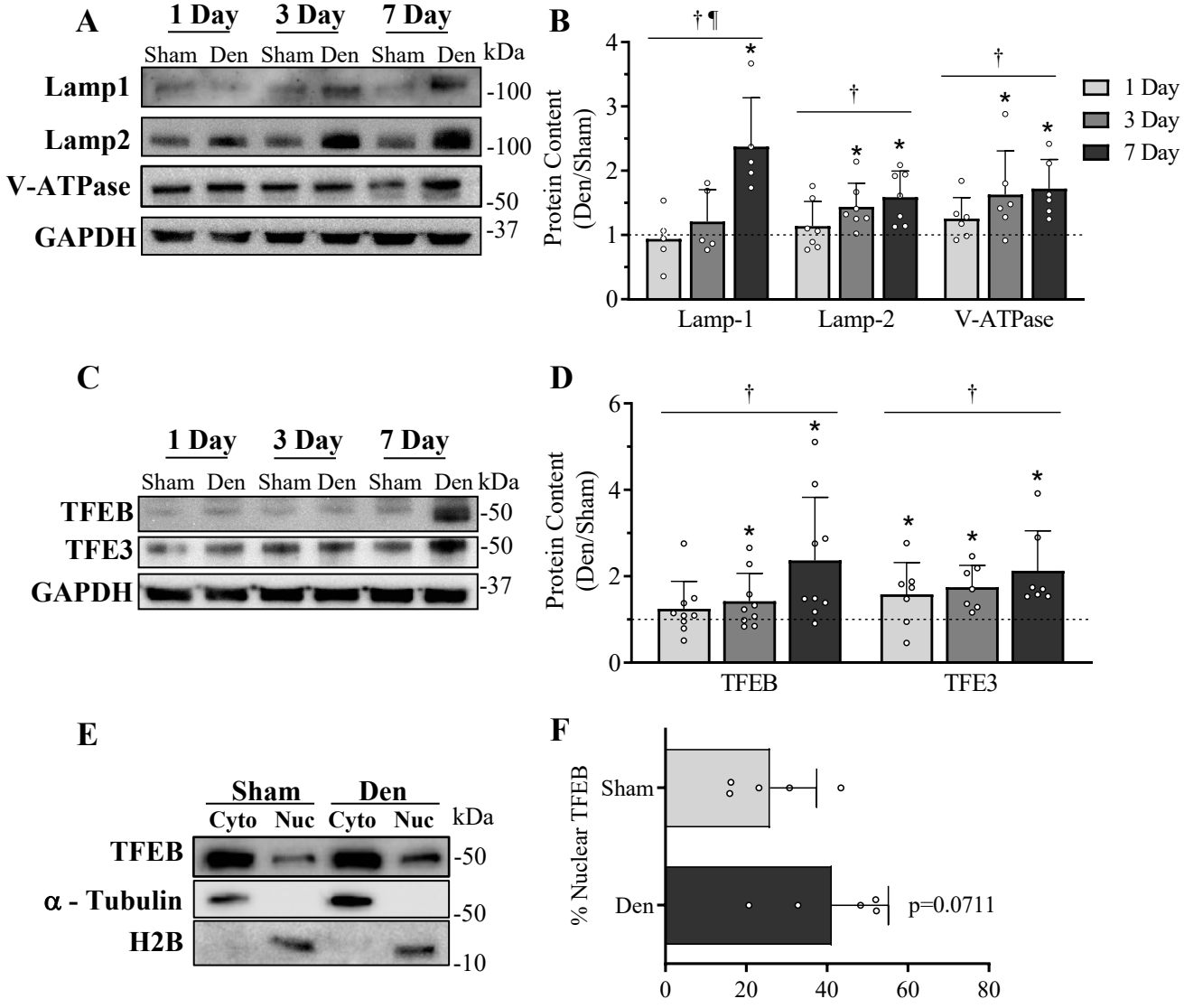
A
1 Day
3 Day
7 Day
Sham Den Sham Den Sham Den kDa
Lamp1
Lamp2
V-ATPase
GAPDH
-100
-100
-50
-37
B
† ¶
†
†
Protein Content (Den/Sham)
1 Day
3 Day
7 Day
Lamp-1
Lamp-2
V-ATPase
C
1 Day
3 Day
7 Day
Sham Den Sham Den Sham Den kDa
TFEB
TFE3
GAPDH
-50
-50
-37
D
†
†
Protein Content (Den/Sham)
TFEB
TFE3
E
Sham
Den
Cyto Nuc Cyto Nuc kDa
TFEB
α - Tubulin
H2B
-50
-50
-10
F
% Nuclear TFEB
Sham
Den
p=0.0711

Figure 7:

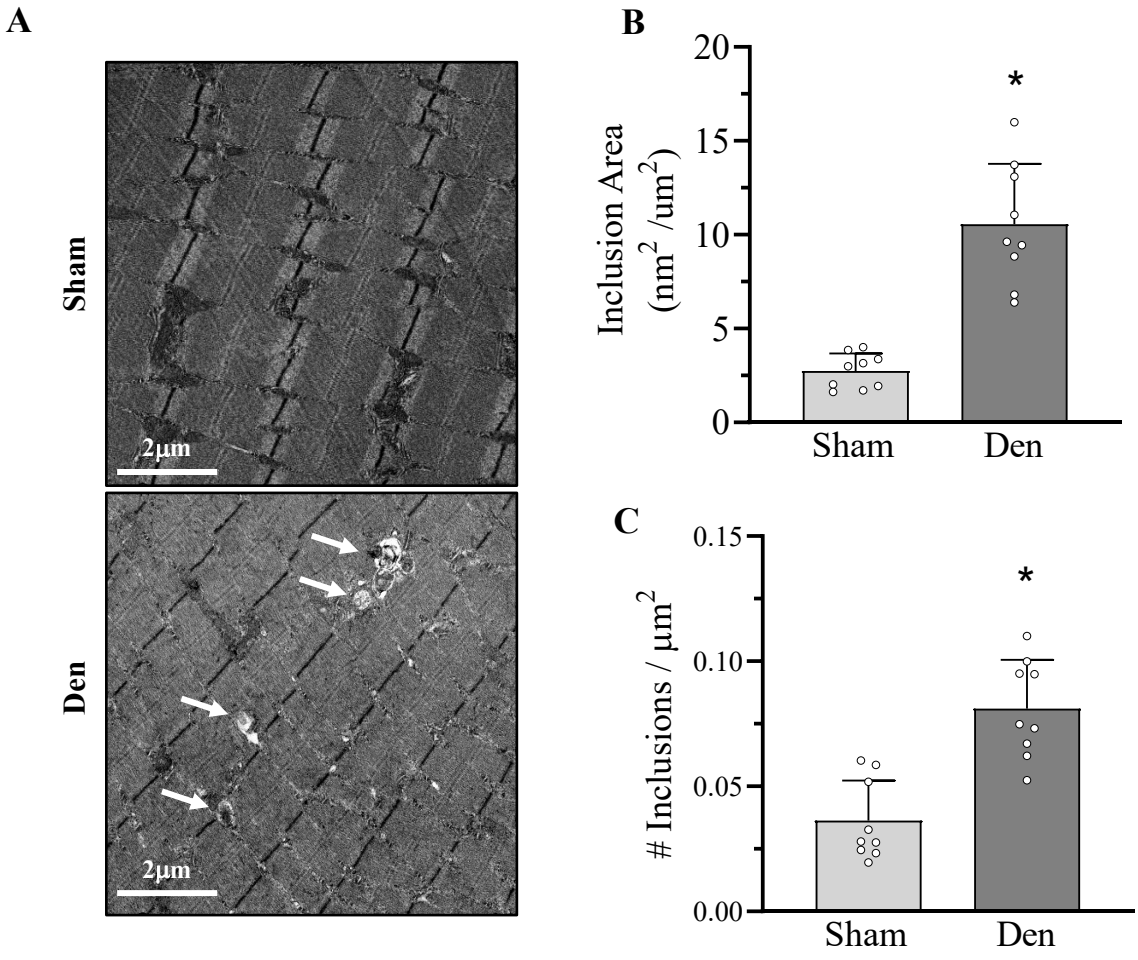
A
Sham
2μm
Den
2μm
B
Inclusion Area
(nm2 /um2)
20
15
10
5
0
*
Sham
Den
C
Inclusions / μm2
0.15
0.10
0.05
0.00
*
Sham
Den

Figure 8:

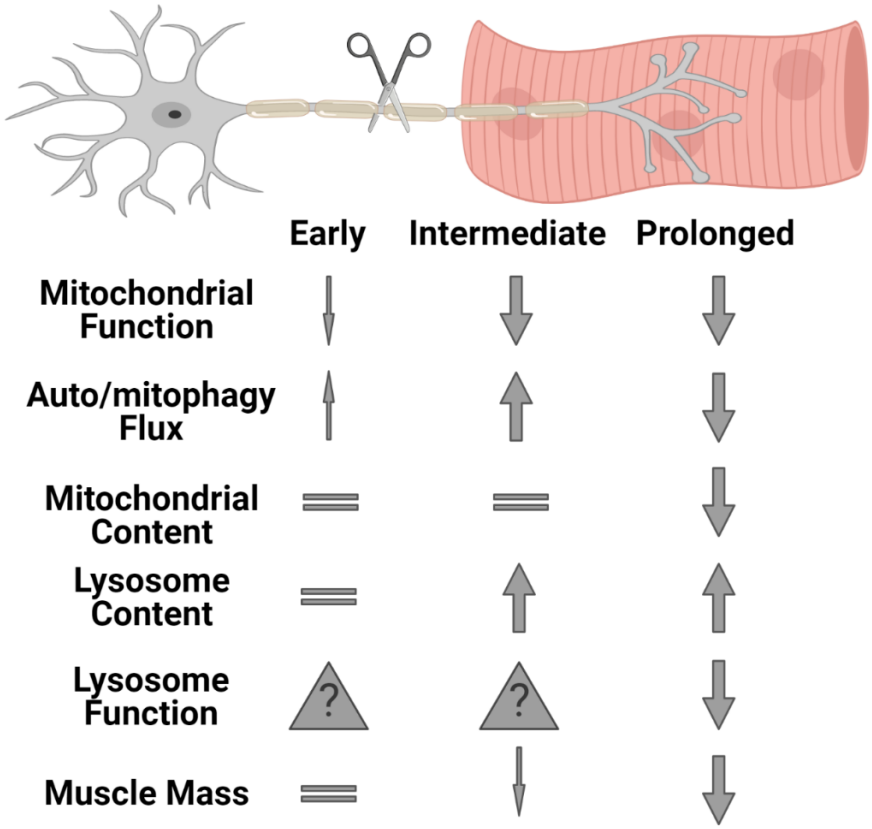
Early
Intermediate
Prolonged
Mitochondrial Function
Auto/mitophagy Flux
Mitochondrial Content
Lysosome Content
Lysosome Function
?
?
Muscle Mass

References:

1. **Hood DA**, **Tryon LD**, **Carter HN**, **Kim Y**, **Chen CCW**. Unravelling the mechanisms regulating muscle mitochondrial biogenesis. *Biochem J* 473: 2295–2314, 2016. doi: 10.1042/BCJ20160009.

2. **Hood DA**, **Memme JM**, **Oliveira AN**, **Triolo M**. Maintenance of skeletal muscle mitochondria in health, exercise, and aging. *Annual Review of Physiology* 81: 19–41, 2019. doi: 10.1146/annurev-physiol-020518-114310.

3. **Ashrafi G**, **Schwarz TL**. The pathways of mitophagy for quality control and clearance of mitochondria. *Cell Death and Differentiation* 20: 31–42, 2013. doi: 10.1038/cdd.2012.81.

4. **Triolo M**, **Hood DA**. Mitochondrial breakdown in skeletal muscle and the emerging role of the lysosomes. *Archives of Biochemistry and Biophysics* 661: 66–73, 2019. doi: 10.1016/j.abb.2018.11.004.

5. **Furuya N**, **Ikeda S-I**, **Sato S**, **Soma S**, **Ezaki J**, **Oliva Trejo JA**, **Takeda-Ezaki M**, **Fujimura T**, **Arikawa-Hirasawa E**, **Tada N**, **Komatsu M**, **Tanaka K**, **Kominami E**, **Hattori N**, **Ueno T**. PARK2/Parkin-mediated mitochondrial clearance contributes to proteasome activation during slow-twitch muscle atrophy via NFE2L1 nuclear translocation. *Autophagy* 10: 631–41, 2014. doi: 10.4161/auto.27785.

6. **Romanello V**, **Guadagnin E**, **Gomes L**, **Roder I**, **Sandri C**, **Petersen Y**, **Milan G**, **Masiero E**, **Del Piccolo P**, **Foretz M**, **Scorrano L**, **Rudolf R**, **Sandri M**. Mitochondrial fission and remodelling contributes to muscle atrophy. *The EMBO journal* 29: 1774–1785, 2010. doi: 10.1038/emboj.2010.60.

7. **Ogata T**, **Yamasaki Y**. Scanning electron-microscopic studies on the three-dimensional structure of mitochondria in the mammalian red, white and intermediate muscle fibers. *Cell and Tissue Research* 241: 251–256, 1985. doi: 10.1007/BF00217168.

8. **Picard M**, **White K**, **Turnbull DM**. Mitochondrial morphology, topology, and membrane interactions in skeletal muscle: a quantitative three-dimensional electron microscopy study. *Journal of Applied Physiology* 114: 161–171, 2013. doi: 10.1152/japplphysiol.01096.2012.

9. **Kirkwood SP**, **Munn EA**, **Brooks GA**. Mitochondrial reticulum in limb skeletal muscle. *The American Journal of Physiology - Cell Physiology* 251: C395-402, 1986. doi: 10.1152/ajpcell.1986.251.3.C395.

10. **Cogswell AM**, **Stevens RJ**, **Hood DA**. Properties of skeletal muscle mitochondria from subsarcolemmal and intermyofibrillar isolated regions. *The American Journal of Physiology - Cell Physiology* 264: C383-389, 1993. doi: 10.1152/ajpcell.1993.264.2.C383.

11. **Hoppeler H**. Exercise-induced ultrastructural changes in skeletal muscle. *International Journal of Sports Medicine* 07: 187–204, 1986. doi: 10.1055/s-2008-1025758.

12. **Krieger DA**, **Tate CA**, **McMillin-Wood J**, **Booth FW**. Populations of rat skeletal muscle mitochondria after exercise and immobilization. *Journal of applied physiology: respiratory, environmental and exercise physiology* 48: 23–8, 1980. doi: 10.1152/jappl.1980.48.1.23.

13. **Reichmann H**, **Hoppeler H**, **Mathieu-Costello O**, **von Bergen F**, **Pette D**. Biochemical and ultrastructural changes of skeletal muscle mitochondria after chronic electrical stimulation in rabbits. *Pflügers Archiv* 404: 1–9, 1985. doi: 10.1007/BF00581484.

14. **Bizeau ME**, **Willis WT**, **Hazel JR**. Differential responses to endurance training in subsarcolemmal and intermyofibrillar mitochondria. *Journal of Applied Physiology* 85: 1279–1284, 1998. doi: 10.1152/jappl.1998.85.4.1279.

15. **Knight JA**. Physical inactivity: associated diseases and disorders. *Annals of clinical and laboratory science* 42: 320–37, 2012.

16. **Bogdanis GC**. Effects of physical activity and inactivity on muscle fatigue. *Frontiers in physiology* 3: 142, 2012. doi: 10.3389/fphys.2012.00142.

17. **Bodine SC**. Disuse-induced muscle wasting. *The Iternational Journal of Biochemistry & Cell Biology* 45: 2200–8, 2013. doi: 10.1016/j.biocel.2013.06.011.

18. **Powers SK**, **Ozdemir M**, **Hyatt H**. Redox Control of Proteolysis During Inactivity-Induced Skeletal Muscle Atrophy. *Antioxidants & Redox Signaling* 33: 559–569, 2020. doi: 10.1089/ars.2019.8000.

19. **Powers SK**, **Wiggs MP**, **Duarte JA**, **Zergeroglu AM**, **Demirel HA**. Mitochondrial signaling contributes to disuse muscle atrophy. *American journal of physiology Endocrinology and metabolism* 303: E31-9, 2012. doi: 10.1152/ajpendo.00609.2011.

20. **Tryon LD**, **Crilly MJ**, **Hood DA**. Effect of denervation on the regulation of mitochondrial transcription factor A expression in skeletal muscle. *American Journal of Physiology Cell Physiology* 309: C228--38, 2015.

21. **Singh K**, **Hood DA**. Effect of denervation-induced muscle disuse on mitochondrial protein import. *American Journal of Physiology - Cell Physiology* 300: C138–C145, 2011. doi: 10.1152/ajpcell.00181.2010.

22. **Tryon LD**, **Vainshtein A**, **Memme JM**, **Crilly MJ**, **Hood DA**. Recent advances in mitochondrial turnover during chronic muscle disuse. *Integrative Medicine Research* 3: 161–171, 2014. doi: 10.1016/j.imr.2014.09.001.

23. **Carter HN**, **Pauly M**, **Tryon LD**, **Hood DA**. Effect of contractile activity on PGC-1 transcription in young and aged skeletal muscle. *Journal of Applied Physiology* 124: 1605–1615, 2018. doi: 10.1152/japplphysiol.01110.2017.

24. **Iqbal S**, **Ostojic O**, **Singh K**, **Joseph A-M**, **Hood DA**. Expression of mitochondrial fission and fusion regulatory proteins in skeletal muscle during chronic use and disuse. *Muscle & Nerve* 48: 963–970, 2013. doi: 10.1002/mus.23838.

25. **O'Leary MF**, **Vainshtein A**, **Iqbal S**, **Ostojic O**, **Hood DA**. Adaptive plasticity of autophagic proteins to denervation in aging skeletal muscle. *American Journal of Physiology-Cell Physiology* 304: C422–C430, 2013. doi: 10.1152/ajpcell.00240.2012.

26. **Ljubicic V**, **Joseph A-M**, **Adhihetty PJ**, **Huang JH**, **Saleem A**, **Uguccioni G**, **Hood DA**. Molecular basis for an attenuated mitochondrial adaptive plasticity in aged skeletal muscle. *Aging* 1: 818–830, 2009.

27. **Carter HN**, **Kim Y**, **Erlich AT**, **Zarrin-khat D**, **Hood DA**. Autophagy and mitophagy flux in young and aged skeletal muscle following chronic contractile activity. *Journal of Physiology* 596: 3568–3584, 2018. doi: 10.1113/JP275998.

28. **Kang C**, **Yeo D**, **Ji LL**. Muscle immobilization activates mitophagy and disrupts mitochondrial dynamics in mice. *Acta Physiologica* 218: 188–197, 2016. doi: 10.1111/apha.12690.

29. **Malicdan MC V.**, **Nishino I**. Autophagy in Lysosomal Myopathies. *Brain Pathology* 22: 82–88, 2012. doi: 10.1111/j.1750-3639.2011.00543.x.

30. **Malicdan MC**, **Noguchi S**, **Nonaka I**, **Saftig P**, **Nishino I**. Lysosomal myopathies: An excessive build-up in autophagosomes is too much to handle. *Neuromuscular Disorders* 18: 521–529, 2008. doi: 10.1016/J.NMD.2008.04.010.

31. **Martina JA**, **Diab HI**, **Li H**, **Puertollano R**. Novel roles for the MiTF/TFE family of transcription factors in organelle biogenesis, nutrient sensing, and energy homeostasis. *Cellular and Molecular Life Sciences* 71: 2483–97, 2014. doi: 10.1007/s00018-014-1565-8.

32. **Ploper D**, **de Robertis EM**. The MITF family of transcription factors: Role in endolysosomal biogenesis, Wnt signaling, and oncogenesis. *Pharmacological Research* 99: 36–43, 2015. doi: 10.1016/J.PHRS.2015.04.006.

33. **Sardiello M**, **Palmieri M**, **di Ronza A**, **Medina DL**, **Valenza M**, **Gennarino VA**, **Di Malta C**, **Donaudy F**, **Embrione V**, **Polishchuk RS**, **Banfi S**, **Parenti G**, **Cattaneo E**, **Ballabio A**. A gene network regulating lysosomal biogenesis and function. *Science (New York, NY)* 325: 473–7, 2009. doi: 10.1126/science.1174447.

34. **Settembre C**, **di Malta C**, **Polito VA**, **Garcia Arencibia M**, **Vetrini F**, **Erdin S**, **Erdin SU**, **Huynh T**, **Medina D**, **Colella P**, **Sardiello M**, **Rubinsztein DC**, **Ballabio A**. TFEB links autophagy to lysosomal biogenesis. *Science (New York, NY)* 332: 1429–33, 2011. doi: 10.1126/science.1204592.

35. **Vainshtein A**, **Desjardins EM**, **Armani A**, **Sandri M**, **Hood DA**. PGC-1α modulates denervation-induced mitophagy in skeletal muscle. *Skeletal Muscle* 5: 9, 2015. doi: 10.1186/s13395-015-0033-y.

36. **Ju J-S**, **Varadhachary AS**, **Miller SE**, **Weihl CC**. Quantitation of autophagic flux in mature skeletal muscle. *Autophagy* 6: 929–35, 2010. doi: 10.4161/auto.6.7.12785.

37. **Adhihetty PJ**, **Ljubicic V**, **Hood DA**. Effect of chronic contractile activity on SS and IMF mitochondrial apoptotic susceptibility in skeletal muscle. *American Journal of Physiology - Endocrinology and Metabolism* 292: 748–755, 2007. doi: 10.1152/ajpendo.00311.2006.

38. **Takahashi M**, **Hood DA**. Protein import into subsarcolemmal and intermyofibrillar skeletal muscle mitochondria. Differential import regulation in distinct subcellular regions. *The Journal of biological chemistry* 271: 27285–27291, 1996.

39. **Perry CGR**, **Kane DA**, **Lin C Te**, **Kozy R**, **Cathey BL**, **Lark DS**, **Kane CL**, **Brophy PM**, **Gavin TP**, **Anderson EJ**, **Neufer PD**. Inhibiting myosin-ATPase reveals a dynamic range of mitochondrial respiratory control in skeletal muscle. *Biochemical Journal* 437: 215–222, 2011. doi: 10.1042/BJ20110366.

40. **Sun N**, **Yun J**, **Liu J**, **Malide D**, **Liu C**, **Rovira II**, **Holmström KM**, **Fergusson MM**, **Yoo YH**, **Combs CA**, **Finkel T**. Measuring in vivo mitophagy. *Molecular Cell* 60: 685–696, 2015. doi: 10.1016/j.molcel.2015.10.009.

41. **Sun N**, **Malide D**, **Liu J**, **Rovira II**, **Combs CA**, **Finkel T**. A fluorescence-based imaging method to measure in vitro and in vivo mitophagy using mt-Keima. *Nature Protocols* 12: 1576–1587, 2017. doi: 10.1038/nprot.2017.060.

42. **Wicks KL**, **Hood DA**. Mitochondrial adaptations in denervated muscle: relationship to muscle performance. *American Journal of Physiology - Cell Physiology* 260: C841–C850, 1991.

43. **Park KHJ**. Mechanisms of muscle denervation in aging: Insights from a Mouse Model of Amyotrophic Lateral Sclerosis. *Aging and Disease* 6 International Society on Aging and Disease: 380–389, 2015.

44. **Jang YC**, **Van Remmen H**. Age-associated alterations of the neuromuscular junction. *Experimental Gerontology* 46 NIH Public Access: 193–198, 2011.

45. **Adhihetty PJ**, **O'Leary MFN**, **Chabi B**, **Wicks KL**, **Hood DA**. Effect of denervation on mitochondrially mediated apoptosis in skeletal muscle. *Journal of applied physiology (Bethesda, Md : 1985)* 102: 1143–1151, 2007. doi: 10.1152/japplphysiol.00768.2006.

46. **Montava-Garriga L**, **Ganley IG**. Outstanding Questions in Mitophagy: What We Do and Do Not Know. *Journal of Molecular Biology* 432 Academic Press: 206–230, 2020.

47. **Yoshii SR**, **Mizushima N**. Monitoring and measuring autophagy. *International Journal of Molecular Sciences* 18: 1865, 2017. doi: 10.3390/ijms18091865.

48. **Lippai M**, **Lőw P**. The Role of the Selective Adaptor p62 and Ubiquitin-Like Proteins in Autophagy. *BioMed Research International* 2014: ., 2014. doi: 10.1155/2014/832704.

49. **Liu WJ**, **Ye L**, **Huang WF**, **Guo LJ**, **Xu ZG**, **Wu HL**, **Yang C**, **Liu HF**. p62 links the autophagy pathway and the ubiqutin-proteasome system upon ubiquitinated protein degradation. *Cellular and Molecular Biology Letters* 21: ., 2016.

50. **O′Leary MFN**, **Vainshtein A**, **Carter HN**, **Zhang Y**, **Hood DA**. Denervation-induced mitochondrial dysfunction and autophagy in skeletal muscle of apoptosis-deficient animals. *American Journal of Physiology-Cell Physiology* 303: C447–C454, 2012. doi: 10.1152/ajpcell.00451.2011.

51. **Klionsky DJ**, **Abdelmohsen K**, **Abe A**, **Abedin MJ**, **Abeliovich H**, **Al E**. Guidelines for the use and interpretation of assays for monitoring autophagy (3rd edition). *Autophagy* 12: 1, 2016. doi: 10.1080/15548627.2015.1100356.

52. **Leermakers PA**, **Kneppers AEM**, **Schols AMWJ**, **Kelders MCJM**, **de Theije CC**, **Verdijk LB**, **van Loon LJC**, **Langen RCJ**, **Gosker HR**. Skeletal muscle unloading results in increased mitophagy and decreased mitochondrial biogenesis regulation. *Muscle and Nerve* 60: 769–778, 2019. doi: 10.1002/mus.26702.

53. **Larsson L**, **Degens H**, **Li M**, **Salviati L**, **Lee Y il**, **Thompson W**, **Kirkland JL**, **Sandri M**. Sarcopenia: Aging-Related Loss of Muscle Mass and Function. *Physiological Reviews* 99: 427, 2019. doi: 10.1152/PHYSREV.00061.2017.

Chapter 5:

The influence of age, sex, and exercise on autophagy, mitophagy and lysosome biogenesis in skeletal muscle

Authors: Matthew Triolo[1,2], Ashley N. Oliveria[1,2], Rita Kumari[1,2], David A. Hood[1,2]

Affiliations: [1] Muscle Health Research Centre, York University, Toronto, Ontario, Canada M3J 1P3

[2] School of Kinesiology and Health Science, York University, Toronto, Ontario, Canada M3J 1P3

Running Title: Regulation of the autophagy lysosome system with age, sex, and exercise

Corresponding Author: David A Hood, PhD
School of Kinesiology and Health Science
Muscle Health Research Centre
York University, Toronto, ON
M3J 1P3, Canada
Tel: (416) 736-2100 ext. 66640
Email: dhood@yorku.ca

Key Words: autophagy, mitophagy, lysosomes, muscle, sex differences, aging, Tfeb

This manuscript has been submitted the journal Skeletal Muscle (November 2021).

Abstract:

Background

Aging decreases skeletal muscle mass and quality. Maintenance of healthy muscle is regulated by a balance between protein and organellar synthesis and their degradation. The autophagy lysosome system is responsible for the selective degradation of protein aggregates and organelles, such as mitochondria (i.e., mitophagy). Little data exist on the independent and combined influence of age, biological sex and exercise on the autophagy system and lysosome biogenesis. The purpose of this study was to characterize sex differences in autophagy and lysosome biogenesis in young and aged muscle, and to determine if acute exercise influences these processes.

Methods

Young (4-6 months) and aged (22-24 months) male and female mice, were assigned to a sedentary, or an acute exercise group. Mitochondrial content, the autophagy-lysosome system and mitophagy were measured via protein analysis. A transcription factor EB (TFEB)-promoter-construct was utilized to examine TFEB transcription, and nuclear-cytosolic fractions allowed us to examine TFEB localization in sedentary and exercised muscle with age and sex.

Results

Our results indicate that female mice, both young and old, had more mitochondrial protein in skeletal muscle than age-matched males, and mitochondrial content was only reduced with age in the male cohort. Although young female mice had a greater abundance of autophagy, mitophagy and lysosome proteins than young males, we measured increases with age irrespective of sex. Interestingly, young sedentary female mice had indices of greater autophagosomal turnover than male counterparts. Exhaustive exercise stimulated autophagic breakdown in young male mice, but

not in the young female mice or aged mice from either sex. Similarly, nuclear TFEB protein was enhanced to a greater extent in young male than in young female mice following exercise, but no changes were observed in aged mice. Finally, TFEB-promoter activity was upregulated following exercise in both young and aged muscle.

Conclusions

The present study demonstrates that biological sex influences mitochondrial homeostasis, the autophagy-lysosome system and mitophagy in skeletal muscle with age. Further, our data suggest that young male mice have a more profound ability to activate these processes with exercise than in the other groups. Ultimately, this may contribute to a greater remodeling of muscle in response to exercise training in males.

Background:

The natural aging process is associated with a progressive loss of muscle mass and function (1, 2), commonly referred to as sarcopenia (3). Since skeletal muscle represents 40% of total body mass and is essential for motor function and whole-body metabolic control (1, 4), these age-related declines are associated with deficits in the quality of life of older individuals, and are related to a higher incidence of falls, hospitalization, and co-morbidities (5). This is problematic when we consider that physical inactivity rates are greater in those that are older, potentiating the negative effects of age on overall health (6–8). It is now known that the maintenance of physical activity throughout the lifespan is an essential preventative measure in age-associated loss in mitochondrial volume and function (9, 10). Thus, there is an evolving need to understand the mechanisms that underly the changes in muscle architecture with age, and how exercise preserves muscle health.

The muscle atrophy observed within aging muscle is achieved by an imbalance protein synthesis and degradation. The autophagy-lysosome system is a proteolytic pathway that is responsible for the breakdown of long-lived, aggregated proteins and organelles (11). Autophagy is an evolutionary conserved recycling mechanism, whereby damaged or dysfunctional cellular components are engulfed in a double membrane autophagosome and delivered to the lysosomes for digestion. Inhibition of autophagy promotes atrophy, neuromuscular junction decay, sarcomere disarrangement and ultimately, weakness (12–16). Further a lack of autophagy attenuates the phenotypic remodeling of muscle associated with exercise training (17–19). Cumulatively, these studies highlight the importance of this proteolytic system in skeletal muscle.

The impact of aging on skeletal muscle autophagy remains controversial (20), but previous reports utilizing “flux” measurements have shown that autophagy is upregulated in aging muscle (21, 22). These alterations in autophagy have implications for the selective degradation of

mitochondria through mitophagy. In fact, in a series of studies, our group has reported enhanced mitophagy in aged muscle (22–24). We have also shown that muscle from aged rodents displayed an accumulation of lysosomal protein and nondegraded lysosomal content, termed lipofuscin (23, 25). This would imply lysosomal dysregulation, which may contribute to a reduced capacity to effectively remove damaged intracellular constituents.

In young, healthy muscle, autophagy and lysosome biogenesis are activated following acute endurance activity (26, 27) to assist in the remodeling of muscle. Over time, aerobic training improves the metabolic capacity of the tissue (28–30), enhancing mitochondrial content concomitant with increases in lysosomal content (31, 32). However, it remains to be seen if these acute-exercise responses occur in aged skeletal muscle, and whether exercise can enhance lysosome capacity to promote the removal of the accumulating damaged constituents.

Recently it was reported that female mice had enhanced catabolic and autophagy signaling in response to hindlimb unloading (33, 34). These findings highlight the importance of examining biological sex as a variable in muscle physiology. Furthermore, a limited analysis on the autophagy-lysosome markers was conducted in aged male and female mice, investigating the impact of prolonged training in these groups. No difference between the sexes was reported. (35). We are unaware of any studies that have examined the influence of biological sex on the autophagy-lysosome system, with a focus on the impact of age and acute exercise.

Thus, the overarching goal of this study was to examine sex differences in autophagic, mitophagic and lysosomal pathways in muscle from young (4-6 mo) and aged (22-24 mo) male and female C57BL6 mice. Based on previous reports (33, 34), we hypothesized that autophagy would be greater in our female cohort. Further, we investigated the utility of acute exercise to

activate these pathways in young and aged muscle, and whether biological sex could influence the exercise response.

Materials and Methods:

Animals

All animal procedures were conducted in accordance with the standards set by the Canadian Council on Animal Care, with the approval of York University Animal Care Committee (YUACC). Young (4-6 months) and aged (22-24 months) male and female C57BL/6 mice were obtained from The Jackson Laboratory. Mice used in this study were ordered at ~2 months old and aged in our facility in accordance with YUACC protocols and guidelines. Food and water were provided *ad libitum*. At the appropriate age, mice were assigned to sedentary or acute exhaustive exercise groups so that the final # of animals/group were n=5/ male; n=4/female groups.

Acute Exhaustive Exercise Protocol

Animals that were assigned to the acute exhaustive exercise group were acclimatized to the treadmill 48 and 24 hours prior to their exercise date. Acclimatization occurred at 0m/minute, 5m/minute and 10m/min for 5 minutes each. On the day of exercise, prior to protocol, resting blood lactate levels were measured via tail blood. Subsequently, animals were placed on the treadmill at a fixed incline of 10%. The acute exhaustive exercise protocol began with a 5m/minute warmup for 5 minutes and a 10m/min run for 10 minutes, followed by increasing speeds at 1m/minute every 2 minutes until exhaustion was achieved. Exhaustion was defined as the inability of the animal to run on the treadmill despite prodding. Immediately following exercise, post-exercise blood lactate measurements were made, animals were cervically dislocated and tissues were harvested for biochemical analysis.

Luciferase Reporter Assay

The TFEB promoter containing -1601 bp region of the canonical promoter was subcloned into a pGL3 vector containing a firefly luciferase reporter (rTfeb-pGL3), under control of the constitutively active CMV promoter, as previously described(27). Ampicillin-resistant bacteria were transformed, and bacterial colonies were then amplified to isolate plasmid DNA using a Maxi Plasmid Isolation Kit (Qiagen). Six days prior to tissue removal, in both the sedentary and exercised groups mice underwent *in vivo* muscle transfection. Briefly, mice were anesthetized using gaseous isoflurane and the lower hindlimbs were shaved and sterilized. One gastrocnemius muscle of each mouse was injected with 30μg of the rTfeb-pGL3 construct and 50ng of renilla luciferase downstream of the CMV promoter (pRL-CMV), used as a marker of transfection efficiency. The contralateral hindlimb was injected with an empty vector (pGL3) and renilla luciferase, both under the control of the CMV promoter. All injections were conducted using a short 29-gage insulin syringe (BD Canada). Immediately after the injection, trans-continuous electrical pulses were applied using an ECM 380 BTX electroporation system (Harvard Apparatus Saint-Laurent, QC, Canada), whereby the muscle were held on either side of the injection site by forceps-style electrodes, followed by ten 100V/cm^2 pulses. Conductive gel was applied to the electrodes to assist with transfection. The anode and cathode orientation were reversed, and another 10 pulses were delivered. Following tissue extraction, frozen gastrocnemius muscle was pulverized to a fine powder at the temperature of liquid nitrogen. Approximately 30mg of powder was diluted in 1X passive lysis buffer (Promega, cat# E1500) supplemented with protease (Roche Mississauga, ON, Canada) and phosphatase (Sigma Oakville, ON, Canada) inhibitors. The sample was then sonicated on ice (3x3seconds) and spun in a microcentrifuge at 4^{o}C for 10 minutes at 16,000g and the supernatant fraction was collected. Using an EG&G Berthold Luminometer

(Lumat LB 7507; Berthold Technologies, Oak Ridge, TN). Following initial background readings of the passive lysis buffer, 20µL of either the rTfeb-PGL3+ pRL-CMV or pGL3+pL-CMV sample tissue were loaded into a test tube and mixed with 100µl of luciferase substrate followed by 100µl of renilla substrate (Promega). Each sample was run in triplicate, and the average was used. The ratio of firefly luciferase reporter (RLU1) to renilla luciferase (RLU2) was taken for both the TFEB-promoter- and the empty vector-injected limbs. Transcriptional activity was expressed as the TFEB promoter data divided by the empty vector.

Mitochondrial Isolations

To isolate intermyofibrillar mitochondrial subfractions, muscles from the animal were pooled (one quadricep, hamstrings from both hindlimbs, triceps from both forelimbs and the pectoralis muscles) adding up to ~400mg. Muscle was minced, homogenized mechanically, and underwent differential centrifugation as previously described(36–38). The final mitochondrial pellets were resuspended in ice-cold buffer (100 mm KCl, 10 mm MOPS, 0.2% BSA). Isolated mitochondria were supplemented with phosphatase inhibitor cocktails as well as protease inhibitors and stored at –80°C for Western blotting procedures.

High Resolution Respiration and ROS-Emission

High-resolution respirometry (Oroboros O2k, Austria) was used to measure oxygen consumption in permeabilized muscle fibers from the lateral portion of the left TA muscle of all mice. Briefly, the muscle was excised, and fibers were mechanically separated in ice cold BIOPS buffer (2.77_{mM} CaK2EGTA, 7.23_{mM} K2EGTA, 7.55_{mM} Na2ATP, 6.56_{mM} MgCl26H2O, 20_{mM} Taurine, 15_{mM} Na2Phosphocreatine, 20_{mM} Imidazole, 0.5_{mM} Dithiothreitol, 50_{mM} MES-Hydrate, pH 7.1). Subsequently, the fibers were permeabilized in BIOPS supplemented with $40_{ug/uL}$ saponin at 4ºC

for 30 minutes with gentle rocking and washed in Buffer-Z (105_{mM} K-MES, 30_{mM} KCl, 10_{mM} KH2PO4, 5_{mM} MgCl2•6H2O, 1_{mM} EGTA, $5_{mg/ml}$ BSA) with gentle rocking. Fibers were then incubated in the chamber with oxygenated Buffer-Z supplemented with 10μM Amplex-Red to simultaneously measure ROS-production, as well as $1_{\mu M}$ Blebbistatin to prevent tetanus of the muscle(39), $25_{U/ml}$ Cu/Zn SOD1 to convert O2- to H2O2 and 2_{mM} EGTA. Following oxygenation and measurement of background values, substrates were added to assess respiration and ROS production simultaneously. Substrates were titrated in three separate protocols as follows. In the first protocol, 5_{mM} glutamate + 2_{mM} malate (Complex I – Basal), 5_{mM} ADP (Complex I – Active), and 10_{mM} succinate (Complex I+II – Active) were added to simultaneously measure O_2 consumption and ROS. In the second protocol, O_2 consumption was measured by first titrating $0.5_{\mu M}$ rotenone, to prevent electron backflow and slip at Complex I and damage to the fiber. Subsequently, 10_{mM} succinate (Complex-II Basal) and 5_{mM} ADP (Complex-II Active) were added. In the final protocol, ROS emission was measured by titrating 10_{mM} of succinate (Complex-II Basal) and 5_{mM} ADP (Complex-II Active). To test for mitochondrial membrane integrity, cytochrome c was added to the chamber. Respiratory function was determined by oxygen flux rates (pmol/s·ml) minus background rates and corrected to fiber mass (pmol/s/mg). ROS-emission was calculated by dividing the rate of ROS-emission (pmol/s/mg) and correcting it by the corresponding respiration rate (pmol H_2O_2/pmol O_2 consumed).

Cytosolic and Nuclear Fractionation

Nuclear and cytosolic fractions from fresh TA muscles of mice were obtained using the NE-PER extraction reagents (38835, Thermo Scientific Scientific) with minor modifications. Briefly, 50~100 mg of the TA muscle was minced on ice and homogenized using a Douce homogenizer in cytosolic extraction reagent (CER) I. Homogenates were then vortexed and let to stand on ice for

10 minutes. Following the addition of CER II solution, samples were briefly vortexed and centrifuged (16,000g) for 10 min. The cytosolic fractions (supernates) were then collected. The remaining pellets, containing nuclei and cellular debris, were washed 3 times in cold 1×PBS and subsequently resuspended in nuclear extraction buffer (NER). Nuclear fractions were then sonicated for 3 seconds x 3 times, and incubated on ice for 40 min. These samples were vortexed every 10 min during the incubation, and subsequently underwent centrifugation (16,000g) for 10 min. The resulting supernatant nuclear fractions were collected. Both the cytosolic and nuclear fractions were stored at -80°C until further analysis.

Whole Muscle Protein Extracts

One quadricep muscle was snap frozen in liquid nitrogen following excision from the animal and stored at -80ºC. The tissue was pulverized to a fine powder at the temperature of liquid nitrogen. Protein extracts were made by diluting (10x) a small amount of powder (~15-20mg) in Sakamoto buffer (20mM HEPES, 2mM EGTA, 1% Triton X-100, 50% Glycerol, 50 mM ß-Glycerophosphate) containing both phosphatase (Sigma) and protease (Roche) inhibitors and rotated end-over-end for 1 hour at 4ºC. Samples were then sonicated on ice (3 seconds x 3 times) and centrifuged (14,000g) for 15 minutes at 4ºC. The supernatant fraction was collected and stored at -80ºC until further analysis.

Western Blotting

All protein concentrations in isolated mitochondria, nuclear and cytosolic fractions and whole muscle samples were determined using the Bradford method. Equal amounts of protein (~20-30µg) were loaded and separated via SDS-PAGE and transferred onto nitrocellulose membranes (Bio-Rad, Mississauga, ON, Canada). Membranes were blocked with wash buffer (0.12% Tris-HCl,

0.585% NaCl, 0.1% Tween, pH 7.5) supplemented with 5% skim milk (w/v) at room temperature for 1 hour with gentle agitation. Membranes were then incubated with primary antibodies overnight at 4ºC for OXPHOS Cocktail (Ab110413, Lot 2101000654, Abcam), Beclin1 (3738, Lot 3, Cell Signaling Technologies), ATG7 (A2856, Lot 078M4843V, Sigma), p62 (Ab56416, Lot GR3285986-1, Abcam), LC3-I/II (4108, Lot 3, Cell Signaling Technologies), Bnip3 (Gift from Dr. L.A. Kirshenbaum), Parkin (4211, Lot 7, Cell Signaling Technologies), VDAC (Ab14734, Lot GR3391163-2, Abcam), Lamp1 (Ab24170, Lot GR3235632-1, Abcam), V-ATPase B1/2 (sc-55544 F-6, Lot I1018, SantaCruz), mature Cathepsin B (D1C7Y, Lot 1, Cell Signaling Technologies), mature Cathepsin D (sc-377299, Lot BO419 , SantaCruz), TFEB whole muscle (MBS120432, Lot 319C2a-3, MyBioSource), TFEB nuc/cyto (A303-673A, Lot 7, Bethyl), TFE3 (HPA023881, Lot 000010514, Sigma), GAPDH (ab8254, Lot GR3317834-1, Abcam), a-tubulin (CP06, Lot D00175772, Calbiochem), H2B (2934, Lot 4, Cell Signaling Technologies). The following day, membranes were washed 3x5minutes in wash buffer and incubated for 1 hour at room temperature with the appropriate HRP-conjugated secondary antibody and subsequently washed 3x5 minutes in wash buffer. The protein density was visualized using enhanced chemiluminescence (1705061, Bio-Rad) with an iBright FL1500 Imaging Station (Fischer Scientific, Oakville, ON, Canada). Band densities were quantified by ImageJ software (NIH) and normalized to corresponding loading controls. All gels were run in a sex-specific manner, with each blot containing either male or female samples. For whole muscle western blots, to have sex-comparisons, an identical, arbitrary control sample, was run in the first lane and all values were controlled back to this band. Representative blots with a break between bands denotes that portion of the image was shifted, without alterations in contrast, to show representative data. All data are represented as combined young and old data, and sex-separated data.

Statistical Analysis

Data were analysed using GraphPad Prism Software (Version 9) and values are represented as means ± SEM. Student's unpaired t-tests were utilized to analyze combined, male and female data to investigate an effect of age. Two-way ANOVAs were used to assess the interaction between age and sex where applicable, and significance was achieved at $p<0.05$. A Bonferroni post-hoc test was used and δ represents a significant difference. Due to the limited sample sizes when the sexes were separated, where post-hoc tests failed to uncover significant differences between groups, independent Student's unpaired t-tests were used to assess the differences between male and female, young and old data. Significance is represented by *, and p values are shown for trends in the data. Three-way ANOVAs were used to assess the independent and interaction effects between age, sex and exercise, significance was achieved at $p<0.05$, and p values are reported for trends in the data set where applicable.

Results:

Physical characteristics of young and aged male, and female mice.

To determine whether aging differentially impacted muscle mass in male and female mice we first measured body mass (g), muscle mass (mg) and muscle mass corrected for body mass (mg/g) in the predominantly fast tibialis anterior (TA) and predominantly slow-twitch soleus (Sol) muscles (Table 1). Overall, body mass was 1.4-fold greater in aged mice versus young counterparts ($p<0.05$). Main effects of age and sex effects were found. Post-hoc tests revealed that both young and aged male mice were significantly larger than age-matched female counterparts ($p<0.05$). Furthermore, aged male mice were 32% heavier than young males, and aged female mice were 28% heavier than young females ($p<0.05$). Raw TA mass (mg) was lower in female mice (sex effect, $p<0.05$) and TA mass was significantly less in young females versus young males (t-test, $p<0.05$). When corrected for body mass, TA mass was 24% smaller in aged mice ($p<0.05$), and a main effect of sex was observed in our separated analysis ($p<0.05$). On average, TA mass/body mass (mg/g) was 28% lower in female mice (post-hoc, $p<0.05$) and 18% less in male mice (t-test, $p<0.05$). Sol mass (mg) was not different between any groups. When corrected for body mass (mg/g), a significant 30% decrease in Sol mass with age was measured in sex-pooled data ($p<0.05$). In a sex-separated analysis, a main effect of age and sex were observed ($p<0.05$). Young females had a 1.4-fold larger Sol mass/body mass than young males (post-hoc, $p<0.05$). With age, male mice had a 24% decline in Sol mass/body mass (t-test, $p<0.05$), whereas females displayed a 36% decline (post-hoc, $p<0.05$).

Exercise capacity in young and aged; male and female mice.

To determine if age and biological sex impact acute exercise capacity, we exposed a cohort of mice to an exhaustive bout of incremental exercise. In our sex-pooled comparison, aged mice

ran for an average of 25 minute less (t-test, $p<0.05$, Fig.1A) accounting for 645 meters of less distance covered (t-test, $p<0.05$, Fig. 1B). In sex-separated comparisons, a main effect of age and an interaction of age and sex were found in run time ($p<0.05$, Fig. 1A). Further analysis revealed 34% and 43% declines in aged male and female mice versus their young counterparts, respectively (post-hoc, $p<0.05$, Fig. 1A). Effects of age, sex, and an interaction of the two variables was measured in distance to fatigue ($p<0.05$, Fig. 1B). Run distance was reduced with age in both male and female mice (post-hoc, $p<0.05$, Fig. 1B). On average young female mice ran 263 meters more than young males (post-hoc, $p<0.05$, Fig. 1B), whereas aged females ran slightly less (28m) than aged males (post-hoc, $p<0.05$, Fig. 1B). Blood lactate was similarly increase with exercise in all groups (t-test, $p<0.05$, Fig. 1C).

Mitochondrial parameters in young and aged, male and female mice.

To understand the divergent endurance capacity with age and sex, we assessed mitochondrial parameters as these organelles are correlated with muscle fatigability. We examined respiration and H_2O_2 emission in permeabilized TA muscle fibers from all groups (Fig. 2A, B). We observed an overall effect of age, whereby aged muscle had lower respiratory capacity (3-way ANOVA, $p<0.05$, Fig. 2A). Independent analyses were performed for each subsequent titration, and we measured a main effect of age for all respiratory measurements (2-way ANOVA, $p<0.05$ Fig. 2A), apart from the Complex I-Basal condition. An interaction between age and sex was found in Complex II-Basal respiration (2-way ANOVA, $p<0.05$ Fig. 2A), however, no post-hoc significance was observed. Overall, no changes were measured in H_2O_2 emission in permeabilized fibers (Fig. 2B), but a trending effect of sex was measured in Complex II-active (2-way ANOVA, $p=0.09$, Fig. 2B), with lower values in female samples.

To determine the effects of age and sex on mitochondrial protein content, we quantified levels of proteins derived from each complex of the electron transport chain (ETC) (Fig. 3). In the sex-grouped data, we found no significant differences in any ETC proteins, and a trending increase in both Complex-V (t-test, $p=0.058$, Fig. 3B) and -II protein (t-test, $p=0.087$, Fig. 3B, E). A main effect of age was observed in both Complex-V (Fig. 3B) and -II (Fig. 3E). Each independent complex (Fig. 3B-F) and total OXPHOS protein (Fig. 3G) exhibited a main effect of sex ($p<0.05$), such that females had more mitochondrial protein. Further, an interaction between age and sex was found in Complex-V ($p<0.05$, Fig. 3B), Complex-II ($p<0.05$, Fig. 3E), Complex-I ($p<0.05$, Fig. 3F), and total OXHOS ($p<0.05$, Fig. 3G) protein, whereby female muscle did not display decrements in mitochondrial protein content with age.

We assessed independent differences between young males and females, and measured 35%, 61%, 38%, and 28% more Complex-V (t-test, $p<0.05$, Fig. 3B), Complex-III (post-hoc, $p<0.05$, Fig. 3C), Complex-II (t-test, $p<0.05$, Fig. 3E), and total OXPHOS (t-test, $p=0.08$, Fig 3G) protein in young females versus young males. The same comparison in aged male and female mice showed that each complex had between 1.8- and 2.1-fold more mitochondrial protein ($p<0.05$, Fig. 3B-F) and 2.1-fold more total OXPHOS in females than in males (post-hoc, $p<0.05$, Fig. 3G).

We then explored independent differences between young and aged muscle from the same-sex mice. In male mice, we observed no change in Complex-V (Fig. 3B) or -II (Fig. 3E) but measured 17% to 39% decreases in all other mitochondrial protein content with age (Fig. 3C, D, F, G). In females, we measured no change in Complex-III (Fig. 3C), -IV (Fig. 3D) or -I (Fig. 3F) protein, but 33% to 47% increases were evident in the remaining mitochondrial proteins (Fig. 3B, E, G) with age in female mice.

Autophagy-related protein expression in aged muscle

To evaluate how aging and biological sex affect the autophagy-lysosome system, we measured upstream autophagy proteins in whole muscle quadriceps samples (Fig. 4 A-C). In combined-sex groups, aging led to a significant 44% increase in Beclin1 protein (t-test, $p<0.05$, Fig. 4B), and a trending 47% increase in Atg-7 protein (t-test, $p=0.09$, Fig. 4C). When the sexes were analyzed separately, no main or interaction effects were measured in Beclin1 protein (Fig. 4B), but a main effect of both age and sex was found in Atg-7 protein (2-way ANOVA, $p<0.05$, Fig. 4C), whereby aging and female muscle displayed increased protein expression.

Independent differences between the groups were then examined for these autophagy proteins. Beclin1 protein was significantly increased by 36% in aged males versus young counterparts (t-test, $p<0.05$, Fig. 4B), whereas female mice displayed no age-effect (Fig. 4B). Atg-7 protein was unchanged in both sexes independently, however both young (t-test, $p<0.05$, Fig. 4C) and aged female mice (post-hoc, $p<0.05$, Fig. 4C) contained ~2-fold more Atg-7 protein in comparison to age-matched male mice.

Autophagosomal protein content in male and female mice with age.

We next wanted to explore how markers of mature autophagosome content are changed in whole muscle samples with age and biological sex in skeletal muscle. Since, these proteins have been shown to change with exercise, we also assessed the impact of exercise in these murine groups. We first measured LC3-II/I as markers of the ratio of mature:immature autophagosomes, respectively. We found a tendency of exercise to reduce LC3-II/I in our combined-group analysis (2-way ANOVA, $p=0.09$, Fig 5.B), with no main effects or post-hoc significance in our sex-separated groups. We observed an overall effect of age on p62 levels in our combined group (2-

way ANOVA, $p<0.05$, Fig. 5C) and a trending 37% increase in p62 protein in our young versus aged sedentary animals (t-test, $p=0.085$, Fig. 5C). In the sex-separated data, a significant main effect of age was observed, along with an interaction between age and acute exercise (3-way ANOVA, $p<0.05$, Fig. 5C). When we assessed the influence of age and exercise in independent sexes, a main effect of age was evident in both males and females (2-way ANOVA, $p<0.05$, Fig. 5C). Independent analyses revealed a significant 33% decrease in p62 protein with exercise in young males (t-test, $p<0.05$, Fig. 5C), and a 25% increase with exercise in young females (t-test, $p=0.05$, Fig. 5C).

Mitophagic protein content in whole muscle and isolated mitochondria

To determine if age and sex impact mitophagy in skeletal muscle, we first probed for the mitophagy markers BNIP3 and Parkin in whole muscle samples (Fig. 6A-C). In the sex-combined group, there were 4.8-fold and 3.6-fold increases in aged muscle BNIP3 and Parkin protein, respectively (t-test, $p<0.05$, Fig. 5 B, C). In sex-separated comparisons, a main effect of age was observed in BNIP3 protein (2-way ANOVA, $p<0.05$, Fig. 6B), and post-hoc comparisons revealed similar, significant increases in aged muscle BNIP3 protein vs sex-matched young counterparts (post-hoc, $p<0.05$, Fig. 6B). A main effect of both age and sex were found in Parkin protein, whereby females, both young and old, had more Parkin than their sex-matched, young, counterparts (2-way ANOVA, $p<0.05$, Fig. 6C). Aging in both sexes led to increases in Parkin protein (Male: t-test, $p<0.05$; Female: post-hoc, $p<0.05$; Fig. 6C).

We also explored whether LC3-II protein, a marker of mature autophagosomes was different in isolated mitochondria from young and old male and female mice (Fig. 6D,E). We observed no effect of age in either sex. Since we have previously reported that acute exercise can stimulate mitophagic breakdown, we assessed whether our exercise stimulus altered

mitochondrially-localized LC3-II. A main effect of exercise was observed, whereby LC3-II protein was decreased with exercise by an average of 20% overall (3-way ANOVA, $p<0.05$, Fig. 6E).

Lysosomal protein content in young and aged, male and female mice.

To assess the end-stage of the autophagy pathway, we evaluated lysosomal protein content in our groups (Fig. 7A-E). Lysosome-associated membrane protein 1 (Lamp1) levels were unchanged with age in the sex-combined group. Alternatively, vesicular ATPase (V-ATPase), mature Cathepsin B, and mature Cathepsin D were all upregulated by 3.6-, 4.0- and 5.5-fold with age, respectively (t-test, $p<0.05$, Fig.7 C, D, E). When sex was separated, all lysosomal proteins showed a significant main effect of age (2-way ANOVA, $p<0.05$, Fig. 7 B-E). A main effect of sex was found in Lamp1 (2-way ANOVA, $p<0.05$, Fig. 7C), vATPase (2-way ANOVA, $p<0.05$, Fig. 7D) and mature Cathepsin D (2-way ANOVA, $p<0.05$, Fig. 7E), whereby these proteins were higher in the female mice. An interaction between age and sex was found for mature Cathepsin D protein (Two-way ANOVA, $p<0.05$, Fig. 7E). Independent analyses for each protein confirmed significant 1.8-3.9-fold increases in all measured lysosomal proteins with age in the male mice ($p<0.05$, Fig. 7 B-E). In female mice, significant 4.4-6.5-fold increases were found with age in each lysosome protein (post-hoc; $p<0.05$, Fig. 7 C-E), except for Lamp1. We quantified higher Lamp1 (post-hoc, $p<0.05$, Fig 7. B) and mature Cathepsin D (t-test, $p<0.05$, Fig 7. D) in young female mice versus young male mice, and elevated mature Cathepsin D in aged females compared to aged males (post-hoc, $p<0.05$, Fig 7. E).

We measured the protein levels of TFEB and TFE3, transcription factors that control the autophagy-lysosome pathway (Fig. 8A-C). TFEB was 3.8-fold greater with age in the sex-combined analysis (t-test, $p<0.05$, Fig. 8B). In the sex-separated analyses, TFEB protein exhibited

main effects of age and sex, and an interaction existed between these variables (2-way ANOVA, $p<0.05$, Fig. 8B), whereby these proteins were greater in aged, versus young muscle, female muscle versus male, and the increase with age was larger in the female cohort. Specifically, TFEB protein was 1.8-fold greater in young females (t-test, $p<0.05$, Fig. 8B) and 2.5-fold greater in aged females (t-test, $p<0.05$, Fig. 8B) when compared to age-matched male counterparts. Compared to young, sex-matched animals, TFEB protein was 3.3-fold greater in aged males (t-test, $p<0.05$, Fig. 8B) and 4.2-fold higher in aged females (post-hoc, $p<0.05$, Fig. 8B). Conversely, TFE3 was 1.5-fold greater in our sex-combined analysis (t-test, $p<0.05$, Fig. 8C). In the sex-separated analyses, TFE3 protein exhibited main effects of age and interaction between age and sex (2-way ANOVA, $p<0.05$, Fig. 8B, C). As such, TFE3 protein was increased 3.3-fold with age in male mice (post-hoc, $p<0.05$, Fig. 8C), an effect not seen in females. A trending increase was also measured in TFE3 protein, whereby young females contained 66% more than young males (t-test, $p=0.057$, Fig. 8C).

Influence of exercise on lysosome biosynthetic pathway

We also wished to explore whether exercise can activate lysosome biosynthesis pathways in both young and aged, male and female mice (Fig 9. A-D). Thus, we measured levels of nuclear TFEB protein in all groups. Sedentary aged, sex-combined muscle exhibited 18% more nuclear TFEB (post-hoc, $p<0.05$, Fig. 9A). In this sex-combined analysis, there was an interaction between age and exercise (2-way ANOVA, $p<0.05$, Fig. 9B). Following cessation of exercise, nuclear TFEB was increased by 30%, whereas this was not evident in aged male or female muscle (post-hoc, $p<0.05$, Fig 9B). However, aged male and female muscle appeared to possess approximately 20% higher basal pre-exercise levels of TFEB in the nucleus, compared to young counterparts (t-test, $p=0.075$ and $p=0.077$ respectively, Fig. 9B). In response to exercise, young male mice

enhanced nuclear TFEB by 40% (post-hoc, $p<0.05$, Fig. 9B), whereas females only upregulated nuclear content by 16% (t-test, $p=0.064$, Fig. 9B). Thus, the fold-change in nuclear TFEB with exercise was greater in males, compared to females (t-test, $p<0.05$, Fig 9C).

We also utilized a TFEB-luciferase promoter activity assay to determine whether exercise stimulates TFEB transcriptional activity. This analysis could only be completed in sex-combined groups. Overall, there was a trending main effect of increase promoter activity with exercise (2-way ANOVA, $p=0.09$, Fig. 9D). There was also a main effect of age (2-way ANOVA, $p<0.05$, Fig. 9D), whereby TFEB promoter activity was reduced with age. Exercise enhanced TFEB promoter activity in both young (t-test, $p=0.069$, Fig. 9D) and aged (t-test, $p<0.05$, Fig. 9D) muscle by 1.9-and 2.5-fold, respectively.

Discussion:

With advancing age there is a progressive loss of muscle mass and function, ultimately resulting in sarcopenia (3, 40). This has global implications, as the aging population is continually rising. Understanding the molecular underpinnings that govern muscle loss with age will guide future therapeutic interventions. It is well established that regular exercise can counteract these deficits, partially through upregulating the production of new healthy mitochondria and stimulating the removal dysfunctional ones through mitophagy (20, 41). Mitophagy is the mitochondrial-specific degradation through the autophagy lysosome system. Previous reports from our group have indicated that acute exercise stimulates lysosome biogenesis (27) and that chronic muscle activity elevates lysosome protein content (42, 43) in young, healthy muscle. These changes are likely to support an enhanced capacity for proteolysis. No studies to date have examined the regulation of lysosome biosynthesis in sedentary or exercised aged muscle, and whether similar mechanisms exist in males and females. The influence of biological sex is an important factor to consider, as therapeutic targets in males and females may differ. To this end, the present study explores how biological sex influences the autophagy-lysosome system in young and aged skeletal muscle. Furthermore, we wanted to examine whether acute exercise can upregulate lysosomal synthetic pathways in aged muscle, and whether the effect was sex-dependent.

To address these aims, we utilized young (4-6 mo) and aged (22-24 mo), male and female C57BL/6 mice, which were either sedentary or exercised acutely. In our analyses, we performed measures in both combined and sex-separated groups, which allowed us to determine if changes we observed were age- and/or sex- dependent.

We confirmed the observation that female mice have a smaller muscle mass, as previously reported (44), and that they also display greater reductions in muscle mass with age. This may be due to a higher abundance of atrophy susceptible Type I muscle fibers in females (45–48). It has been reported that female rodents have greater loss of muscle mass with hindlimb unloading due to elevated catabolic signaling (33, 49, 50). Based on our findings, this seems to be true with age as well. A balance between protein synthesis and degradation is required to maintain muscle mass. Our observation that female mice undergo a greater degree of atrophy with age may be due to greater anabolic resistance, and/or accelerated protein degradation. Here, we have explored the latter pathway, with a focus on the autophagy-lysosome system.

Aging leads to decrements in endurance capacity (20, 41), which we reproduce in the current study. We also report that young female mice have greater exercise capacity than their male counterparts. We can discount the possibility that males and females where not similarly exhausted, as post-exercise lactate levels were similar amongst all groups. Thus, the longer distance to exhaustion in young female mice may be due to the greater abundance of mitochondrial proteins that we measured in our female cohort. Supportively, others have found that young females have higher mitochondrial content (35, 51) and have more fatigue-resistant muscle (52–54). However, we cannot discount the possibility that these differences in mitochondrial content and exercise capacity are simply a product of young female mice being more active in their cage behavior (55, 56). Furthermore, the aging-induced reduction in exercise tolerance was greater in our female cohort. This result was surprising as only our male animals showed declines in mitochondrial content with age. This could also be explained by an age-related deterioration of mitochondrial function in females; however our data did not indicate any sex differences in respiratory capacity, or reactive oxygen species production, between our males and females. Thus,

it is clear that other mechanisms may influence the divergence in exercise capacity with age in male and female rodents.

Protein aggregates and mitochondria are degraded by the autophagy-lysosome system. Since aberrations in this proteolytic system are associated with muscle dysfunction (12–16), we wanted to investigate whether age and biological sex similarly, or differentially, influenced this system. Like previous studies (22, 23, 57), our results support an increase in autophagy-related proteins such as the nucleation-inducing protein Beclin1 (58, 59), and the LC3 maturation protein ATG7 (59) with age. However, sex influences this response, since both young and old females had a greater abundance of ATG7 protein in comparison to age-matched counterparts, a finding that has been reported previously in avian muscle (57). These data would imply that females have a greater capacity to form mature autophagosomes via the conversion of LC3-I to LC3-II.

To delineate whether these upstream markers influence autophagosomal turnover, we measured LC3-I as well as its downstream lipidated form LC3-II, which is a marker of mature autophagosomes [60]. In addition, we assessed the levels of p62, an adaptor protein responsible for tethering the autophagosome to removable cellular constituents (60–62). Importantly, these proteins are degraded by lysosome proteolysis. Thus, declines in p62 protein, without change and/or deficits in LC3-II/I would indirectly suggest higher levels of autophagic breakdown. It should be noted that these measures do not directly indicate true autophagic flux. Thus, future research investigating gene expression changes and utilizing "flux" measures will be useful in determining whether age, biological sex or acute exercise impact autophagy and mitophagy similarly or differentially. Our finding that young female mice have less p62 protein than young male mice, with greater levels of ATG7 and no difference in LC3-II/I would suggest that females have greater basal autophagy in muscle, similar to a previous report (63). We also found that aged

muscle contains a higher abundance of p62 and total LC3 (data not shown), indicative of greater autophagic signaling with age, regardless of sex. Thus, the sex-difference in basal autophagy was not observed with age, and overall, these results suggest that young females have greater basal autophagy than young males.

Acute endurance exercise is a stimulus for autophagosomal turnover in young muscle (26). Thus, we wanted to examine if sex and/or age influence this response. In young male mice we measured reductions in p62 protein in the exercised group. LC3-I was similarly changed (data not shown). These findings, in addition to our main effect of exercise in decreasing whole muscle LC3-II protein imply that exhaustive exercise is a stimulus for autophagic clearance in young male muscle. In contrast, increases in p62 protein were observed in age-matched females. Thus, autophagosomal breakdown is not similarly induced between the sexes with acute exercise. Since female muscle appears to have accelerated basal autophagy, exercise may be insufficient to further augment this pathway. In aged muscle, these exercise effects were not apparent, regardless of sex. Overall, these findings suggest that acute exhaustive exercise stimulates autophagy predominantly in young male muscle.

With an interest in how these changes may translate to mitochondrial degradation through mitophagy, we assessed levels of proteins involved in targeting these organelles for digestion at the lysosomes. In whole muscle samples, we found an overall increase in both BNIP3 and Parkin with age. However, the increase with age was much more prominent in female mice. This may suggest divergent regulation of mitophagy-targeting mechanisms in male and female skeletal muscle. To assess autophagosome-bound mitochondria directly, we probed for LC3-II in isolated mitochondria, as done previously (23–25, 42, 64–66). Contrary to our hypothesis, we failed to measure any increase in mitochondrial LC3-II with age. This contrasts to a previous report from

Chen et al., however, in their study aged mice were considerably younger (18 months), compared to those used here (22-24 months) (24). Further, we measured an overall effect of exercise in reducing mitochondrial LC3-II protein, suggesting that mitophagic clearance is occurring universally. When these acute exercise-induced changes are repeated in a chronic manner, they likely contribute to the training-induced enhancement in mitochondrial quality observed as a result of training (22). Ultimately, these observations indicate that mitophagy signaling is elevated in the muscle from aged mice, and that exercise can stimulate the degradation of mitochondria regardless of age, or sex.

Lysosomes act as the terminal step of the autophagic pathway whereby they degrade substrates via their low pH and the presence of digestive enzymes. These organelles play an integral role not just in autophagy, but also in mitochondrial quality control through mitophagy (67). In muscle from aged rodents and humans the presence of non-digestible lysosomal content, termed lipofuscin is apparent (23, 68). The presence of such structures is indicative of lysosome dysfunction, which may limit the capacity for autophagic and mitophagic breakdown. Our group and others have reported that aging leads to an accumulation of lysosomal proteins (22, 69), which we recapitulate in the present study. This could be explained by the greater levels of TFEB and TFE3 protein, transcription factors that mediate lysosome biogenesis, in the muscle from aged animals in this study. Uniquely, we also uncovered that young and aged female mice have a greater abundance of lysosomal protein in whole muscle samples as compared to age-matched males. This may in part be explained by the higher levels of TFEB and TFE3 in female muscle. This abundance of lysosome protein in female muscle may serve to support the observed increase in autophagy in females, but more research utilizing direct flux measurements, along with assessments of lysosomal function, are required as a function of age and sex.

TFEB is considered the master transcriptional regulator of lysosome biogenesis (70, 71). Our work in the past has uncovered that chronic contractile activity, as a model of endurance exercise training, upregulates lysosome content in young healthy muscle (22, 42, 43). This is due to acute-exercise inductions in the transcriptional activation of TFEB, as well as enhanced nuclear localization of the protein (27). We also observed this nuclear localization and transcriptional activation of the TFEB promoter construct in young mice. When we analyzed this response in males versus females, the relative shift of TFEB to the nucleus was greater in the male cohort. This finding matches that of the exercise autophagy data. Cumulatively these findings imply that the autophagy-lysosome system is more responsive to exercise in young male, compared to female muscle, and future work should look at mechanisms that underly such changes.

Finally, we wanted to examine these mechanisms in aged muscle, as increasing lysosomal content though exercise could in theory enhance the capacity for autophagic/mitophagic degradation. We hypothesized that the muscle from aged animals would exhibit a blunted lysosome biosynthetic pathway due to attenuated kinase signaling (24, 25, 72, 73). Supportively, an upregulation of nuclear TFEB protein post-exercise was only found in young animals. However, although aging led to an overall decrease in TFEB transcription as measured by promoter-reporter activity level, exercise was able to upregulate it to the level observed in young muscle. Thus, although aging blunts aspects of autophagosomal turnover and lysosome biosynthesis with acute exercise, it enhances TFEB expression, which, if repeated over time, may serve to re-establish lysosome function and homeostasis.

Conclusions:

Collectively, our studies reveal that aging and exercise have differential effects on the autophagy-lysosome system in skeletal muscle, which is dependent on biological sex. First, we show that in female mice, there is a greater abundance of mitochondrial, autophagy and lysosome proteins. Second, we observed that female mice have a greater index of skeletal muscle autophagosome clearance than male mice. We also demonstrate that acute exercise stimulates autophagosome turnover and lysosome biogenesis in young males, but not in young females or in aged animals from either sex. Finally, and most importantly, exercise was able to activate TFEB promoter activity regardless of age, which can promote lysosome biogenesis. This finding provides merit to further explore the vitality of exercise in re-establishing autophagy-lysosome homeostasis in aged muscle. More work is required to delineate the impact of biological sex on mechanisms that contribute to sarcopenia, as future therapies must be targeted accordingly.

Table and Figure Legends:

Table 1. Animal body weight and muscle characteristics. Body mass (g), muscle mass (mg) and muscle mass corrected for body weight (mg/g) in combined and sex-separated young and aged muscle. Values are means ± SEM. #, $p<0.05$ main effect of age; †, $p<0.05$ main effect of sex; ⁋, $p<0.05$ interaction of age and sex. Different letters represent post-hoc significance at $p<0.05$. *$p<0.05$, t-test between young vs old within the same sex; δ $p<0.05$ t-test between male and females at the same age. N=10/male group, N=8/female group.

Figure 1. Exercise capacity in young and aged, male and female mice. A. Time to fatigue in minutes. B. Distance to fatigue in meters. C. Blood lactate (mM). Values are means ± SEM. Main effects are represented on graph at $p<0.05$. *$p< 0.05$, t-test between indicated groups. δ $p<0.05$, post-hoc significance. N=5/male group, N=4/female group.

Figure 2. Mitochondrial respiration and reactive oxygen species in young and aged, male and female mice. A. Oxygen consumption rates and B. H_2O_2 emission in the indicated respiratory states. All values are reported as means ± SEM. Main effects of a 3-way ANOVA are represented on the graph at $p<0.05$. Main effects of 2-way ANOVA are represented on graph at $p<0.05$. # $p<0.05$, main effect age. N=10/male group, N=8/female group

Figure 3. Mitochondrial protein content in young and aged, male and female mice. A. Representative western blot from male (top panel) and female (bottom panel) mice for OXPHOS protein. B-F. Quantification of each independent mitochondrial protein. B. Complex-V protein (ATP5A) protein, C. Complex-III (UQCRC2) protein, D. Complex-IV (MTCO1) protein, E. Complex-II (SDH8), and F. Complex I (NDUFB8) protein. G. Quantification of total OXPHOS. All values were corrected to Ponceau stain (P.S), and values are reported as means ± SEM, in A.U.

Main effects of 2-way ANOVA are represented on graph at $p<0.05$. δ $p<0.05$, post-hoc significance. *$p< 0.05$, t-test between indicated groups. N=10/male group, 8/female group.

Figure 4. Upstream autophagic proteins in young and aged, male and female mice. A. Representative western blots for Beclin1 and ATG7. B. Quantification of Beclin1 protein in combined and sex-separated groups. C. Quantification of ATG7 protein in combined and sex-separated groups. All values were corrected to GAPDH and are reported as means ± SEM, in A.U. Main effects of 2-way ANOVA are represented on graph at $p<0.05$. δ $p<0.05$, post-hoc significance. *$p< 0.05$, t-test between indicated groups. N=10/male group, 8/female group. Dashed line break in representative blot are different sections from the same blot.

Figure 5. Autophagosomal proteins in sedentary and acute-exercised young and aged, male and female mice. A. Representative western blots for p62, LC3-I and LC3-II. B. Quantification of LC3-II/I protein in combined and sex-separated groups. C. Quantification of p62 protein in combined and sex-separated groups. All values were corrected to GAPDH and are reported as means ± SEM, in A.U. Main effects of a 3-way ANOVA are represented on the graph at $p<0.05$. Main effects of 2-way ANOVA are represented on graph at $p<0.05$. # $p<0.05$, main effect age. δ $p<0.05$, post-hoc significance. *$p< 0.05$, t-test between indicated groups. N=5/male group, 4/female group.

Figure 5. Mitophagy protein content in the muscle and mitochondria in young and aged, male and female mice. A. Representative western blots for BNIP3 and Parkin in whole muscle samples. B. Quantification of BNIP3 protein in combined and sex-separated groups. C. Quantification of Parkin protein in combined and sex-separated groups. D. Representative western blots for LC3-II in isolated mitochondria with or without exercise in young and aged, male and

female mice. E. Quantification of LC3-II protein in combined and sex-separated groups. Whole muscle values were corrected to GAPDH. Isolated mitochondria values were corrected to VDAC. Values are reported as means ± SEM, in A.U. Main effects of a 3-way ANOVA are represented on the graph at $p<0.05$. Main effects of 2-way ANOVA are represented on graph at $p<0.05$. δ $p<0.05$, post-hoc significance. *$p< 0.05$, t-test between indicated groups. N=10/male group, 8/female group in A-C, and N=5/male group, 4/female group in D-E. Line break in representative blot are different sections from the same blot.

Figure 7. Lysosome proteins in young and aged, male and female mice. A. Representative western blots for Lamp1, vATPase, mature Cathepsin B and mature Cathepsin D. B. Quantification of Lamp1 protein in combined and sex-separated groups. C. Quantification of vATPase protein in combined and sex-separated groups. D. Quantification of mature Cathepsin B protein in combined and sex-separated groups. E. Quantification of mature Cathepsin D protein in combined and sex-separated groups. All values were corrected to GAPDH and are reported as means ± SEM, in A.U. Main effects of 2-way ANOVA are represented on graph at $p<0.05$. δ $p<0.05$, post-hoc significance. *$p< 0.05$, t-test between indicated groups. N=10/male group, 8/female group.

Figure 8. Lysosome transcription factor proteins in young and aged, male and female mice. A. Representative western blots for TFEB and TFE3 protein. B. Quantification of TFEB protein in combined and sex-separated groups. C. Quantification of TFE3 protein in combined and sex-separated groups. All values were corrected to GAPDH and are reported as means ± SEM. Main effects of 2-way ANOVA are represented on graph at $p<0.05$. δ $p<0.05$, post-hoc significance. *$p< 0.05$, t-test between indicated groups. N=10/male group, 8/female group. Line break in representative blot are different sections from the same blot.

Figure 9. TFEB protein localization and promoter activity in sedentary and acute-exercised young and aged, male and female mice. A. Representative western blots for TFEB protein in nuclear and cytosolic fractions in sedentary and exercised male and female mice. B. % nuclear TFEB protein in combined and sex-separated male and female mice. C. Fold-change in nuclear TFEB protein in each group examined. D. TFEB promoter activity (luciferase; RLU) in young and aged, sedentary, and exercised mice. In A-C, cytosolic values were corrected to a-tubulin, nuclear values were corrected to H2B, and reported as mean ± SEM, in A.U. Main effects of 2-way ANOVA are represented on graph at $p<0.05$. # $p<0.05$, main effect age. δ $p<0.05$, post-hoc significance. *$p< 0.05$, t-test between indicated groups. N=5/male group, 4/female group in B-C. N=6/group in D.

Tables and Figures:

Table 1:

		Combined		Male		Female		Statistics
		Young	Aged	Young	Aged	Young	Aged	
Body Mass (g)		30.73 ± 1.27	41.35 ± 1.91*	34.65 ± 1.01^{A}	45.72 ± 2.45^{*,B}	25.83 ± 0.976^{C}	35.89 ± 1.62^{*,A}	# †
Muscle Mass (mg)	TA	51.41 ± 1.41	53.49 ± 3.95	54.61 ± 1.34^{A}	58.70 ± 3.95^{A}	47.43 ± 1.97$^{\delta, A}$	46.98 ± 5.58^{A}	†
	Sol	10.32 ± 0.49	9.60 ± 0.76	10.01 ± 0.42^{A}	9.95 ± 0.916^{A}	10.51 ± 1.00^{A}	9.15 ± 1.32^{A}	
Muscle Mass (mg/g body weight)	TA	1.70 ± 0.06	1.31 ± 0.10*	1.59 ± 0.05$^{A, B}$	1.30 ± 0.12$^{*, A,B}$	1.85 ± 0.08^{A,C}	1.34 ± 0.17$^{*, A, B, D}$	#
	Sol	0.34 ± 0.03	0.24 ± 0.02*	0.29 ± 0.02^{A}	0.22 ± 0.02$^{*, A}$	0.409 ± 0.04^{B}	0.26 ± 0.04$^{*, A}$	# †

Figure 1:

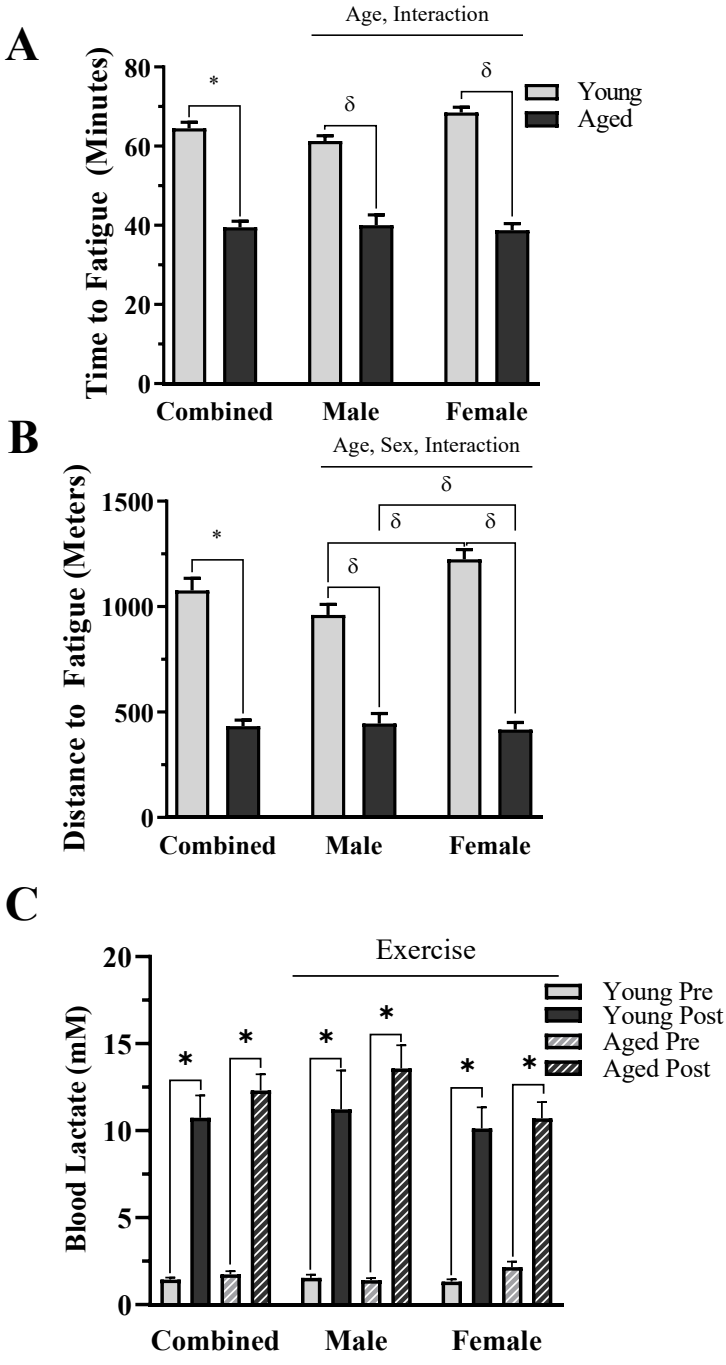
A
Age, Interaction
Time to Fatigue (Minutes)
80
60
40
20
0
*
δ
δ
Young
Aged
Combined
Male
Female
B
Age, Sex, Interaction
Distance to Fatigue (Meters)
1500
1000
500
0
*
δ
δ
δ
Combined
Male
Female
C
Exercise
Blood Lactate (mM)
20
15
10
5
0
Young Pre
Young Post
Aged Pre
Aged Post
Combined
Male
Female

Figure 2:

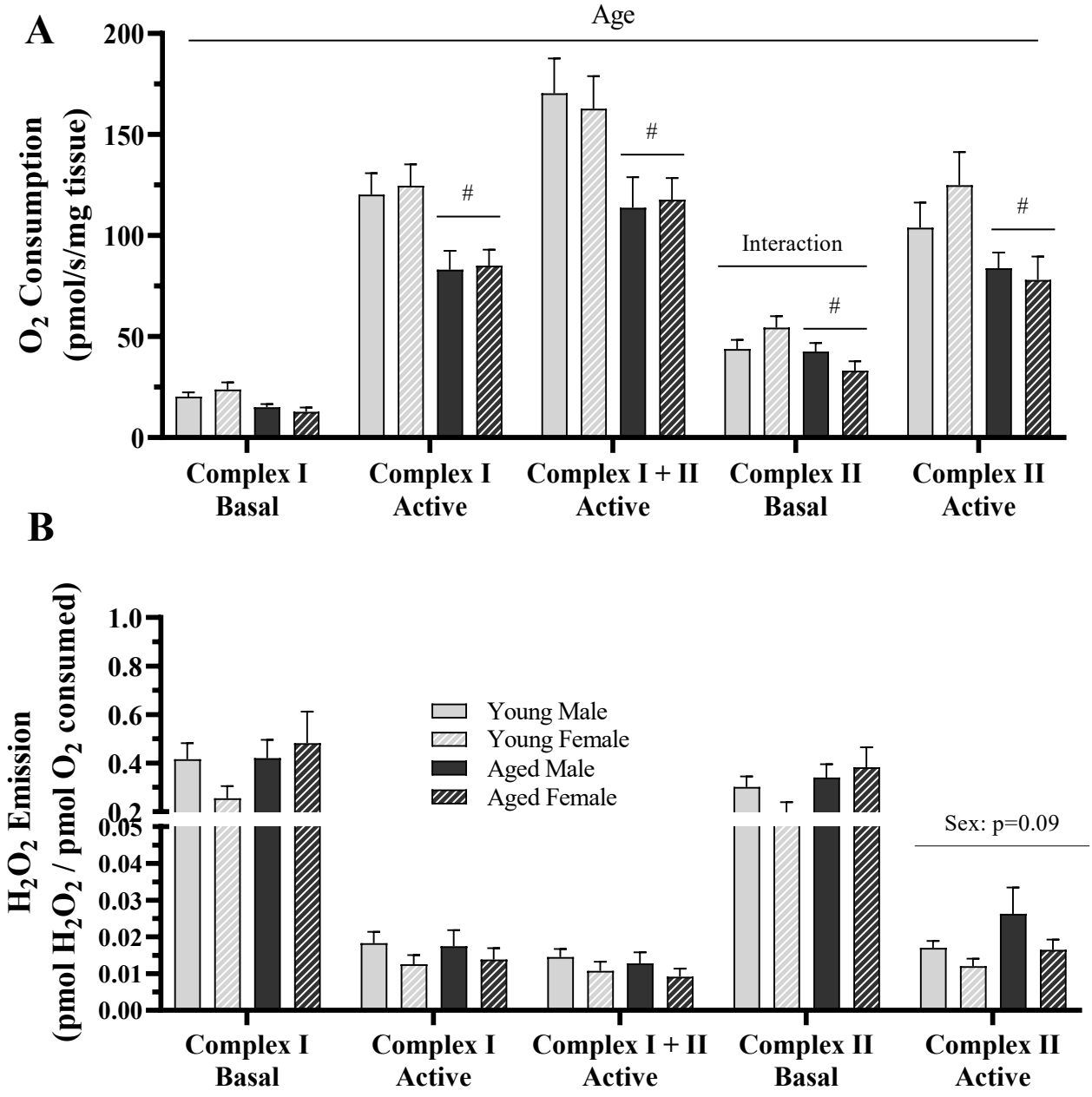
A
Age
O_2 Consumption (pmol/s/mg tissue)
200
150
100
50
0
#
#
Interaction
#
#
Complex I Basal
Complex I Active
Complex I + II Active
Complex II Basal
Complex II Active
B
H_2O_2 Emission (pmol H_2O_2 / pmol O_2 consumed)
1.0
0.8
0.6
0.4
0.2
0.05
0.04
0.03
0.02
0.01
0.00
Young Male
Young Female
Aged Male
Aged Female
Sex: p=0.09
Complex I Basal
Complex I Active
Complex I + II Active
Complex II Basal
Complex II Active

Figure 3:

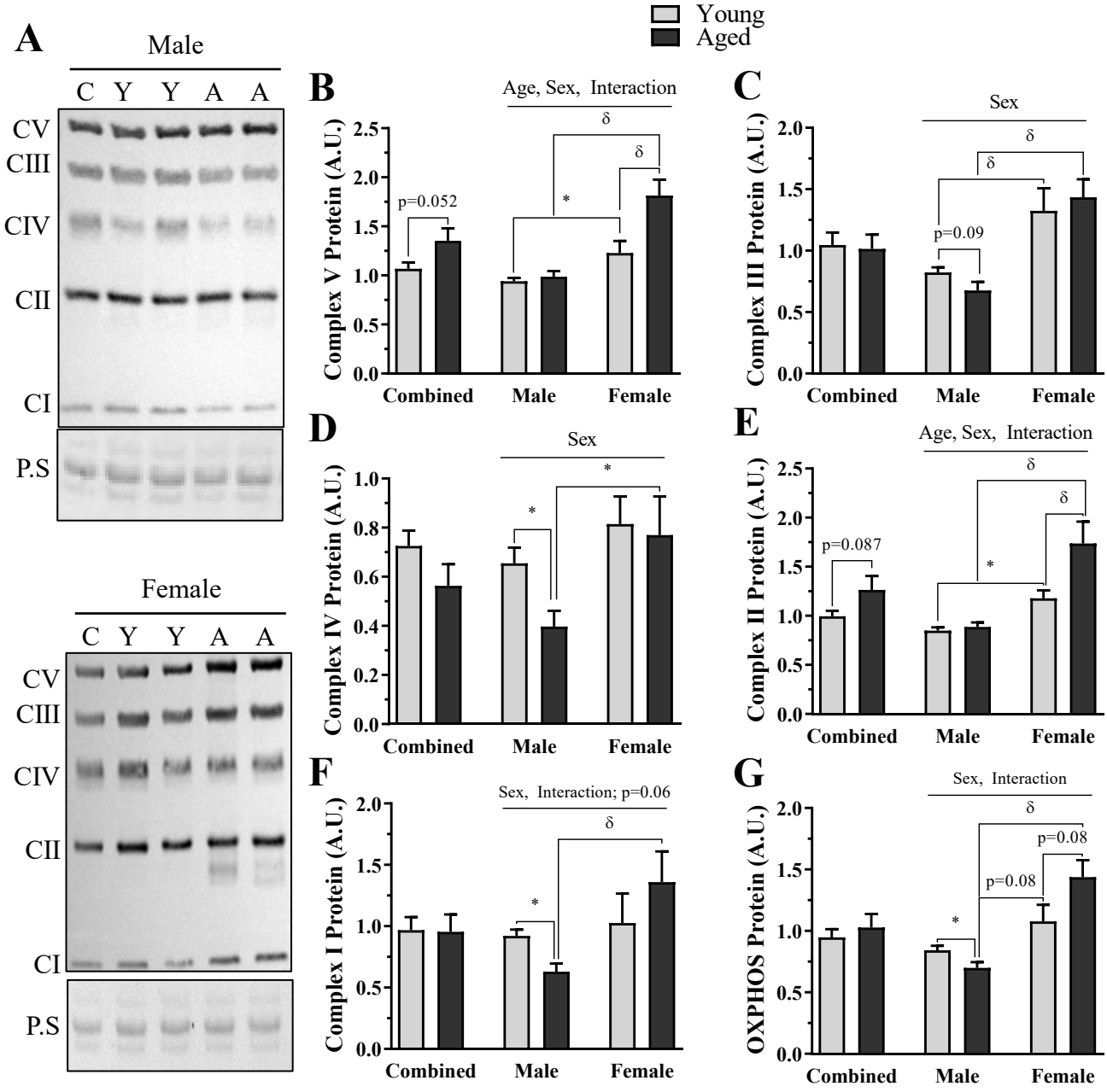
A
Male
C Y Y A A
CV
CIII
CIV
CII
CI
P.S
Female
C Y Y A A
CV
CIII
CIV
CII
CI
P.S
Young
Aged
B
Age, Sex, Interaction
Complex V Protein (A.U.)
p=0.052
Combined
Male
Female
C
Sex
Complex III Protein (A.U.)
p=0.09
D
Sex
Complex IV Protein (A.U.)
E
Age, Sex, Interaction
Complex II Protein (A.U.)
p=0.087
F
Sex, Interaction; p=0.06
Complex I Protein (A.U.)
G
Sex, Interaction
OXPHOS Protein (A.U.)
p=0.08
p=0.08

Figure 4:

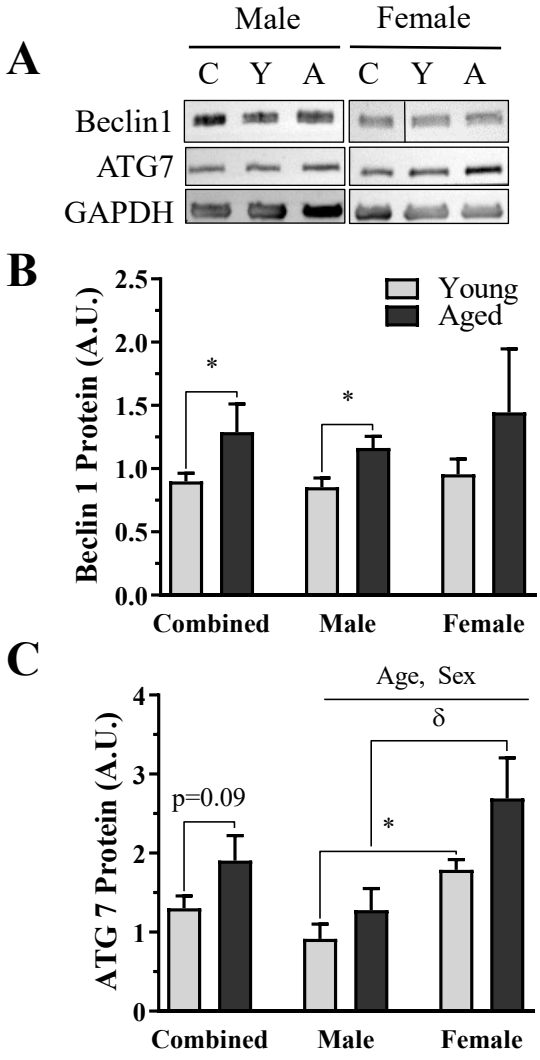
A
Male
Female
C Y A C Y A
Beclin1
ATG7
GAPDH
B
Young
Aged
Beclin 1 Protein (A.U.)
2.5
2.0
1.5
1.0
0.5
0.0
*
*
Combined
Male
Female
C
Age, Sex
δ
ATG 7 Protein (A.U.)
4
3
2
1
0
p=0.09
*
Combined
Male
Female

Figure 5:

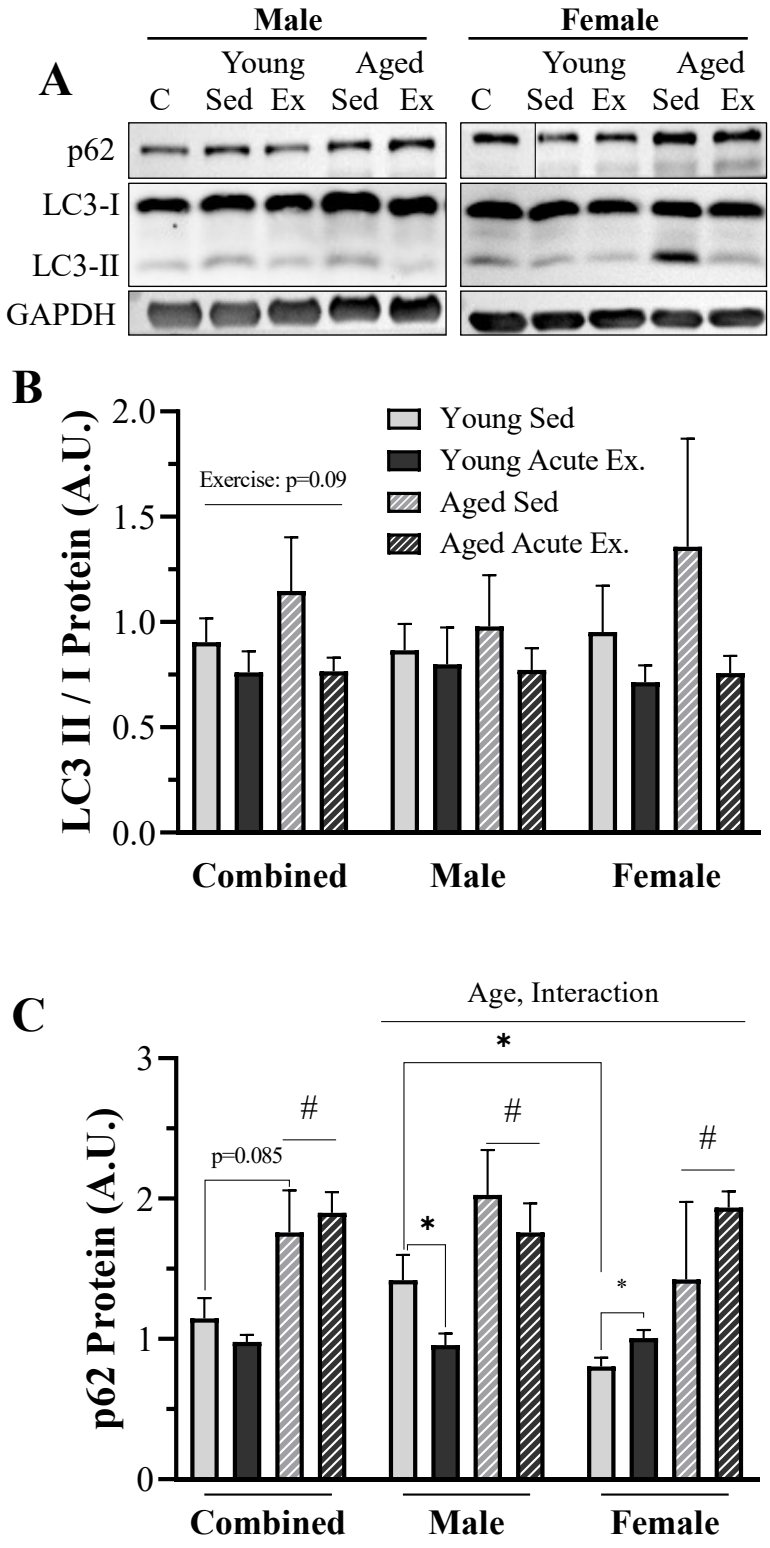
A
Male
Female
Young
Aged
C
Sed
Ex
Sed
Ex
p62
LC3-I
LC3-II
GAPDH
B
LC3 II / I Protein (A.U.)
2.0
1.5
1.0
0.5
0.0
Exercise: p=0.09
Young Sed
Young Acute Ex.
Aged Sed
Aged Acute Ex.
Combined
Male
Female
C
p62 Protein (A.U.)
3
2
1
0
Age, Interaction
*
#
p=0.085
Combined
Male
Female

Figure 6:

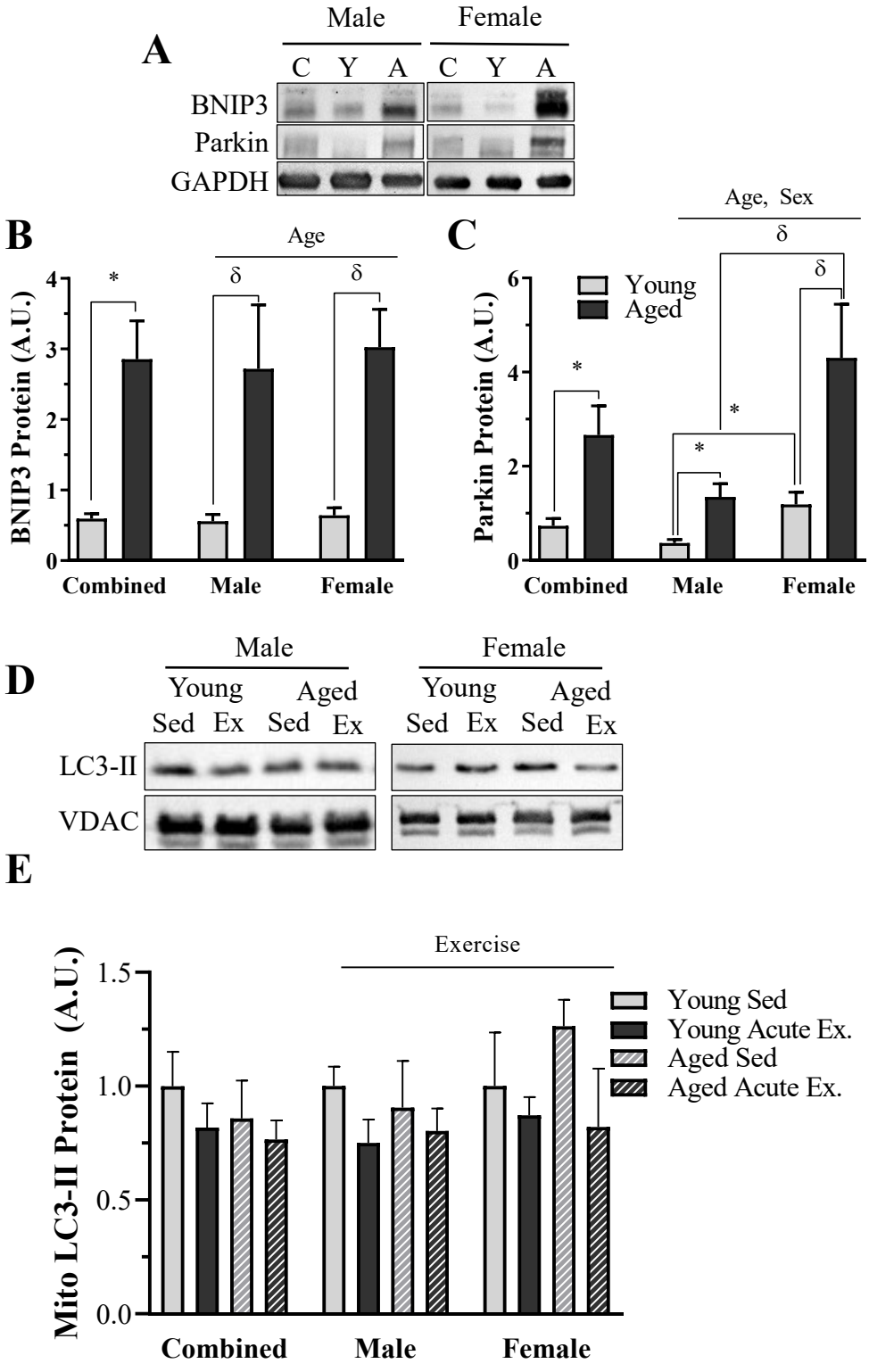
A
Male
Female
C Y A C Y A
BNIP3
Parkin
GAPDH
B
Age
BNIP3 Protein (A.U.)
Combined
Male
Female
C
Age, Sex
Young
Aged
Parkin Protein (A.U.)
Combined
Male
Female
D
Male
Female
Young
Aged
Sed Ex Sed Ex
LC3-II
VDAC
E
Exercise
Mito LC3-II Protein (A.U.)
Young Sed
Young Acute Ex.
Aged Sed
Aged Acute Ex.
Combined
Male
Female

Figure 7:

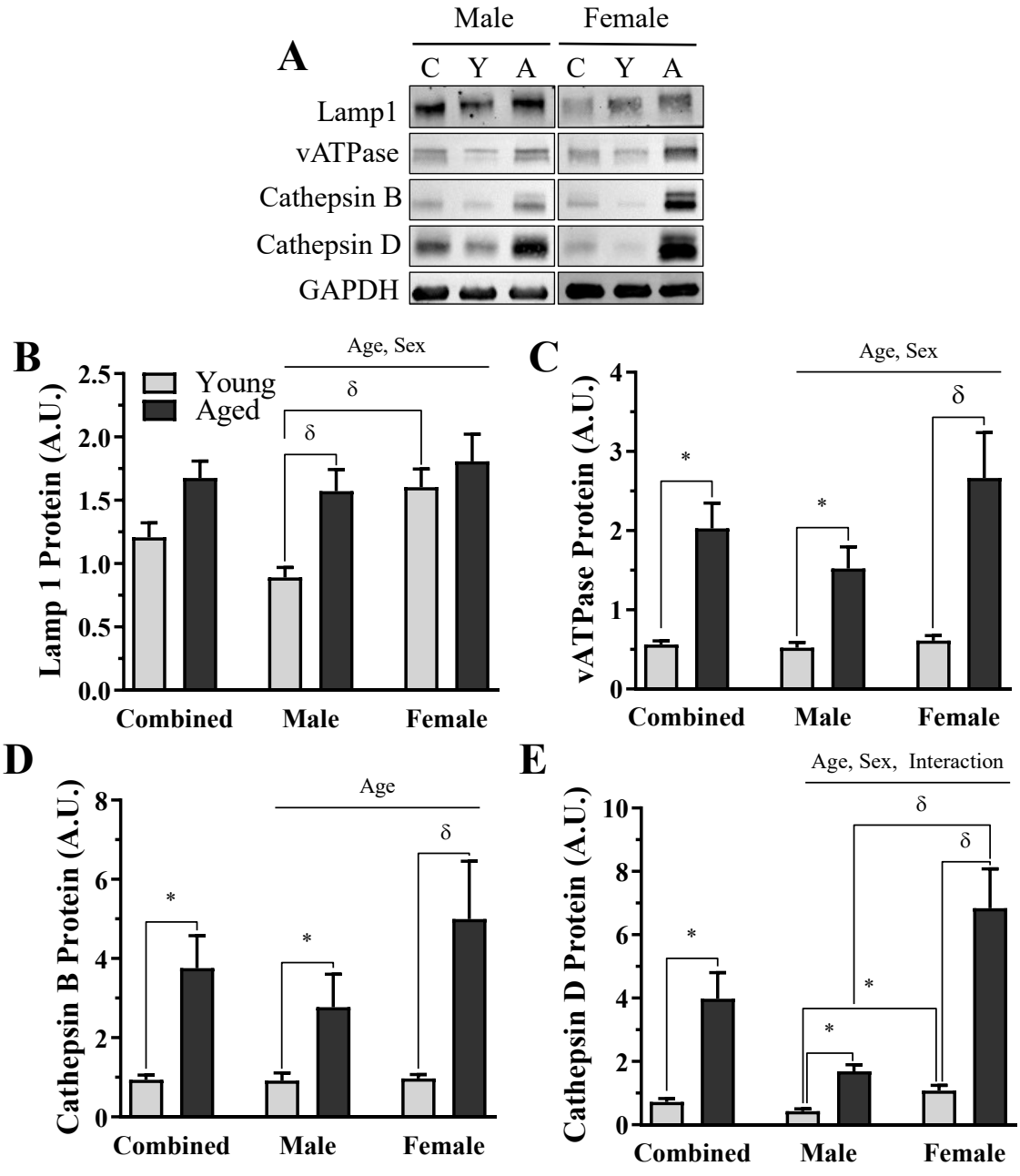
A
Male
Female
C Y A C Y A
Lamp1
vATPase
Cathepsin B
Cathepsin D
GAPDH
B
Young
Aged
Age, Sex
δ
δ
Lamp 1 Protein (A.U.)
2.5
2.0
1.5
1.0
0.5
0.0
Combined
Male
Female
C
Age, Sex
δ
*
*
vATPase Protein (A.U.)
4
3
2
1
0
Combined
Male
Female
D
Age
δ
*
*
Cathepsin B Protein (A.U.)
8
6
4
2
0
Combined
Male
Female
E
Age, Sex, Interaction
δ
δ
*
*
*
Cathepsin D Protein (A.U.)
10
8
6
4
2
0
Combined
Male
Female

Figure 8:

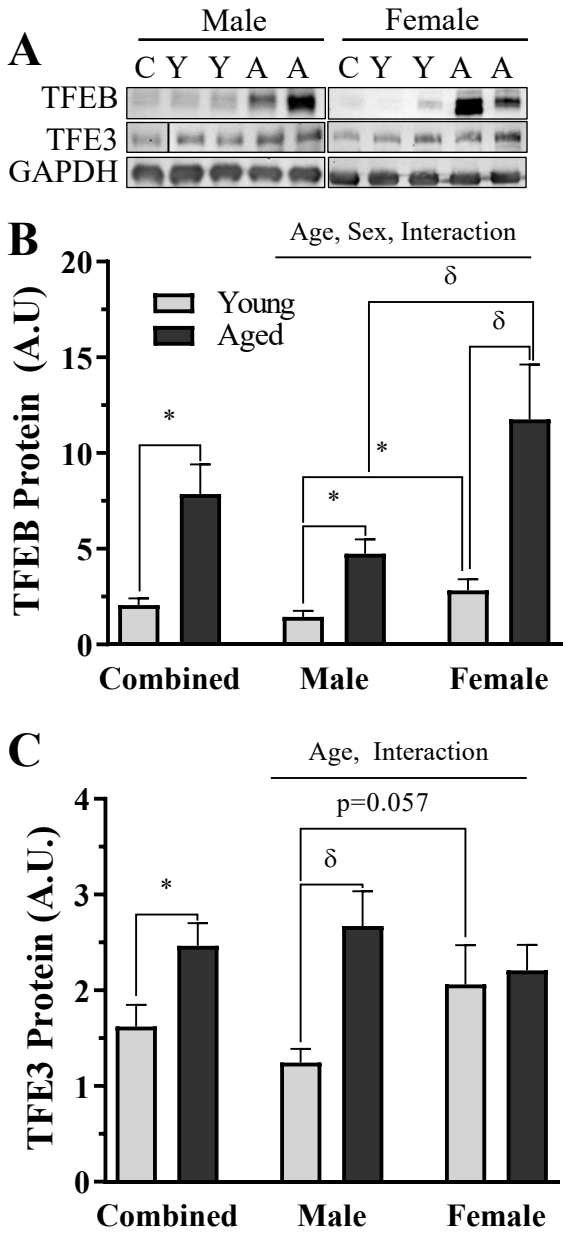
A
Male
Female
C Y Y A A C Y Y A A
TFEB
TFE3
GAPDH
B
Age, Sex, Interaction
δ
δ
Young
Aged
*
*
*
TFEB Protein (A.U)
20
15
10
5
0
Combined
Male
Female
C
Age, Interaction
p=0.057
δ
*
TFE3 Protein (A.U.)
4
3
2
1
0
Combined
Male
Female

Figure 9:

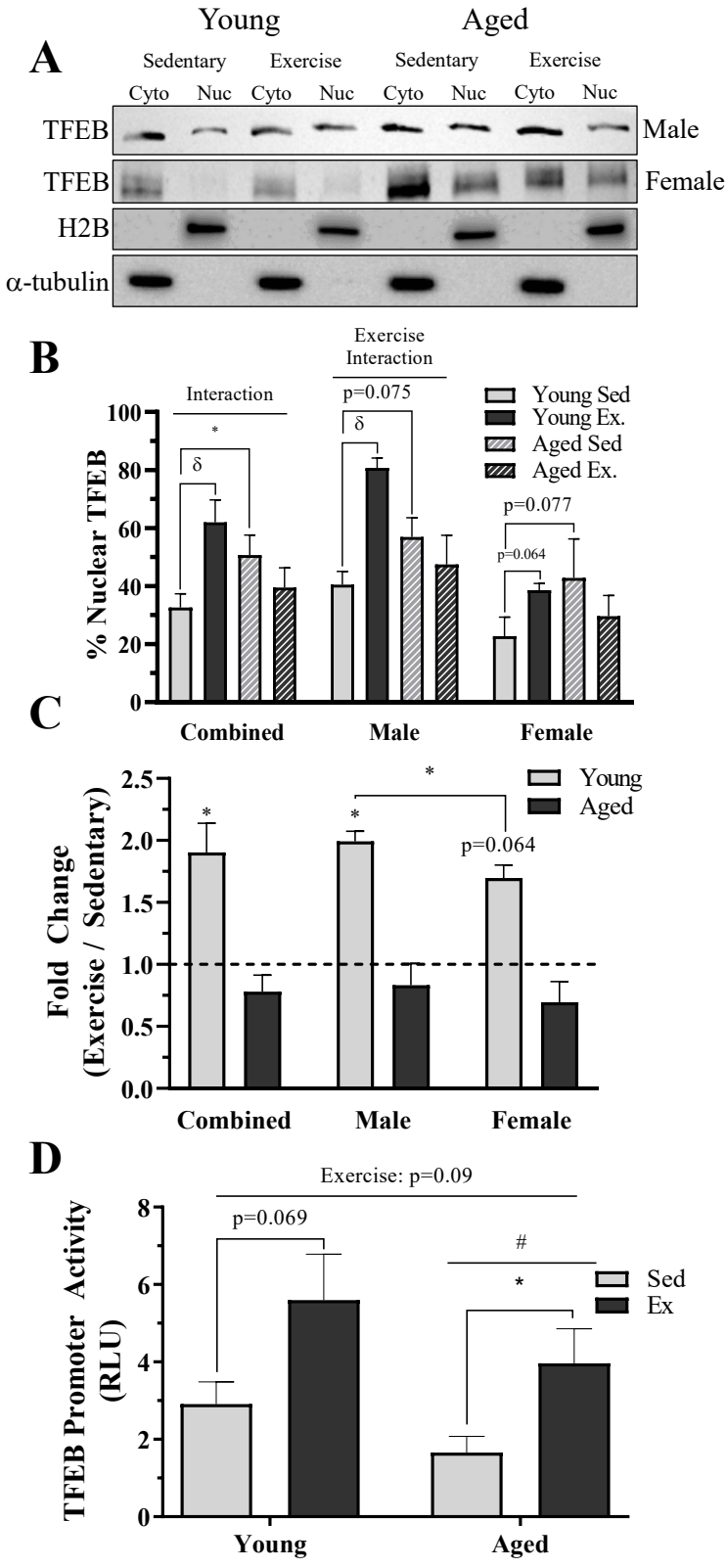
Young
Aged
A
Sedentary
Exercise
Sedentary
Exercise
Cyto
Nuc
Cyto
Nuc
Cyto
Nuc
Cyto
Nuc
TFEB
Male
TFEB
Female
H2B
α-tubulin
B
Exercise Interaction
Interaction
p=0.075
Young Sed
Young Ex.
Aged Sed
Aged Ex.
% Nuclear TFEB
p=0.077
p=0.064
Combined
Male
Female
C
Young
Aged
Fold Change (Exercise / Sedentary)
p=0.064
Combined
Male
Female
D
Exercise: p=0.09
p=0.069
Sed
Ex
TFEB Promoter Activity (RLU)
Young
Aged

References:

1. **Janssen I**, **Heymsfield SB**, **Wang Z**, **Ross R**. Skeletal muscle mass and distribution in 468 men and women aged 18–88 yr. *Journal of Applied Physiology* 89: 81–88, 2000. doi: 10.1152/JAPPL.2000.89.1.81.

2. **Janssen I**, **Heymsfield SB**, **Ross R**. Low relative skeletal muscle mass (sarcopenia) in older persons is associated with functional impairment and physical disability. *Journal of the American Geriatrics Society* 50: 889–96, 2002.

3. **Larsson L**, **Degens H**, **Li M**, **Salviati L**, **Lee Y il**, **Thompson W**, **Kirkland JL**, **Sandri M**. Sarcopenia: Aging-Related Loss of Muscle Mass and Function. *Physiological Reviews* 99: 427, 2019. doi: 10.1152/PHYSREV.00061.2017.

4. **Argilés JM**, **Campos N**, **Lopez-Pedrosa JM**, **Rueda R**, **Rodriguez-Mañas L**. Skeletal Muscle Regulates Metabolism via Interorgan Crosstalk: Roles in Health and Disease. *Journal of the American Medical Directors Association* 17: 789–796, 2016. doi: 10.1016/J.JAMDA.2016.04.019.

5. **Rejeski WJ**, **Mihalko SL**. Physical Activity and Quality of Life in Older Adults. *The Journals of Gerontology Series A: Biological Sciences and Medical Sciences* 56: 23–35, 2001. doi: 10.1093/gerona/56.suppl_2.23.

6. **McPhee JS**, **French DP**, **Jackson D**, **Nazroo J**, **Pendleton N**, **Degens H**. Physical activity in older age: perspectives for healthy ageing and frailty. *Biogerontology* 17: 567–80, 2016. doi: 10.1007/s10522-016-9641-0.

7. **Caspersen CJ**, **Pereira MA**, **Curran KM**. Changes in physical activity patterns in the United States, by sex and cross-sectional age. *Medicine and science in sports and exercise* 32: 1601–9, 2000.

8. **Azagba S**, **Sharaf MF**. Physical Inactivity among Older Canadian Adults. *Journal of Physical Activity and Health* 11: 99–108, 2014. doi: 10.1123/jpah.2011-0305.

9. **Joseph A-M**, **Adhihetty PJ**, **Buford TW**, **Wohlgemuth SE**, **Lees HA**, **Nguyen LM-D**, **Aranda JM**, **Sandesara BD**, **Pahor M**, **Manini TM**, **Marzetti E**, **Leeuwenburgh C**. The impact of aging on mitochondrial function and biogenesis pathways in skeletal muscle of sedentary high- and low-functioning elderly individuals. *Aging cell* 11: 801–9, 2012. doi: 10.1111/j.1474-9726.2012.00844.x.

10. **Zampieri S**, **Pietrangelo L**, **Loefler S**, **Fruhmann H**, **Vogelauer M**, **Burggraf S**, **Pond A**, **Grim-Stieger M**, **Cvecka J**, **Sedliak M**, **Tirpakova V**, **Mayr W**, **Sarabon N**, **Rossini K**, **Barberi L**, **de Rossi M**, **Romanello V**, **Boncompagni S**, **Musaro A**, **Sandri M**, **Protasi F**, **Carraro U**, **Kern H**. Lifelong Physical Exercise Delays Age-Associated Skeletal Muscle Decline. *The Journals of Gerontology Series A: Biological Sciences and Medical Sciences* 70: 163–173, 2015. doi: 10.1093/gerona/glu006.

11. **Pohl C**, **Dikic I**. Cellular quality control by the ubiquitin-proteasome system and autophagy. *Science* 366: 818–822, 2019.

12. **Raben N**, **Hill V**, **Shea L**, **Takikita S**, **Baum R**, **Mizushima N**, **Ralston E**, **Plotz P**. Suppression of autophagy in skeletal muscle uncovers the accumulation of ubiquitinated proteins and their potential role in muscle damage in Pompe disease. *Human Molecular Genetics* 17: 3897–908, 2008. doi: 10.1093/hmg/ddn292.

13. **Masiero E**, **Agatea L**, **Mammucari C**, **Blaauw B**, **Loro E**, **Komatsu M**, **Metzger D**, **Reggiani C**, **Schiaffino S**, **Sandri M**. Autophagy Is Required to Maintain Muscle Mass. *Cell Metabolism* 10: 507–515, 2009. doi: 10.1016/j.cmet.2009.10.008.

14. **Carnio S**, **LoVerso F**, **Baraibar MA**, **Longa E**, **Khan MM**, **Maffei M**, **Reischl M**, **Canepari M**, **Loefler S**, **Kern H**, **Blaauw B**, **Friguet B**, **Bottinelli R**, **Rudolf R**, **Sandri M**. Autophagy Impairment in Muscle Induces Neuromuscular Junction Degeneration and Precocious Aging. *Cell Reports* 8: 1509–1521, 2014. doi: 10.1016/j.celrep.2014.07.061.

15. **Paré MF**, **Baechler BL**, **Fajardo VA**, **Earl E**, **Wong E**, **Campbell TL**, **Tupling AR**, **Quadrilatero J**. Effect of acute and chronic autophagy deficiency on skeletal muscle apoptotic signaling, morphology, and function. *Biochimica et Biophysica Acta - Molecular Cell Research* 1864: 708–718, 2017. doi: 10.1016/j.bbamcr.2016.12.015.

16. **Nemazanyy I**, **Blaauw B**, **Paolini C**, **Caillaud C**, **Protasi F**, **Mueller A**, **Proikas-Cezanne T**, **Russell RC**, **Guan KL**, **Nishino I**, **Sandri M**, **Pende M**, **Panasyuk G**. Defects of Vps15 in skeletal muscles lead to autophagic vacuolar myopathy and lysosomal disease. *EMBO Molecular Medicine* 5: 870–890, 2013. doi: 10.1002/emmm.201202057.

17. **Lira VA**, **Okutsu M**, **Zhang M**, **Greene NP**, **Laker RC**, **Breen DS**, **Hoehn KL**, **Yan Z**. Autophagy is required for exercise training-induced skeletal muscle adaptation and improvement of physical performance. *FASEB journal : official publication of the Federation of American Societies for Experimental Biology* 27: 4184–93, 2013. doi: 10.1096/fj.13-228486.

18. **Grumati P**, **Coletto L**, **Schiavinato A**, **Castagnaro S**, **Bertaggia E**, **Sandri M**, **Bonaldo P**. Physical exercise stimulates autophagy in normal skeletal muscles but is detrimental for collagen VI-deficient muscles. *Autophagy* 7: 1415–23, 2011. doi: 10.4161/AUTO.7.12.17877.

19. **He C**, **Bassik MC**, **Moresi V**, **Sun K**, **Wei Y**, **Zou Z**, **An Z**, **Loh J**, **Fisher J**, **Sun Q**, **Korsmeyer S**, **Packer M**, **May HI**, **Hill JA**, **Virgin HW**, **Gilpin C**, **Xiao G**, **Bassel-Duby R**, **Scherer PE**, **Levine B**. Exercise-induced BCL2-regulated autophagy is required for muscle glucose homeostasis. *Nature* 481: 511–515, 2012. doi: 10.1038/nature10758.

20. **Triolo M**, **Hood DA**. Manifestations of Age on Autophagy, Mitophagy and Lysosomes in Skeletal Muscle. *Cells 2021, Vol 10, Page 1054* 10: 1054, 2021. doi: 10.3390/CELLS10051054.

21. **Baehr LM**, **West DWD**, **Marcotte G**, **Marshall AG**, **de Sousa LG**, **Baar K**, **Bodine SC**. Age-related deficits in skeletal muscle recovery following disuse are associated with neuromuscular junction instability and ER stress, not impaired protein synthesis. *Aging* 8: 127–146, 2016. doi: 10.18632/aging.100879.

22. **Carter HN**, **Kim Y**, **Erlich AT**, **Zarrin-khat D**, **Hood DA**. Autophagy and mitophagy flux in young and aged skeletal muscle following chronic contractile activity. *Journal of Physiology* 596: 3568–3584, 2018. doi: 10.1113/JP275998.

23. **O'Leary MF**, **Vainshtein A**, **Iqbal S**, **Ostojic O**, **Hood DA**. Adaptive plasticity of autophagic proteins to denervation in aging skeletal muscle. *American Journal of Physiology-Cell Physiology* 304: C422–C430, 2013. doi: 10.1152/ajpcell.00240.2012.

24. **Chen CCW**, **Erlich AT**, **Crilly MJ**, **Hood DA**. Parkin is required for exercise-induced mitophagy in muscle: impact of aging. *American Journal of Physiology-Endocrinology and Metabolism* 315: E404–E415, 2018. doi: 10.1152/ajpendo.00391.2017.

25. **Carter HN**, **Kim Y**, **Erlich AT**, **Zarrin-khat D**, **Hood DA**. Autophagy and mitophagy flux in young and aged skeletal muscle following chronic contractile activity. *The Journal of Physiology* 596: 3567–3584, 2018. doi: 10.1113/JP275998.

26. **Vainshtein A**, **Hood DA**. The regulation of autophagy during exercise in skeletal muscle. *Journal of applied physiology (Bethesda, Md : 1985)* 120: 664–73, 2016. doi: 10.1152/japplphysiol.00550.2015.

27. **Erlich AT**, **Brownlee DM**, **Beyfuss K**, **Hood DA**. Exercise induces TFEB expression and activity in skeletal muscle in a PGC-1α-dependent manner. *American Journal of Physiology-Cell Physiology* 314: C62–C72, 2018. doi: 10.1152/ajpcell.00162.2017.

28. **Kim Y**, **Triolo M**, **Hood DA**. Impact of Aging and Exercise on Mitochondrial Quality Control in Skeletal Muscle. *Oxidative medicine and cellular longevity* 2017: 3165396, 2017. doi: 10.1155/2017/3165396.

29. **Carter HN**, **Chen CCW**, **Hood DA**. Mitochondria, Muscle Health, and Exercise with Advancing Age. *Physiology* 30: 208–223, 2015. doi: 10.1152/physiol.00039.2014.

30. **Hood DA**, **Memme JM**, **Oliveira AN**, **Triolo M**. Maintenance of skeletal muscle mitochondria in health, exercise, and aging. *Annual Review of Physiology* 81: 19–41, 2019. doi: 10.1146/annurev-physiol-020518-114310.

31. **Kim Y**, **Hood DA**. Regulation of the autophagy system during chronic contractile activity-induced muscle adaptations. *Physiological Reports* 5: e13307, 2017. doi: 10.14814/phy2.13307.

32. **Ju J-S**, **Jeon S-I**, **Park J-Y**, **Lee J-Y**, **Lee S-C**, **Cho K-J**, **Jeong J-M**. Autophagy plays a role in skeletal muscle mitochondrial biogenesis in an endurance exercise-trained condition. *Journal of Physiological Sciences* 66: 417–430, 2016. doi: 10.1007/s12576-016-0440-9.

33. **Rosa-Caldwell ME**, **Lim S**, **Haynie WA**, **Brown JL**, **Deaver JW**, **Silva FM da**, **Jansen LT**, **Lee DE**, **Wiggs MP**, **Washington TA**, **Greene NP**. Female mice may have exacerbated catabolic signalling response compared to male mice during development and progression of disuse atrophy. *Journal of Cachexia, Sarcopenia and Muscle* 12: 717–730, 2021. doi: 10.1002/JCSM.12693.

34. **Rosa-Caldwell ME**, **Lim S**, **Haynie WS**, **Jansen LT**, **Westervelt LC**, **Amos MG**, **Washington TA**, **Greene NP**. Altering aspects of mitochondrial quality to improve

musculoskeletal outcomes in disuse atrophy. *Journal of Applied Physiology* 129: 1290–1303, 2020. doi: 10.1152/JAPPLPHYSIOL.00407.2020.

35. **White Z**, **Terrill J**, **White RB**, **McMahon C**, **Sheard P**, **Grounds MD**, **Shavlakadze T**. Voluntary resistance wheel exercise from mid-life prevents sarcopenia and increases markers of mitochondrial function and autophagy in muscles of old male and female C57BL/6J mice. *Skeletal Muscle 2016 6:1* 6: 1–21, 2016. doi: 10.1186/S13395-016-0117-3.

36. **Adhihetty PJ**, **Ljubicic V**, **Hood DA**. Effect of chronic contractile activity on SS and IMF mitochondrial apoptotic susceptibility in skeletal muscle. *American Journal of Physiology - Endocrinology and Metabolism* 292: 748–755, 2007. doi: 10.1152/ajpendo.00311.2006.

37. **Cogswell AM**, **Stevens RJ**, **Hood DA**. Properties of skeletal muscle mitochondria from subsarcolemmal and intermyofibrillar isolated regions. *The American Journal of Physiology - Cell Physiology* 264: C383-389, 1993. doi: 10.1152/ajpcell.1993.264.2.C383.

38. **Takahashi M**, **Hood DA**. Protein import into subsarcolemmal and intermyofibrillar skeletal muscle mitochondria. Differential import regulation in distinct subcellular regions. *The Journal of biological chemistry* 271: 27285–27291, 1996.

39. **Perry CGR**, **Kane DA**, **Lin C Te**, **Kozy R**, **Cathey BL**, **Lark DS**, **Kane CL**, **Brophy PM**, **Gavin TP**, **Anderson EJ**, **Neufer PD**. Inhibiting myosin-ATPase reveals a dynamic range of mitochondrial respiratory control in skeletal muscle. *Biochemical Journal* 437: 215–222, 2011. doi: 10.1042/BJ20110366.

40. **Santilli V**, **Bernetti A**, **Mangone M**, **Paoloni M**. Clinical definition of sarcopenia. *Clinical Cases in Mineral and Bone Metabolism* 11: 177–80, 2014.

41. **Hood DA**, **Memme JM**, **Oliveira AN**, **Triolo M**. Maintenance of skeletal muscle mitochondria in health, exercise, and aging. *Annual Review of Physiology* 81: 19–41, 2019. doi: 10.1146/annurev-physiol-020518-114310.

42. **Kim Y**, **Triolo M**, **Erlich AT**, **Hood DA**. Regulation of autophagic and mitophagic flux during chronic contractile activity-induced muscle adaptations. *Pflugers Archiv* 471: 431–440, 2019. doi: 10.1007/s00424-018-2225-x.

43. **Kim Y**, **Hood DA**. Regulation of the autophagy system during chronic contractile activity-induced muscle adaptations. *Physiological Reports* 5, 2017. doi: 10.14814/phy2.13307.

44. **Staron RS**, **Hagerman FC**, **Hikida RS**, **Murray TF**, **Hostler DP**, **Crill MT**, **Ragg KE**, **Toma K**. Fiber Type Composition of the Vastus Lateralis Muscle of Young Men and Women: *http://dx.doi.org/101177/002215540004800506* 48: 623–629, 2016. doi: 10.1177/002215540004800506.

45. **Gao Y**, **Arfat Y**, **Wang H**, **Goswami N**. Muscle Atrophy Induced by Mechanical Unloading: Mechanisms and Potential Countermeasures. *Frontiers in Physiology* 9: 235, 2018. doi: 10.3389/FPHYS.2018.00235.

46. **Brocca L**, **Cannavino J**, **Coletto L**, **Biolo G**, **Sandri M**, **Bottinelli R**, **Pellegrino MA**. The time course of the adaptations of human muscle proteome to bed rest and the underlying mechanisms. *The Journal of Physiology* 590: 5211, 2012. doi: 10.1113/JPHYSIOL.2012.240267.

47. **DB T**, **RE H**, **D S**, **KM B**. Time course of soleus muscle myosin expression during hindlimb suspension and recovery. *Journal of applied physiology (Bethesda, Md : 1985)* 63: 130–137, 1987. doi: 10.1152/JAPPL.1987.63.1.130.

48. **Mauvais-Jarvis F**. Sex differences in metabolic homeostasis, diabetes, and obesity. *Biology of Sex Differences* 6, 2015. doi: 10.1186/S13293-015-0033-Y.

49. **Rosa-Caldwell ME**, **Lim S**, **Haynie WS**, **Jansen LT**, **Westervelt LC**, **Amos MG**, **Washington TA**, **Greene NP**. Altering aspects of mitochondrial quality to improve musculoskeletal outcomes in disuse atrophy. *Journal of Applied Physiology* 129: 1290–1303, 2020. doi: 10.1152/JAPPLPHYSIOL.00407.2020.

50. **Yoshihara T**, **Natsume T**, **Tsuzuki T**, **Chang S**, **Kakigi R**, **Sugiura T**, **Naito H**. Sex differences in forkhead box O3a signaling response to hindlimb unloading in rat soleus muscle. *The Journal of Physiological Sciences 2018 69:2* 69: 235–244, 2018. doi: 10.1007/S12576-018-0640-6.

51. **Colom B**, **Alcolea M**, **Valle A**, **Oliver J**, **Roca P**, **García-Palmer F**. Skeletal Muscle of Female Rats Exhibit Higher Mitochondrial Mass and Oxidative-Phosphorylative Capacities Compared to Males. *Cellular Physiology and Biochemistry* 19: 205–212, 2007. doi: 10.1159/000099208.

52. **Hicks AL**, **Kent-Braun J**, **Ditor DS**. Sex differences in human skeletal muscle fatigue. *Exercise and sport sciences reviews* 29: 109–112, 2001. doi: 10.1097/00003677-200107000-00004.

53. **Lundsgaard A-M**, **Kiens B**. Gender Differences in Skeletal Muscle Substrate Metabolism – Molecular Mechanisms and Insulin Sensitivity. *Frontiers in Endocrinology* 0: 195, 2014. doi: 10.3389/FENDO.2014.00195.

54. **Ansdell P**, **Thomas K**, **Hicks KM**, **Hunter SK**, **Howatson G**, **Goodall S**. Physiological sex differences affect the integrative response to exercise: acute and chronic implications. *Experimental Physiology* 105: 2007–2021, 2020. doi: 10.1113/EP088548.

55. **Broida J**, **Svare B**. Sex Differences in the Activity of Mice: Modulation by Postnatal Gonadal Hormones. *Hormones and Behaviour* 18: 65–78, 1984. doi: 10.1016/0018-506x(84)90051-5.

56. **König C**, **Plank A-C**, **Kapp A**, **Timotius IK**, **von Hörsten S**, **Zimmermann K**. Thirty Mouse Strain Survey of Voluntary Physical Activity and Energy Expenditure: Influence of Strain, Sex and Day–Night Variation. *Frontiers in Neuroscience* 0: 531, 2020. doi: 10.3389/FNINS.2020.00531.

57. **Piekarski A**, **Khaldi S**, **Greene E**, **Lassiter K**, **Mason JG**, **Anthony N**, **Bottje W**, **Dridi S**. Tissue Distribution, Gender- and Genotype-Dependent Expression of Autophagy-

Related Genes in Avian Species. *PLoS ONE* 9: 112449, 2014. doi: 10.1371/JOURNAL.PONE.0112449.

58. **Kang R**, **Zeh HJ**, **Lotze MT**, **Tang D**. The Beclin 1 network regulates autophagy and apoptosis. *Cell death and differentiation* 18: 571–580, 2011. doi: 10.1038/cdd.2010.191.

59. **Yu L**, **Chen Y**, **Tooze SA**. Autophagy pathway: Cellular and molecular mechanisms. *Autophagy* 14 Taylor and Francis Inc.: 207–215, 2018.

60. **Yoshii SR**, **Mizushima N**. Monitoring and measuring autophagy. *International Journal of Molecular Sciences* 18: 1865, 2017. doi: 10.3390/ijms18091865.

61. **Lippai M**, **Lőw P**. The Role of the Selective Adaptor p62 and Ubiquitin-Like Proteins in Autophagy. *BioMed Research International* 2014: ., 2014. doi: 10.1155/2014/832704.

62. **Liu WJ**, **Ye L**, **Huang WF**, **Guo LJ**, **Xu ZG**, **Wu HL**, **Yang C**, **Liu HF**. p62 links the autophagy pathway and the ubiqutin-proteasome system upon ubiquitinated protein degradation. *Cellular and Molecular Biology Letters* 21: ., 2016.

63. **Oliván S**, **Calvo AC**, **Manzano R**, **Zaragoza P**, **Osta R**. Sex Differences in Constitutive Autophagy. *BioMed Research International* 2014, 2014. doi: 10.1155/2014/652817.

64. **Chen CC**, **Erlich AT**, **Hood DA**. Role of Parkin and endurance training on mitochondrial turnover in skeletal muscle. *Skeletal Muscle* 8: 1–14, 2018. doi: 10.1186/s13395-018-0157-y.

65. **Vainshtein A**, **Desjardins EM**, **Armani A**, **Sandri M**, **Hood DA**. PGC-1α modulates denervation-induced mitophagy in skeletal muscle. *Skeletal Muscle* 5: 9, 2015. doi: 10.1186/s13395-015-0033-y.

66. **Vainshtein A**, **Tryon LD**, **Pauly M**, **Hood DA**. Role of PGC-1α during acute exercise-induced autophagy and mitophagy in skeletal muscle. *American Journal of Physiology Cell Physiology* 308: C710-9, 2015. doi: 10.1152/ajpcell.00380.2014.

67. **Triolo M**, **Hood DA**. Mitochondrial breakdown in skeletal muscle and the emerging role of the lysosomes. *Archives of Biochemistry and Biophysics* 661: 66–73, 2019. doi: 10.1016/j.abb.2018.11.004.

68. **Hütter E**, **Skovbro M**, **Lener B**, **Prats C**, **Rabøl R**, **Dela F**, **Jansen-Dürr P**. Oxidative stress and mitochondrial impairment can be separated from lipofuscin accumulation in aged human skeletal muscle. *Aging Cell* 6: 245–256, 2007. doi: 10.1111/j.1474-9726.2007.00282.x.

69. **Fernando R**, **Castro JP**, **Flore T**, **Deubel S**, **Grune T**, **Ott C**. Age-Related Maintenance of the Autophagy-Lysosomal System Is Dependent on Skeletal Muscle Type. *Oxidative Medicine and Cellular Longevity* 2020, 2020. doi: 10.1155/2020/4908162.

70. **Napolitano G**, **Ballabio A**. TFEB at a glance. *Journal of cell science* 129: 2475–2481, 2016.

71. **Settembre C**, **di Malta C**, **Polito VA**, **Garcia Arencibia M**, **Vetrini F**, **Erdin S**, **Erdin SU**, **Huynh T**, **Medina D**, **Colella P**, **Sardiello M**, **Rubinsztein DC**, **Ballabio A**. TFEB

links autophagy to lysosomal biogenesis. *Science (New York, NY)* 332: 1429–33, 2011. doi: 10.1126/science.1204592.

72. **Ljubicic V**, **Joseph A-M**, **Adhihetty PJ**, **Huang JH**, **Saleem A**, **Uguccioni G**, **Hood DA**. Molecular basis for an attenuated mitochondrial adaptive plasticity in aged skeletal muscle. *Aging* 1: 818–830, 2009.

73. **Ljubicic V**, **Hood DA**. Specific attenuation of protein kinase phosphorylation in muscle with a high mitochondrial content. *American Journal of Physiology-Endocrinology and Metabolism* 297: E749–E758, 2009. doi: 10.1152/ajpendo.00130.2009.

Chapter Six: Summary, Conclusion and Future Direction

6.1. SUMMARY AND CONCLUSIONS

Skeletal muscle displays a high degree of plasticity, responding to the demands placed upon it. With both chronic muscle disuse and advancing age, there are declines in muscle mass (i.e., atrophy) concomitant with deficits in mitochondrial and tissue quality (1–3). With age, this process is referred to as sarcopenia. In recent years, significant advances have been made to uncover the processes that underly denervation atrophy and age-related sarcopenia. Although there are multiple mechanisms involved in these phenotypic changes, of particular interest is protein and organelle turnover mediated by the autophagy-lysosome system. This has implications of mitochondrial health, as this system is responsible for the selective degradation of these organelles through mitophagy. Presently, it remains unclear as to whether there are similar or divergent effects of these two stimuli on the regulation autophagy and mitophagy in muscle.

There are many positive influences of a single bout of exercise on muscle health, one of which is the activation of autophagy and mitophagy. This is integral as mitophagy acts to prune the mitochondrial pool and eliminate non-functional components, thereby creating space for newly synthesized, properly functioning components. Over time, these acute exercise-induced changes in proteolysis, coupled with the biogenesis of new constituents such as mitochondria, leads to a healthier tissue. As such, endurance-style exercise is a potent stimulus for both muscular and mitochondrial restoration in muscle (1, 3, 4). However, this “renovation” of the muscle is blunted in senescent muscle (1, 3, 4). Thus, there is a need to understand how acute exercise differentially influences the autophagy-lysosome system in young versus aged muscle.

Finally, in various tissues, muscle included, sex differences are apparent in mitochondrial and autophagic regulation (5, 6). However, many of these reports are characterizations in young-healthy muscle. Thus, the regulation of autophagy, mitophagy and lysosome biogenesis remains largely unexplored in the context of aging and acute exercise.

The overall goal of this Dissertation was to understand the molecular signaling and the proteins involved in mediating autophagy, mitophagy and lysosome content in skeletal muscle, employing in-vivo techniques. Through the manuscripts and supplemental work, we will 1) further our understanding of these processes during two conditions of muscle atrophy; 2) provide insight into the temporal regulation of these processes at the early phases of denervation; 3) uncover mechanistic differences in a sex-specific manner; and 4) elucidate whether exercise can activate these processes to remodel muscle in an age- and sex- dependent manner. Advancing knowledge in these areas swill help us understand the molecular basis autophagy, mitophagy and lysosome biosynthesis during conditions of muscle wasting, and has become the focus of my doctoral work.

Objective 1: We first investigated temporal changes in skeletal muscle mitochondria, the autophagy-lysosome system and mitophagy in response to denervation. We had previously shown that in response to 7 days of denervation, there are declines in autophagy flux, but elevations in mitophagy flux (7), which corresponds to a time in which mitochondrial (8) and lysosomal (9) impairments are present. To determine the events preceding this change at 7 days, we unilaterally denervated Sprague-Dawley rats for 1, 3, or 7 days. We also isolated the two distinct subpopulations of mitochondria (subsarcolemmal, SS; Intermyofibrillar, IMF) to determine how their response differs to denervation. We hypothesized that autophagy and mitophagy flux would be enhanced with denervation to eliminate the accumulating dysfunctional mitochondria and damaged proteins typically observed with denervation. We further hypothesized that lysosome

content will be upregulated throughout the course of denervation to enhance the capacity for this accumulating autophagic demand. We measured indices of mitochondrial impairment as early as 1-day post-denervation, suggesting that mitochondrial dysfunction precedes atrophy, which was apparent at 3 days. Denervation also upregulated both autophagic and lysosomal protein content in a time-dependent manner, which may be explained by our observed increase in nuclear TFEB protein. This upregulation of lysosome content may serve as a mechanism to enhance the capacity for autophagosomal degradation. We also treated a subset of animals with the microtubule destabilizer colchicine via intraperitoneal injection for 2 days prior to sacrifice. This allowed us to measure autophagic and mitophagic flux, at least up to the point of lysosome delivery. We found that autophagy and SS mitophagy flux were enhanced in the early (i.e., 1 and 3 days) timepoints, whereas IMF mitophagy flux was unchanged. We also demonstrated, using transgenic mt-Keima mice, that mitophagy flux is enhanced at the early 1-day post-denervation timepoint. Although we saw these divergent effects early in our time-course, we measured a global deficit in autophagy and mitophagy flux at 7-days post-denervation. This is a finding that we attribute to accumulating lysosomal impairment, as observed by the presence of vacuolar inclusions. This study provides evidence that autophagy and mitophagy flux are biphasic, increasing early post-denervation, followed by later decrements. Further, we provide insight into how lysosome content may be upregulated in denervation, through an early increase in nuclear TFEB, and that this capacity may be blunted to due organelle dysfunction.

Objective 2: Work from our group has reported increases in autophagic flux (10), mitophagic flux (11), and lysosome biogenesis (12) in young healthy muscle following the cessation of acute exercise. However, the impact of biological sex and the influence of age have yet to be studied in this context. Furthermore, the interaction of these two variables on the aforementioned

mechanisms remain undefined. Thus, our goal with this objective was two-fold. First, we wanted to examine the effect of biological sex on the regulation of autophagy, mitophagy and lysosome biogenesis at baseline (sedentary) in young versus old muscle. Second, we aimed to understand how both sex and aging influence the acute exhaustive exercise response of these processes. Thus, for this study, we compared young (4-6 months) and aged (22-24 months) male and female mice, who were either assigned to a sedentary, or an acute exercise group.

In regard to our first aim, exploring sex differences in sedentary young and aged muscle, we hypothesized that mitochondrial content would be reduced in aged animals, irrespective of biological sex. To our surprise we uncovered that in skeletal muscle female mice, regardless of age, contain more mitochondria, and that age-related declines in mitochondrial content is male specific. We next hypothesized, based on previous reports (5, 13), that there would be greater levels of autophagy and mitophagy in female mice. However, we were unsure how age would impact these processes in muscle, as it has not been explored in the past. In support of our hypothesis, we measured a greater abundance of autophagy and lysosome-related protein in young female mice versus male counterparts. Inference, based on p62 and LC3 protein in whole muscle samples support the notion that the muscle from females have greater level of autophagosomal clearance. This seems to be the case in aged females as well. Furthermore, in support of our hypothesis, young and aged females have greater autophagy and mitophagy proteins versus age-matched male counterparts. Finally, both aged muscle from both male and female mice had a greater relative abundance of nuclear TFEB than that of young sex-matched counterparts. Thus, in sedentary animals, we uncovered a sex difference that is not age-dependent, the first time this has been reported. Specifically, there is greater autophagy in the muscle from female mice in comparison to age-matched males.

The second aim within this objective was to assess how exercise can moderate autophagy and lysosome biogenesis with a focus on sex differences and aging. We hypothesized that the exercise-induced elevation in autophagosomal clearance and lysosome biogenesis would be age-specific, whereby young animals would have a greater response than aged animals. This is based on previous literature showing that aging muscle has a blunted response to exercise-induced adaptations (1, 3, 4). Unexpectedly, we found that exercise in young males was able to stimulate autophagosome clearance, measured via western blotting for related proteins. This observation that was not matched in young females. Regarding lysosome biogenesis, we utilized a TFEB-promoter activity assay, and found that exercise stimulated TFEB transcription. Although both young males and females had an upregulation of nuclear TFEB protein, which may promote autophagy and lysosome related gene expression, the exercise-induced effect was greater in the male mice. Thus, in young muscle, we uncovered, for the first time, that biological sex influences the autophagy and lysosome response to endurance-style exercise. Finally, in support of our hypothesis, aged muscle did not show any evidence of increases in autophagosomal degradation or increases in nuclear TFEB protein, irrespective of sex. However, an important finding was that aged muscle was able to upregulate TFEB-promoter activity to a greater extent than that of young muscle, which may indicate that the exercise can, at least in part, stimulate lysosome biosynthesis. Thus, our major findings from this portion of the study are that exercise can serve to remodel skeletal muscle of young animals, an effect that is impacted by biological sex. However, it seems that with aging, the ability of acute exhaustive exercise to stimulate autophagy and lysosome biogenesis is blunted. These findings have major implications of the design of exercise-based interventions to slow the progression of sarcopenia in males and females.

Overall Conclusion: Denervation is a potent model of skeletal muscle disuse and can mimic aspects of the aging phenotype. In contrast, aging is a multifactor process that leads to muscle atrophy and functional decline. In recent years significant advances have been made to uncover mechanisms that underly the wasting of muscle in these two models. Although denervation and aging are inherently different, through these studies we successfully uncovered a common modulation of the autophagy-lysosome system. Specifically, there is an upregulation in autophagy, mitophagy and lysosome-related protein expression, which likely serve to enhance the capacity for autophagic breakdown. Our work investigating these processes in young and aged muscle provides novel insight into how biological sex can influence both the aging-phenotype and the acute exercise-induced plasticity of the muscle. Work from this Dissertation contributes to are understanding of how muscle undergoes wasting in various physiological conditions. This advanced knowledge will undoubtedly be beneficial in the development of future therapeutic strategies aimed at maintaining skeletal muscle health.

6.2. EXPERIMENTAL LIMITATIONS AND FUTURE DIRECTIONS

Based on our findings from the studies within this dissertation, the autophagy-lysosome system undergoes significant changes in denervated and aged muscle. Furthermore, exercise has the capacity to enhance the health of the muscle through the activation of autophagic clearance and lysosome biogenesis, at least in young muscle. Finally, we have identified biological sex as an integral factor to consider in studies on muscle biochemistry and plasticity. However, several questions remain due to 1) the experimental limitations of our work and 2) the future directions that we envision, based on our findings. These are outlined below:

1 – Assessing sex differences in denervation-atrophy

Based on our findings in Chapter 5 there is a clear need to study muscle physiology in a sex-specific manner. This step is necessary to ensure that as we develop therapeutic strategies, they must be optimized based on such biological factors. However, in our first manuscript, we have only utilized young, healthy, male rats and mt-keima mice. Thus, future work should aim to examine basal and denervation-induced changes in the autophagy, mitophagy and lysosome system with more consideration for sex.

2 – Examining these processes in other muscle fiber types

In our denervation model (Chapter 4), we transect the peroneal nerve, which acts as a complete disuse model in both the tibialis anterior and extensor digitorum longus muscles. Although the data we generate are valuable, the changes we see are specific to a predominantly fast-twitch muscle group. Thus, future work should explore whether similar regulation exists in tonic, predominantly slow-twitch muscle such as the soleus. Furthermore, due to experimental limitations in our second manuscript, we assessed whole muscle markers in the mixed-fiber type quadricep muscle, TFEB-promoter activity in the mixed gastrocnemius muscle, nuclear protein in the predominantly fast tibialis anterior muscle, and isolated mitochondria from the remaining muscle (hamstrings, triceps, pectoralis muscle). Thus, future studies should examine muscle-specific changes, as there is a divergent response to aging in slow versus fast muscle, as discussed in Chapter 2.4.1.1. This work will delineate how aging, sex and acute exercise interact to influence muscle autophagy, and may lead to novel treatments for age-related sarcopenia.

3 – Assessing autophagy and mitophagy flux by alternative means

In Chapter 5, we have interpreted changes in autophagy based on static, "snapshot" measures of early autophagy and late stage autophagosomal proteins. Although we can make inferences based on this data set, the strength of our analysis is limited. Power in this interpretation would come from the utilization of appropriate "flux" measurements. We have done so successfully in our first manuscript (Chapter 4) via the utilization of colchicine as a method to inhibit autophagosomal breakdown. This allowed for us to compare the difference between a condition treated with saline vs colchicine. A model such as this would be valuable to further understand sex-differences differences in autophagy and mitophagy with aging and exercise. Granted, this method comes with three shortcomings of this experimental model. The first is that it requires 2-times the number of animals, which can be rather costly. Second, this assay only captures "flux" up to the point of transport to the lysosomes. Thus, the model discounts the role of lysosomes in autophagy. Finally, as a microtubule destabilizer, treatment with colchicine likely comes with off-target effects. For example, although treatment with this agent prevents autophagosomal transport, it also stops other essential cell trafficking events. To circumvent this confounding variable, future studies should utilize appropriate fluorescent probes (i.e., tandem-tags, pH sensitive fluorophores, as reviewed in Chapter 2.2.5. of this Dissertation) and associated microscopy to measure autophagy. In this Dissertation, we have begun to explore the utility of such methods. We have successfully developed an *in vivo* model to monitoring mitophagy in muscle through the utilization of mt-keima mice (Appendix A.3., Figure S3-S6). At the present time, this model has been applied in young and aged mouse muscle, and in control and 1,3, and 7 day-denervated muscle (Appendix A.3., Figure S7-S8). Further utilization of these methods, in

adjunct to methods we have utilized in Chapter 4 and 5 of this thesis will provide a clearer picture into sex-differences in muscle autophagy with age and/or denervation.

4 - Assessing and targeting lysosome function

Another major limitation of the current manuscripts was our inability to directly assess lysosome function. For example, in our denervation study (Chapter 4), we are making inferences based on a variety of factors (i.e., inhibited autophagy/mitophagy flux, accumulation of lysosome proteins, TEM quantifications of vacuolar inclusions). In our aging study (Chapter 5) we do not measure lysosome function, but rather infer it based on previous studied. Thus, in both manuscripts assessing lysosome function directly would allow us to understand whether lysosome abnormalities are implicated in the pathophysiology of denervation and sarcopenia. This may in fact stimulate investigation into the merit of treating lysosomes in the prevention of atrophy. Importantly, this limitation is not exclusive to our group. At present, assays to measure function of these organelles have gained traction *in vitro*, but have seldom been applied successfully in muscle, *in vivo*. Focusing on hallmarks of lysosome impairments, such as loss of acidification, membrane instability and swelling of the organelles, may stimulate work of this nature (14). We have, as part of this Dissertation, attempted to understand how we can explore indices of lysosome function in muscle. In fact, we show, *in vitro*, that treating myoblasts with the lysosome-deacidifier chloroquine promotes lysosome swelling (Appendix A.4.; Supplemental Figure 9), suggesting that lysosome impairments are associated with organellar swelling.

If lysosome impairment is in fact implicated in denervation-atrophy or age-related sarcopenia, then there would be value in examining if restoration of organelle function is indeed protective. This has been done in experimental models of various neuropathies. Specifically, TFEB overexpression (15–17) and activation via the small molecule curcumin analog C1 (18) induces

autophagy and lysosome-related gene expression and reduces pathophysiology. Furthermore, AAV-mediated TFEB overexpression attenuated the pathophysiology of Pompe Disease in mouse skeletal muscle (19). Overall, future studies should explore the vitality of treating muscle wasting with lysosomal therapies.

6.3. REFERENCES

1. **Hood DA**, **Memme JM**, **Oliveira AN**, **Triolo M**. Maintenance of skeletal muscle mitochondria in health, exercise, and aging. *Annual Review of Physiology* 81: 19–41, 2019. doi: 10.1146/annurev-physiol-020518-114310.

2. **Tryon LD**, **Vainshtein A**, **Memme JM**, **Crilly MJ**, **Hood DA**. Recent advances in mitochondrial turnover during chronic muscle disuse. *Integrative Medicine Research* 3: 161, 2014. doi: 10.1016/J.IMR.2014.09.001.

3. **Carter HN**, **Chen CCW**, **Hood DA**. Mitochondria, muscle health, and exercise with advancing age. *Physiology* 30: 208–223, 2015. doi: 10.1152/physiol.00039.2014.

4. **Kim Y**, **Triolo M**, **Hood DA**. Impact of Aging and Exercise on Mitochondrial Quality Control in Skeletal Muscle. *Oxidative Medicine and Cellular Longevity* 2017, 2017. doi: 10.1155/2017/3165396.

5. **Gottlieb RA**, **Andres AM**, **Sin J**, **Taylor D**. Untangling Autophagy Measurements: All Fluxed Up. *Circulation Research* 116: 504, 2015. doi: 10.1161/CIRCRESAHA.116.303787.

6. **Rosa-Caldwell ME**, **Greene NP**. Muscle metabolism and atrophy: let's talk about sex. *Biology of Sex Differences 2019 10:1* 10: 1–14, 2019. doi: 10.1186/S13293-019-0257-3.

7. **Vainshtein A**, **Desjardins EM**, **Armani A**, **Sandri M**, **Hood DA**. PGC-1α modulates denervation-induced mitophagy in skeletal muscle. *Skeletal Muscle* 5: 9, 2015. doi: 10.1186/s13395-015-0033-y.

8. **Singh K**, **Hood DA**. Effect of denervation-induced muscle disuse on mitochondrial protein import. *American Journal of Physiology - Cell Physiology* 300: C138-145, 2011. doi: 10.1152/ajpcell.00181.2010.

9. **O'Leary MF**, **Vainshtein A**, **Iqbal S**, **Ostojic O**, **Hood DA**. Adaptive plasticity of autophagic proteins to denervation in aging skeletal muscle. *American Journal of Physiology-Cell Physiology* 304: C422–C430, 2013. doi: 10.1152/ajpcell.00240.2012.

10. **Vainshtein A**, **Tryon LD**, **Pauly M**, **Hood DA**. Role of PGC-1α during acute exercise-induced autophagy and mitophagy in skeletal muscle. *American Journal of Physiology Cell Physiology* 308: C710-9, 2015. doi: 10.1152/ajpcell.00380.2014.

11. **Chen CCW**, **Erlich AT**, **Crilly MJ**, **Hood DA**. Parkin is required for exercise-induced mitophagy in muscle: impact of aging. *American Journal of Physiology-Endocrinology and Metabolism* 315: E404–E415, 2018. doi: 10.1152/ajpendo.00391.2017.

12. **Erlich AT**, **Brownlee DM**, **Beyfuss K**, **Hood DA**. Exercise induces TFEB expression and activity in skeletal muscle in a PGC-1α-dependent manner. *American Journal of Physiology - Cell Physiology* 314: C62–C72, 2017. doi: 10.1152/ajpcell.00162.2017.

13. **Oliván S**, **Calvo AC**, **Manzano R**, **Zaragoza P**, **Osta R**. Sex Differences in Constitutive Autophagy. *BioMed Research International* 2014, 2014. doi: 10.1155/2014/652817.

14. **Wang F**, **Gómez-Sintes R**, **Boya P**. Lysosomal membrane permeabilization and cell death. *Traffic* 19: 918–931, 2018. doi: 10.1111/tra.12613.

15. **Arotcarena M-L**, **Bourdenx M**, **Dutheil N**, **Thiolat M-L**, **Doudnikoff E**, **Dovero S**, **Ballabio A**, **Fernagut P-O**, **Meissner WG**, **Bezard E**, **Dehay B**. Transcription factor EB overexpression prevents neurodegeneration in experimental synucleinopathies. *JCI Insight* 4, 2019. doi: 10.1172/JCI.INSIGHT.129719.

16. **Decressac M**, **Mattsson B**, **Weikop P**, **Lundblad M**, **Jakobsson J**, **Björklund A**. TFEB-mediated autophagy rescues midbrain dopamine neurons from α-synuclein toxicity. *Proceedings of the National Academy of Sciences of the United States of America* 110: E1817, 2013. doi: 10.1073/PNAS.1305623110.

17. **Decressac M**, **Mattsson B**, **Weikop P**, **Lundblad M**, **Jakobsson J**, **Björklund A**. TFEB-mediated autophagy rescues midbrain dopamine neurons from α-synuclein toxicity. *Proceedings of the National Academy of Sciences* 110: E1817–E1826, 2013. doi: 10.1073/PNAS.1305623110.

18. **Song J**, **Malampati S**, **Zeng Y**, **Durairajan SSK**, **Yang C**, **Tong BC**, **Iyaswamy A**, **Shang W**, **Sreenivasmurthy SG**, **Zhu Z**, **Cheung K**, **Lu J**, **Tang C**, **Xu N**, **Li M**. A small molecule transcription factor EB activator ameliorates beta-amyloid precursor protein and Tau pathology in Alzheimer's disease models. *Aging Cell* 19, 2020. doi: 10.1111/ACEL.13069.

19. **Gatto F**, **Rossi B**, **Tarallo A**, **Polishchuk E**, **Polishchuk R**, **Carrella A**, **Nusco E**, **Alvino FG**, **Iacobellis F**, **de Leonibus E**, **Auricchio A**, **Diez-Roux G**, **Ballabio A**, **Parenti G**. AAV-mediated transcription factor EB (TFEB) gene delivery ameliorates muscle pathology and function in the murine model of Pompe Disease. *Scientific Reports* 7: 15089, 2017. doi: 10.1038/s41598-017-15352-2.

Appendices

APPENDIX A: ADDITIONAL DATA

A.1 Kinase response to denervation

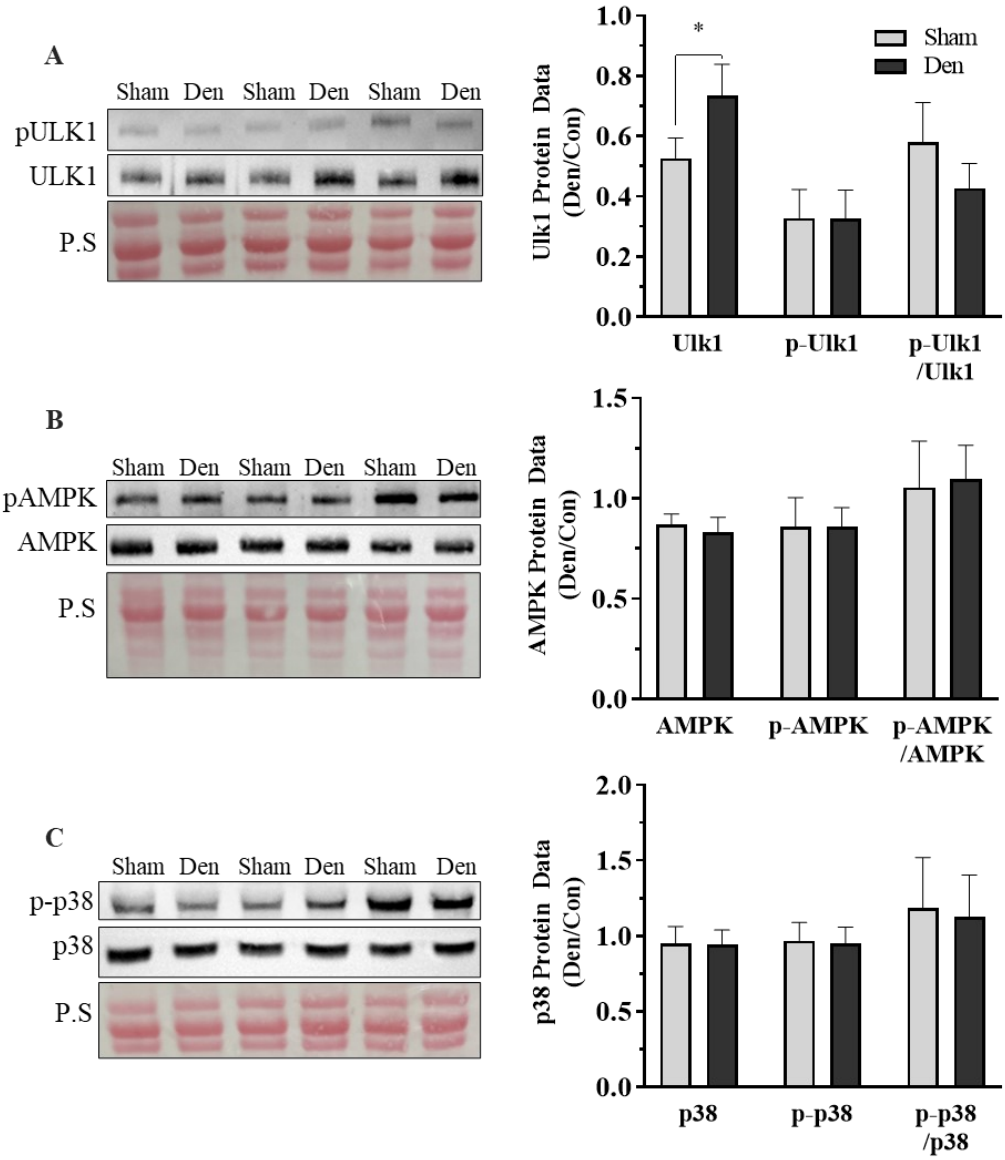

Figure S1: Upstream kinases and autophagy markers with 1 day of denervation. A. Representative blot and data summary for Ulk1 protein. Ulk1 protein content was elevated with 1 day of denervation, but no changes in activity via phosphorylation were measured. **B.** Representative blot and data summary for AMPK protein. AMPK protein content and activity via phosphorylation were unchanged. **C.** Representative blot and data summary for p38 protein. p38 protein content and activity via phosphorylation were unchanged. All values are represented are raw values corrected to ponceau stain (P.S). All values are mean ± SEM. N=6 for all data.

A.2 Impact of denervation on mitochondrial quality control

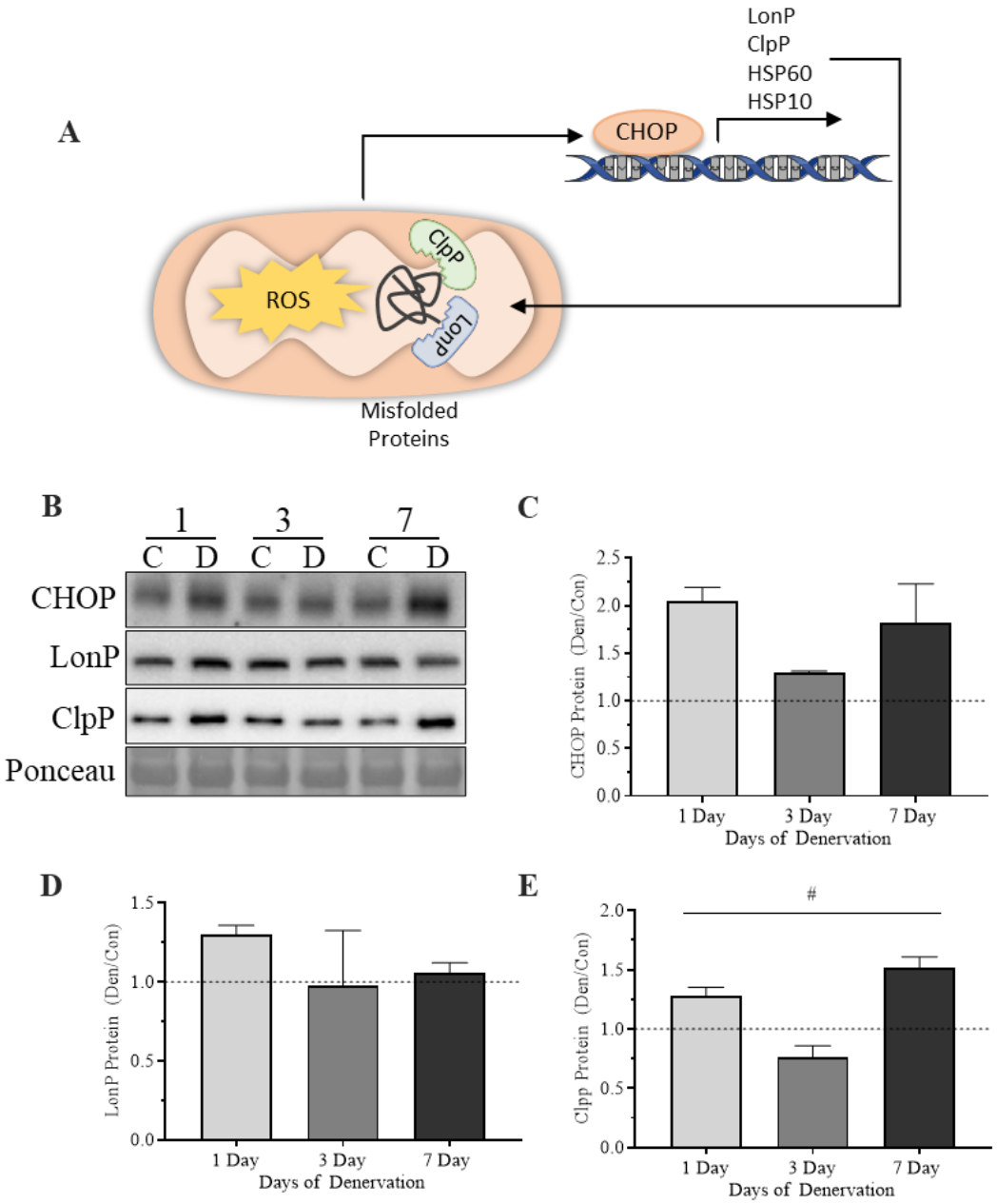

Figure S2: Mitochondrial quality control (MQC) proteins during denervation. A. Schematic of mitochondrial quality control. In response to mitochondrial ROS production and protein misfolding, there is retrograde signaling which leads to the activation of CHOP protein. CHOP acts a transcription factor that promotes the expression of various chaperones and proteases, some of which are mitochondrial. These proteases then localize to the mitochondria where they help eliminate proteotoxicity. **B.** Representative wester blot images for MQC protein targets in 1,3, and 7-day denervated TA muscle. Ponceau was used as a loading control. Quantification of **C.** CHOP **D.** LonP, and **E.** ClpP protein throughout the course of denervation. All values are mean ± SEM. N=2/group.

A.3 mt-Kiema for assessing mitophagy flux in aged muscle

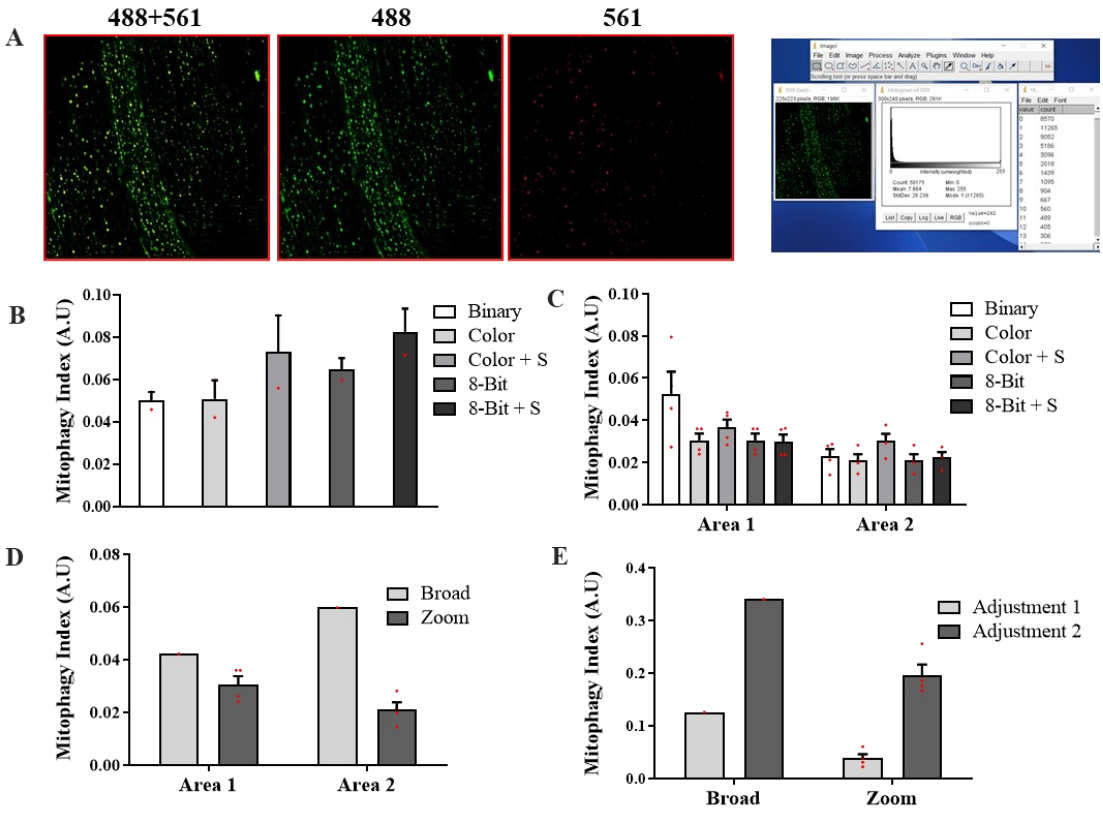

Figure S3: Comparison of mt-keima quantification methods in ImageJ. The Gastrocnemius muscle of mt-keima mice was excised from anesthetized animals and imaged immediately post-removal. **A.** Representation of how images are separated for quantification purposes. Images were taken using sequential imaging at 488-TRICT (green) and 561-TRITC (red), with all imaging parameters remaining the same (laser power and gain). Subsequently, images were separated into their independent channels for quantification purposes. The histogram feature in Image J was utilized to count all the colored pixels and background pixels. Mitophagy index was calculated as follows Mitophagy = Red Pixels / Total Green + Red Pixels. This was done using different variants of the image (binary image, colored image, colored+sharpened image, 8bit image and 8bit+sharpened image). **B.** Broad images were taken using a 20x objective for 3 different areas of the gastrocnemius muscle. Subsequently, each area was analyzing using the above quantification methods. Each method showed a similar mitophagy index. **C.** Each area was imaged using a zoom feature and quantified similarly. Each data point represents 1 zoomed image (4 quadrants per area). Areas and imaging parameters displayed consistent mitophagy indices. Colored images were selected going forward. **D.** To assess the effect of post-hoc image adjusted on our quantification we compared our standard quantification parameters (Adjustment 1) to one in which we sharpened the 561-TRITC (red) image (Adjustment 2). Sharpening the 561-TRITC led to elevated mitophagy values. **E.** Similarly, these adjustments had the same effect when conducted in TA muscle for both broad and zoomed images. Mice were 8-month-old males. All values are mean ± SEM.

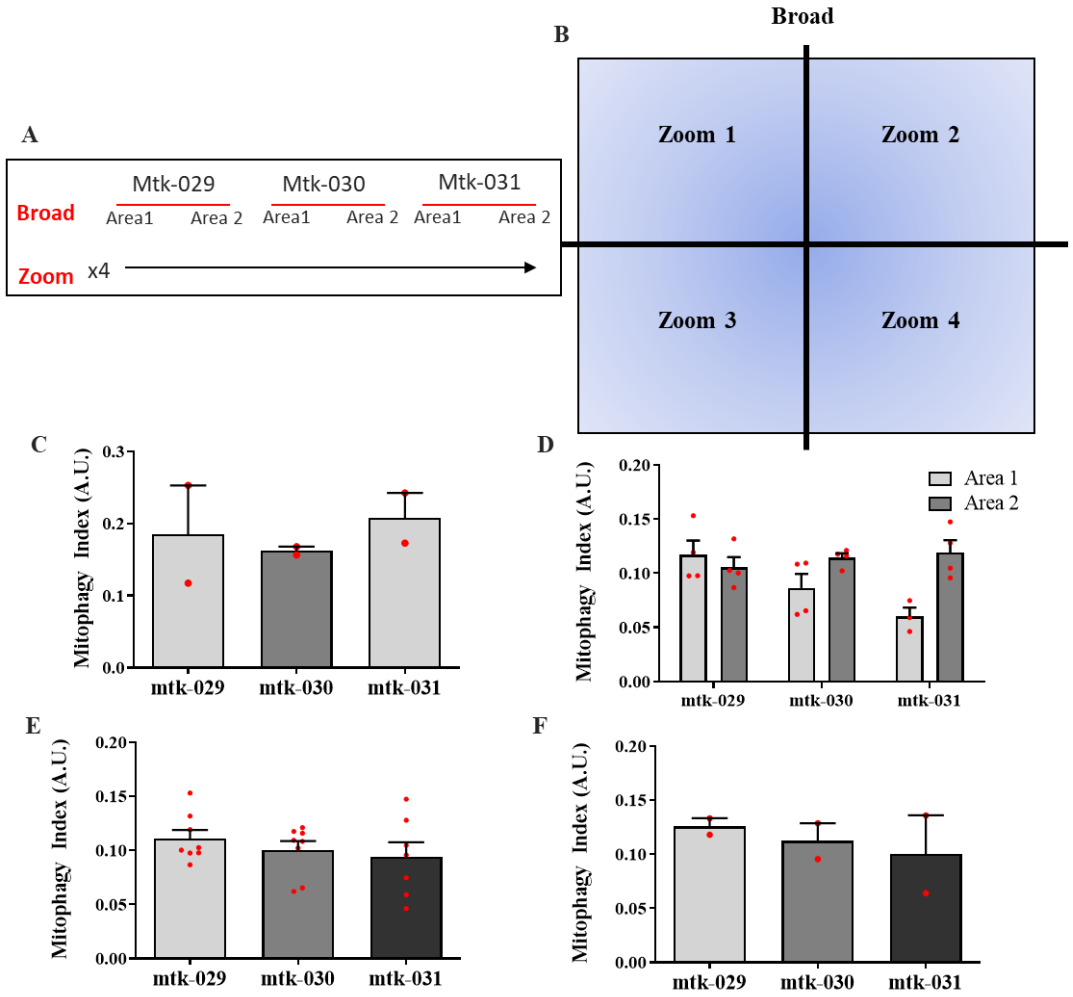

Figure S4: Evaluation of mt-Kiema quantification consistency between animals, whereby mitophagy measurements are similar among three animals. The TA muscle of mt-keima mice was excised from anesthetized animals and imaged immediately post-removal. Images were taken using sequential imaging at 488-TRICT (green) and 561-TRITC (red). Imaging parameters were consistent between animals (laser power and gain). **A.** Imaging workflow; two areas of the muscle were imaged per animal. First a broad image was taken with a 20x objective of "Area 1" followed by zoomed images of each quadrant of this area. Subsequently, "Area 2" was imaged. **B.** A schematic of the broad and zoomed images. **C.** Broad images were quantified in each animal, each data point representing one broad image. **D.** Zoomed images were quantified in the two different areas of each animal, each data point representing one quadrant or 1/4th of a full field of view. **E.** Each data point from the two areas were combined for each animal; each data point represents one quadrant of one area. **F.** An average of each area's zoomed images represents each data point. Mice were 8-month old males. All values are mean ± SEM.

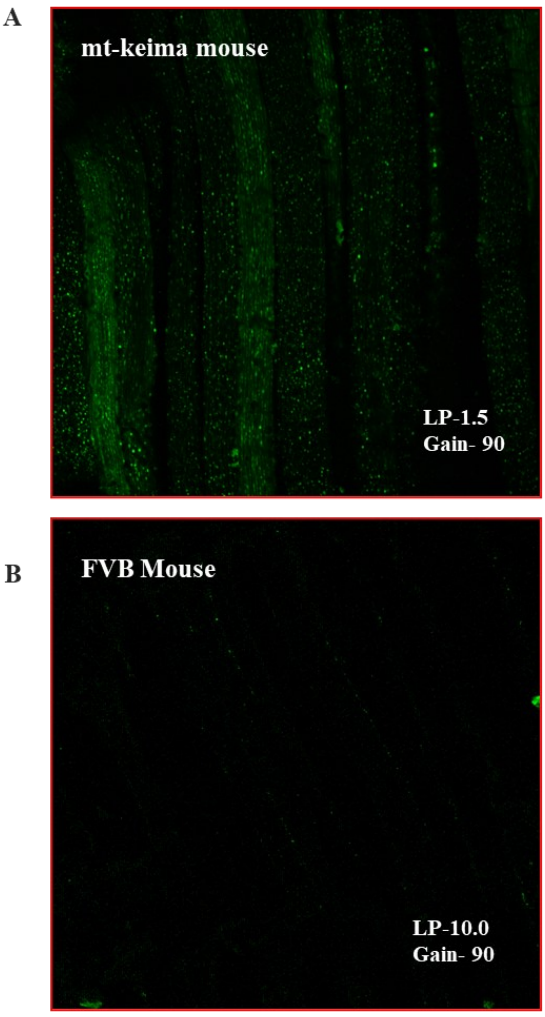

Figure S5. Comparison of green fluorescence (488-FITC) in mt-keima and FVB mouse TA-muscle. Wild-type FVB and mt-keima mice were imaged for green fluorescence to confirm that the green emission was indicative of mt-keima. **A.** Representative confocal microscopy image of the TA muscle using the 488 laser and FITC emission filter in a mt-keima mouse. Laser power was set to a "low" setting (1.5) with a gain of 90, whereby green fluorescence is present. **B.** Representative confocal microscopy image of the TA muscle using the 488 laser and FITC emission filter in and FVB mouse. Laser power was set to a "very high" setting (10.0) with a gain of 90, whereby green fluorescence was not observed. Mice were 8-month-old females.

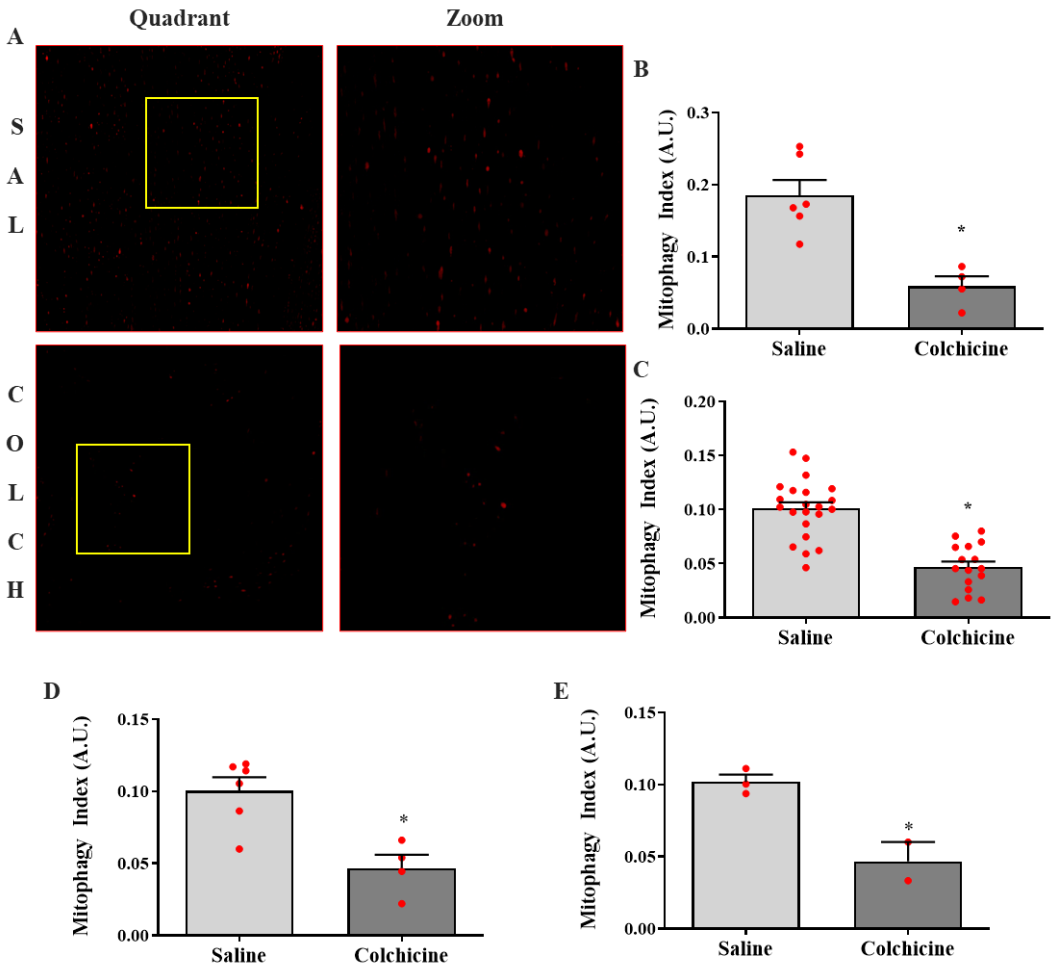

Figure S6: Two days of 0.4mg/kg/day of IP-colchicine reduces red fluorescence in the TA muscle of mt-Keima mice. Mice were treated with IP colchicine or volume-matched saline for 2 days prior to sacrifice. **A.** Representative confocal microscopy images using the 561 laser and TRITC emission filter. Left panels represent a quadrant (1/4th of an area within a TA muscle). Right panels represent a zoomed image of a region of the quadrant. B-E. Quantification of 561-kiema utilizing different quantification parameters. **B.** Each data point represents one broad area of an animal's TA muscle. Each animal was imaged in two broad areas. **C.** Each data point represents one quadrant zoom of the broad areas in (B). **D.** Each data point represents the average of each areas four zoomed images. E. Each data point represents the average of the zoomed images from all areas within an animal. Mice were 8-month old males. All values are mean ± SEM. * represents significance using an unpaired t-test at $p<0.05$.

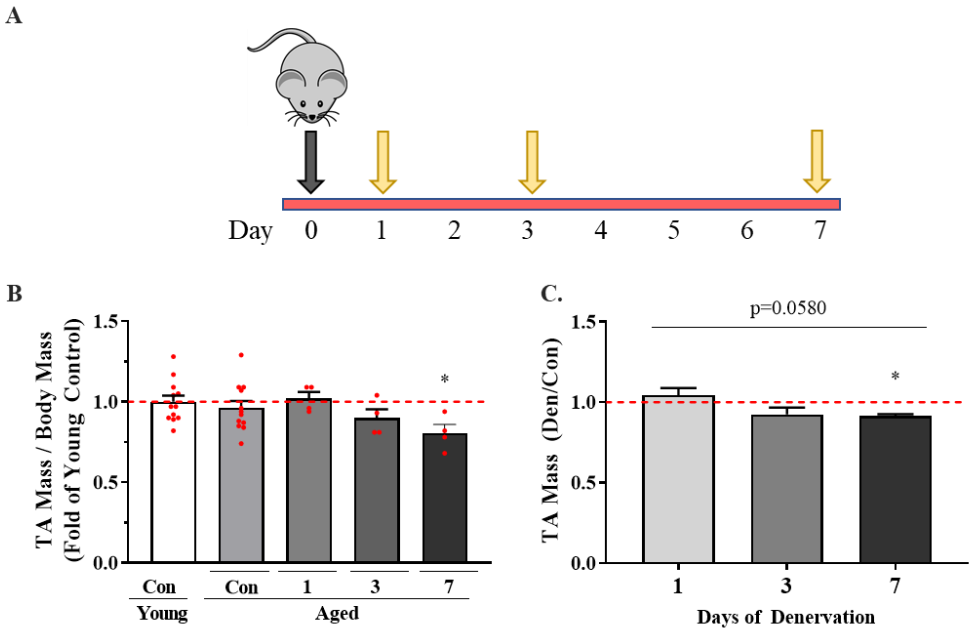

Figure S7: Study Design and Tissue Date on the influence of aging and denervation in mt-Keima mice. Young (4-6) and aged (16-19) month old mt-keima were used. Young mice were used as a control, whereas aged mice underwent unilateral denervation for 1, 3 or 7 days. The contralateral limb was used as a sham-operated internal control. **A.** Representative time-course of deneravation in aged mt-keima mice. **B.** Tibialis anterior mass corrected for body mass, represented as a fold of young control muscle, whereby 7-days of denervation led to a significant reduction in TA mass. **C.** Tibialis anterior mass in aged mt-keima mice represented as denervated / control. A trend in muscle mass reduction over the course of denervation was found. 7 days of denervation led to significant reductions in muscle mass vs time-matched control. All values are mean ± SEM. * represents significance using an unpaired t-test at $p<0.05$.

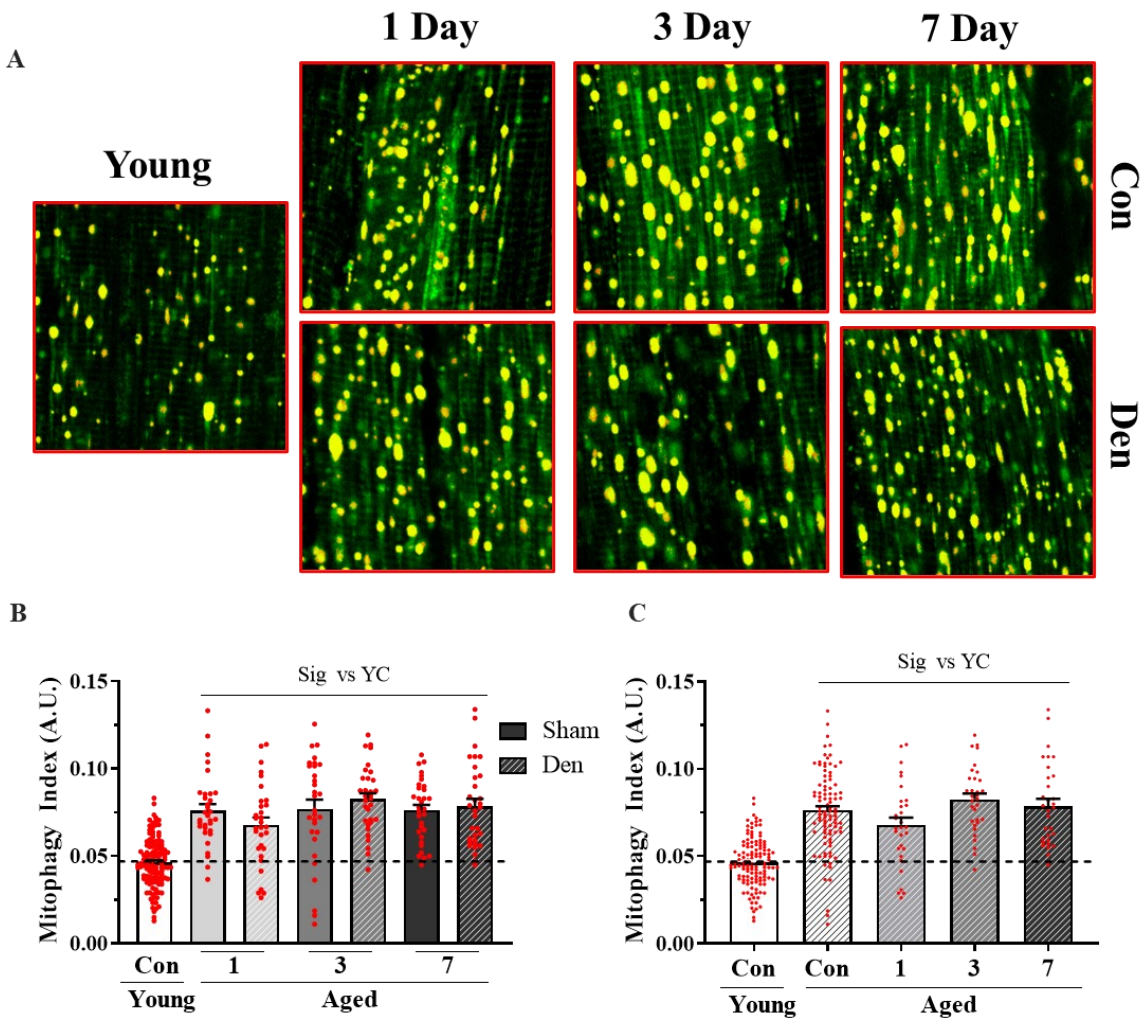

Figure S8: Aging enhances mitophagy in mt-keima imce, with no further changes in response to 1, 3 or 7 days of denervation. A. Representative confocal microscopy images using the 561-excitation laser and TRITC emission filter (red) and the 488-excitation laser and FITC emission filter (green)in young control TA muscle, and aged sham-operated (top row) and denervated (bottom row) muscle for 1, 3 or 7 days. **B.** Quantification of mitophagy (mitophagy index) in young control and separated aged sham-and-denervated muscle. **C.** Quantification of mitophagy (mitophagy index) in the TA muscle of young control, grouped aged sham-operated and 1, 3 or 7 day denervated mice. In young mice 12 biological replicates were used and 8 images were taken at random resulting in 32 data points. In aged mice, for each group, 4 biological replicates were used, and 8 images were taken at random resulting in 32 data points/group. All values are mean ± SEM. * represents significance using an unpaired t-test at $p<0.05$.

A.4 Assessing Lysosome Function *in vitro*

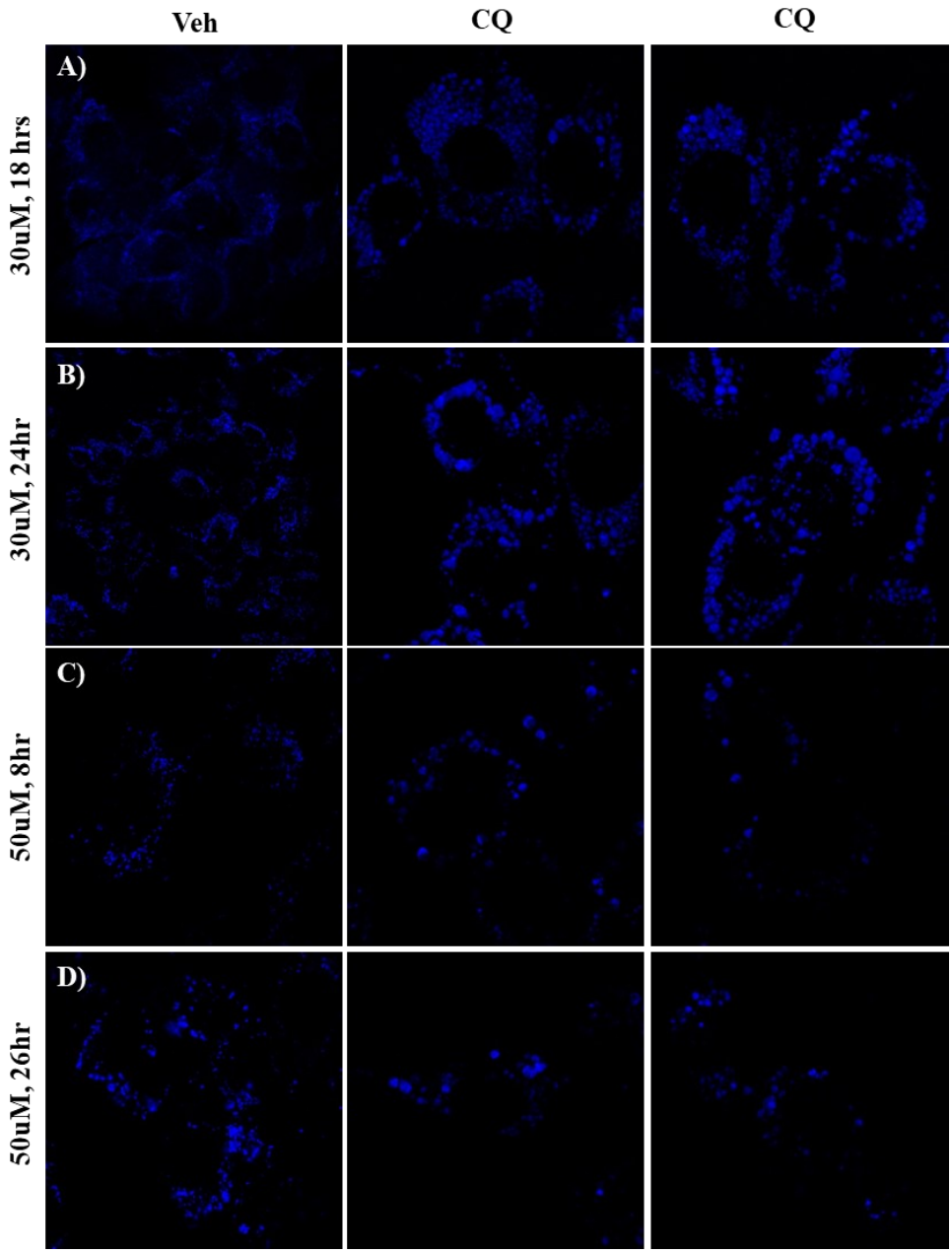

Figure S9: **Utilizing Lysosome Swelling as an indicator of dysfunction in vitro.** C2C12 myoblasts were cultured according to established protocols (DMEM + 10% FBS). 24 hours after being plated in 6-well plates, cells were treated with 30mM or 50mM of chloroquine (CQ) or volume matched vehicle (Veh). 30mM treatment was done for 18hrs (A) or 24hrs (B). 50mM treatment was for 8hrs (C) or 26 hours (D). All images were captured using a 60x objective.

A.5 Autophagy-lysosome markers in human muscle with aging

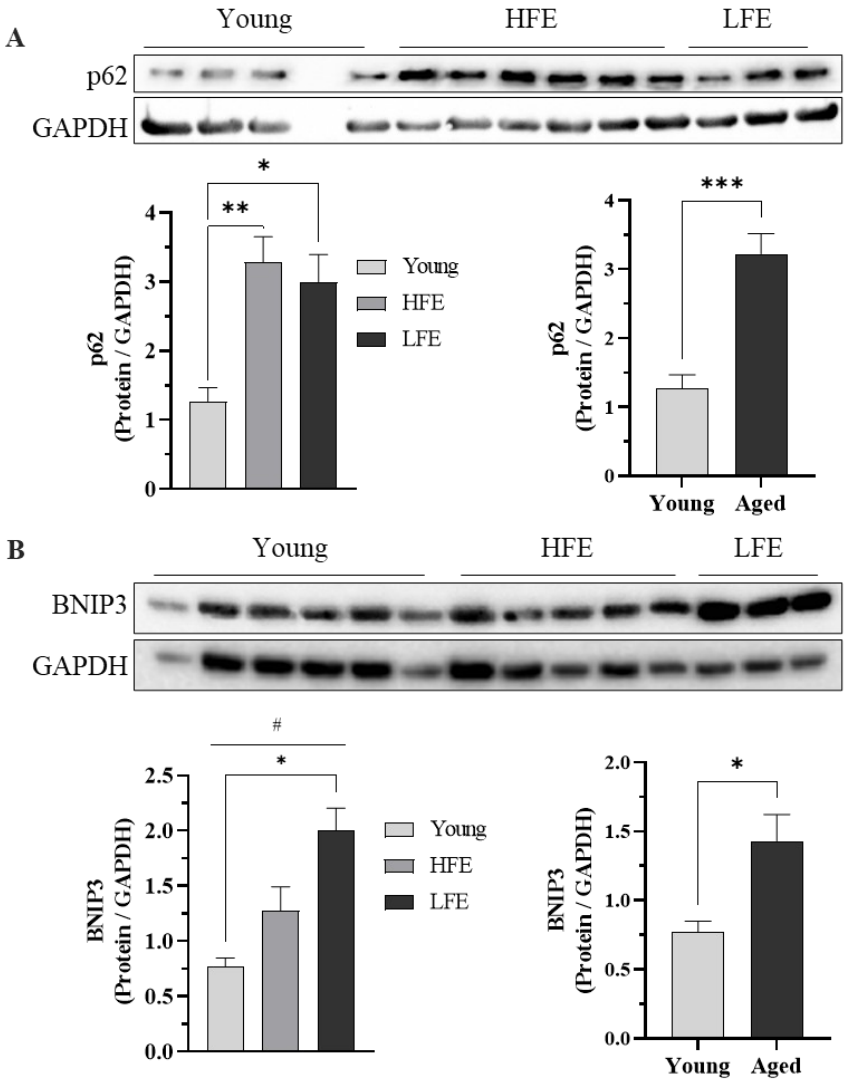

Figure S10: Autophagy and mitophagy markers in human skeletal muscle from young, high functioning elderly (HFE) and low functioning elderly (LFE). A. p62 protein is elevated in both HFE and LFE, leading to an overall age effect. **B.** The mitophagy marker BNIP3 is only significantly upregulated in the muscle from the HFE versus young, but an overall effect of age was observed. Values are represented as N=9, N=11 HFE, N=3 LFE. # represents a significant one-way ANOVA. * represents a significant difference between indicated groups. $p<0.05$.

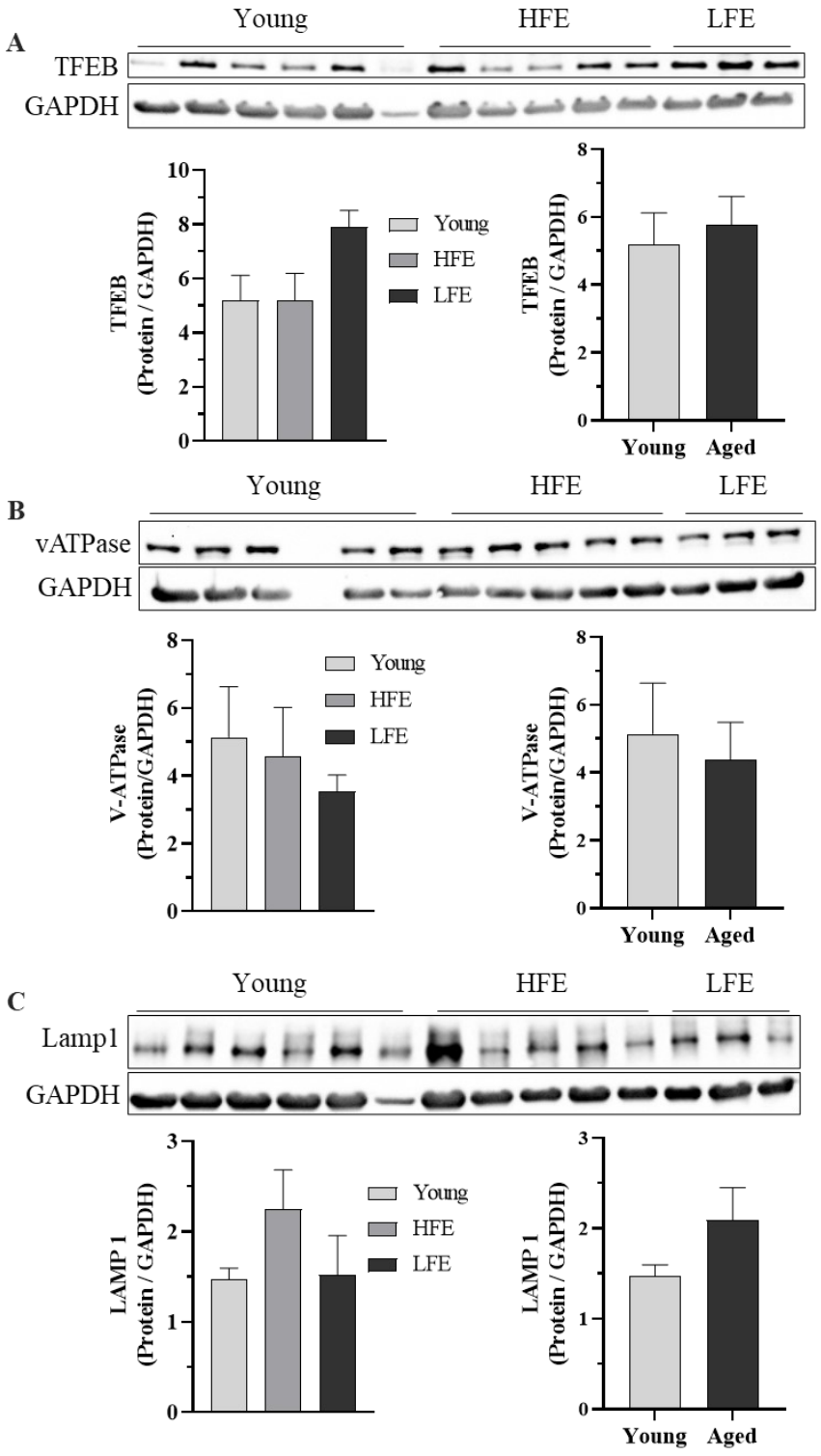

Figure S11: Lysosome markers in human skeletal muscle from young, high functioning elderly (HFE) and low functioning elderly (LFE). A. TFEB protein is unchanged with age in both LFE and HFE. **B.** vATPase is unhanged with age in both LFE and HFE. **C.** LAMP1 is unchanged with age in LFE and HFE. Values are represented as N=9, N=11 HFE, N=3 LFE.

APPENDIX B: OTHER CONTRIBUTIONS TO SCIENCE

PEER REVIEWED ARTICLES:

1. **Triolo M**, Hood DA. (2021) Manifestations of Age on Autophagy, Mitophagy and Lysosomes in Skeletal Muscle. *Cells*. 10(5).
2. Hood DA, Memme JM, Oliveira AN, **Triolo M**. (2019) Maintenance of skeletal muscle mitochondria in health, exercise, and disease. Annual Reviews of Physiology. 81.19-41.
3. **Triolo M,** Hood DA. (2019) Mitochondrial breakdown in skeletal muscle and the emerging role of the lysosomes. Archives in Biochemistry and Biophysics. 661. 61-71.
4. Kim Y, **Triolo M,** Erlich A, Hood DA. (2019) Regulation of autophagic and mitophagic flux during chronic contractile activity-induced muscle adaptations. Pflügers Archiv - European Journal of Physiology. 471. 431-440.
5. Beyfuss K, Erich A, **Triolo M,** Hood DA. (2018) The role of p53 in determining mitochondrial adaptations to endurance training in skeletal muscle. Scientific Reports. 8.
6. Kim Y, **Triolo M,** Hood DA. (2017) Impact of aging and exercise on mitochondrial quality control in skeletal muscle. Oxidative Medicine and Cellular Longevity. 2017:3165396.

BOOK CHAPTERS

Cheema N, Triolo M, Hood DA. Ch.27 - Exercise training, mitochondrial adaptations and aging. pp 413-432 in The Routledge Handbook on Biochemistry of Exercise. ISBN: 978-0-367-22383-0

ABSTRACTS, POSTERS & ORAL PRESENTATIONS:

1. **Triolo M,** Kumari R, Hood DA. The effect of age, sex, and acute exercise on the autophagy-lysosome system in skeletal muscle. *Canadian Society for Exercise Physiology (CSEP) 2021.* Virtual, ON. October 15, 2021 (Poster Presentation).
2. **Triolo M,** Hood DA. Mitophagy undergoes time-dependent changes in response to hindlimb denervation. APS Integrative Physiology of Exercise Conference 2020. Nov 9-13. Online. (Poster Presentation).
3. **Triolo M,** Hood DA. Denervation-induced muscle disuse is associated with alterations in mitochondrial clearance. *Canadian Society for Exercise Physiology (CSEP) 2020.* Virtual, ON. October 23, 2020 (Poster Presentation).

4. **Triolo M,** Slavin M, Moradi N, Hood DA. Regulation of The Autophagy-Lysosome System in Response to Hindlimb Denervation. *MHRC Muscle Health Awareness Day 11.* Toronto, ON. May 22, 2020 (Oral Presentation).
5. **Triolo M**, Slavin M, Kim Y, Carter HN, Hood DA. Lysosomal Alterations in skeletal muscle plasticity – an investigation of age, exercise and disuse. *APS Experimental Biology 2020.* San Diego, CA. April 2020. (Poster Presentation)
6. **Triolo M,** Cheema N, Slavin M, Moradi N, Hood DA. Skeletal muscle autophagy and mitophagy are altered in the time course of hindlimb denervation. *MitoNET 2019*. Toronto, ON. November 8-9, 2019 (Poster Presentation).
7. **Triolo M,** Slavin M, Moradi N, Hood DA. The effects of hindlimb denervation on the regulation of autophagy and mitophagy. *NHLBI Mitochondrial Biology Symposium.* Bathesda, MD. September 24-26, 2019 (Poster Presentation).
8. Slavin M, **Triolo M,** Hood DA. Autophagy in Hindlimb Denervated Rats. *MHRC Muscle Health Awareness Day 10.* Toronto, ON. May 24 2019. (Poster Presented by Slavin).
9. **Triolo M,** Slavin M, Hood DA. Hindlimb Denervation Alters the Regulation of Autophagy and Mitophagy. *APS Experimental Biology 2019*. Orlando, Fl. April 2019 (Poster presentation).
10. **Triolo M,** Oliveira A, Hood DA. The effect of age and acute exhaustive exercise on skeletal muscle mitochondria and lysosomal biogenesis. *Canadian Society for Exercise Physiology (CSEP) 2018.* Niagara Fall, ON. November 1 2018 (Poster Presentation).
11. **Triolo M,** Oliveira AN, Hood DA. The effects of age and acute endurance exercise on skeletal muscle mitochondria and lysosomal biogenesis. *MHRC Muscle Health Awareness Day 9.* Toronto, ON. May 24 2018 (Poster Presentation).
12. Kim Y, **Triolo M,** Erlich A, Lai J, Hood DA. Autophagy and Mitophagy Flux in Skeletal Muscle during Chronic-Contractile Activity. *APS Experimental Biology 2018*. San Diego, Ca. April 2018 (Poster presented by Kim).
13. **Triolo M,** Oliveira AN, Hood DA. The effect of age and exercise on muscle mitochondrial function and signaling towards mitophagy. *Ontario Exercise Physiology 2018*. Barrie, ON. January 2018 (Oral Presentation).

14. Beyfuss K, Erlich A, **Triolo M,** Hood DA. Role of p53 in exercise-training induced mitochondrial adaptations: a comparison of two mouse models. *Ontario Exercise Physiology 2017*. Barrie, ON. January 2018 (Presented by Beyfuss).
15. **Triolo M,** Hood, DA. The impact of skeletal muscle disuse on mitochondrial content and mitophagy flux. *MitoNET 2017*. Toronto, ON. September 30 2017 (Poster Presentation).
16. **Triolo M**, Tryon L, Hood, DA. Skeletal muscle disuse is associated with reductions in mitochondrial content and elevations in mitophagy in the rat hindlimb. *MHRC Muscle Health Awareness Day 8*. Toronto, ON. May 26 2017 (Poster Presentation).
17. Kim Y, **Triolo M,** Hood, DA. Autophagy vs. mitochondrial adaptations in skeletal muscle during endurance training. *MHRC Muscle Health Awareness Day 8.* Toronto, ON. May 26 2017 (Poster presented by Kim).
18. Kim Y, **Triolo M**, Hood, DA. Regulation of autophagy during chronic contractile activity-induced muscle adaptations. *APS Experimental Biology 2017*. Chicago, IL. April 2017 (Poster presented by Kim).
19. **Triolo M**, Tryon L, Hood, DA. The effects of denervation on skeletal muscle autophagy and mitochondrial proteases. *Ontario Exercise Physiology 2017*. Barrie, ON. January 2017 (Oral Presentation).